University of Stavanger

Faculty of Science and Technology

MASTER'S THESIS

Study program/ Specialization: **Petroleum Engineering**	**Spring semester, 2010** **Open**
Writer: **Henriette Strøm**	Henriette Strøm (Writer's signature)

Faculty supervisor: **Merete Vadla Madland**

External supervisor: **Kari Nordaas Kulkarni**

Title of thesis:

The use of sea water tracer as a tool for history matching of the Statfjord Fm simulation model

Credits: **30sp**

Key words: The Statfjord field Statfjord Fm reservoir simulation model Gas Cap Water Injection History matching Tracer Statfjord field predictions	Pages: 141 + Enclosure: ..... Stavanger, 15.06.2010 Date/year

University of Stavanger

Statoil

The use of sea water tracer as a tool for history matching of the Statfjord Fm simulation model

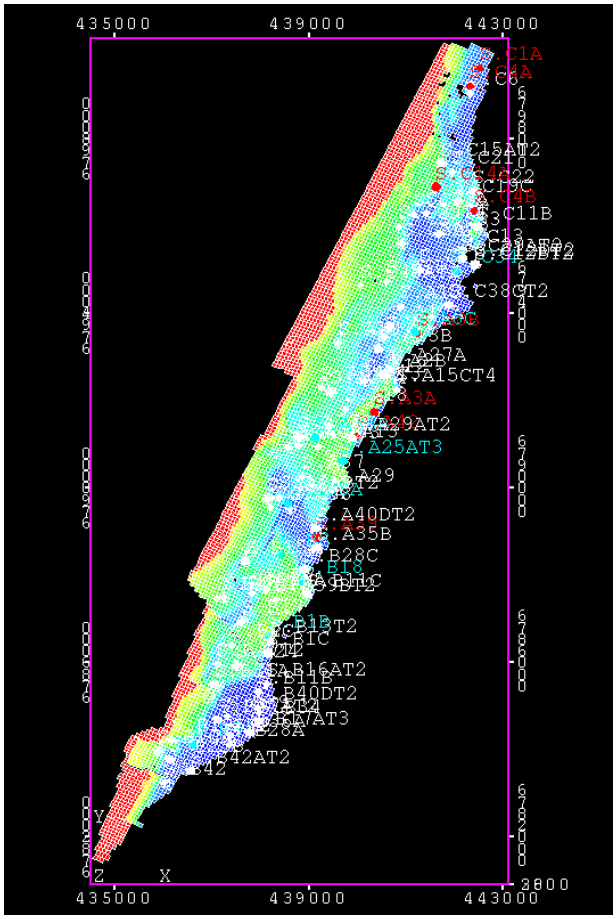

By

Henriette Strøm

Master Thesis, Spring 2010

Acknowledgments

I would like to give a special and huge thanks to my supervisor at Statoil, Kari Nordaas Kulkarni. Despite being very busy, she has taken the time to give me help and guidance. Her enthusiasm and knowledge has been essential for completing my thesis. I am grateful for all that she has taught me, and for being the best supervisor I could ask for.

I am thankful for Merete Vadla Madland for being my supervisor at the University of Stavanger. Knowing that she has had a very tight schedule this semester, it means a lot to me that she took the time for me. With her knowledge and kindness, she has been both very helpful and supportive.

A special thanks also goes to Oddvar Husby, Andreas Bielinski and Egil Stangeland, who have all helped me whenever I needed it. They have supported me and given me valuable information and guidance.

Thanks also to Egil Stangeland and Goro E. Müller for giving the opportunity to write my thesis at Statfjord PETEK at Statoil. It has been a very interesting study, where I have learned very much.

I would like to give a huge thanks to Harald Steensland and Grete Marie Dysjaland, who have also been writing their theses at Statoil. We have had very interesting discussion, where we have shared our knowledge. They have both been very supportive and helpful whenever I needed.

I would like to thank Eva Stevenson for giving me the best support during this semester. A huge thanks also goes to my family and friends.

Thanks again to all.

Stavanger, June 2010

Henriette Strøm

Henriette Strøm

Abstract

In this study, the Statfjord Fm reservoir simulation model was set up to track injected sea water. The sea water itself thereby forms a tracer in the simulation model. This *sea water tracer* was included with the intent of comparing modeled sea water production with observations. The observed data was the sea water cut (fraction of sea water in produced water), calculated from the concentration of sulphate and magnesium in produced water. Comparisons of observations and model results have been used to further history match the model, by analyzing both the sea water cut and the breakthrough times of sea water in production wells.

The sea water cut match for some wells was found to be unsatisfactory, indicating a potential for improvement of the simulation model. Analysis of these results provided information about flow patterns in the reservoir, and indicated presence of additional faults and regions where permeability might be different from that used in the model.

The objective of this study was to improve the sea water cut match in the model, for a selection of Upper Statfjord producers. Statfjord A wells and Statfjord B wells north of the F-11 fault were considered when history matching. These regions were prioritized as most of the upflank water injection took place there.

The first attempt to improve the sea water cut match focused on the relative permeability of water, as water breakthrough times are sensitive to changes in water mobility. In the model, most producers had sea water breakthrough too late, indicating that increased water mobility could improve the match. After implementing a new water relative permeability curve, the sea water cut match was improved, but at the cost of a too high water production volume. To achieve a satisfactory match, additional changes were also applied, mostly in the form of modifying the transmissibility of existing faults, introducing new faults, and by changing permeability in selected layers to encourage fingering of water.

Upflank producers are close to the injectors, and the modeled sea water cut was often too high. Further, the modeled breakthrough times for most downflank producers were too late, indicating that the model had underestimated the degree to which injected water could move downflank. Upflank wells could not be matched on sea water breakthrough times as sea water was in place at the start of production. Nevertheless, the SWC match has been generally improved. The sea water breakthrough times and the sea water cut for downflank producers have improved significantly.

This study has been the first step in a process to consider injected sea water when history matching the Statfjord Fm model. Because only some of the Statfjord Fm producers have been considered, discrepancies may have been introduced in the match for the remaining wells. This should be accounted for in any subsequent full match of the field.

Table of Contents

List of Figures

List of Tables

1 Introduction

The Statfjord Field is the largest producing oil field in the North Sea. Having produced for over 30 years, since 1979, the field is also one of the oldest North Sea fields. A pressure depletion process – the Statfjord Late Life project (SFLL) – is currently being performed to extract gas from remaining oil. The recovery factor for the field is exceptionally high, at 65% for oil and 53% for gas prior to SFLL. At the expected end of the field life in 2020, these recovery factors are estimated to become 68% and 74%, respectively.

Two main reservoirs comprise the Statfjord Field: the Brent Gp and the Statfjord Fm. Pressure maintenance has been the primary drainage strategy in both reservoirs, though the injection patterns have been very different. In the Brent Gp, downflank water injection was used from 1981, assisted by WAG injection from 1997, until 2008, when SFLL was initiated. In the Upper Statfjord Fm, miscible gas injection was used, creating a gas cap in the reservoir. In 1997, gas cap water injection was started, assisted by continued gas injection. Lower Statfjord has been drained by downflank water injection and some WAG injection. All injection in Statfjord Fm was stopped at the start-up of SFLL in 2007.

Reliable simulation models are important for optimizing, managing and establishing a production prognosis for the reservoir. Simulation models for both the Brent and Statfjord reservoirs have been developed. Aspects of three-phase flow, critical gas saturation and hysteresis processes results in a complex drainage process. Uncertainties regarding liberation and migration of gas during SFLL make it essential to have a good simulation model. History matching is a vital tool for improving the model, by matching various parameters and to compare the response to observed data. However, history matching is a complex process, even more so because the Statfjord Field is large and has a complex drainage history.

This study will attempt to further history match the Statfjord Fm model. The water production has proven to be difficult to match, presumably because of gas cap water injection in Upper Statfjord. By considering previously neglected data– the sea water cut, this study aims to provide additional insight into the movement of the injected water. To consider the sea water cut when history matching, both observed data and simulation results are needed. Natural tracers in sea water provide data about the location of sea water when injection water reaches producers. And a sea water tracer can be implemented in the simulation model. Comparisons of observations and simulation results give additional information that can be used to improve the simulation model.

2 The Statfjord Field

The Statfjord Field was discovered by well 33/12-1 on August 10, 1973, and production started in November 1979. The field is located about 200km off the coast of Norway, on the western margin of the North Sea Rift System (map shown in Figure A.1 in the appendix). Being 25 km long and having an average width of 4 km, it is the largest producing oil field in Europe. Figure A.2 illustrates the size of the field.

Development of the field has been done using three Condeep platforms. Statfjord A started in November 1979, followed by Statfjord B in November 1982 and Statfjord C in June 1985. Several tie-ins have also been established, including satellite fields (Statfjord East, Statfjord North, Statfjord North Flank and Sygna) and the Snorre platform; see Figure A.3.

The company Mobil discovered the Statfjord Field and Statoil took over as operator in January 1987.

The current ownership interests for the Statfjord Unit are [25]:

- Norwegian owners:
    - o StatoilHydro ASA (operator) 44.33688%
    - o ExxonMobil Exploration and Production Norway A/S 21.36717%
    - o Norske ConocoPhillips AS 10.32747%
    - o A/S Norske Shell 8.54687%
    - o Enterprise Oil Norge AS 0.89030%
- UK owners:
    - o ConocoPhillips (UK) Ltd 4.84377%
    - o Centrica Resources Ltd 9.68754%

The Statfjord Field consists of three reservoirs: the Statfjord Formation, the Brent Gp and Cook Fm. A lithostratigraphic overview is shown in Figure A.5. Brent and Statfjord are further subdivided into Upper and Lower Statfjord and Upper and Lower Brent (Figure 2.1), on the basis of significant pressure barriers.

The field has a relatively uniform Main Field block, dipping about 7 degrees to the west, separated by steep normal cross-faults. To the east, the East Flank is a geologically complex gravitational collapse zone, and is highly faulted. In addition, the East Flank contains reworked Brent sediments. The communication between Main Field and East Flank is generally good, despite the many faults and complexity. A cross section through the field is shown in Figure A.4.

Figure A.7 shows the Statfjord A, B and C areas and the major fault F-11 that divides the B area.

Lithostrat.			LITHO_Statfjord
Viking		Rew. Brent	Rew. Brent
BRENT	Upper Brent	Tarbert	Tarbert
		Ness	Ness 2
			Ness 1
	Lower Brent	Etive	Etive
		Rannoch	Rannoch 2
			Rannoch 1
		Broom	Broom
DUNLIN		Drake	Drake
		Cook	Cook2
			Cook 1B
			Cook 1A
		Burton	Burton
		Amundsen	Amundsen 2
			Amundsen 1
STATFJORD	Upper Statfjord	Nansen	Nansen
		Eiriksson	Eiriksson
	Lower Statfjord	Raude	Raude 2
			Raude 1

Figure 2.1: General lithostratigraphic Column for the Statfjord Field

The oil recovery factor for Statfjord is very high, exceeding 65% of STOIIP. Cumulative oil production is over 650 MSm^3. Oil and gas production, reserves and STOIIP/GIIP for Brent, Cook and Statfjord is shown in Figure A.6. Plateau production was reached in 1986 and maintained for about 8 years at an oil rate of about 110000 Sm^3/day [25].

This study will focus on the Statfjord Fm reservoir. Therefore, the Statfjord Fm will be described in more detail regarding reservoir structure, properties and drainage strategies used.

2.2 The Statfjord Fm

The Statfjord Fm is a sandstone reservoir of Lower Jurrasic to Upper Triassic age, with the oil trapped along the crest. A shale layer separates Upper and Lower Statfjord, forming a pressure barrier. Upper Statfjord consists of the Nansen member at the top and the Eiriksson member at the bottom. The Lower Statfjord consists of the Raude member. See Figure 2.2. The reservoir properties in the Statfjord Fm have an improving quality upwards.

Based on a pressure study, communication across the F-11 fault in the SFB area (see Figure A.7) is believed to be open for Eiriksson-Eiriksson and tight for Eiriksson-Raude.

<table>
<tr><td rowspan="3">STATFJORD Fm.</td><td rowspan="2">UPPER STATFJORD</td><td>Nansen</td></tr>
<tr><td>Eiriksson</td></tr>
<tr><td>LOWER STATFJORD</td><td>Raude</td></tr>
</table>

Figure 2.2: Reservoir zonation of the Statfjord Formation

Nansen Member

Nansen is composed of shallow marine sandstones. It is 5-15m thick and has excellent reservoir properties. It reflects a fluvio-deltaic enovironment with mouthbar sands and tidal channels, marking the onset of marine conditions.

Eiriksson Member

The Eiriksson member is a 40-60m thick sequence of fluvial dominated sand deposits with fairly good properties. Eiriksson consists mostly of coastal plain deposits, but shows an upwards trend towards a marine environment. It consists of more than 80% sandstone.

Raude Member

A fieldwide shale layer is found on top of Raude and acts as a barrier between the Upper and Lower Statfjord. Raude consists of seven main zones, each characterized by a lower sand layer of braided stream deposits overlaid by floodplain claystones. A high proportion of the sand deposits in upper Raude are amalgamated, providing extensive sandstone sheets with good productivity. Lower Raude has fewer amalgamated channel units, typically resulting in lower productivity due to the more restricted stratigraphy and limited aquifer support [25].

2.3 Reservoir properties of the Statfjord Fm

The STOOIP of the Statfjord Fm is approximately 220 million Sm^3, from where approximately 150 million Sm^3 is found in the Upper Statfjord. Reservoir data for the Statfjord Fm is presented in Table 2.1 and 2.2 [25].

Reservoir and Fluid Properties	
Datum Depth	2701.0 m TVD MSL
Datum Pressure	404.3 BARA
Datum Temperature	96.7 Deg. C
Oil-Water Contact north	2829.9 m TVD MSL
Oil-Water Contact central	2814.0 m TVD MSL
Oil-Water Contact south	2806.3 m TVD MSL
Oil gradient	0.0655 bar/m
Bubble point Pressure	200 bar
Formation volume factor of original reservoir oil	1.48 m^3/Sm^3
Solution gas-oil-ratio of original reservoir oil	156.6 Sm^3/Sm^3
Viscosity of original reservoir oil	0.36 mPa s
Viscosity of injected gas	0.032 mPa s
Viscosity of water	0.36 mPa s

Table 2.1: Reservoir and Fluid Properties [25].

Average Reservoir Properties	Nansen	Eiriksson	Raude
Porosity, percent	29	25	20
Permeability, mD	2000-5000	800-1000	100-300
Horizontal permeability, mD	5000	1250	100
Net/gross, percent	100	70	40
Water saturation, percent	11	15	20

Table 2.2: Average Reservoir Properties [25].

2.4 Reservoir Development plan

2.3.1 History

For 28 years the main drainage strategy for the Statfjord reservoir has been pressure maintenance by water and gas injection into the main reservoirs. The Brent reservoir first produced from pressure depletion until pressure maintenance by down flank water injection was established in 1981 for Lower Brent and 1982 for Upper Brent. Due to the lack of gas export pipeline the first years, the gas produced was injected upflank in the Statfjord Fm, providing pressure maintenance. This process was also miscible, resulting in a very high recovery. The initial drainage strategy is illustrated in Figure 2.3.

In 1986, gas export from the Statfjord Field started through pipelines in the Statpipe and the UK FLAGS system. As the oil production declined, associated gas production was reduced. Upflank water injection was started in addition to gas injection in Upper Statfjord reservoir in 1997 when there was not enough gas to maintain the reservoir pressure. Therefore, water-alternating-gas (WAG) injection combined with gas cap water injection (GCWI) was initiated in

1997 in Upper Statfjord to replace gas injection. The decision to inject water upflank is described in chapter 4. Lower Statfjord was developed by downflank water injection assisted by limited WAG injection.

With less gas injection in Statfjord Fm, some gas was available for WAG injection in Brent, which started in 1997 and was very successful. After injecting 16 GSm3 of WAG gas, an additional 11 MSm^3 of oil was produced as of 2007. The drainage strategy until 2007 is illustrated in Figure 2.4 [25].

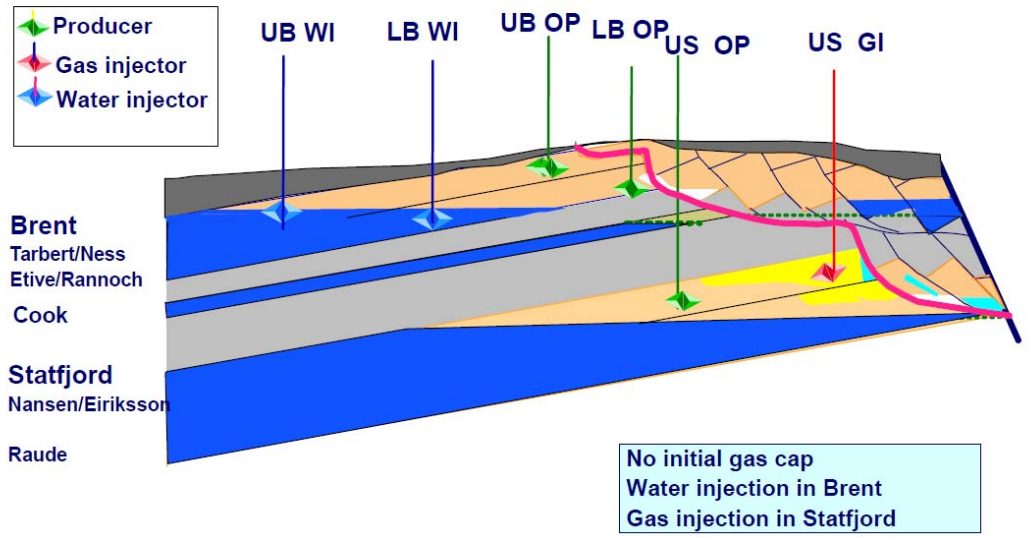

Figure 2.3: Illustration of the initial drainage strategy on the Statfjord Field [25].

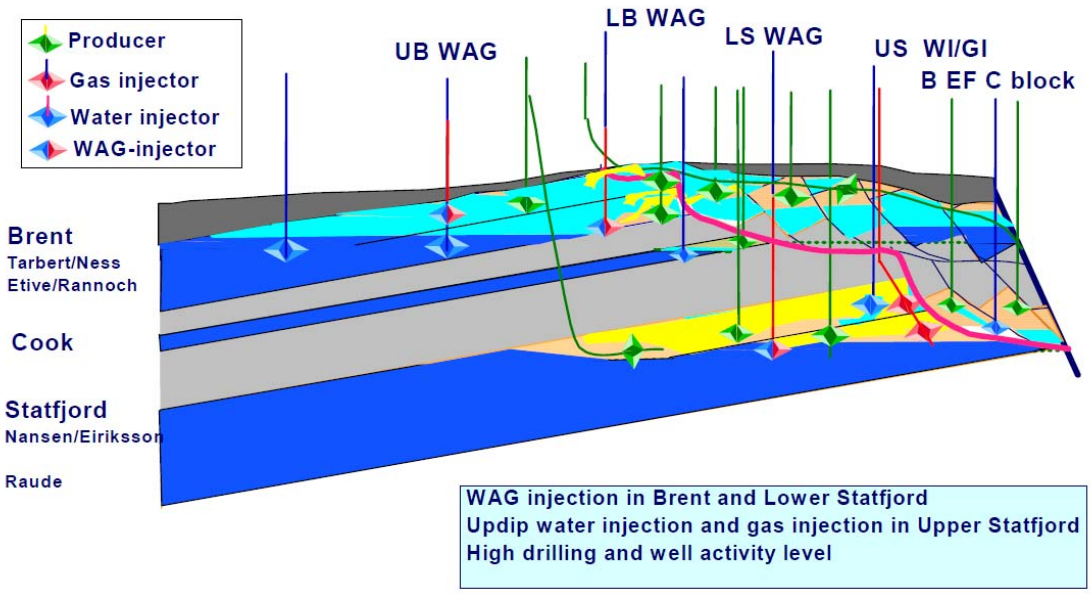

Figure 2.4: Illustration of drainage strategy on the Statfjord Field from 1995-2007 [25].

2.3.2 Present; Statfjord Late life project

In order to extend the production life of the Statfjord Field it was required to change drainage strategy from pressure maintenance to depressurization. Depletion of the reservoirs has converted the Statfjord field from an oil field to a gas field, see Figure 2.5. This new strategy is called Statfjord Late Life (SFLL). The new drainage strategy was found to increase ultimate gas recovery factor from 53% to 74% and oil recovery factor from 65% to 68%. The lifetime of the Statfjord Field will be extended by approximately 10 years, up to 31.12.2020 for SFB and SFC, and 31.12.2012 for SFA [7]. The Statfjord Late Life project was sanctioned by the partners and the Norwegian Government in 2005. Two years after, in 2007, pressure depletion of Upper Statfjord Fm started. In October 2008, depletion started in Brent and Lower Statfjord [25].

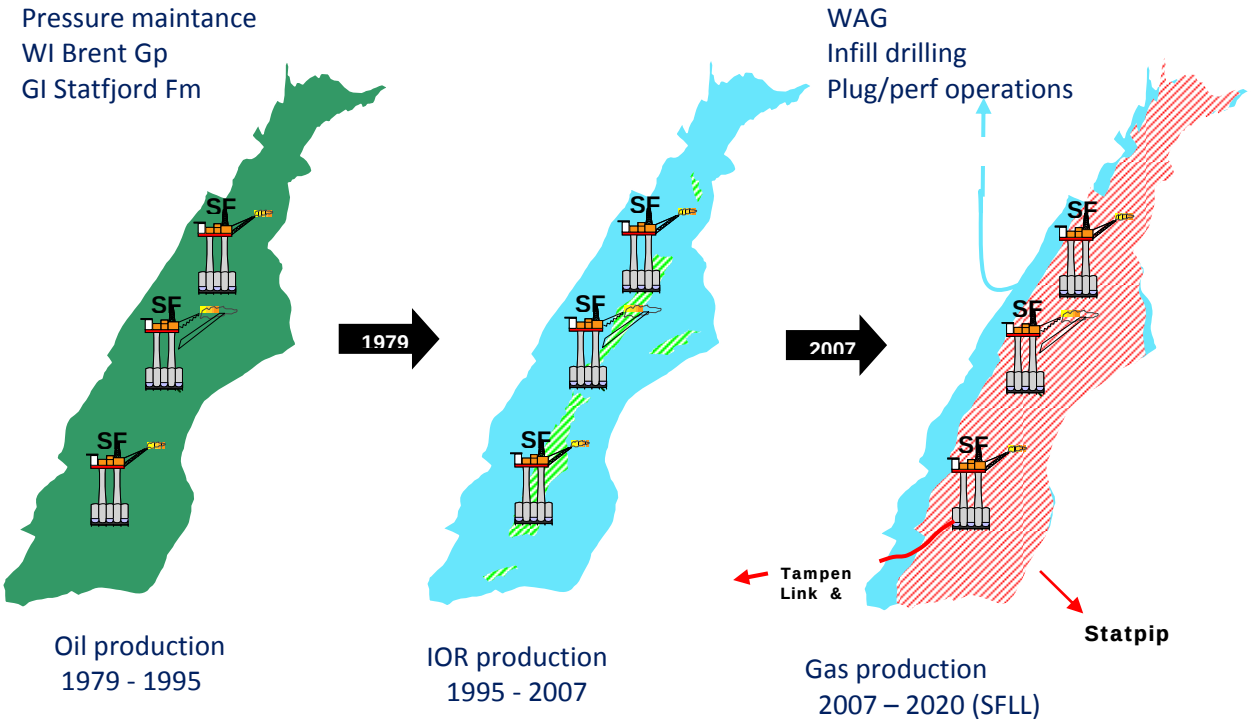

Figure 2.5: SFLL – From oil to gas. (From pressure maintenance to pressure depletion)[24]

An extensive reduction in pressure below the bubble point will cause gas to liberate from the remaining oil. The free gas will, once above critical gas saturation, move towards the crest of the field where it can be produced. In the Statfjord Fm, gas production will be mostly from the previously injected gas. However, much of the injected gas is trapped in water from GCWI. The gas will be released from water as the pressure drops, though there is some uncertainty as to how much and fast this process is. Statfjord Fm will be the main supplier of gas in the first few years of SFLL, before Brent Gp takes over. The development of free gas and gas associated with oil for both Brent and Statfjord during SFLL is shown in Figure A.8.

Figure 2.6 illustrates the major steps of the depressurization process, including (a) start-up, (b) start-up for gas liberation from solution, (c) gas cap establishment and (d) the final pressure depletion phase, when the aquifer wells (ESP) are introduced to support the pressure depletion rate [25].

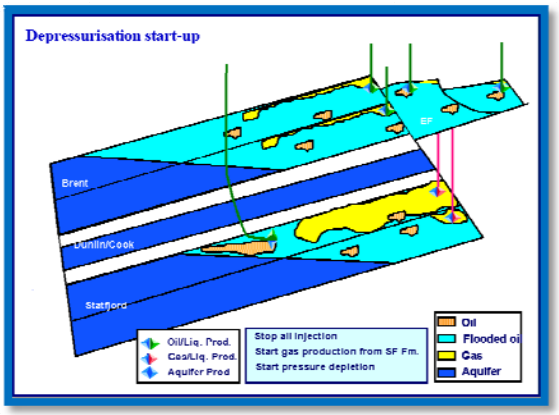

a) Depressurisation start-up - Current stage

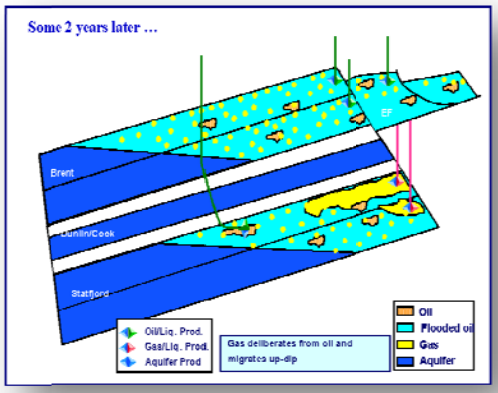

b) Gas starts to liberate from solution

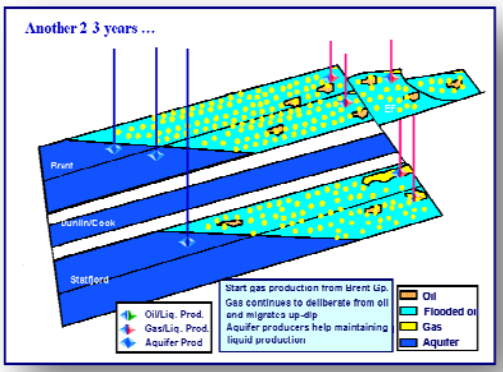

c) Brent Gp. becomes the main gas contributor

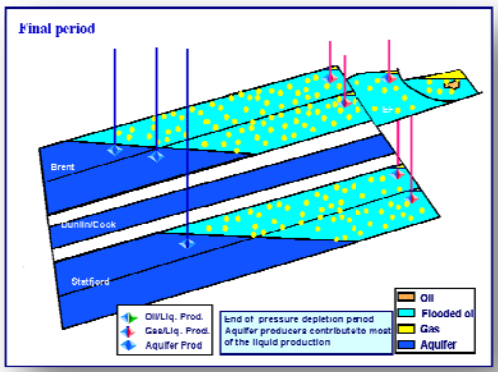

d) Aquifer producers maintain pressure depletion rate

Figure 2.6: SFLL Drainage Strategy [25].

3 Theory

3.1 Miscibility

Two phases are miscible if they can mix and form a homogenous mixture. Miscible fluids are soluble in oil so there will be no inter-facial force between the oil and the solvent, hence no interfacial tensions and capillarity either exists between the two fluids. Therefore the residual oil saturation can theoretical become zero in the case of miscible displacement. In contrast, immiscible fluids are fluids that do not mix physically or chemically, two phases that cannot mix to form a homogenous mixture. In a water flood or an immiscible gas flood, the displacing fluid is not soluble in the displaced oil. The displacement results in residual oil saturation due to the inter-facial forces between the displacing fluid and the displaced oil [4].

Reservoir temperature and pressure, the composition of the injected fluid and composition of the oil are four important factors which influence the degree of miscibility. To achieve miscible conditions between the oil and the injected fluid a certain pressure for a given temperature must prevail, which is defined as minimum miscibility pressure (MMP). Both pressure control of the reservoir and control over the intermediate composition of the injected gas must be preformed to achieve controlled miscible drive operations [2].

3.1 Relative permeability

Relative permeability relates the effective permeability with the absolute permeability. When a fluid occupies only a fraction of the total pore volume, effective permeability must be used. Relative permeability is defined as effective permeability divided by the absolute permeability.

$$k_{rl} = \frac{k_l}{k}, l = o, g, w \qquad [3.1]$$

where

k_{rl} : Relative permeability
k_l : Effective permeability
k : Absolute permeability

Even though relative permeability depends on the structure of the porous medium it is common to assume that relative permeability only is a function of the saturation distribution. With this assumption it becomes simpler to determine the relative permeability with experimental work. Most often two-phase systems are used. In a water/oil system relative permeability of water and of oil are measured as functions of water saturation, while in an oil/gas system the relative permeabilities of oil and gas are determined from the gas saturation. Figure 3.1 illustrates the phase relative permeability dependence on saturation in two-phase oil/water and gas/oil systems. The endpoints S_{wr}, S_{owr}, S_{gr} and S_{ogr} are of critical importance. S_{wr} is the critical water saturation. S_{owr} is the critical oil saturation in the oil/water system. S_{gr} is the critical gas saturation and S_{ogr} is the critical oil saturation in the oil/gas system. The four curves in Figure 3.1 will be the relative permeability input to a simulator, k_{rw}, k_{row}, k_{rg} and k_{rog}.

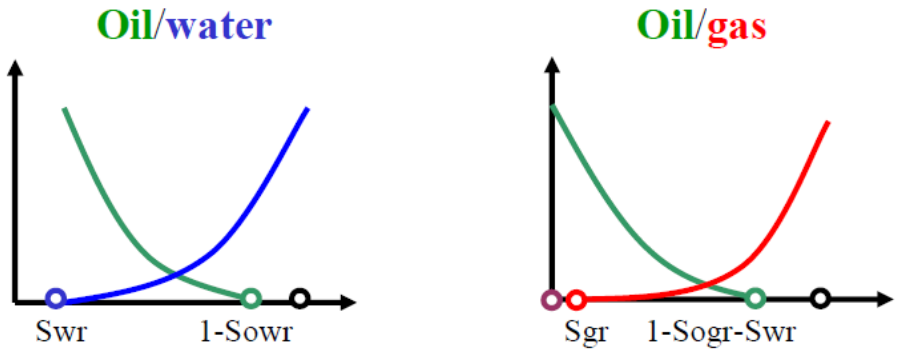

Figure 3.1: Two-phase relative permeability data [17].

Three phase relative permeabilities are required if water, oil and gas flow simultaneously in a reservoir. The relative permeabilities k_{rw}, k_{row}, k_{rg} and k_{rog}, are obtained similarly as for the two-phase measurements, while the relative permeability of oil, k_{ro}, is a function for S_w and S_g. K_{ro} can be constructed using the curves measured in two-phase systems [17].

Generally, the relative permeability values are normalized prior to scaling. With normalization both saturation and relative permeability end points are 0 or 1. Figure 3.2 illustrates how this is done using the normalized saturations

$$S'_w = \frac{S_w - S_{wr}}{1 - S_{wr}} \quad [3.2]$$

$$S''_w = \frac{S_w - S_{wr}}{1 - S_{wr} - S_{owr}} \quad [3.3]$$

With resulting normalized relative permeabilities $k^t_{rw} = k^t_{rw}(S'_w)$ and $k^t_{row} = k^t_{row}(S''_w)$.

If normalizes saturation functions have been input to the model, the curves may be scaled by varying S_{wr}, S_{gr}, S_{owr}, S_{ogr} and by specifying new end point relative permeabilities such as

KRW = $k_{rw,max}$

KRG = $k_{rg,max} = k_{rg}\,(1 - S_{wr})$

KRO = $k_{ro,max} = \begin{cases} K_{row}(S_{wr}) \\ k_{rog}(0) \end{cases}$

The actual and normalized relative permeabilities are then related through

$$k_{rw}(S_w) = KRW \cdot k^t_{rw}(S'_w)$$

$$k_{row}(S_w) = KRO \cdot k^t_{row}(S''_w)$$

Figure 3.2: Normalization of relative permeabilities and saturations using eqs. 3.2 and 3.3 [17].

3.2 Mobility

Mobility, λ, is a measure of the ability of a fluid to move through interconnected pore space. It can be calculated as the ratio between permeability, k, and viscosity, μ:

$$\lambda_l = \frac{k_l}{\mu_l} = \frac{k_{rl}k}{\mu_l} \qquad l = w, o, g \tag{3.4}$$

The mobility ratio can be found by dividing displacing phase mobility to displaced phase mobility:

$$M = \frac{\lambda_{\text{displacing phase}}}{\lambda_{\text{displaced phase}}} \tag{3.5}$$

If M = 1 the two phases flows at equal velocities resulting in a piston-like displacement. M < 1 indicates that there is a stable displacement. M > 1 is an unfavorable mobility ratio and will make the displacement unstable.

When describing a miscible displacement process, mobility and mobility ratio are some of the most important parameters. Waterflooding performance in multi-layered composite linear reservoirs is mainly controlled by the mobility ratio [3].

3.3 Transmissibility

Having a fluid flow through porous media, transmissibility is defined as [9]:

$$T = \frac{\beta_c k A}{\mu \Delta L} \quad [3.6]$$

The transmissibility may be included in Darcy's law for horizontal flow through porous media:

$$q = \frac{\beta_c k A}{\mu} \frac{\Delta P}{\Delta L} = T\, \Delta P \quad [3.7]$$

where :

T : transmissibility
q: flow rate
β_c: transmissibility conversion factor
k: permeability
A: cross-sectional area
μ: viscosity
ΔL: segment length
ΔP: pressure difference

The reservoir is divided into grid blocks where each block is assign given values such as permeability, porosity and saturation. No variations of the assigned values are allowed for in a given grid block. The block permeability does not say how easy fluid will flow between different blocks, therefore transmissibility is introduced. Transmissibility describes the communication that occurs between the grid blocks. Transmissibility is a function of permeabilities and is defined so that $T_x(I)$ is between blocks I and (I+1) as shown in Figure 3.3.

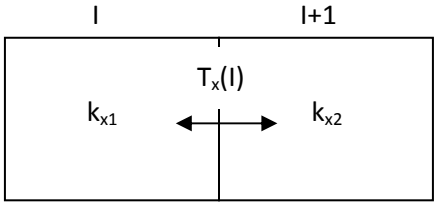

Figure 3.3: Transmissibility in x-direction between two grid blocks.

3.4 Dominating Force (Viscous & Gravitational)

Viscous forces are governed by the viscosity-ratio, VR:

$$VR = \frac{\mu_{displacing\ fluid}}{\mu_{displaced\ fluid}} \quad [3.8]$$

Gravitational forces are measured by the gravity reference rate, GRR:

$$GRR = \frac{\kappa_l A}{\mu_l} \cdot g \cdot \Delta\rho \cdot sin\theta \quad [3.9]$$

where:

K_l: effective permeability to a liquid at 100% liquid saturation
μ_l: viscosity of oil for a gas/oil system and the viscosity of water for a water/gas system
ρ: density

Dandona and Morse [1] have concluded that when flooding at rates above the gas-oil GRR, oil displacement by gas becomes unstable and ineffective. Water flooding through a gas cap will yield higher oil recoveries than gas flooding under these conditions. Under stable conditions, down-dip gas flood may recover more oil than a water flood when gas is present.

The gravity reference rate refers to the maximum rate of gravity drainage. Injection rate divided by the GRR should give a measure of the dominance of forces, increasing when viscous forces increase. Viscous forces tend to be dominating compared to gravitational forces when the viscosity-ratio increases. This causes a piston-like displacement effect. If the viscous-ratio is decreasing, the gravitational forces dominate and tonguing tends to occur.

The viscous- to gravity force ratio can be defined as:

$$F_{vg} = \frac{u_w \mu_g L}{\kappa \Delta\rho g H} \quad [3.10]$$

where:

L: total length of the linear reservoir model
H: total height/thickness of the flow model
κ: permeability in the flow direction
u_w: velocity of injected water

This definition is modified to cover the case where water is injected in the gas cap, displacing the gas if rates are high enough [20].

As the viscous- to gravity force ratio increases, the viscous force becomes more dominant for the flow. Low values for the ratio indicates gravitational dominance.

3.5 Viscous Fingering

Viscous fingering is when a more viscous fluid is unstably displaced by a less viscous fluid. As the low viscosity fluid moves through the more viscous fluid it will begin to form fingers. This phenomenon can influence reservoir flow behavior and have an unfavorable impact on recovery. Having a homogeneous medium, the fingers often display a symmetric pattern. The symmetry can however be lost if there is

some heterogeneity in the system. In addition to a reservoir heterogeneity problem, fingering can also be a fluid displacement problem. Most reservoir simulators do not accurately model fingering effects. By using a very fine grid to cover the area of interest, the model accuracy can be approved. The benefits associated with such a grid are seldom sufficient to justify the additional cost [10].

3.6 Hysteresis

Hysteresis [5] is when the effects of an input into a system are experienced with a certain delay in time. For reservoir simulation, a hysteresis effect in both capillary pressure and relative permeability occurs when there is a reversal in the direction of saturation change.

For reservoir rocks with a wettability preference for a specific phase, a change from a drainage to imbibitions process causes the nonwetting phase to be trapped by the wetting phase. This entrapment of the nonwetting phase results in hysteresis of the relative permeability to this phase. Relative permeability hysteresis will increase the stability of the injected water-gas mixture in a WAG process.

Capillary pressure hysteresis can be caused by pore structure effects or contact angle hysteresis. Contact angle hysteresis is the difference between the advancing and receding contact angles between two phases. (Advancing contact angle is measured as the contact angle when volume is added to the maximum before the interfacial area increases. Receding contact angle is measured when the maximum fluid volume is removed from the drop without the interfacial area decreasing.)

4 Gas cap water injection

Water injection in the gas cap allows for pressure maintenance while at the same time avoiding a rise of the oil-water contact. Water injection downflank would obviously result in a much more rapid rise of the OWC. Production wells can thus continue producing from the same zones. With a lack of gas to inject, water injection provides an alternative.

It also turns out that injection of water in a gas cap is considerably more stable than water injection in an oil zone. This is due to the high mobility of gas, giving a much lower mobility ratio with water injection in gas. When injecting in oil, water has a stronger tendency to finger in layers with high permeability. Figure 4.1 presents a comparison of upflank water injection in oil (left) and in a gas cap, illustrating how injection in a gas cap is more stable than in the case of an oil zone, where the water moves faster through a high permeability channel [14].

Experience with upflank water injection is limited.

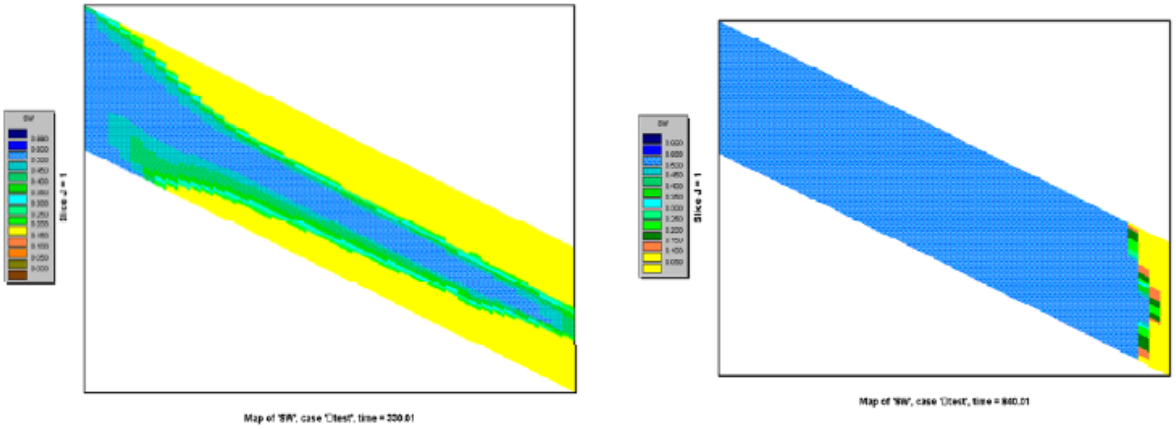

Figure 4.1: Comparison of water-oil and water-gas displacement[14].

4.1 IOR potential with upflank GCWI in Upper Statfjord

Because less gas was available for injection, studies were initiated to look into alternative methods for pressure maintenance. The potential of using GCWI was assessed by Hegre et al. in 1994 by developing a refined element model. Only SFA was considered since 4 of the then 8 gas injectors were in the SFA area. This allows flexible gas injection while some injectors were used for water injection. The element model was used to compare different production scenarios. The alternatives considered [11]:

- Reference case
- WAG injection
- Gas cap water injection, supplemented by WAG injection

Figure 4.2 and 4.3 shows the simulated oil production rate and cumulative oil production for these three cases, respectively.

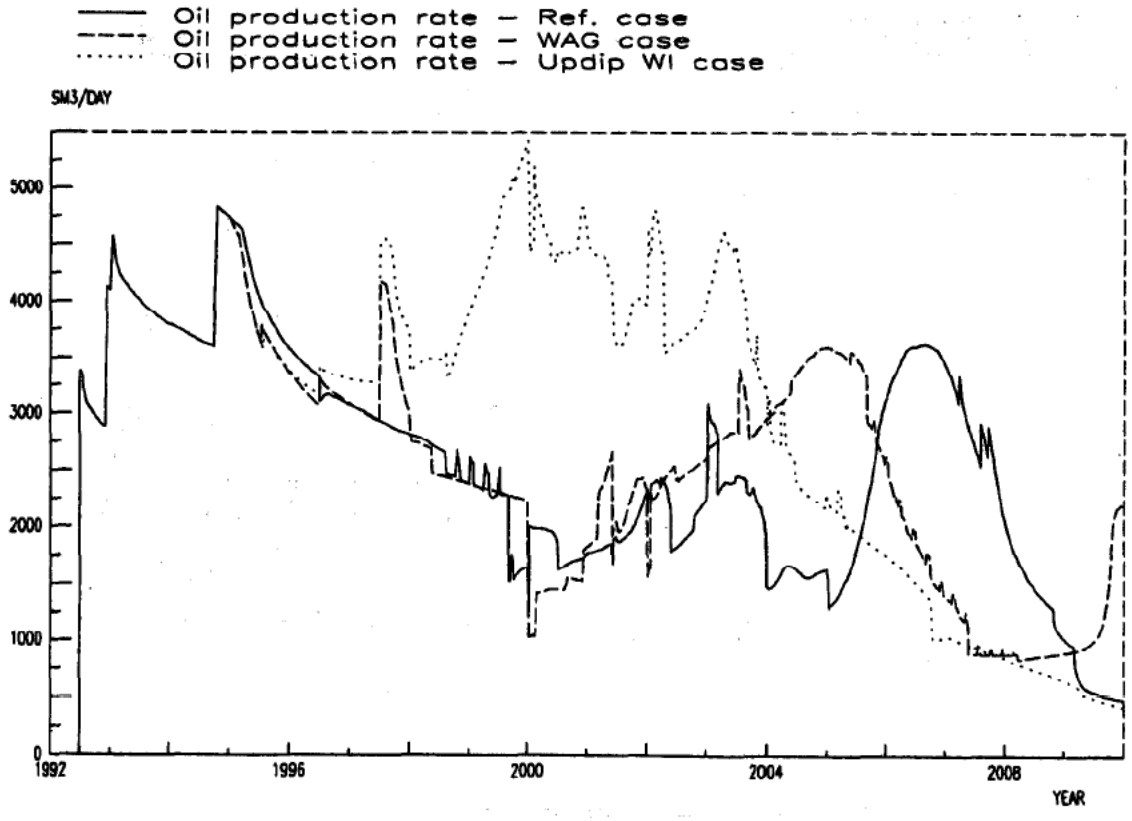

Figure 4.2: Oil production rates for reference case, upflank WAG and upflank WI [11].

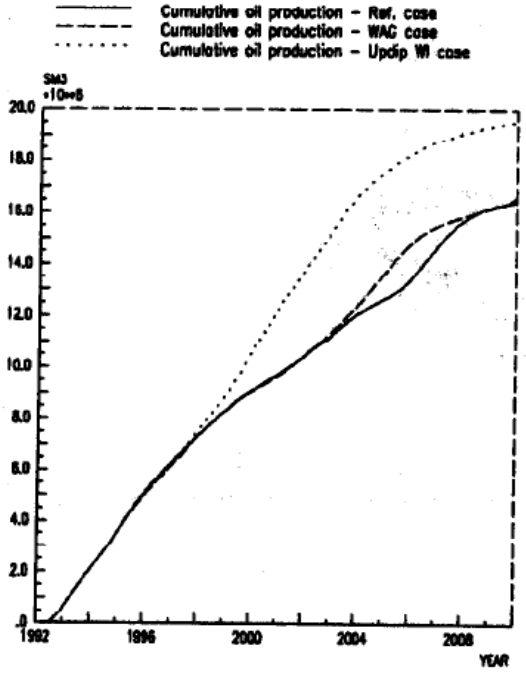

Figure 4.3: Cumulative oil production for reference case, upflank WAG and upflank WI [11].

Two other scenarios were also considered:

- Pressure maintenance by (continued) gas injection
    - Results showed less oil production compared to upflank WAG/GCWI injection, making it less favorable.
- Supplementing gas injection with downflank water injection
    - Results indicated higher cumulative oil production compared to the upflank WAG/GCWI cases, but not enough to justify the added cost of drilling additional downflank water injectors.

Upflank water injection was chosen in the Statfjord Fm for the following reasons:

- Less gas available for injection, implying that water injection was necessary for pressure maintenance (keeping reservoir pressure above the gas-oil miscibility pressure).
- Using less gas in Statfjord Fm allows for some gas to be used for WAG injection in Brent.
- Existing upflank gas injectors could also be used for water injection.
- Reservoir simulations indicating accelerated and increased recovery of about 5%, better sweep and less problems with gas production constraints.

This was done only in Upper Statfjord because most of the gas injected until 1994 went into Upper Statfjord. Due to a field-wide barrier between Upper and Lower Statfjord, most of the injected water would remain in Upper Statfjord, but with some uncertainty around major faults.

The revised drainage strategy was also implemented in the Full Field Simulation (FFM) model, including downflank WAG injection in Lower Statfjord. Results from FFM confirmed the results from the element model. FFM showed an improved oil recovery of 8%. Sensitivity analysis was also performed on selected parameters, and did not indicate any particular disadvantages with GCWI [11].

4.2 Experience from upflank GCWI in Upper Statfjord

Gas cap water injection in Statfjord was successful in the sense that the gas cap contains much of the injected water, displacing the oil in the lowermost parts of Eiriksson. That said, the success of the strategy also depends on production well coverage and flexibility of injection points and phase.

The upflank movement of the OWC was considerably reduced with upflank WI, as expected. However, GCWI does not represent a stable process, and water has eventually reached the aquifer, resulting in a rise in the OWC and drowning of some producers. Injector A-3A shows the best result, due to it being located structurally high with faults and large volumes of gas separating it from the the downflank producers. Figure 4.4 shows simulation results that illustrate water movement around A-3A at different times. In general, oil recovery has been improved because oil was pushed towards the wedge zone producers [6].

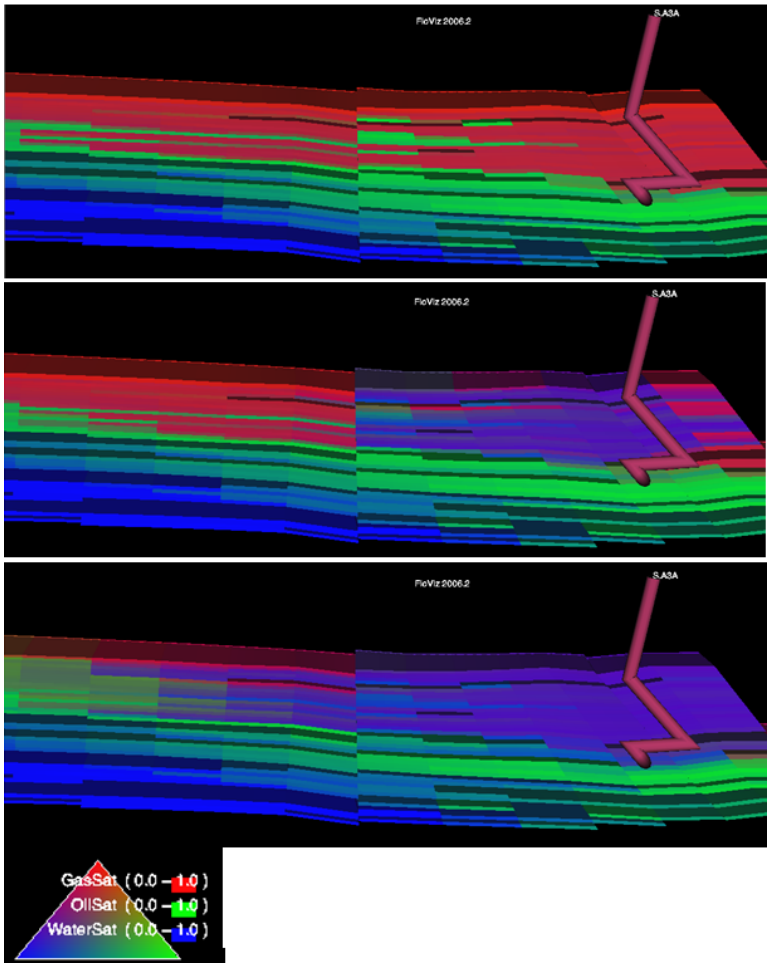

Figure 4.4: Illustration of the water-gas displacement from injector A-3A US (1996-1998-2000).

Downsides of GCWI:

- Uncertainties regarding the locations of oil and gas, making well planning difficult. It has been difficult to predict the movement of injected water.
    - Some drilled wells where it was expected to find oil turned out to be without oil, e.g. A-40D and A-18C.
- Gas is trapped in upflank water, only parts of which will be recovered when pressure is drawn down during SFLL. The amount of water in the gas cap is uncertain, including how fast released gas can be produced.

If enough gas had been available for injection, the movement of the different phases would have been easier to control. It is generally agreed that GCWI was necessary and the only option for keeping the voidage at an acceptable level. Voidage replacement is considered more important than which phase to inject [6].

5 Reservoir simulation

Reservoir simulation is one of the most powerful tools available to a reservoir engineer and has become the standard for solving reservoir engineering problems. It is a tool made to predict performance under various operating strategies by combining physics, mathematics, reservoir engineering and computer programming. The reservoir simulation software enables building of models that predict the movement of oil and gas flowing in the reservoirs under the surface of the earth. Some advantages and disadvantages are given in the following table:

Advantages of Reservoir Simulation	Disadvantages of Reservoir Simulation
The analytical limitations of simpler methods are overcome	Modeling requires a significant amount of reasonable data
Data variation within a reservoir can be applied; homogeneity is not a requirement	Modeling requires a significant amount of knowledgeable manpower and time
The effect of uncertainty in the reservoir description can be analyzed with sensitivity testing	Results are not unique, i.e. the same answer can be obtained by varying several different parameters
After matching history, many different methods of operating the reservoir in the future can be investigated and an optimum plan of reservoir management can be formulated	Simulation has limitations that a casual user/observer may not fully comprehend
Continual performance monitoring is available	
The computational burden is reduced for the engineer and additional time is available for analyzing results	Software/hardware costs are greater than analytical methods
A common tool is employed in arbitration and unitization decisions	

Table 5.1: Advantages and disadvantages of reservoir simulation[18].

5.1 Model input data

To be able to perform reservoir simulations, enormous amounts of input data are required. The table below shows the properties needed, and how the properties can be found.

Property	Sources
Permeability	Pressure transient testing, core analyses, correlations, well performance
Porosity, Rock compressibility	Core analyses, Well logs
Saturations	Well logs, core analyses pressure cores, single-well tracer test
Relative permeability and capillary pressure	Laboratory core flow test
Fluid property (PVT) data	Laboratory analyses of reservoir fluid samples
Faults, boundaries, fluid contacts	Sesmic, pressure transient testing
Aquifers	Seismic, material balance calculations, regional exploration studies
Fracture spacing, orientation, connectivity	Core analyses, well logs, seismic, pressure transient tests, interference testing, wellbore performance
Rate and pressure data, completion and workover data	Field performance history

Table 5.2: Data required for a simulation study and sources[10].

Because the input data exhibits strong heterogeneities the reservoir must be divided into grid blocks to be able to simulate the variations. Especially petrophysical data like permeability and porosity exhibits strong heterogeneities. The grid is also needed for numerical computations [17].

5.2 Black-Oil models

The simplest and most commonly used model for reservoir simulation is the Black-Oil model. This is the model used for reservoir simulations of the Statfjord Field.

The Black- Oil model is based on six assumptions [17]:

- There are three phases in the reservoir; oil, gas and water
- There are three components; oil, gas and water
- No phase transfer between water and hydrocarbons take place
- A part of the gas component can be dissolved in oil and flow together with the oil component in an oil phase
- The oil component cannot exist in gas phase, which means that all of the oil component is in oil phase
- The temperature in the reservoir is constant

The notation black-oil for oil components can be used to distinguish oil component from oil phase. This is done to avoid confusion when gas is dissolved in oil and flows together with the oil component in the oil phase. This is demonstrated in figure 5.1 that shows that when the oil phase from the reservoir is produced, it is split into one oil component and one gas component. It can therefore be concluded that some of the gas component has been dissolved in the oil phase in the reservoir.

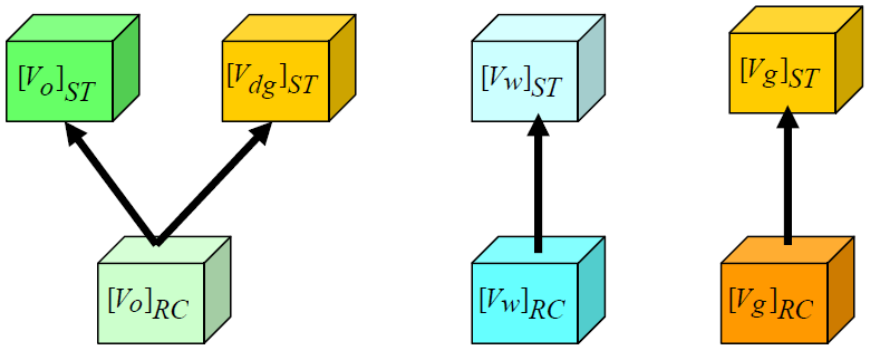

Figure 5.1 Fluid at reservoir conditions and standard conditions [17].

From the above assumptions and the three-phase Darcy's law, the Black-Oil mass balance equations can be given as follows:

Water:

$$\nabla \cdot \left[\frac{[k]k_{rw}}{\mu_w B_w}(\nabla p_w - \gamma_w \nabla d)\right] + Q_w = \frac{\partial}{\partial t}\left(\varphi \frac{S_w}{B_w}\right) \quad [5.1]$$

Oil:

$$\nabla \cdot \left[\frac{[k]k_{ro}}{\mu_o B_o}(\nabla p_o - \gamma_o \nabla d)\right] + Q_o = \frac{\partial}{\partial t}\left(\varphi \frac{S_o}{B_o}\right) \quad [5.2]$$

Gas:

$$\nabla \cdot \left[\frac{[k]k_{rg}}{\mu_g B_g}(\nabla p_g - \gamma_g \nabla d)\right] + \left[\frac{[k]k_{ro}R_s}{\mu_o B_o}(\nabla p_o - \gamma_o \nabla d)\right] + Q_g = \frac{\partial}{\partial t}\left(\varphi \frac{S_g}{B_g} + \varphi \frac{R_s S_o}{B_o}\right) \quad [5.3]$$

where:

[k]: permeability
k_r: relative permeability
μ: viscosity
B: volume factor
p: phase pressure
γ: g·ρ, where ρ is the phase density
d: vertical distance for a reference level to a point
Q: q/ρ^s, where q is the flow rate and ρ^s is the density at standard conditions
φ: porosity
S: saturation

The sub notes w,o and g represent water, oil and gas respectively.

In the above equations, the phase pressures and the saturations are the unknowns that need to be determined from simulation. They are determined based on position and time. Once the pressures and saturations are determined, the flow parameters can be found from the above given mass balance equations and three additional equations. These three equations are called constraint equations, and are given as follows:

Capillary pressure oil/water:

$$P_{cow}(S_w) = p_o - p_w \quad [5.4]$$

Capillary pressure gas/water:

$$P_{cgo}(S_g) = p_g - p_o \quad [5.5]$$

Saturation equation:

$$S_w + S_o + S_g = 1 \quad [5.6]$$

There are now six unknowns and six equations. Two pressures and one saturation are eliminated by the three constraint equations. The three mass balance equations can then be used to determine the remaining unknowns [17].

5.3 History matching

To be able to predict the future field performance, the reservoir model must be able to reproduce the field history. A history match is therefore performed in order to make the numerical data fit the observed historical field data. The main goal of the history matching process is to improve predictability of the numerical model and to reduce uncertainty in the predictions.

History matching is done by changing uncertain fluid and reservoir parameters to make them better fit the field of interest. There are several paths and changes that can be performed in the reservoir simulation model that will lead to a representable solution. Consequently, a history match is not unique and there may be reservoir parameters that are not tested by a history match. This is why it is very important to have a best possible geomodel as a fundament for the matching process. Thorough evaluation of seismic, well, and field data should be the base for the geomodel. The model should be consistent with observed production data.

History matching is done through trial and failure to minimize the error. There is no well defined procedure for history matching, but trends can be established during the process. Some points that can be used to help perform a history match are [13]:

- Define the objectives of the study, and the expected and product
- Familiarize with field and well performance
- Match the overall reservoir energy level
- Match gas/oil ratio, water-cut performance and pressure (WFT and BHP) for individual wells

- Match the tubing head pressure to assure a smooth transition from history mode to prediction mode

Input parameters frequently altered in a history matching procedure are [17]:

- Absolute permeability
- Aquifer size and transmissibility
- Transmissibility reduction across faults
- Relative permeability and capillary pressure curves
- Porosity and rock compressibility

During the history matching procedure, a clear strategy must be followed and only one parameter should be changed at a time. A perfect match cannot be expected. A general comment has been made that " a good history match is obtained when you run out of time or money" [17].

5.4 Forecasting future performance

When the history matching is done, prediction runs needs to be performed. During the change from history mode to prediction mode, the model must switch smoothly without marked discontinuities in well capacities.

Predictions help visualize future performance of the reservoir for different operating strategies. A variety of scenarios can be explored and the strategy with the most desirable performance can then be chosen. From prediction runs, types of performance predictions that may be generated include [17]:

- Oil production rates
- WOR and GOR performance
- Reservoir pressure performance
- Well pressure performance
- Position of fluid fronts
- Recovery efficiency by area
- Information concerning facility requirements
- Estimated ultimate recovery

6 Reservoir Simulators

Reservoir simulators are referred to a computer program that is written to solve the equations for flow of fluids in a reservoir. The reservoir simulator begins with reading the applied input data and then initializing the reservoir. Information for time dependent data is then read, which includes well and field control data. An iteration process between calculated flow coefficients and unknown variables is performed, which can improve the material balance. When a satisfied solution to the iterative process is complete, flow properties are updated and output files created before the next time step calculations begins[10]. The simulator can give predictions on future reservoir performance, and can therefore be used to find the optimal recovery mechanism for future production.

6.1 ECLIPSE

ECLIPSE is a reservoir simulator which solves the mass balance equations by numerical methods for approximating the solutions to the differential equations. The program is owned by Schlumberger Information Solutions. ECLIPSE software covers all the different reservoir models, specializing in blackoil, compositional and thermal reservoir simulation. Providing fast and accurate prediction of dynamic behavior of the reservoir makes ECLIPSE the industry's most robust reservoir engineering software[23].

ECLIPSE comes in two main versions:

- ECLIPSE 100 solves the Black Oil model on corner-point grids.
- ECLIPSE 300 solves compositional and thermal models.

ECLIPSE 100 is used as the reservoir simulator in this study. It is a fully-implicit, three phase, 3D, general purpose black oil simulator with gas condensate options. Both gas dissolving in oil and oil vaporizing in gas can be simulating using ECLIPSE 100. Hysteresis can also be modeled in the simulation, both relperm and capillary pressure hysteresis. Also an alternative three phase hysteresis model is available for processes where all three phases are present simultaneously[21].

6.1.1 Structure of ECLIPSE data input file

An ECLIPSE data input file is split into sections, where each section is introduced by a keyword. The sections must come in a certain order, where some sections are required while some can be optional. An overview of the sections in specified order are shown [21]:

RUNSPEC

The first section, runspec, contains the run title, start date, units, numbers of blocks, wells, tables, flags for phases or components present and option switches.

GRID

The grid section determines the basic geometry of the simulation grid and various rock properties, like porosity, absolute permeability, net-to-gross ratios, in each grid cell. From these input data the grid block pore volumes, mid-point depths and inter-block transmissibilities are calculated.

EDIT

The edit section contains instructions for modifying the parameters computed in the grid section, and is of course optional.

PROPS

The props section of the input data contains pressure and saturation dependent properties of the reservoir fluids and rocks.

REGIONS

The section regions is optional and splits computational grid into regions for calculation of PVT properties, saturation properties, initial conditions and fluids in place. If the section is omitted all grid blocks are put in one region.

SOLUTION

The solution section contains sufficient data to define the initial state (pressure, saturations, and compositions) of every grid block in the reservoir.

SUMMARY

The summary section is optional and it specifies a number of variables that are to be written to Summary files after each time step. The results can be plotted graphically.

SCHEDULE

The schedule section specifies the operations to be simulated, like production and injection controls and constraints. Also specifies the times at which output reports are required. Vertical flow performance curves and simulator tuning parameters may also be specified in the schedule section.

The body of sections that are not frequently changed are often held in separate files, which is included in the data file using the INCLUDE keyword. Two examples are shown to illustrate the use of the keyword INCLUDE. The first example is from the grid section, where different faults are included. Note that a line that starts with '--` is only a comment line and is not read by the simulator. The other example shows that the history file of the reservoir is included in the section schedule.

```
---------------------- GRID SECTION ----------------------
GRID

INCLUDE
 '/project/stf2007-1/FFM2005/STATFJORD/INCLUDE_RUM/GRID/25107_BASE4.FAULTS' /
```

```
---------------------- SCHEDULE SECTION ----------------------
SCHEDULE
INCLUDE
'sf_hist_100223_V1_1.sch' /
```

As mentioned every section is introduced with a specified keyword, also input data and program options are specified using keywords. Some keywords may occur in any section of the input file, while most of the keywords can only be used in specific sections. The data for a keyword follows after the keyword on a new line and is terminated with a slash. Text or data written after a slash will be read as a comment. Two examples are shown to illustrate the use of keywords:

```
639.000000 days from start of simulation ( 1 'NOV' 1979 )
DATES
 1 'AUG' 1981 /
/

WCONHIST
    'S.A12'      'OPEN'      'ORAT'   4026.646      0.000 651054.625  5* /
    'S.A33'      'OPEN'      'ORAT'   2824.645    142.290 441521.906  5* /
    'S.A38'      'OPEN'      'ORAT'   2655.323    193.677 411814.031  5* /
     'S.A7'      'OPEN'      'ORAT'   1689.484     73.452 259358.672  5* /
/

WCONINJE
    'S.A29'       'GAS'  1*      'RATE' 1676366.250  5* /
    'S.A3A'       'GAS'  1*      'RATE' 1519418.875  5* /
    'S.A42'       'GAS'  1*      'RATE' 1378664.375  5* /
/


Hysteresis input
EHYSTR
   0.1   0  0.1 1* KR /


COPY
 'SWCR'  'ISWCR'    1 65 1 262 1 46 /
 'SGU'   'ISGU'                     /
 'ISWCR'   'ISWL'   1 65 1 262 1 46 / hysteresis water saturations
 'SWU'   'ISWU'                      /
 'SGL'   'ISGL'                      / hysteresis gas saturations
 'SOGCR' 'ISOGCR'                    / hysteresis oil saturations
 'SOWCR' 'ISOWCR'                    /
 /
```

6.2 Software used for viewing the simulation results

6.2.1 FLOVIZ

Simulation model data can be displayed in FLOVIZ, which provides a 3D visualization of the reservoir. FLOVIZ has been designed to interface efficiently with the ECLIPSE reservoir simulators. Grid blocks and well locations are visualized, and the camera angle can be altered horizontally or vertically and a full 360

degree rotation can be animated. A comprehensive and flexible IJK Slicer panel makes it possible to view the different layers and grid cells. Different properties can be shown and are represented by coloring the grid blocks. Both initial and recurrent properties can be viewed. FLOVIZ also provides a time animation of the model, which allows us to view the recurrent properties for different times in the simulation[22].

In the process of history matching of the Statfjord Fm model, FLOVIZ was used extensively to track the injected water at different time step. Figures from FLOVIZ are given throughout the thesis.

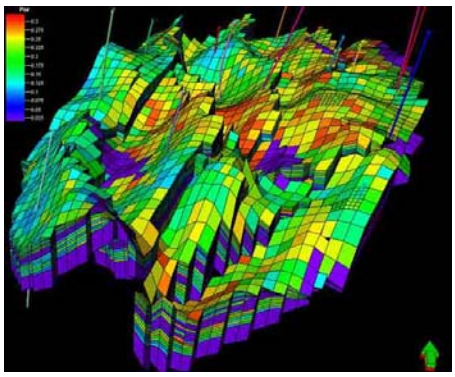

Figure 6.1: 3D Simulation model[23].

6.2.2 S3GRAF

S_3graf is a program that makes it possible to plot the simulation results. Observed data can also be plotted in the program, which makes it possible to compare the data with the simulation data. It can be very helpful and necessary to plot the parameters of interest versus ex. time. Showing the data in graphical form gives a quick, but credible way of making qualitative statements concerning the result of the simulations.

S_3graf was extensively used to compare observed seawater cut with simulated sea water cut versus time for different wells. The plots made it quick and easy to see how the history matching of the sea water cut changed during different simulation runs. A standard input file for S_3graf was made to make it easy to make new plots for the different simulation runs. The section “variables” was the only section that had to be modified for new plots. This section is shown below. Plots made in S_3graf to analyze results are given throughout the thesis.

```
------------------------------------------------------------
-- SEA WATER TRACER, COMPARISON OF SIMULATION AND OBSERVATIONS

-- Works only in S3Graf
------------------------------------------------------------

------------------------------------------------------------
-- Variables
------------------------------------------------------------
INCLUDE variables-statfjord.INC

ASSIGN NAME1%     =     V1
ASSIGN NAME2%     =     V2
```

```
ASSIGN FOLDER1%    =      HIST_STATFJORD_V1
ASSIGN FOLDER2%    =      HIST_STATFJORD_V2
ASSIGN RUN1%       =      STATFJORD_TR_BASE_V1
ASSIGN RUN2%       =      STATFJORD_TR_BASE_V2
```

6.2.3 RESVIEW

RESVIEW has been developed by Roxar ASA and is used to display and process the result of simulations. Like FLOVIZ, RESVIEW provides a 3D visualization of the reservoir. RESVIEW also has the functions to rotate, slice, peel and to view time animation of the model. Reservoir simulation grids, initial and recurrent properties can be handled in RESVIEW [16]. The "viewer" is not easy to learn and is therefore not so much used as earlier. RESVIEW has mainly been used in this thesis to define different faults.

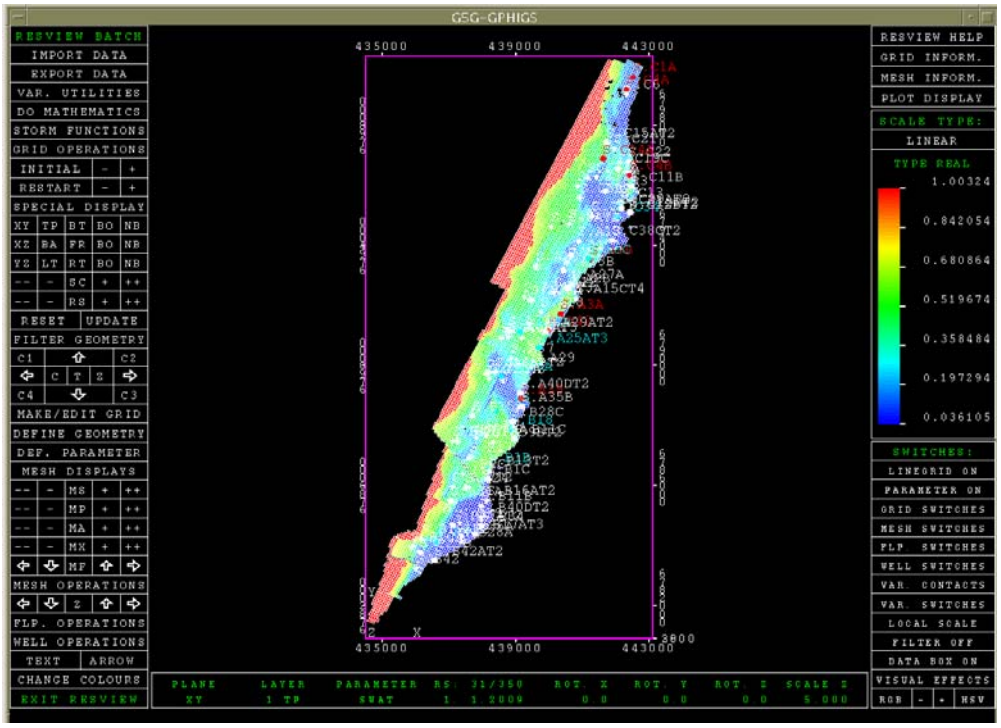

Figure 6.2: RESVIEW working window.

7 The Statfjord full field simulation model

The Statfjord field is 24 km long and has an average width of 4 km, which makes it the largest producing oil field in Europe. Because of the size, and the fact that it have produced from multiple mechanisms including gas injection, upflank gas cap water injection, WAG injection for pressure maintenance, a full-field model (FFM) is necessary to answer many depletion planning questions and to evaluate the benefits of large scale or field wide projects. In 2007 a new drainage strategy was implemented to the Statfjord field, where the drainage strategy went from pressure maintenance to depressurization. The new drainage strategy made it even more important to have a reliable FFM to be able to further optimize and assess the reservoir development during the reservoir pressure drawdown.

The former FFM was based on work from 1996, and the updated simulation work indicated weaknesses in the interpretation. A new 3D seismic survey from 2002 formed the basis for making the new FFM2005 geomodels. The former FFM2003 models were not able to predict the oil production satisfactorily, it was found to be rather optimistic compared to updated field and well potential extrapolations. The new FFM was also intended to improve estimation of oil production, which however turned out to be difficult [13].

The overall FFM2005 project covers three main phases:

- Structural modeling
- Geocellullar sequence stratigraphic, facies and property modeling
- Numerical reservoir simulation, including both history matching and predictions

The Statfjord field consists of three main reservoirs, the Brent Gp, the Cook Fm, and the Statfjord Fm. As now communication exists between the main reservoirs, separate models have been created. One FFM for Brent Gp, and one FFM for the Statfjord Fm. A simulation model for the Cook reservoir was also created in 1996, but is currently not in use. The models can be run separately in ECLIPSE where they are implemented as Black Oil models. The Statfjord Fm model is further presented since it is the one considered in this study.

7.1 Statfjord Fm model

The geological model contains 96 layers. In the reservoir simulation model FFM2005 the Statfjord Fm was upscaled from the original 96 layers to 46 layers. A layer overview of both the reservoir simulation model FFM2005 and the geomodel are shown in Table 7.1.

Cartesian grids were constructed using a corner point geometry scheme with vertical displacement over faults. A 65 x 262 x 46 simulation grid was made, giving 783 380 grid blocks in the simulation model. 251 000 of the grid blocks are active. The lateral dimensions were the same as the full field geological grid, except that the vertical dimensions of the simulation grid was doubled. The cell dimensions are 75 x 75 x 3 m with the grid orientation parallel to the OWC to best reprocess the contact movement, and obtain flow perpendicular to grid [13]. The main grid characteristics are summarized in Table 7.2.

Lithostratigraphy		Lithostratigraphy Statfjord	Sequence Stratigraphy Statfjord	Geomodel FFM2005	Dynamic Reservoir Simulation Model FFM2005
STATFJORD	Nansen	Nansen	RUM_SF.11 Top	1-4	1-2
	Eiriksson	Eiriksson	RUM_SF.10 Top	5-39	3-19
			RUM_SF.9 Top		
			RUM_SF.8 Top		
	Raude	Raude 2	RUM_SF.8 Base	40-51	20-24
			RUM_SF.7 Top	52-63	25-30
			RUM_SF.6 Top	64-78	31-37
			RUM_SF.5 Top	79-88	38-42
		Raude 1	RUM_SF.4 Top	89-96	43-46
			RUM_SF.3 Top		
			RUM_SF.2 Top		

Table 7.1: Reservoir zonation and grid layer in the geomodel and simulation model.

Grid characteristics	
Grid dimension	65 x 262 x 46
Total grid cells	783 380
Active grid cells	251 000
Cell dimensions	75 x 75 x 3 m

Table 7.2: Simulation: Grid summary.

One of the dynamic model design criteria was a 24 hour turnaround for a history match run. ECLIPSE had to extrapolate PVT-properties beyond input, and thereby slowing down to unacceptable running times. The parallel option was therefore activated in the model to be able to run the model within acceptable runtime. The Statfjord Fm model runs in approximately six hours on four processors, were approximately equal amounts of CPU time are spent on each domain during the history match [13].

7.2 History matching of the Statfjord Fm model

To history match the Statfjord Fm reservoir simulation model, an iteration process was performed:

1. Global pressure matching, adjusting large scale parameters.
    - Aquifer tuning, vertical permeability, vertical communication between Upper and Lower Statfjord and resizing shale and fault transmissibility.
2. Individual well phase matching, adjusting local parameters.
    - Tuning local fault transmissibilities and implementation of local shales
    - Attempts to tune gas distribution with connection factor multipliers [13].

7.3 Match quality

For both the field and individual wells, the pressure match is considered good. The 100 bar pressure depletion and build up and the pressure difference between Eiriksson and Raude is captured by the model.

On a field level, the oil and gas match is good. Water production was harder to match due to water production in the early SFA wells. In addition, some parts of Raude gave too much water and the up flank water movement in SFB turned out to be difficult to control. North of Fault F11, attempts to match up flank water production were not successful. Wells here experience late water breakthrough and excessive water production later.

Hysteresis has been introduced to trap gas in water in upflank water injection, with a critical gas saturation set to 30% after water sweep.

Statfjord A

The oil and gas match is good in SFA. The water match is fairly good, but is missing the early water production, especially from A-38, A-33 and A-7. From 2003, water production is too low, mainly due to A-15 CT4, A-26 A, A-26 BT2, A-40 B and A-13 B.

Statfjord B

The oil and gas match is good also in SFB. Water production is too low in the period 1998 – 2001, mainly due to B-10 A and B-15. From 2002 – 2006, water production is too high, caused primarily by B-28 C, B-15 A, B-2 C, B-31 A and B-23 B.

Statfjord C

The production match for SFC is good overall [13].

History matching of the Statfjord Fm model is an ongoing process and changes are constantly performed to achieve a better match.

8 Tracing injected water

In the Statfjord Fm, the drainage strategy has changed from up-flank gas injection to up-flank water injection before entering into the Statfjord late life project. Having a good simulation model is important to get reliable predictions of the pressure depletion and gas production during the new drainage strategy. However, history matching of the simulation model has shown to be difficult due to the large number of wells and a complicated drainage pattern. In this study a sea water tracer has been introduced in the model to help understanding the drainage pattern and to improve the match between the simulation model and well observations. With some simple additions to the simulation model code, the model also calculates sea water concentration, production rates and cumulative production which are compared to true data. The up-flank water injection has a large impact on the gas production prediction, which makes it an important history matching parameter.

8.1 Tracers

A tracer is a fluid, radioactive compound or chemical dissolved in a fluid that is injected in a well with the intention of later producing it. Predicting how and where the fluids are moving in the reservoir can be done with knowledge of the amount injected and later produced. A lack of a breakthrough in a producer may indicate the presence of a fault that hinders the movement of the injected fluid. A quick breakthrough, on the other hand, may indicate the presence of a high permeability channel that results in fingering of the injected fluid.

An ideal water or gas tracer must meet two requirements:

- It must follow the path and velocity of the phase with which it is injected
- It must be easy to identify when produced

Gas tracers can be divided into:

- Inorganic gases (e.g. tritiad hydrogen, krypton-85, xenon-133
- Organic gases (e.g. methane, ethane, propane)

Tracers available for waterflooding can be divided into:

- Non-radioactive isotopes
- Radioactive molecules (e.g. tritated water (HTO), $14C^-$labelled thiocyanate ($S14CN^-$))
- Non-radioactive chemicals (e.g. thiocyanate (SCN^-), fluorinated bezoic acids)

8.2 Definition of water cut and sea water cut

Sea water cut is the main parameter used in this thesis to history match the Statfjord Fm simulation model with true data. Also water cut has been an important parameter. Definition of sea water cut and water cut is given below. Seen from the equations it is obvious that both sea water cut and water cut must be a number between zero and one.

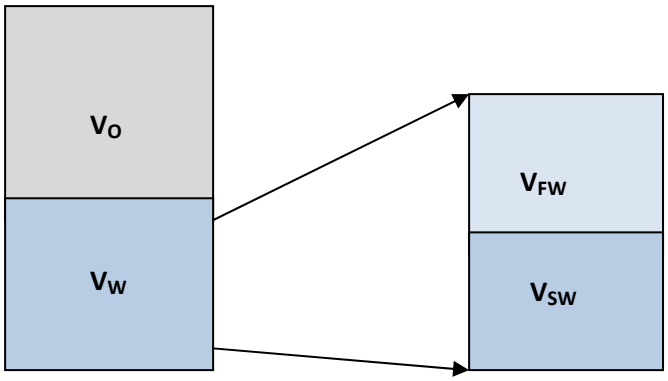

Figure 8.1: Illustration of stock tank fluids.

The water cut (WCT) is defined as the water fraction of produced liquid, oil and water:

$$WCT \overset{\text{def}}{=} \frac{V_W}{V_W + V_O} \quad [8.1]$$

where
V_W : Volume of produced water
V_O : Volume of produced oil

The seawater cut (SWC) is defined as the sea water fraction of produced water, sea water and formation water:

$$SWC \overset{\text{def}}{=} \frac{V_{SW}}{V_{SW} + V_{FW}} \quad [8.2]$$

where
V_{SW} : Volume of produced sea water
V_{FW} : Volume of produced formation water

Figures from FLOVIZ showing the sea water cut in the different grid blocks will be used. Therefore it is important to note the difference from sea water cut produced by a well and the sea water cut in a grid block. The same equation as for sea water cut can be used for sea water cut in a grid block. But SWC ≠ $SWC_{grid\ block}$ since a well most often produces from several grid blocks. SWC = $SWC_{grid\ block}$ only if a well produces from only that specific grid block.

$$SWC_{grid\ block} \overset{\text{def}}{=} \left(\frac{V_{SW}}{V_{SW} + V_{FW}}\right)_{\text{grid block}} \quad [8.3]$$

8.3 Natural water tracers

Water injection is a well used EOR method, where typical sea water is the source that is injected into the reservoir. Table 8.1 shows how the ion composition typically varies between sea water and the water originally present in the reservoir. The chemical and isotope signature of the sea water differs from formation water. This makes it possible to track the injected water by ion content that only exist in the injected water. These ions function as natural tracers.

Ion	FW [mg/l]	SW [mg/l]
Na^{2+}	8.640	11.150
K^{+}	190	420
Mg^{2+}	70	1.410
Ca^{2+}	300	435
Ba^{2+}	60	0
Sr^{2+}	50	7
Cl^{-}	14.300	20.310
SO_4^{2-}	0	2.800
HCO_3^{-}	1.100	150
HA_c (organic aids)	397	0
TDS (total dissolved solids)	25.107	36.675

Table 8.1: Typical ion composition of formation water and seawater[19].

The concentration of the ions found in the injected water can be affected by chemical reactions with the matrix or the reservoir formation water, and can therefore not be assumed to behave as ideal sea water tracers. On the other hand, hydrogen and oxygen isotope data are ideal sea water tracers. Hydrogen isotope data would be preferred to use, because they represent water itself and is also not much affected by diagenetic reactions in the sediments[8]. But, since isotope data are often not available, ion content can be used as natural tracer. Data on ion content are more likely to be available as they are often recorded, e.g. for formation damage surveillance. From a North Sea field case, Huseby et al. (2005) had geochemical information available from the field's producers, and showed that some of the ions behaved almost as ideal sea water tracers, i.e. without sorption to the matrix, ion exchange with the matrix or scale formation. The natural tracers available for the study were Ca^{2+}, SO_4^{2-}, K^{+}, Ba^{2+}, Sr^{2+}, Mg^{2+}, Sr^{2+}, and Cl^{-}. From cross-plots of pairs of the compounds, Ca^{2+}, Ba^{2+} and Sr^{2+} were found to be non-ideal tracers. Further, cross-plots of the ion concentrations in the produced water revealed that SO_4^{2-} was the best-suited sea water tracer in the investigated case[12].

Water samples from the Statfjord field are taken from a test separator. The test separator is used for many wells, therefore when a water sample is taken there might still be water left from the previous well. This might result in uncertainty in the measurement and care must be taken into account. Data from the water samples is stored in a database, and can be accessed from the software DBR or Prosty. The data was exported to excel, with columns for well name, sample date and concentrations for the different ions that were measured. The data also contained sea water cut measured from Mg^{2+} and SO_4^{2}, which was the two columns that were of interest for this thesis. Figure 8.2, illustrates the differences found from SWC based on sulphate and magnesium. A cross-plot was also made from the sea water cuts based on sulphate and magnesium. The plots where made to evaluate if these two ions could be used as natural tracers in this study. For that the two ions would be ideal tracers, the sea water fraction estimated from one ion should equal the fraction estimated from the other ion, also a cross-plot of the fractions should yield a straight line[12].

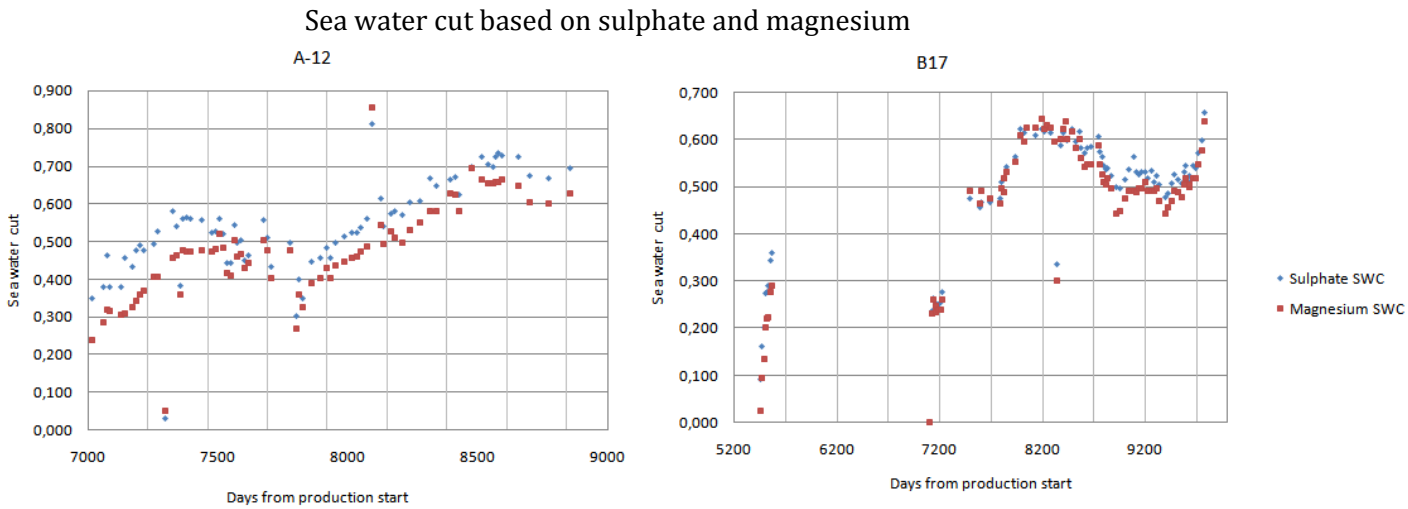

Figure 8.2: Comparison of SWC from sulphate and magnesium for well A12 and B17.

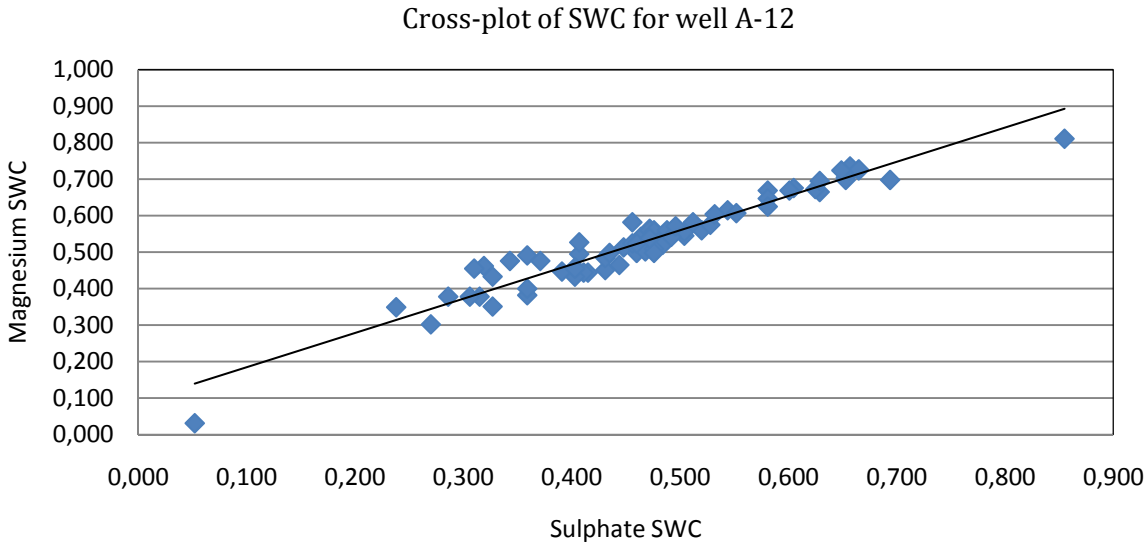

Figure 8.3: Cross-plot of SWC based on sulphate and magnesium for well A-12.

From Figure 8.2 one can see that some wells had a good match (B-17), while others had a noticeable deviation (A-12). The cross-plot in Figure 8.3 shows that for the well A-12 the fractions yield a straight line. The data was not expected to be more accurate. From this it was decided to use the average of the two sea water cuts to represent the sample sea water cut.

$$SWC = \frac{SWC_{SO_4^{2-}} + SWC_{Mg^{2+}}}{2} \quad [8.4]$$

Table 8.2 shows the data that were collected from the database and the calculated sea water cut.

Well	Sample date	Sample date (days)	SO4 Sw	Mg Sw	SO4 SWC	Mg SWC	SWC
A-01	20.11.1998 00:00	6959	1,100	5,800	0,011	0,058	0,035
A-02	20.04.1990 00:00	3823	5,200	1,400	0,052	0,014	0,033
A-02	27.04.1990 00:00	3830	3,900	1,500	0,039	0,015	0,027
:	:	:	:	:	:	:	:
:	:	:	:	:	:	:	:
B-19	08.05.1992 00:00	4572	55,700	48,700	0,557	0,487	0,522
B-19	15.05.1992 00:00	4579	58,000	50,300	0,580	0,503	0,542
B-19	24.05.1992 00:00	4588	56,900	50,100	0,569	0,501	0,535
:	:	:	:	:	:	:	:
C-42	17.12.2009 14:38	11005	86,900	87,100	0,869	0,871	0,870
C-42	01.01.2010 00:00	11019	109,500	82,300	1,000	0,823	0,912

Table 8.2: Calculated sea water cut for the different Statfjord Fm wells.

For simplicity we will assume that the initial concentrations of the ions, sulphate and magnesium, are zero in the formation water. This assumption was also made in the case by Huseby et al. (2005) [12], and is reasonable in view of the much smaller sulphate and magnesium content in the formation water compared to sea water.

8.4 Tracer tracking in the Simulation Model

The ECLIPSE Tracer Tracing option is a general facility to follow the movement of a “marked” fluid or fluid elements during a simulation run. Any fluid element can be considered as a tracer in the simulator, compared to ex. tracers that are added to the injected phase. The tracers in the simulator are to be regarded as passive. They will therefore not affect the PVT properties of the phase in which they are set in. The tracer concentrations are updated fully-implicitly at the end of each time-step after the oil, water and gas flows have been computed. In this study a water tracer has been implemented into the simulation. The tracer is set to trace the injected sea water.

8.5 Implementing sea water tracer in the simulation model

The Tracer Tracking option in Eclipse was used in this study to be able to trace the movement of the injected water in the Statfjord Fm. There is no sea water in the reservoir initially and therefore the concentration of the tracer is zero at start of the simulation. The history file is included under the section schedule, this file contains the production and injection history. To define what to be traced for the water tracer, the keyword WTRACER is used in the history file. The keyword sets tracer concentrations for the injection wells. When a well starts to inject water for the first time the keyword WTRACER is used to define that all water injected from the well is to be traced in the simulation. The concentration is therefore set to one. This is done for all the water injectors so the tracer tracks all the injected water. An example for the well B-8 is shown.

```
WCONINJE
    'S.B34'       'GAS'  1*      'RATE' 2965064.500  5* /
     'S.B8'     'WATER'  1*      'RATE'    934.935  5* /
/
WTRACER
      'S.B8'      SW    1     /
```

After defining sea water as the fluid to be traced, the tracer tracking function must be activated. This is done in the RUNSPEC section where the keyword TRACERS is used. The keyword represents the maximum tracers to be defined in water, oil and dry gas phase. The keyword TRACER is used in the PROPS section to define tracer name and which phase the tracer is associated with. As shown in the following one tracer is activated in the water phase and the tracer is named SW (sea water).

```
---------------------- RUNSPEC SECTION ----------------------
------ TRACER ------
TRACERS
--    Specification of number of tracers and solution scheme.
--    MAX-OIL-TR  MAX-WAT-TR  MAX-GAS-TR  MAX-ENV-TR  NUM-DIFF-CTRL
      0           1           0           0           *           /

---------------------- PROPS SECTION ----------------------
------ TRACER ------
TRACER
      SW    WAT   /
/
```

The keyword TBLK is used in the SOLUTION section, which specifies the initial concentration of the tracer in each grid block. The keyword TBLK must be followed by the letter F or S and then the name of the tracer which is being initialized. F stands for free state while S stands for solution state. All water tracers are in free state. Therefore, in this case the keyword becomes TBLKFSW. As mentioned there is no sea water in place in the reservoir initial and the concentration is set to zero in all 783 380 grid blocks. The keyword RPTSOL is also used in the SOLUTION section, where the list of mnemonics followed after the keyword controls the output of the data that are written to the print file. In the implementation TBLKSW is added to the list of mnemonics.

```
---------------------- SOLUTION SECTION ----------------------
RPTSOL
      RESTART=2 FIP=3 FIPRESV PRESSURE SOIL SWAT SGAS RS TBLKFSW  /

------ TRACER ------
TBLKFSW
      783380*0    /
```

As mentioned before the Summary section contains the keywords that define which variables that are to be written to the summary file. Different keywords are added to the SUMMARY section to include data outputs on field and well tracer production rates, cumulative tracer production, tracer production concentrations and tracer volume in the reservoir. The keywords are shown below. Note that F stands for field, W for well and G for group. The groups are SFA, SFB and SFC.

```
---------------------- SUMMARY SECTION ----------------------
------ TRACER ------
-- tracer production rate
FTPRSW
/
GTPRSW
/
WTPRSW
/
```

```
-- tracer production total
FTPTSW
/
GTPTSW
/
WTPTSW
/

-- tracer production concentration
FTPCSW
/
GTPCSW
/
WTPCSW
/

-- tracer in place
FTIPTSW
/
```

The ECLIPSE Tracer Tracking option allows up to 50 tracers to be defined in a single run. To define more than one tracer the same procedure as described above must be preformed for each tracer. An example where an additional tracer is added to trace the injected sea water from A-3A is shown:

The name of the tracer is defined to be SW1, and is only set to trace water injected fromA-3A.

```
WCONINJE
    'S.A39'       'GAS'  1*      'RATE' 312580.656  5* /
    'S.A3A'     'WATER'  1*      'RATE'      8.484  5* /
    'S.A42'       'GAS'  1*      'RATE' 482322.594  5* /
/

WTRACER
      'S.A3A'     SW    1     /
      'S.A3A'     SW1   1     /
/


---------------------- RUNSPEC SECTION ----------------------
------ TRACER ------
TRACERS
--    Specification of number of tracers and solution scheme.
--    MAX-OIL-TR  MAX-WAT-TR  MAX-GAS-TR  MAX-ENV-TR  NUM-DIFF-CTRL
      0           2           0           0           *           /

---------------------- PROPS SECTION ----------------------
------ TRACER ------
TRACER
      SW    WAT   /
      SW1   WAT   /
/

---------------------- SOLUTION SECTION ----------------------
RPTSOL
      RESTART=2 FIP=3 FIPRESV PRESSURE SOIL SWAT SGAS RS TBLKFSW  TBLKSW1 /
```

```
------ TRACER ------
TBLKFSW
      783380*0    /
TBLKFSW1
      783380*0    /
```

8.6 Comparing observed sea water cut with simulation results

Natural tracer data is a valuable additional source of information that can help reduce the uncertainty in a reservoir simulation model. Comparing the observed SWC with the result from the simulation can be used in the history matching process of the simulation model. The SWC curves can be used to obtain information about reservoir structures, such as faults and interwell permeability variations in the form of highly permeable channels.

After a simulation run plots of the observed and simulated SWC were made for all wells in the Statfjord Fm. To check the quality of the match two main considerations were accounted for:

- Time of sea water breakthrough
- Sea water cut

The only change made in the first simulation run was implementing the tracer in the reservoir simulation model. This simulation run will be referred to as the" base case simulation" **(BCS)**. All changes made later in the reservoir model will always be compared to the BCS.

8.7 Sea water production data

In addition to sea water cut data, tracer production rates, cumulative tracer production and tracer volume in the reservoir were written to the summary file. To be able to compare these simulation results with true data it was necessary to calculate the observed data.

The sea water production rate can be found from multiplying SWC with water production rate:

$$q_{sw} = SWC \cdot q_w \qquad [8.5]$$

where:
q_{sw}: sea water production rate
q_w: water production rate

From equation 8.6 the cumulative production volume of sea water from a given well can be estimated:

$$V_{sw,tot} = \sum_{m=1}^{T} V_{sw,m} = \sum_{m=1}^{T} SWC_m \cdot V_{w,m} \qquad [8.6]$$

where:
m: (1…..,T), the number of months since the well started production
T: number of months passed since startup at the end point
$V_{sw,tot}$: total cumulative production volume of sea water
$V_{sw,m}$: monthly production volume of sea water
$V_{w,m}$: monthly production volume of water

Monthly sea water production can be determined from the monthly sea water cut multiplied with monthly production volume of water:

$$V_{sw,m} = SWC_m \cdot V_{w,m} \quad [8.7]$$

Then average monthly sea water production rates can be found from:

$$q_{sw,m} = \frac{V_{sw,m}}{\Delta t} \quad [8.8]$$

To be able to calculate production volumes and rates; firstly, dates were converted to the first day of that day's month. If there were many samples for one month an average was used to represent that month's sea water cut. If there were months were there had been non water samples, interpolation was used to calculate sea water cut. Since only rough estimates of production volume and rates were seeked, this was a reasonable approximation. Months with no water production was removed.

Table 8.3 was created to view the results, and the table was also converted to a format that allowed the calculated results to be plotted in S3GRAF.

Well	Date	Days	Vw [Sm3]	SWC	Vsw [Sm3]	qsw [Sm3/d]	Vsw,kum [Sm3]
A10	01.10.2002	8370	6850	0,3750	2569	84,4	2569
A10	01.11.2002	8401	24343	0,3505	8532	280,3	11101
:	:	:	:	:	:	:	:
:	:	:	:	:	:	:	:
B17	01.03.2001	7791	185425	0,4983	92397	3035,6	92397
B17	01.04.2001	7822	177389	0,5360	95081	3123,8	187478
B17	01.05.2001	7852	166312	0,5430	90307	2967,0	277785
:	:	:	:	:	:	:	:
C42	01.01.1997	6271	90454	0,3313	29967	984,6	29967
C42	01.02.1997	6302	21978	0,1450	3187	104,7	33154

Table:8.3 Calculated sea water production data for the different Statfjord Fm wells.

Some producers did not have regularly water samples taken, which makes the estimates of sea water production rates and volumes less accurate.

The monthly sea water production rates were also summarized for all wells, and Figure 8.4 shows the comparison of the simulated results and the calculated.

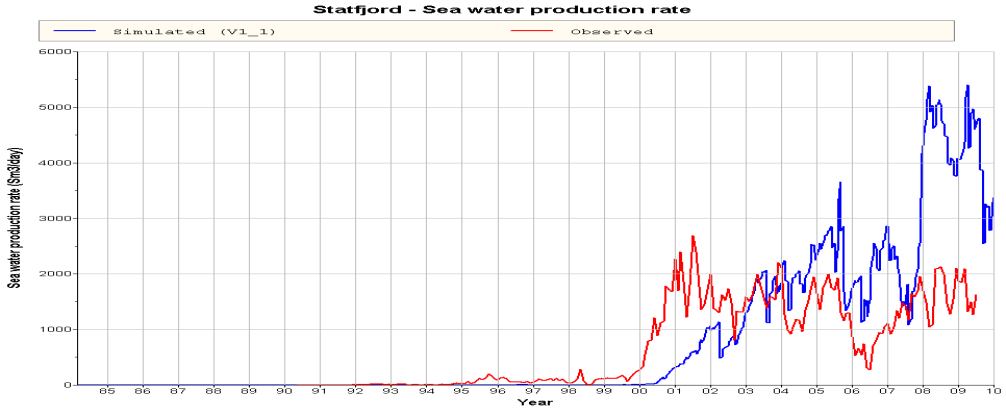

Figure 8.4: Statfjord – Sea water production rate

8.8 Additional considerations

Sea water cut is the main parameter that is to be history matched in this study. The effect of changes made in the simulation model to better match the SWC with observed data will also be checked for:

- Water cut
- The gas-oil ratio,GOR

GOR is defined as the ratio of the gas and oil volumes:

$$GOR \overset{\text{def}}{=} \frac{V_g}{V_o} \qquad [8.9]$$

where:
V_g: gas volume
V_o: oil volume

GOR is not defined when there is no oil production, $V_o = 0$.

- Production rates
    - Water production rate
    - Sea water production rate
    - Oil production rate – Example for A-17A is shown in Figure 8.5
    - Gas production rate

- Total production volumes
    - Total water production
    - Total sea water production
    - Total oil production
    - Total gas production

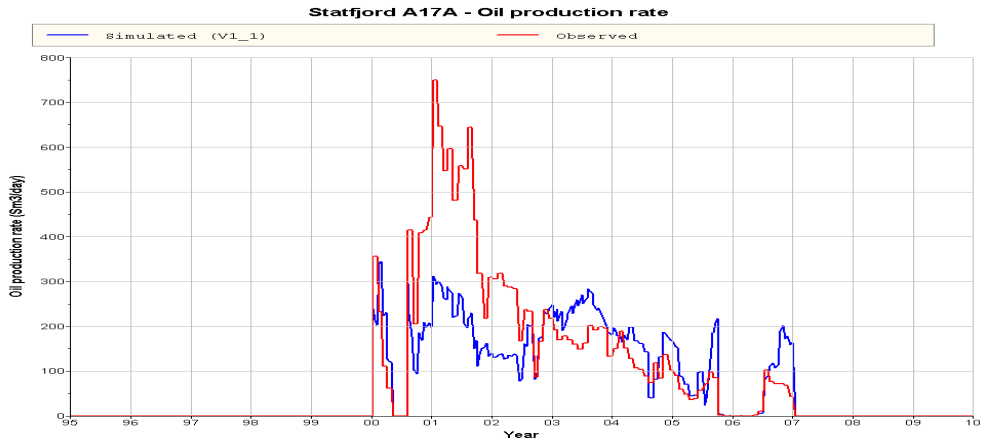

Figure 8.5: Well A-17A – Oil production rate.

9 Focus area: Upper Statfjord, A and B area north of F-11

Upflank GCWI started in Upper Statfjord in 1997 and was stopped in 2007. Since then 76.1 M Sm^3water has been injected. One of the consequences from upflank water injection was lost control over where the different phases were located in the reservoir. The simulation model did no longer correspond well with observed data. Especially the sea water production from the producers had a bad match. Since no upflank water injectors are located south of the F-11 fault, the producers in this area has had little sea water production. This study focuses on history matching of the sea water cut for the Upper Statfjord producers in SFA and SFB north of the major fault F-11. This chapter gives an overview of the production and injection history of the region in focus of this study.

9.1 Producers and perforation history

The production wells have produced from the field at different time steps, and the perforation history is quite complex. Perforations are often closed and new ones taken to produce from different layers in the reservoir, and then at a later time step the old perforations may be reopened. Some production wells also produced from the Statfjord Fm and from the Brent reservoir at the same time, which makes it difficult to estimate which part of the reservoir that contributes most to oil and water production.

This study focuses on 23 production wells, where all are located in SFA and SFB north of the fault F-11. Table 9.1 describes the production history for the wells at the time of interest for this study. Wells that were closed or had older perforations in the history before start of the upflank water injection is of less interest since this study focuses mainly on the sea water movement in the reservoir.

Reservoir zone	Well MF	Well EF
US	B-6BT2 [Eiriksson 02.00-07.00 ⇨ Nansen 07.00-08.00]	
	A-34AT3 [Eiriksson 10.96-03.03] B-15 [Eiriksson 03.94-08.01]	B-21B [Raude MF12.00-11.05 ⇨ Eiriksson EF 11.05-] A-18D[Eiriksson EF 01.09-]
	A-2B [Eiriksson/Nansen 11.2007-] A-10 [Eiriksson/Nansen 01.96-10.02] A-26A [Eiriksson 06.00-11.03 ⇨ Eiriksson/Nansen 11.03-05.04] A-26BT2 [Eiriksson 05.04-12.05 ⇨ Eiriksson/Nansen 12.05-01.06] A-32A [Eiriksson 03.97-04.99 ⇨ Eiriksson/Nansen 04.99-04.02] A-37A [Eiriksson 07.97-10.00 ⇨ Eiriksson/Nansen 10.00-10.01] A-40B [Eiriksson 09.01-03.02 ⇨ Eiriksson/Nansen 03.02-06.04] A-40DT2 [Eiriksson/Nansen 03.07-] B-1C [Raude 02.08-10.08 ⇨ Eiriksson/Nansen 10.08-] B-11C [Eiriksson/Nansen 04.07-]	
US simultaneously with LS	A-12 [Raude/Eiriksson 10.95-02.04] A-15CT4 [Raude 06.03-11.06 ⇨ Raude/Eiriksson 11.06-09.07] A-17A [Raude/Eiriksson 08.00-06.05 ⇨ Eiriksson/Nansen 07.05-12.06] A-35B [Raude 05.07-06.08 ⇨ Raude/Eiriksson/Nansen 06.08-01.10]	A-10AT2 [Raude /Eiriksson 04.03-07.03 ⇨ Eiriksson 07.03-08.04 ⇨ Eiriksson/Nansen 08.04-03.10]

US simultaneously with UB/LB	A-2A [Eiriksson 06.02-05.06 ⇨ Eiriksson/Ness EF 05.06-03.07] B-15A [Eiriksson 03.02-04.02 ⇨ Eiriksson/Rannoch 04.02-09.05 ⇨ Eiriksson/Rannoch/Ness 09.05-] B-17 [Eiriksson /Rannoch EF/Etive EF 06.98-09.06]	

Table 9.1: Production history for the focus wells in Upper Statfjord.

From Table 9.1 one can see that 5 production wells produced from Upper Statfjord simultaneously as Lower Statfjord, while 3 wells produced simultaneously as the Brent reservoir. Especially wells that have production simultaneously with Brent must be carefully considered. If there is sea water produced from the well, it can be difficult to determine if the water comes from Statfjord Fm or Brent. The sea water breakthrough might be caused from the Brent reservoir, and it can then be impossible to determine sea water breakthrough in the Statfjord Fm. There are 46 layers in the simulation model and the perforations changes and the layers the wells were producing from must also be carefully considered when trying to history match the sea water production.

Table B.1 and B.2 in appendix summarizes the perforation history of the production wells in Upper Statfjord A and B area respectively. Each well is listed in an individual column. The columns illustrate the perforation history to each well, which layers that are perforated and the time that the perforations were opened. Different shades of the color green is used to show new perforations when the older ones were closed. Dark green was used for the first perforations, while lighter green was used for new ones. Note that if new perforations were taken, but the earlier ones were not closed, the same shade of green was used. The perforation history was found from examining the history file that was included in the scchedule section in the ECLIPSE input file.

9.2 Water/WAG injectors

There have been 8 injectors contributing to the upflank water that has been injected into Upper Statfjord:

- The WAG injector A-3A started water injection in January 1996 and has since then injected 16.8 M Sm^3.
- A-25AT3 was drilled in June 1999 as a dedicated water injector and has injected 16.6 M Sm^3
- A-8C which was a WAG injector started water injection in December 2000, and has injected 6.3 M Sm^3.
- The WAG injector B-18 was the first upflank water injector in the B-area. The well started water injection in February 1998. The cumulative water injection adds up to 8.8 M Sm^3.
- B-1B, which was a pure water injector started injection in April 2000, has injected 20.2 M Sm^3.
- C-34 was in 1999 converted to a WAG injector and started in December the same year to inject water. The well has injected 1.7 M Sm^3.
- C-4A, a WAG injector, started water injection in May 2001. Injected 1.5 M Sm^3.
- C-4B, also a WAG injector, started water injection in July 2003. Injected 4.2 M Sm^3.

The total amount of water injected adds up to 76.1 M Sm^3, where 39.7 M Sm^3 was injected in SFA , 29.0 M Sm^3 in SFB and 7.4 M Sm^3 in SFC. The much larger amount of water injected into SFA and SFB was one of the reasons for choosing the focus area of this study. The volumes injected are summarized in Table 9.2. Figure 9.1 shows the location of the Water/WAG injectors, both for all upflanks injectors and for only the injectors in focus of this study.

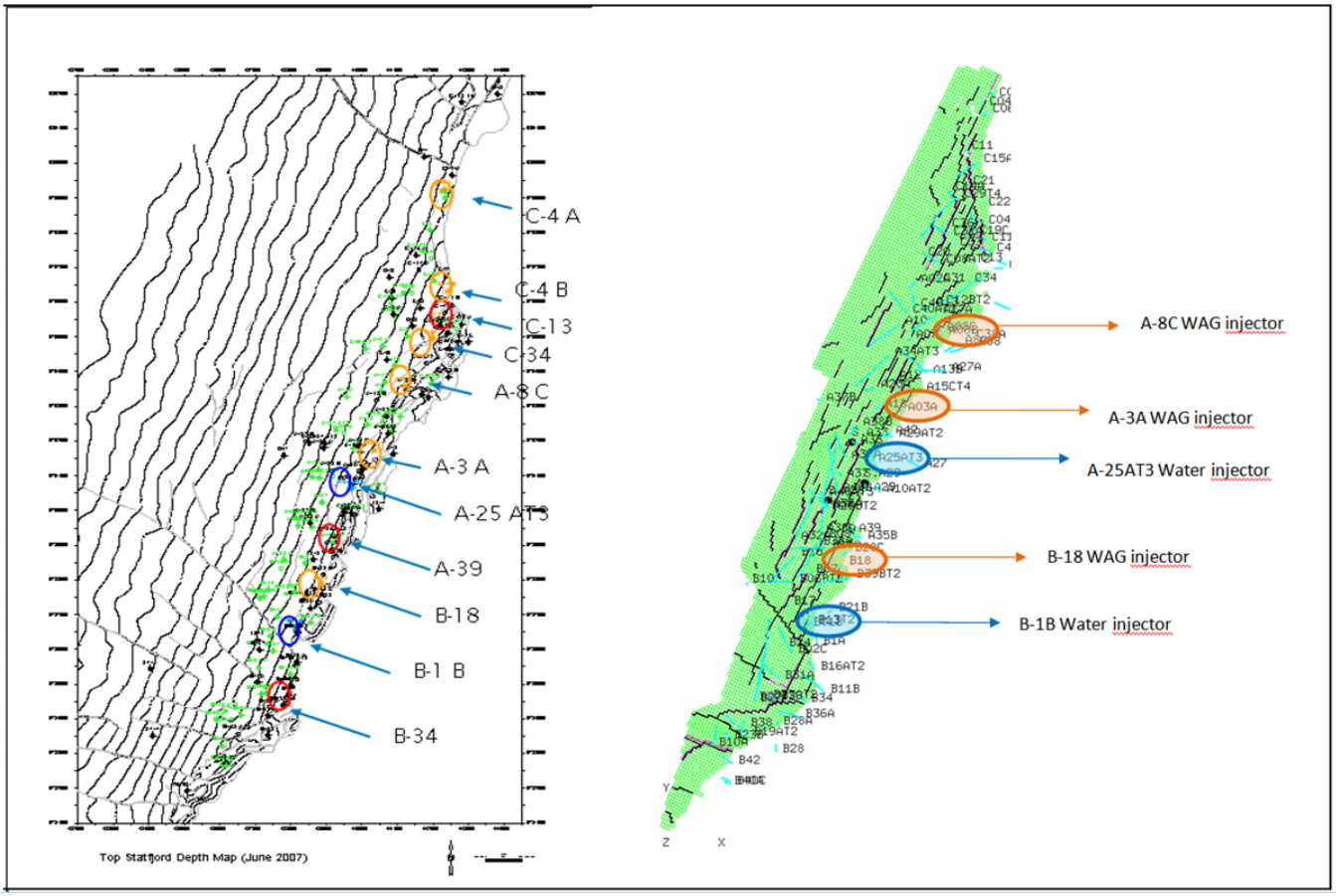

Figure 9.1: Location of different injectors in Upper Statfjord. Blue indicates pure water injectors, orange WAG injectors and red pure gas injectors.

Well	A-3A	A-8C	A-25AT3	B-1B	B-18	C-34	C-4A	C-4B
Volume of injected water [M Sm^3]	16.8	6.3	16.6	20.2	8.8	1.7	1.5	4.2
	SFA			SFB		SFC		
	39.7			29.0		7.4		
	Upper Statjord							
	76.1							

Table 9.2: Volumes of injected upflank water in Upper Statfjord.

Table B.3 in appendix summarizes the perforation history of the Water/WAG injectors in the Statfjord Fm. Each well is listed in an individual column and the color blue is used to easily show which layers that are opened. The time that the perforations were opened is also shown.

Water tracers have been injected in some wells and are summarized in Table 9.3 and 9.4 for Upper and Lower Statfjord respectively. These tracers give valuable information for this study because they can be used to verify communications paths between injectors and producers.

Injection Well	Tracer inj. Date	Reservoir	Formation	Tracer	Observation Well	Formation	Breakthrough date	# days	Distance from inj. (m)	Velocity (m/d)
A-08 C	27.11.2002	US	Eiriksson	HTO	A-02 A	Dunlin / LB	Not detected		1317	
					A-12	Raude / Eiriksson	20.09.2003	297	1561	5.26
					A-17 A	Eirikson / Raude	07.07.2003	222	471	2.12
					C-8 A	Eirikson / Nansen / Ness	Not detected			
B-01 B	04.11.2003	US	Nansen/Eiriksson	2,4,5-TFBA	B-15 A	Ra1/Ei MF	Not detected		1770	
					B-17	Et EFB	10.05.2006	918	620	0.68
					B-2 C	Eirikson	Not detected		876	
					B-21 B	Raude / Eiriksson	Not detected		544	
					B-38A	Raude / Eirksson /Cook	(05.01.2007)	(1158)	1030	
B-18	07.03.2003	US	Eiriksson	3,4 DFBA	A-26 BT2	Eiriksson / Nansen / Cook / Rannoch	12.04.2005	767	1950	2.54
					B-15 A	Ra1/Ei MF	05.10.2005	943	940	1.00
					B-17	Et EFB	Not detected		1545	
					B-21 B	Raude / Eiriksson	(18.03.2007)	(1472)	1099	
					B-38A	Raude / Eirksson /Cook	Not detected			
C-04 A	23.09.2002	US	UStatfjord	2,6 DFBA	C-15 A	Eiriksson	11.06.2003	261	1870	7.16
					C-19 C	Raude Eiriksson	Not detected		2840	
					C-29	Eiriksson	Not detected		2740	
C-04 B	04.04.2003	US	UStatfjord	4-FBA	C-15 A	Eiriksson	19.08.2004	503	1365	2.71
					C-29	Eiriksson	16.06.2004	439	1120	2.55
					C-31 A	Eiriksson	13.03.2005	2313	1060	0.46
					C-8 A	Eirikson / Nansen / Ness	Not detected		1560	

Table 9.3: Water tracer detections and flow velocities for Upper Statfjord [25].

Lower Statfjord - water tracer breaktrough										
Injection Well	Tracer inj. Date	Reservoir	Formation	Tracer	Observation Well	Formation	Breakthrough date	# days	Distance from inj. (m)	Velocity (m/d)
A-38 B	11.10.2003	LS	Raude	2,6 DFBA	A-13 B	Raude	Not detected		2159	
					A-15 CT4	Raude / Eiriksson / Rannoch	Not detected		1738	
					A-29 AT2	Raude	Not detected		822	
C-14 A	04.04.2003	LS	Raude	3,4 DFBA	C-11 B	Raude	Not detected		1525	
					C-19 C	Raude Eiriksson	Not detected		875	
					C-29	Eiriksson	(15.12.2004)	(621)	205	

Table 9.4: Water tracer detections and flow velocities for Lower Statfjord [25].

10 Status of the "Base Case Simulation"

The BCS is used as the reference case; all changes made in the history matching process will be compared not only to observed data but also to the BCS. A detailed description of the status of the BCS is therefore given in this chapter.

Figure B.3 to B.7 in the appendix illustrates the upflank water movement from each injector in focus of this study. An overview of how the upflank water approaches each well in BCS is given in chapter 11.

10.1 Sea water cut match for "Base Case Simulation"

The BCS was compared to the observed data, where the quality of the match was determined by sea water breakthrough time and sea water cut. A label for each well with the result from the match was added on a map with well locations. In addition to the result, color codes of the labels were used to indicate the quality of the match for sea water cut:

- Dark blue indicates too high sea water cut
- Light blue indicates too low sea water cut
- Dark red indicates no sea water breakthrough in the simulation
- Green indicates acceptable sea water cut match

Figure B.1 and B.2 in the appendix shows the maps covering Upper Statfjord A and B area respectively. The focus area of this study does not cover Statfjord B area south of the F-11 fault, these labels are therefore colored grey. From the labels one can see that the wedge zone producers in general have too low sea water cut, while the producers upflank have too high. The regional pattern seems to be that the upflank water moves too slowly down to the wedge zone producers, resulting in too late sea water breakthrough. The breakthrough time of the sea water is in general 1-2 years late in the base case simulation model.

10.2 "Base Case Simulation" run with several tracers

Having 46 different layers in the simulation model it can sometimes be difficult to observe which water injector that is contributing to producing sea water in a specific producer. There are five water injectors in the focus area of this study. In addition to the tracer implemented in the simulation model, which tracks all injected water, five more tracers were added, and these tracers track water from only one specific water injector. The simulation run made it easy to follow the water movement from each water injector and thereby observe which injector that caused sea water production in the producing wells.

The new water tracers were defined as follows:

- A-8C: SW1
- A-3A: SW2
- A-25AT3: SW3
- B-18: SW4
- B-1B: SW5

Table 10.1 presents an overview of the relationship between injectors and producers, including:

- Which injector causes sea water breakthrough
- The perforated layers for producers and injectors
- Time of sea water breakthrough, both observed and simulated
- Layer(s) where sea water breakthrough occurs
- Time between simulated and observed sea water breakthrough

Injection well	Start of injection	Formation {layer}	Tracer in simulation	Production well	Formation	{layer} peforated in US	Breakthrough date	Breaktrough in simulation	{layer} with SW in simulation	ΔSWBT [months]
A-8C	nov.00	Eiriksson {11-13,17-19}	SW1	A-2A	Eiriksson/Ness	{10-14}	Not detected	Not detected	..	..
				A-17A	Raude/Eiriksson/Nansen	{1,3,9-12,18-19}	oct.01	aug. 01	{1,3,12,18-19}	-2
A-3A	jan.96	Eiriksson/ Nansen {1-4} {6-10} {14-18}	SW2	A-10	Eiriksson/Nansen	{1-4,7-10}	mar. 01	Not detected	..	_
				A-12	Eiriksson/Raude	{12-19}	jan. 99	feb.00	{17-19}	13
				A-34AT3	Eiriksson	{1-2,7,9}	jun. 01	nov.02	{1-2,7}	17
				A-2B	Eiriksson/Nansen	{2-5,7,9-18}	From start	From start	{2-5,7,9-18}	..
				A-15CT4	Raude/Eiriksson	{9-10,12-13}	From start	From start	{9-10,12-13}	..
				A-37A	Eiriksson/Nansen	{1-3,6-10,12-15,17-19}	des. 99	jan.01	{3,7-10,13-15,17-19}	13
A-25AT3	jun.99	Eiriksson {6-8} {11,13-15}	SW3	A-37A	Eiriksson/Nansen	{1-3,6-10,12-15,17-19}	des. 99	jan.01	{3,7-10,13-15,17-19}	13
				A-18D	Eiriksson	{3-4,6-7}	From start	From start	{3-4,6-7}	..
				A-10AT2	Eiriksson/Nansen (EF)	{10-13}{6}{3-4}	From start	From start	{10-13}{6}{3-4}	..
B-18	feb.98	Eiriksson {3-4} {6} {8} {13-14} {18}	SW4	A-26A	Eiriksson/Nansen	{1-3,14-19}	From start	Not detected	..	_
				A-26BT2	Eiriksson/Nansen	{3-6}	From start	Not detected	..	_
				A-40DT2	Eiriksson/Nansen	{1-5,7-12,14}	From start	From start	{12,14}	..
				A-35B	Eiriksson/Nansen/Raude	{1-2,4-6,10-11,16}	From start	jul.08	{1-2,4-6,16}	1
				A-32A	Eiriksson/Nansen	{1-4}	mar. 00	apr.00	{1-4}	1
				B-15A	Eiriksson/Rannoch/Ness	{7,9-12}	From start	From start	{7,9-12}	..
				B-15	Eiriksson	{4-12}	sep. 99	jan.01	{4-11}	18
				B-6BT2	Eiriksson/Nansen	{1-2,11,17-19}	From start	Not detected	..	_
				B-17	Eiriksson/Rannoch/Etive	{14-19}	?	mar.03	{15,17}	..
				B-11C	Eiriksson/Nansen	{1-10,12-16,18-19}	From start	From start	{5,10,15-16,18-19}	..
				B-1C	Eiriksson/Nansen	{1-6,8-14,16,18-19}	From start	From start	{16,18-19}	..
				B-21B	Eiriksson EF	{12-19}	Not detected	From start	{19}	-48
B-1B	apr.00	Eiriksson/ Nansen {2,5-6}	SW5	B-1C	Eiriksson/Nansen	{1-6,8-14,16,18-19}	From start	From start	{1-6,8-12}	..
				A-35B	Eiriksson/Nansen/Raude	{1-2,4-6,10-11,16}	From start	jul.08	{1-2,4-6,16}	1
				B-11C	Eiriksson/Nansen	{1-10,12-16,18-19}	From start	From start	{5,10,15-16,18-19}	..

Table 10.1: Water tracer detections for Upper Statfjord wells.

11 History matching of sea water cut for the Upper Statfjord focus wells

The primary focus of this study is to match the sea water cut, both breakthrough times and SWC after breakthrough. When history matching, changes were made both on a field level and more locally around specific wells. Field level adjustments include changing relative permeability curves. Fault communication and permeability have been altered to obtain a better match for individual wells.

While the sea water cut match is the primary focus, the fluid match for both oil, water and gas have been monitored while history matching. If the changes applied to improve the sea water cut match also result in an improvement for oil, water and gas production, the changes are considered more plausible.

A trial and error process has been used when history matching. Changes that did not result in any significant improvement were not included in the subsequent runs.

11.1 Keywords used in ECLIPSE for history matching

A description of the keywords that have been used for the history matching process is given below [21]:

SATNUM

SATNUM is used to define different regions within the reservoir where different saturation functions can be specified.

INCLUDE

The keyword INCLUDE is used to make ECLIPSE open and read a file which input is to be taken into account. After ECLIPSE has read the file it is closed, and the program continuous to read input from the main file. After the keyword the name of the file which is to be read must be followed.

EQUALS

The keyword EQUALS is used to assign or replace the value of a property for a box of grid cells within the reservoir grid. The keyword has been used extensively in this study to assign or replace permeability and transmissibility within the reservoir model.

SWOF

The keyword SWOF is used to define water/oil saturation functions versus water saturation. It can be used in runs containing both oil and water as active phases. After the keyword to input tables of water relative permeability, oil-to-water relative permeability and water-oil capillary pressure as function of water saturation must be defined. SGOF can be used to define the gas/oil saturation functions if also gas is an active phase.

FAULTS

FAULTS is used to define a set of faults, the keyword may be used more than once. After the keyword the fault trajectory and the name of the fault must be defined.

MULTFLT

When a fault is defined by the FAULT keyword MULTFLT can be used to modify the transmissibility across the fault. The keyword is followed by the name of the fault defined in the FAULTS keyword and the transmissibility multiplier. A multiplier of zero yields a sealing fault, values between zero and one gives different degree of leaky faults.

PERMX PERMY

The keywords PERMX and PERMY are both used to set the horizontal permeability. PERMX specifies the permeability values in the X-direction, while PERMY specifies values in the Y-direction. In the Statfjord Fm model the permeability in the X-direction is always equal to the permeability in the Y-direction. This will therefore also be done during the history match of the sea water cut. Hence, PERMX = PERMY.

MULTX MULTY

An alternative to change the permeability in the X- and Y-direction is to change the transmissibility in the same area by using the keywords MULTX and MULTY. The transmissibility between a cell and its neighbour involves the permeability values of both cells. ECLIPSE calculates the transmissibility between two grid blocks based on their permeability. By changing the transmissibility the relative variation in permeability in the area that is to be modified will be preserved. This is the main difference between changing transmissibility and changing permeability. The keywords MULTX and MULTY define a multiplier for the transmissibility in X- and Y- direction. A multiplier less than one indicate a flow restriction compared to the original conditions, while a multiplier higher than one indicate that it is easier to flow between the grid blocks. A multiplier of zero can be used to create a sealing condition and will not allow flow.

MULTZ

MULTZ is used to adjust the vertical communication. ECLIPSE calculates the vertical transmissibility in the same manner as horizontal transmissibility. MULTZ defines a multiplier for the vertical transmissibility and works the same way as MULTX and MULTY. MULTZ can be used to emulate the effect of a barrier between two layers. E.g. by sealing vertical transmissibilities a shale layer may be simulated without requiring any actual cells for the shale.

NNC

NNC can be used to set non-neighbor connection values explicitly. The keyword enables a specified transmissibility between any two grid blocks. The cells that are to be linked together and the required transmissibility value must be defined after the keyword.

11.2 Modifying the water relative permeability curve for history matching

Relative permeability curves are often modified in the reservoir simulation model during the lifetime of a field, and are one of the most useful physical quantities available for performing a history match. Relative permeability curves are often obtained from experimental work on flooding cores in a laboratory. Flooding cores will however correspond to a much smaller scale compared to the flow through the drainage area of a well. Therefore, the laboratory curves may not be representative for the flow on reservoir scale [10].

Many of the wells located on the wedge zone had too late sea water breakthrough and too low SWC. The first attempt to improve the match was therefore to change the water relative permeability curve. By modifying this, the mobility of water is changed. It was desired to increase the mobility of water to get earlier breakthrough times and increase the level of the sea water cut. For the oil-water curves, a straight-line was used for water to get a higher mobility. The base case water relative permeability is shown in Figure 11.1, and the adjusted one in Figure 11.2. The base case (Figure 11.1) water relative permeability has a more “creeping” form.

When using the straight-line curve for the whole field, the breakthrough for sea water occurred earlier, as seen in Figure 11.4. However, having a higher water mobility has also (expectedly) resulted in a higher water production (Figure 11.3). This could be because the model has previously been matched on water cut, and not also on sea water cut.

The model grid blocks are much coarser than the actual structure in the reservoir. As such, the water will in reality tend to finger in what is only a part of the layers used in the model. This effect is more pronounced if the reservoir is homogenous, as the flow will then be more gravitationally unstable. In the model, the water will move slower as the saturation in the entire grid block has to increase for the water to be mobile. For this reason, the breakthrough times in the model will be too late. To compensate for this, the new straight-line curve with higher water mobility is used. This allows the water to move through the coarser grid blocks faster at lower water saturations, and give an earlier breakthrough. Because Lower Statfjord (Raude Mb) is fairly heterogeneous and the flow tends to be less affected by gravitational forces, the straight-line relperm should not be used. However, Upper Statfjord is homogeneous and an upscaling of the water relative permeability is necessary.

To use different relative permeability curves in Upper and Lower Statfjord, the SATNUM keyword in the REGIONS section was used to apply the new curve only in US:

```
EQUALS
 SATNUM 1 1 65 1 262  1 19 /
 SATNUM 2 1 65 1 262  20 46 /
/
```

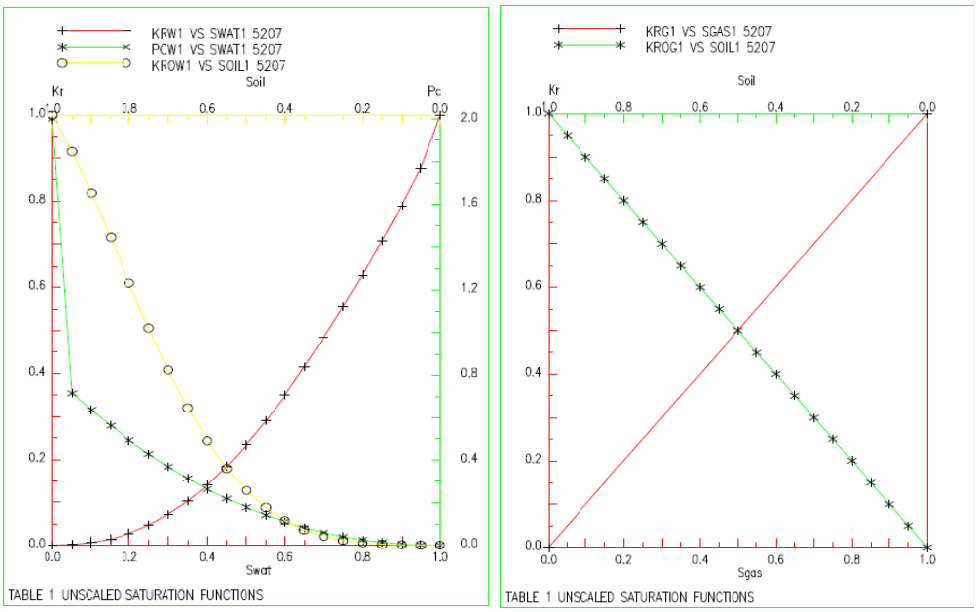

Figure 11.1: Base case relative permeability curves for oil-water (left) and gas-oil (right) [15].

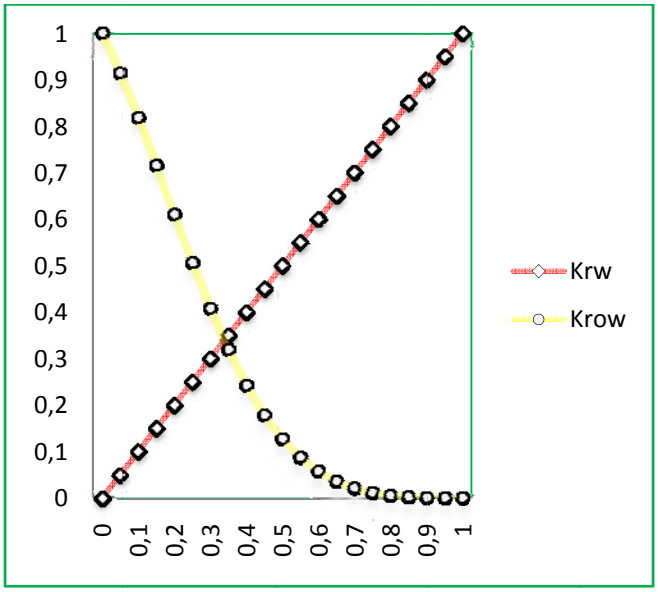

Figure 11.2: New straight-line curve for water in oil-water system.

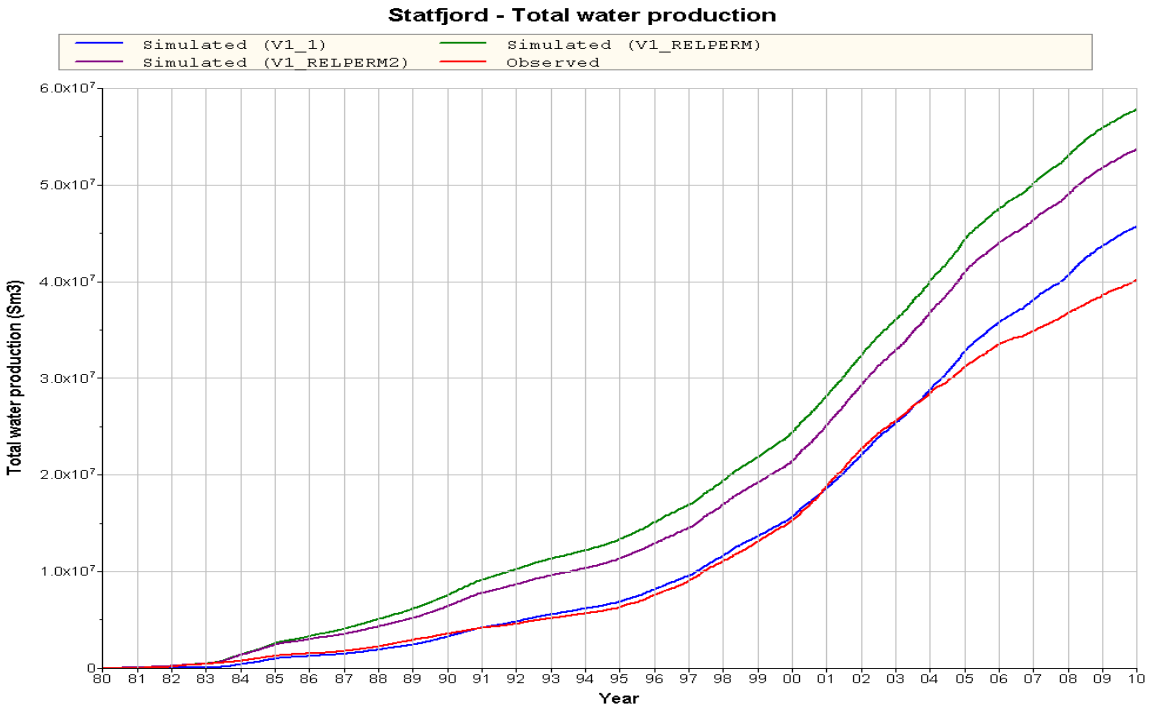

Figure 11.3: Total water production from Statfjord Fm, comparing different oil-water relative permeabilities. Curve "V1_RELPERM" uses the straight-line water relperm for the whole field, whereas "V1_RELPERM2" uses it only in Upper Statfjord.

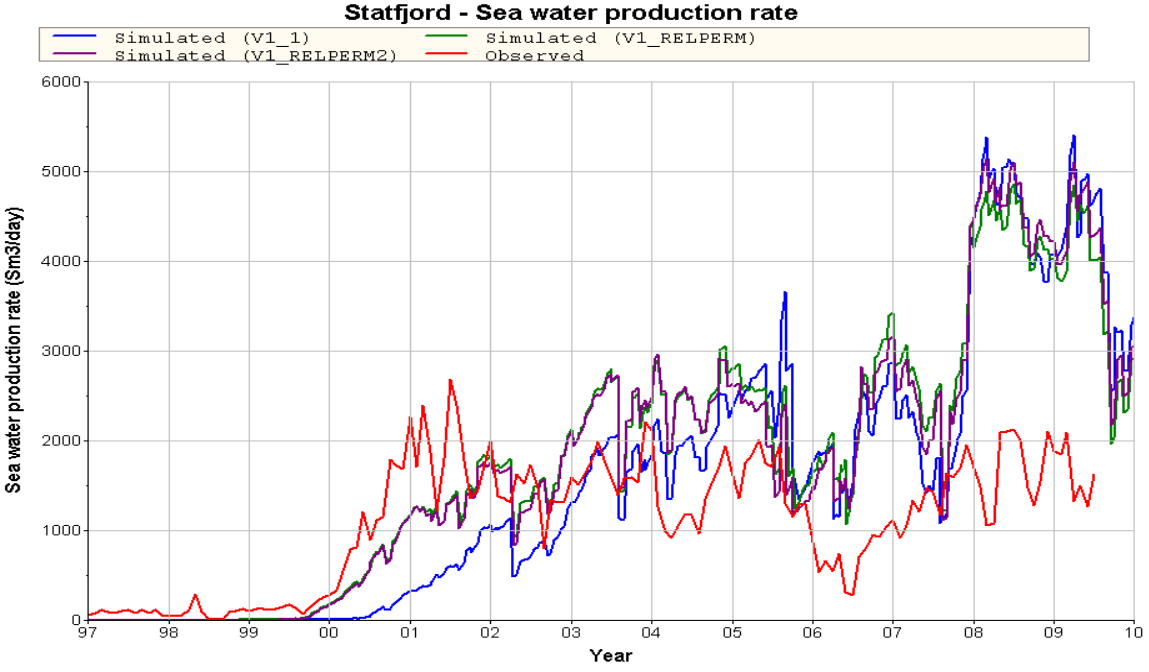

Figure 11.4: Sea water production rate from Statfjord Fm, comparing different oil-water relative permeabilities. Curve "V1_RELPERM" uses the straight-line water relperm for the whole field, whereas "V1_RELPERM2" uses it only in Upper Statfjord.

11.3 History matching of individual wells

The new straight-line relative permeability has always been used when making local adjustments to improve the match for individual wells. In the following, the wells matched will be presented with

- **BCS status** – the match quality of the base case.
- **New relperm** – the match quality *after* applying the new relative permeability curve for Upper Statfjord with higher water mobility.
- **Changes** – the changes that were introduced near the given well.
- **Result** – match quality after applying both local and field level changes.

Details about the modifications that have been made are given in appendix C. This includes the Eclipse input data and images showing the regions in which these changes have been applied.

Plots of SWC and WCT vs time for the individual wells are shown in appendix D. In each plot, four lines are included:

- Simulated (BCS)
- Simulated (RELPERM) – Simulation with the new water-oil relperm (section 11.2).
- Simulated (RELPERM+CHANGES) – Simulation with the new relperm *and* local modifications.
- Observed – Historical data.

Wells will be sorted by their location (north to south):

- Downflank SFA wells.
- Upflank SFA wells.
- Downflank SFB wells.
- Upflank SFB wells.

Producers located in Statfjord A area

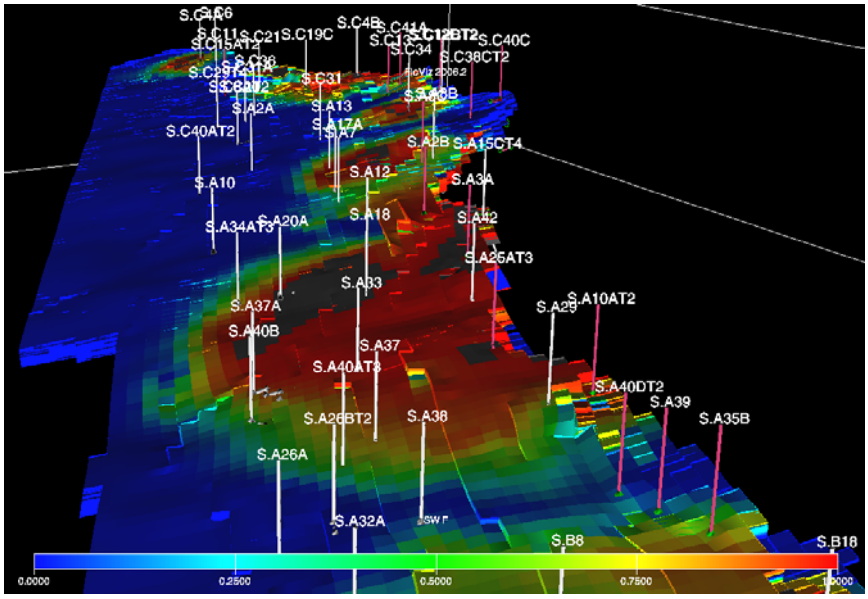

Figure 11.5: SWC; overview of Upper Statfjord A in 2009, showing the uppermost layer.

Downflank SFA wells (north to south)

- **A-2A [Eiriksson MF 06.02-05.06 ⇨ Eiriksson MF/Ness EF 05.06-03.07]**

(Figure D.1)

A-2A was in June 2002 converted from a WAG injector in Raude to a producer in Upper Statfjord wedge zone. SWBT was observed 5 months after the well started production. The water injector C-34 is located east and upflank for A-2A, and the water most likely came from this well. The injector A-8C located southeast for A-2A could also be responsible for the produced sea water. In the end of 2002 a tracer was added to the injected water from A-8C, however, it was not detected in A-2A, indicating that the sea water produced came from injector C-34.

BCS status: The water injected in C-34 and A-8C does not reach the producer A-2A in the simulation model. A-2A was earlier a WAG injector, and when the well started production in Eiriksson, the pressure difference seems to move the water upwards in the grid block column around the well. Hence, A-2A produces its own sea water. The SWC is 0.55 at start, but decreases quickly to below 0.1. SWBT is approximately the same, and the trend of SWC magnitude is almost identical compared to observed data.

New relperm: No change.

Changes: Because the match is already quite good, no local changes were made. It is assumed that the well does indeed produce its own water, because of the "unusual" SWC trend. However, from 2006, the observed SWC starts increasing slightly, while the simulated SWC approaches zero. This may indicate that water from nearby injectors A-8C and C-34 reached the well. But since the well is closed already in 2007, a conclusion cannot be drawn.

Result: The resulting match is very close to BCS. Thus, no changes for other wells have affected A-2A.

- **A-17A [Raude MF 12.99-08.00 ⇨ Raude/Eiriksson MF 08.00-06.05 ⇨ Eiriksson/Nansen MF 07.05-12.06]**

(Appendix C.2.5, Figure D.2)

A-17A had SWBT in the middle of 2001. A-17A is located downflank and southwest of injector C-34 and downflank of injector A-8C. Water tracer injected in A-8C was later produced in A-17A, which revealed that sea water came from A-8C.

BCS status: During the first few months of production from Raude, virtually only water is produced in BCS instead of the observed gas production. The high water production rate during this period has resulted in a poorly matched cumulative water production for the well.

In the Raude/Eiriksson perforations from August 2000, SWBT occurs in August 2001, approximately the same as observed.

New relperm: Breakthrough occurs in May 2001, a bit earlier than in BCS. The SWC also increases faster and reaches a higher value, resulting in a worse match.

Changes: A fault was added between the injector A-8C and the well, in order to slow the breakthrough of sea water and lower the SWC.

Result: The SWBT occurs a couple of months later, and the SWC was lowered slightly by the fault. Different fault transmissibility factors were tested, but the results were almost indistinguishable for factors below 0.1. Considering production only from August 2000 onwards, the total water production is well matched.

- **A-10 [Eiriksson/Nansen MF 01.06-10.02]**

(Appendix C.2.1, Figure D.3)

A-10 is located at the wedge zone and lies north of the WAG injector A-3A. SWBT was observed in March 2001. The well produced from below the OWC, and the sea water concentration was low. It did not reach a higher value than 30%.

BCS status: No sea water shows up in BCS for A-10. Both water from injector A-3A and A-8C approaches the producer, which makes it difficult to see which injector that causes SWBT. BCS shows slight fingering in layer {9-10} from both injectors, where the water from A-8C is closest to the well in 2009.

New relperm: Still no sea water before the well is shut. WCT is also relatively unchanged.

Changes: Different attempts were made to get the sea water to the well earlier, by increasing the transmissibility in selected layers and using a low MULTZ to stop water from moving downwards in the stratigraphy. After increasing transmissibility in layers {4,7} and using a MULTZ of 0.1 between {7} and {8}, a sea water breakthrough was registered in the middle of 2001.

Result: Compared to BCS, sea water breakthrough occurs several years earlier, but is still a few months late and too low. The match of total water, oil and gas production has worsened slightly, but since the SWC is the primary concern, it was chosen to keep the changes.

- **A-12 [Raude/Eiriksson MF 10.95-02.04]**

(Appendix C.2.3, Figure D.4)

A-12 lies north for the WAG injector A-3A. The well has produced sea water from January 1999, and the early SWBT must be caused by the injector A-3A since A-8C did not start injection before November 2000. Even though the well has an early SWBT, the WCT in the well is low, not higher than 20%. However, the increase in WCT in 2003 might be from A-8C. A tracer added to the injected water and later produced in A-12, has verified that water from A-8C did reach the well. The WCT at end of production was over 90%.

BCS status: BCS has SWBT in February 2000, and is thus 13 months late. A-3A is responsible for the sea water production; water injected from A-8C does not reach A-12 in the simulation. Water travels fastest in layer {17-19}, which first reaches A-12. The other layers, which the well is producing from, get sea water next year. SWC is also too low in the simulation, approximately 20%.

New relperm: Breakthrough occurs 6 months earlier and the SWC is higher.

Changes: Permeability was increased to 6 Darcy in layer {14} from about 1 Darcy in BCS, though this is not supported by the A-12 well log, which shows permeability in the lower half of Eiriksson only reaching 500mD. It was also attempted to increase permeability in layer {17-19}, but this did not improve the results.

Result: The SWC match has improved, with a well timed SWBT and a correct SWC. However, this has resulted in excessive water production in the first few years after breakthrough.

- **A-34AT3[Eiriksson MF 10.96-03.03]**

(Appendix C.2.10, Figure D.5)

Like the producer A-10, well A-34AT3 is also located at the wedge zone and north of the injector A-3A. Some produced sea water is observed in June 2001, but the SWC does not reach a higher value than 5%. The well produces from below the OWC, and has had an increasing WCT. The WCT is 45% in the beginning and ends at a WCT of almost 100%.

BCS status: Sea water in BCS is not observed before November 2002 when new perforations are opened in Nansen. The sea water comes from the injector A-3A.

New relperm: No change.

Changes: In an attempt to get a lower water production, a fault was added just east of the well with a transmissibility factor of 0.01.

Result: While the fault did result in lower water production, it had the additional effect of causing a SWBT, only a couple months late with the same increasing trend.

- **A-37A [Eiriksson MF 07.97-10.00 ⇨ Eiriksson/Nansen MF 10.00-10.01]**

(Appendix C.2.12, Figure D.6)

A-37A is a horizontal wedge zone producer directly downflank from A-25AT3. A-37A was the first producer that experienced SWBT. The first SW was produced from the well in December 1999. After this the SWC increased rapidly and Eiriksson was totally water flooded in October 2000. Production from Nansen then started, but also here the SWC increased rapidly and was soon totally water flooded as well. The observation of WCT and SWC indicated that a massive waterfront came toward the well with a piston like displacement. A-25AT3 started injection of water in June 1999, and can be responsible for the SWBT. By the BT time A-25AT3 had injected 1.1Mill Sm^3 while A-3A had injected 7.2 Mill Sm^3. A-3A lies approximately 1.2 km north from A-37A and could also have caused SWBT. The well produced 2.26 Mill Sm^3 oil before it was closed, which was three times more than expected from RTD.

BCS status: BCS has SWBT in January 2001, and is 13 months late. Sea water from injectors A-3A and A-25AT3 are both responsible for SWBT. The well has a too low SWC, almost 80% before Nansen is opened, and 40% after.

New relperm: SWBT occurs a few months earlier, but the SWC magnitude is unchanged.

Changes: The transmissibility of the fault between A-25AT3 and A-37A was increased by a factor of 100 in the northern end of the fault, and by a factor of 5 in the southern end. This distinction was made to

conserve the match for nearby wells A-26A and A-26BT2. In addition, permeability in layer {2} was increased to 2 Darcy.

Result: The combination of these changes and the new relperm resulted in an earlier SWBT and a higher SWC after breakthrough. In addition, changes for A-40B have also been beneficial for A-37A, giving a higher SWC. Breakthrough is now only a few months late. The WCT match after 2000 is better. Total water and gas production has improved, whereas the oil production worsened.

- **A-40B [Eiriksson 09.01-03.02 ⇨ Eiriksson/Nansen 03.02-06.04]**

(Appendix C.2.13, Figure D.7)

A-40B was drilled in August 2001 and lies just south of the well A-37A. When production started in Eiriksson in September 2001, the layers were already waterflooded by injection water, most likely from A-25AT3. New perforations were therefore made in Nansen, where oil was found. The WCT in Nansen started at 50%, and increased to 80%. The initial SWC was 20%.

BCS status: In Eiriksson, the SWC is also far too low. The simulated SWC in Nansen is much too low, and SWBT does not occur until the middle of 2003, making it over 2 years late. The same can be said for the WCT (both Eiriksson and Nansen). The injected water comes from A-25 AT3 in the simulation.

New relperm: The SWC is higher and produced from start in both Eiriksson and Nansen, but is still too low.

Changes: Permeability around A-40B in BCS ranges from 100-600mD in layer {15-16}. This was increased to 4000mD, in agreement with the well log, which shows several high permeability zones in the middle of Eiriksson. Layer {15-16} was chosen on the basis that it was open only during the first production period (09.01-03.02), when the SWC was particularly low in BCS compared to observations.

Result: During the first production period, sea water is produced at production startup, but the SWC is still too low, only reaching 35%, whereas observations indicate roughly 60%. For the second production period (03.02-06.04), changes for nearby wells have improved both the WCT and the SWC. Total production for water, oil and gas have all improved.

- **A-26A [Eiriksson MF 06.00-11.03 ⇨ Eiriksson/Nansen MF 11.03-05.04]**

(Appendix C.2.7, Figure D.8)

A-26A lies south of A-37A and was placed here to be able to produce the oilbank forming in front of the injected water from A-25AT3. The well produced better than anticipated. This could be because it also produced oil that was displaced by the waterfront from injector B-18. The upflank injector B-18 lies south of A-26A. The well had a SWC of 0.05 at start of production and it increased almost linearly to 0.35 in November 2003. When production in Nansen started the SWC decreased to almost 0.20. The WCT, on the other hand continued to increase and the well was totally water flooded and therefore closed and sidetracked.

BCS status: No sea water shows up in BCS. Both water injected in A-25AT3 and B-18 approaches the well, and makes it very difficult to determine which of the injectors that causes SWBT in A-26A.

New relperm: Some sea water arrives at the well in 2003, but is still over 2 years late.

Changes: Transmissibility was increased by 50% in layers {14-17} in an attempt to get water earlier from B-18. The well log for A-26A indicates several zones where permeability reaches 4 Darcy. BCS has the highest in layer {16} of about 1 Darcy and lowest in layer {14} with 100-300mD.

Result: The resulting SWC matches observations both in terms of breakthrough time and magnitude. This is both due to the changes mentioned and the inclusion of a fault near A-32A. In addition, the WCT match has improved significantly. Total production volumes for water, sea water, oil and gas have all improved.

- **A-26BT2 [Eiriksson MF 05.04-12.05 ⇨ Eiriksson/Nansen MF 12.05-01.06]**

(Appendix C.2.8, Figure D.9)

In May 2004 A-26A was sidetracked to A-26BT2. At start the well had a WCT of 0.7 and a SWC of 0.15. The SWC increased rapidly to 0.45 and remained rather stable during the lifetime of the producer. The WCT kept increasing and the well was totally water flooded at end of production.

BCS status: Very little sea water shows up in BCS, and A-26BT2 has the same problem as A-26A. However, in April 2005 water tracer from B-18 was detected in A-26BT2. So water from injector B-18 should have reached the well. Since A-26A lies next to A26BT2, it may indicate that A-26A also should have received sea water from B-18.

New relperm: No change.

Changes: In layers {4-6}, a permeability of around 0.5-1 Darcy is used in BCS. A-26BT2 has no well log, but A-26A is very close, and the log from this well shows permeability reaching 10 Darcy in the uppermost Eiriksson layers. To get water earlier from B-18, transmissibility has been increased by a factor of 9; this is considered reasonable given the large difference between BCS and well log permeability.

Result: The SWC match has improved, now with sea water in place at start of production and a correct SWC. The WCT match has also improved. Total water, sea water and gas production volumes are now better, whereas the oil total is now too high instead of too low.

- **A-32A [Eiriksson MF 03.97-04.99 ⇨ Eiriksson/Nansen MF 04.99-04.02]**

(Appendix C.2.9, Figure D.10)

A-32A is located further south of the wells A-26A and A-26BT2. SWBT was observed in March 2000 and must be caused by injector B-18. The SWC increases to 40% before the well is closed in March 2002.

BCS status: SWBT in BCS occurs at a similar time as observed. Water from injector B-18 reaches the well in 2000, while water injected from B-1B reaches the well in 2003 ({1-3}). The SWC is too high, almost 35% throughout the lifetime of the well.

New relperm: SWBT and FWBT are now about a year too early. This has also resulted in excessive water production.

Changes: A fault directly east of A-32A was extended south by 6 grid blocks in order to get a slower SWBT. The original fault used a transmissibility factor of 0.001, the factor for the extension was set to 0.01.

Result: SWBT is with the fault extension better than BCS, both with a slightly earlier breakthrough and a lower SWC after breakthrough. The total water production has been lowered compared to the new relperm, but is still too high. Total oil and gas production has improved slightly.

Upflank SFA wells (north to south)

- **A-2B [Eiriksson/Nansen MF 11.2007-]**

(Figure D.11)

A-2B is a SFLL producer that is located upflank between the injectors A-8C and A-3A. The well has produced mostly gas and water, some small amounts of oil has also been produced. The well has produced at rather stable gas rates.

BCS status: The well gets sea water injected from A-3A from start of production. Sea water is located in every layer the well is producing from. SWC magnitude is in general 20% too high in the simulation.

New relperm: No change.

Changes: In order to reduce the SWC, it was attempted to add a fault between A-2B and injector A-3A. While this did improve the match, it had a negative effect on the match for A-10 by hindering the movement of water downflank. The small improvements for A-2B were considered less important than the loss of sea water at A-10, so the fault was removed.

Result: No change compared to BCS since the fault was not included.

- **A-15CT4 [Raude/Eiriksson MF 11.06-09.07]**

(Appendix C.2.4, Figure D.12)

A-15CT4 lies south of the producer A-2B and north of the injector A-3A. The well first produced from Raude and then in November 2006 production also started in Eiriksson. In June 2007 the well had a WCT of 96.2%, with a SWC of approximately 60%.

BCS status: Sea water is located in every layer the well produced from at start of production. The produced sea water comes from A-3A. When the well starts production in Eiriksson the WCT is almost 100%. The well only produces sea water in the simulation model, which gives a SWC of almost 100%. The simulated SWC is 40% higher than observed.

In Raude, sea water samples are somewhat ambiguous. Only two high SWC samples exist, whereas most samples are below 10%. Presumably, the samples with a high SWC are wrong. The data is therefore interpreted as indicating a SWC below 10%, making the simulated SWC too high.

New relperm: Total water production goes down slightly. SWBT in Raude occurs much later, in June 2006, and the SWC only reaches 5%. In Eiriksson, no changes are observed based on the new relperm.

Changes: Changes for other wells turned out to result in a SWC of nearly 100% in Eiriksson. To get a lower SWC, a fault was added between the well and the injector A-3A.

Result: In Raude, water production was lost, though the observed rate only averaged 150Sm^3/d. The fault added to lower SWC in Eiriksson was not the cause of the loss of water in Raude, however.

A slight drop in SWC did occur in Eiriksson, but only from 95% to 85%. The fault therefore had limited effect on the match for the well.

- **A-18D [Eiriksson MF 01.09-]**

(Appendix C.2.6, Figure D.13)

A-18D is a SFLL producer and was drilled in the beginning of 2009. The well is located in the same EF block as A-10AT2.

BCS status: Compared to observed data the well produces too much water in BCS and too little oil and gas. The well produces sea water from injector A-25AT3 from start. SWC is 20% too high. Note that this well only has one water sample.

New relperm: No change.

Changes: Two faults were added for the EF block with A-10AT2 and A-18D; see changes for A-10AT2.

Result: Simulated SWC is lower, consistent with results for A-10AT2. With only one water sample, no conclusion can be drawn regarding the quality of the SWC match. The WCT is unchanged and the cumulative water and gas production has improved slightly. Still, very little oil production occurs.

- **A-10AT2 [Raude EF/Eiriksson EF 04.03-07.03 ⇨ Eiriksson EF 07.03-08.04 ⇨ Eiriksson/Nansen EF 08.04-03.10]**

(Appendix C.2.2, Figure D.14)

A-10AT2 produces from the EF and is located south of the injector A-25AT3. The well has not produced much water. The EF block, with the well A-10AT2 and A-18D, ran out of gas in 2010. A-10AT2 was then closed.

BCS status: The well produces sea water from injector A-25AT3 from start. Both WCT and SWC are too high in BCS. The water production rate is also too high (by a factor of 5).

New relperm: For production after 08.04, the SWBT is delayed with about 6 months. After breakthrough, though, the same SWC is reached.

Changes: The well produces from Nansen, but the simulation model does not include grid blocks for Nansen at the location of the well. Layer {3} is the first perforated layer in the model. Since the water front progresses faster in Nansen {1-2}, it was attempted to increase communication by a factor of 2 between {2} and {3} to get earlier SWBT. However, no change was observed.

The model does not reflect the true geometry in this area. There are no EF blocks in the model. Hence A-10AT2 is producing from the MF. No fault had previously been implemented to separate the EF block

(with A-10AT2 and A-18D) from MF. Faults were now added to reduce communication with the wells, which in turn should result in lower water production and SWC. Two faults were defined, one to the north and west and one to the south. The southern fault was given a higher transmissibility, in order to match gas production (from A-39).

Result: SWBT has been delayed by an additional 4 months, which was expected after the inclusion of the fault. But, the SWC now drops from the beginning of 2008, similar to observations. The water production rate has now dropped almost down to the observed value. The WCT shows a similar delay as the SWC, indicating that no formation water is being produced. Cumulative production for all three phases has improved substantially.

- **A-40DT2 [Eiriksson/Nansen MF 03.07-]**

(Figure D.15)

A-40DT2 is a SFLL producer, which is located just north of the injector B-18. The well produces sea water from start. SWC is approximately 40% from start and increases to 70% at the end of 2009.

BCS status: Sea water in BCS is also observed from start of production. The SWC is approximately 45% too low. The small amount of sea water produced in BCS is caused by the injector B-18. Water injected from A-25AT3 is also very close to A-40DT2.

New relperm: Limited change, but slightly higher SWC.

Changes: A fault was added to separate an East Flank block from Main Field, as described in the changes for A-10AT2. This fault does not isolate A-40DT2 from MF, but has nonetheless had a positive effect on the well. The quality of the resulting match meant that no further changes were necessary.

Result: Both the SWBT and SWC is now well matched, with a similar improvement for the WCT.

- **A-35B [Raude MF 05.07-06.08 ⇨ Raude/Eiriksson/Nansen MF 06.08-01.10]**

(Appendix C.2.11, Figure D.16)

A-35B is located south of A-40DT2. A-35B first produced from Raude, and was in June 2008 opened in Eiriksson and Nansen. The WCT has been high throughout the lifetime of the well, on average 90%. SWC has on average been 45%.

BCS status: BCS has SWBT in July 2008, which makes it only 1 month late. The well has a WCT below 10%, when it should be 90%. SWC magnitude is also too low. Both injected sea water from B-1B and B-18 has reached the well when SWBT occurs in BCS.

New relperm: A higher SWC is reached after opening the new perforations in 06.08. The WCT also increases.

Changes: Permeability was increased to 5 Darcy in layers {27-29} in an attempt to increase the amount of water at the well. Well logs show permeability in some zones reaching several Darcy, whereas BCS uses only about 100mD.

Result: The SWC now rises to about the observed value after breakthrough. Water and sea water production rates have improved as a result of this. Total oil and gas production has also improved.

Producers located in Statfjord B area

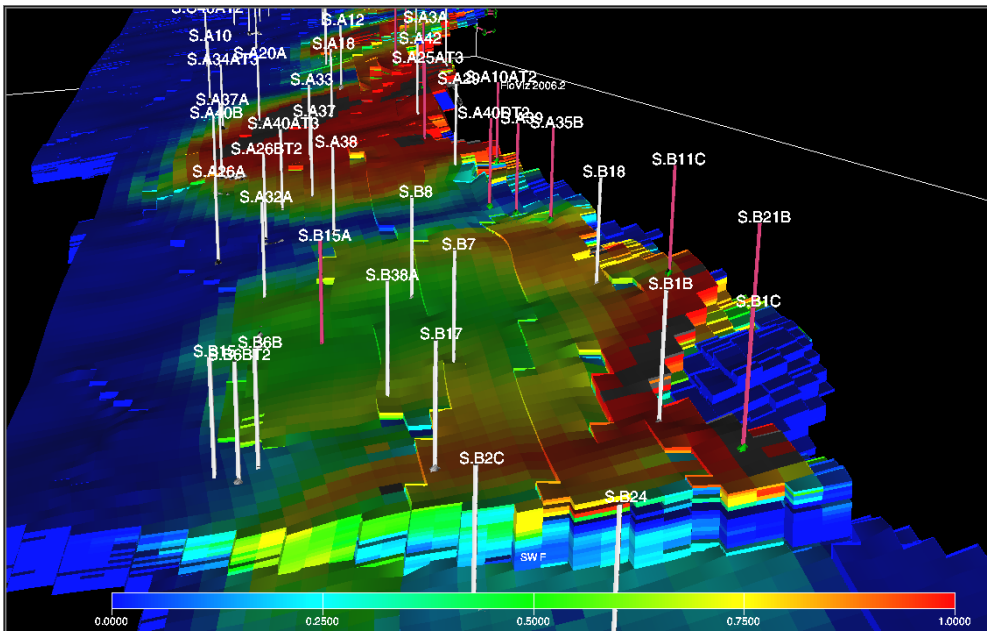

Figure 11.6: SWC; overview of Statfjord B north of F-11 in 2009, showing the uppermost layer.

Downflank SFB wells (north to south)

- **B-15A [Eiriksson MF 03.02-04.02 ⇨ Eiriksson/Rannoch MF 04.02-09.05 ⇨ Eiriksson/Rannoch/Ness MF 09.05-]**

(Figure D.17)

B-15 was in March 2002 sidetracked to B-15A, which is a horizontal well to the northern Statfjord B area. B-15A is located just west of the injectors B-18 and B-1B. When the well was drilled several local oil-water contacts were observed in different layers of sand, indicating that the upflank water seemed to be sliding on the shales.

BCS status: The simulated well experiences excessive amounts of water and sea water. This could be caused by an allocation error as the well is co-producing with the Brent Gp in the East Flank. The well is located in a complicated area with a more isolated middle Eiriksson Mbr, and upflank water flows on both top and bottom of the Eiriksson Mbr. The sea water produced comes from the well B-18 at start of production, and water from B-1B reaches the well the year after.

New relperm: Slight increase in water production.

Changes: Because the well has simultaneous production with Brent, it was not possible to history match the sea water cut, so no changes have been applied. This is connected to the large uncertainties

associated with allocation of water production when the well produces from both Brent and Statfjord, which in turn makes it virtually impossible to estimate the SWC from Brent and Statfjord separately.

Result: The changes made for other wells have only had a minor influence on B-15A.

- **B-15 [Eiriksson MF 03.94-08.01]**

(Appendix C.2.17, Figure D.18)

B-15 was the first producer in the B area that had SWBT. SWBT was observed in September 1999. B-15 was a horizontal wedge zone producer downflank south of B-18. The WCT kept increasing, and the well watered out in March 2001. The SWC was 75% at the end of production.

BCS status: The simulated well misses the observed sea water breakthrough in 1999. Sea water does not move as rapidly as expected to B-15, and SWBT in the simulation is not observed before January 2001. SWBT occurs two years late and is caused by the injector B-18. Water from B-1B reaches the well the year after SWBT. A high permeability channel not included in the geomodel may be present in the area because of the early SWBT and the high observed SWC.

New relperm: SWBT occurs a year earlier and the SWC rises to about 40%.

Changes: Transmissibility has been increased by a factor of 3 in layer {11}, in order to encourage fingering of water and get an earlier breakthrough. BCS uses 500-800mD in the same area. Well logs indicate some zones with permeability up to 1 Darcy.

From 1994-1999, the well has a too high WCT. A fault slightly west of the well has been extended 4 grid blocks to the south, in an attempt to stop water from reaching the well. The fault extension has the same transmissibility as the rest of the fault.

Result: The simulated SWBT now occurs in the middle of 1999, and the SWC increases to about 70%, both in agreement with observations. The WCT match is nearly unchanged up to 1999, but has improved considerably after. Total oil production has also improved somewhat. However, total water production has become too high and gas production too low.

The WCT match for 1994-1996 is nearly unchanged, and is slightly lower from 1996-1999, presumably due to the fault extension.

- **B-6BT2 [Eiriksson MF 02.00-07.00 ⇨ Nansen MF 07.00-08.00]**

(Appendix C.2.15, Figure D.19)

B-6BT2 was drilled in February 2000 as a horizontal well. The well is located downflank south of B-18. The purpose of B-6BT2 was to be able to produce the oil that had been penetrated by the injector B-38A in lower part of Eiriksson. The horizontal position of B-6BT2 was positioned at 2805-2809, which was expected to be close to the OWC. Eiriksson was, however, already water flooded by the injector B-18. The following perforations in Nansen also showed that the uppermost layers were water flooded. The well produced with WCT of almost 100% and SWC increasing from 10% to 25%.

BCS status: No sea water shows up in BCS. Sea water from injector B-18 does not reach the well before 2005, which makes the SWBT about 5 years late.

New relperm: No change.

Changes: Transmissibility was increased by a factor of 4 in Nansen layers {1-2}. In BCS, permeability ranges from 1200-1600mD. The well log for B-6BT2 was not available, but the log from nearby B-15 shows permeability reaching 10 Darcy in the uppermost layer.

Result: A SWBT now occurs at about June 2000, only a few months late. Oil production has also gone up somewhat, with a corresponding drop in water production.

- **B-17 [Eiriksson MF/Rannoch EF/Etive EF 06.98-09.06]**

(Figure D.20)

B-17 is located downflank of the injector B-1B. The water production from Well B-17 may be erroneously allocated from 2003 onwards in the Prosty production data base. A PLT survey carried out in 2003 indicated a water rate of 1000 Sm3/d from the Statfjord Fm, while the production data base indicates only 300 Sm3/d in the same period. SWBT is observed in February 1999, and is most likely from the Brent reservoir since water injection from B-1B started in April 2000. In Statfjord, the injector that can provide SWBT first is B-18, which starts injection in February 1998. However, tracer added to B-18 injection water in March 2003 was never detected in B-17, indicating poor communication between B-17 and B-18. Therefore, the initial SWBT should be attributed to Brent.

BCS status: The simulated well experience sea water production from Statfjord Fm in June 2003. The simulated SWBT cannot be compared to the observed since the first sea water produced came from Brent. The sea water produced in Brent results in a high SWC for the well, and because most of the water is from Brent, the SWC for the well in Statfjord Fm is unknown. In the simulation, water from B-18 reaches the well first, and one year later the water from B-1B has also reached the well.

New relperm: SWBT occurs 5 months earlier and has a higher SWC magnitude.

Changes: Because the well has simultaneous production with Brent, it was not possible to history match the sea water production, so no changes have been applied.

Result: The well has been affected somewhat by other changes.

Upflank SFB wells (north to south)

- **B-11C [Eiriksson/Nansen MF 04.07-]**

(Appendix C.2.16, Figure D.21)

B-11C is a SFLL producer located south of the injector B-18. The well has produced small amount of water, only 2.0 x 10^5 Sm^3. Sea water produced is only 0.5 x 10^5 Sm^3.

BCS status: B-11C produces water injected from both injectors B-18 and B-1B from start. SWC is too high in the simulation model. From start SWC is 30% too high, while at end it is only 5% too high.

New relperm: Only minor changes; for the first few months of production, the WCT and SWC are slightly better matched.

Changes: Permeability in BCS ranges from 2000-2500mD in Nansen. In an attempt to reduce sea water production, this was reduced to 500mD in a small region around the well. The B-11C well log shows permeability averaging about 500mD in Nansen. A fault was also added between B-11C and the injector B-18, also to lower sea water production. The transmissibility factor of the fault was 0.001.

Result: For unknown reasons, the well no longer produces oil. As a result the WCT is now too high. However, the SWC has gone down, as intended. It turned out that the SWC in B-11C was extremely sensitive to changes for other wells. In addition the water, sea water and gas production rates are better matched. It turned out that B-11C was sensitive to changes made for other wells. It is therefore not entirely clear which changes caused the final result.

- **B-21B [Raude MF 12.00-11.05 ⇨ Eiriksson EF 11.05-]**

(Appendix C.2.18, Figure D.22)

B-21B is located north of the injector B-1B and produces from the East Flank. The well has not produced sea water. When the well was opened in Eiriksson the WCT was below 10%, while when producing from Raude the WCT reached 55%.

BCS status: The East Flank where B-21B is situated is not isolated from the main field in the simulation. Water from B-18 reached the well January 2007, and B-1B the year after. The SWC then increases rapidly to 80%.

New relperm: In Eiriksson, sea water cut has been reduced considerably for the first two years, but the SWC still rises to over 70% eventually.

Changes: Faults have been introduced (using RESVIEW) to separate the east flank block from the main field. In Upper Statfjord, MULTFLT has been set to 0.0001, and to 0.1 in Lower Statfjord. It was discovered that a very low MULTFLT in LS resulted in a loss of water production here, and it was therefore set to 0.1.

Result: With fairly good communication across the fault in LS, the water cut was maintained at a similar level as BCS. In US, the low fault communication resulted in a loss of water production, thereby also eliminating the unwanted sea water breakthrough.

- **B-1C [Raude MF 02.08-10.08 ⇨ Eiriksson/Nansen MF 10.08-]**

(Appendix C.2.14, Figure D.23)

B-1C is a SFLL producer located just south of the injector B-1B. The well was first perforated in Raude, but since only water was found and no gas it was decided to close the well. B-1C was then opened in Upper Statfjord, where gas production began. B-1C has only produced 2.5×10^4 Sm^3 of sea water. Water production from Raude continued when producing from Upper Statfjord since Raude was not possible to isolate.

BCS status: In the simulation B-1C produces water injected from B-1B. There is very small amount of water in BCS, which has caused a numerically unstable WCT and SWC. Raude is closed in BCS, which might explain why the water production is so low.

New relperm: No change.

Changes: A fault was added, just north of and in parallel with the F-11 fault, to stop sea water coming from B-1B. The presence of this additional fault is considered plausible since small faults often form near major faults. In addition, layers {29-30} were opened in the simulation to produce formation water instead of sea water (to take into account the Raude contribution). Also:

- The transmissibility factor (in cP·m^3/day·bar) for the connection with the well in {29} and {30} was increased from about 1 and 3 to 15.
- Permeability was increased layer {30} to 4000mD from what was only 5-100mD in BCS. The well log from nearby B-13 shows permeability reaching several Darcy in Lower Statfjord, indicating a severely underestimated permeability in BCS.

However, the new fault also hindered production of formation water from Raude, so different fault transmissibility factors were used in Upper and Lower Statfjord. In Upper Statfjord, a factor of 0.01 was used, and in Raude, it was set to 1.

Result: A stable SWC of 30%, closer to the observed SWC of 10%. However, this was not a result of the fault, more likely due to the opening of layers {29-30} and the increase in permeability in {30}. None of the changes have resulted in any water production after October 2008. It is unclear why the opening of layers {29-30} are not contributing with water production after being opened, but it might be due to too low Raude pressure.

It was chosen to keep the fault because it turned out to result in lower water production in B-11C.

12 History matching summary

The changes and results presented in chapter 11 in addition to field and platform level results will be summarized in this chapter. Plots for the field and individual platforms are given in appendix E.

Tables 12.1 and 12.2 provide a summary of breakthrough times for

- Observations
- Base Case Simulation (BCS)
- History matched simulation

For all three cases, the breakthrough time is listed (columns "SWBT"). Based on the time of SWBT, the time difference between breakthrough in the simulation and in observations has been calculated, both for BCS and the history matched simulation (columns ΔSWBT):

- When an observed SWBT has occurred, and never in the simulation before the well is closed, ΔSWBT is calculated using the end date of the well, with the implication that ΔSWBT would have been even larger had the well remained open. In these cases, ΔSWBT is therefore denoted with a "larger than" symbol.
- When breakthrough occurs in the simulation before being observed, ΔSWBT is negative.
- When breakthrough occurs from start in both the simulation and observations, ΔSWBT is not defined (marked by "—").

A comparison of the SWC in the simulation before and after history matching has also been included (column SWC). This comparison simply states whether the match has improved, worsened or is approximately the same.

12.1 Downflank wells

The time between observed and simulated breakthrough (ΔSWBT), including the SWC after breakthrough, has improved for all downflank wells.

Southern SFA wells

In particular, the match for downflank wells in the southern half of the SFA area has improved significantly. This includes A-37A, A-40B, A-26A, A-26BT2 and A-32A. These wells all had a late SWBT in BCS. The injectors that have given a SWBT in these wells are A-25AT3 and B-18. The time of SWBT is now very well matched for these producers, making it the region with the best match for ΔSWBT. Changes made to improve the SWC, have not only improved the SWC match – cumulative production volumes for water, oil and gas are now also significantly better matched.

An important change in this area was to increase the communication through a fault just west of injector A-25AT3. This has allowed more water to move downflank earlier, especially towards producers A-37A and A-40B. Also, water from injector B-18 now moves faster after permeability was increased in selected layers in the region between B-18 and producers A-26A and A-26BT2. A-32A produced excessive amounts of water with the new relperm, and a fault was therefore extended to delay the arrival of sea water.

Northern SFA wells

The SWC match for producer A-34AT3 has improved. The simulated SWBT is now only a few months late and the SWC never exceeds 5%, as observed.

A-10 and A-12 are situated just north of A-34AT3, with injectors A-3A and A-8C closest. It proved to be difficult to match A-10 and A-12 simultaneously. Both had a late SWBT, and it was known that initial breakthrough in A-12 and A-10 was from A-3A, since A-8C had not started injecting at the time of breakthrough. Various changes were made to get an earlier breakthrough in A-12 and A-10. But after matching the SWBT and SWC, water production was far too high in both wells. A-10 proved to be particularly difficult, with breakthrough being over 2 years late in BCS, fairly radical changes were needed. Even after introducing a high permeability zone in two layers in upper Eiriksson, breakthrough was only just detected before A-10 was closed. To maintain the match for A-12, this high permeability zone was created *around* A-12 (east and north), as it would have otherwise resulted in even higher water production and a premature SWBT in A-12. Despite the high water production, the final SWC match has improved significantly for both A-10 and A-12.

Located further north is A-17A, for which the new relperm resulted in a too high SWC and early SWBT. A fault was therefore introduced to compensate for the new relperm, by hindering the movement of water from injector A-8C. The changes have also resulted in better matched water and gas production, while the oil production is now too low. Nearby well A-2A had a well matched SWC in BCS, and no changes were implemented.

SFB wells

Both B-15 and B-6BT2 receive water from injector B-18. B-15 has sea water breakthrough 18 months late, with a far too low SWC after breakthrough. In B-6BT2, SWBT is never detected in BCS, though the well is only open for 6 months, making breakthrough at least 6 months late. A high permeability region has been introduced around both wells, and has resulted in much better matched breakthrough times and SWC.

As B-15A and B-17 produced simultaneously with Brent, significant uncertainties are tied to observed data, in particular the SWC (water samples show the *combined* well SWC from Brent and Statfjord). This makes it nearly impossible to match the SWC for Statfjord, since it was known that Brent was contributing with sea water.

Well	Observed	BCS		History matched		
	SWBT	SWBT	ΔSWBT	SWBT	ΔSWBT	SWC
A-2A	Nov. 02	From start	< -5 months	From start	--	Same
A-17A	Oct. 01	Aug. 01	-2 months	Aug. 01	-2 months	Same
A-10	Mar. 01	Never	> 2 years	Jun. 01	3 months	Improved
A-12	Jan. 99	Feb. 00	13 months	Jan. 98	-1 year	Improved
A-34AT3	Jun. 01	Nov. 02	17 months	Jul. 01	1 month	Same
A-37A	Dec. 99	Jan. 01	13 months	Dec. 99	0	Improved
A-40B	From start	Nov. 01	3 months	From start	0	Improved
A-26A	From start	Never	> 4 years	Nov. 00	5 months	Improved
A-26BT2	From start	Never	> 2 years	From start	--	Improved

A-32A	Mar. 00	Apr. 00	1 month	Mar. 00	0	Improved
B-15A	From start	From start	--	From start	--	Same
B-15	Sep. 99	Jan. 01	18 months	Oct. 99	1 month	Improved
B-6BT2	From start	Never	> 6 months	May 00	3 months	Improved
B-17	?	Mar. 03	?	Mar. 03	?	Same

Table 12.1: Wells situated downflank

12.2 Upflank wells

The upflank wells were challenging to match, more so than the downflank wells. Since the upflank wells are close to the injectors (which are also located upflank), sea water is almost always produced from startup.

SFA wells

A-2B is fairly well matched in BCS; some changes were attempted, but the small improvements did not weigh up for the discrepancies that resulted for nearby wells. The match for A-15CT4, just south of A-2B, was also difficult to improve. Both A-2B and A-15CT4 have a too high SWC, both above 80%. In the region around A-2B and A-15CT4, various faults were added to limit sea water production, but this did not improve the match. However, a single fault between A-15CT4 and injector A-3A was kept, but still with only minor improvements.

A-10AT2 and A-18D are located in an EF block, which was not isolated from the Main Field in BCS. Therefore, faults were added to separate the block from MF. For A-18D this has had a positive effect on cumulative production volumes (water, oil and gas). With only one water sample, it is difficult to conclude whether the SWC match improved or not. For A-10AT2, SWBT was delayed by over a year, but cumulative production volumes for water, oil and gas have all improved. The overall match for A-10AT2 and A-18D has improved significantly, though this is apparent from WCT and SWC plots.

Both the WCT and SWC for A-40DT2 were too low in BCS, and were improved considerably due to changes for nearby wells. Permeability was raised in a specific layer around A-35B, which resulted in a better matched WCT and SWC.

SFB wells

Around B-11C, permeability was lowered in Nansen, and a fault was added between it and injector B-18. Both of these changes were implemented to lower the SWC, which was initially too high in BCS. This did result in a lower SWC, albeit only slightly. B-11C turned out to be very easily affected by other changes, even those far from the well; most often raising the SWC in B-11C. Strangely though, a fault added just south of B-1C helped to lower the SWC in B-11C.

B-21B is situated in an EF block, which (like the block with A-10AT2 and A-18D) was not separated from the Main Field in BCS. Virtually no water production was observed, whereas BCS has both a high WCT and SWC. By isolating the EF block with faults, simulated water production disappeared almost entirely, resulting in a very good match.

B-1C proved to be one of the most difficult wells to history match. This was mainly due to the lack of formation water in the simulation, as the well did produce water at a low SWC, which is believed to be water from Raude (which was unsuccessfully closed earlier). All attempts to produce water from Raude in the simulation failed, possibly due to the low pressure in Raude.

Well	Observed	BCS		History matched		
	SWBT	SWBT	ΔSWBT	SWBT	ΔSWBT	SWC
A-2B	From start	From start	--	From start	--	Same
A-15CT4	From start	From start	--	From start	--	Same
A-18D	From start	From start	--	From start	--	Same
A-10AT2	From start	From start	--	Mar. 06	19 months	Improved
A-40DT2	From start	From start	--	From start	--	Improved
A-35B	From start	Jul. 08	1 month	From start	--	Improved
B-11C	From start	From start	--	From start	--	Improved
B-21B	Never	From start	< -4 years	Never	--	Improved
B-1C	From start	From start	--	From start	--	Improved

Table 12.2: Wells situated upflank

12.3 Field and platform results

The term "field" will be used in the following to represent the Statfjord Fm only. The new relative permeability for Upper Statfjord has been applied field wide, and is therefore the only change that affects SFC and the southern half of SFB. When discussing field level results, SFA and SFB will therefore be given the most attention.

The sea water production rate was initially too low in BCS, with SWBT approximately a year late (see Figure 12.1). The combined effect of the new relperm and local changes resulted in an improved match the first few years after breakthrough. The match is also better overall. Plots for the individual platforms are shown in Figures E.1-E.3. The most significant improvements are seen for SFA. For SFB, the only notable changes have occurred for the first year after breakthrough and the last 3 years (2007-2010), where the match has improved. SFC has only minor differences compared to BCS.

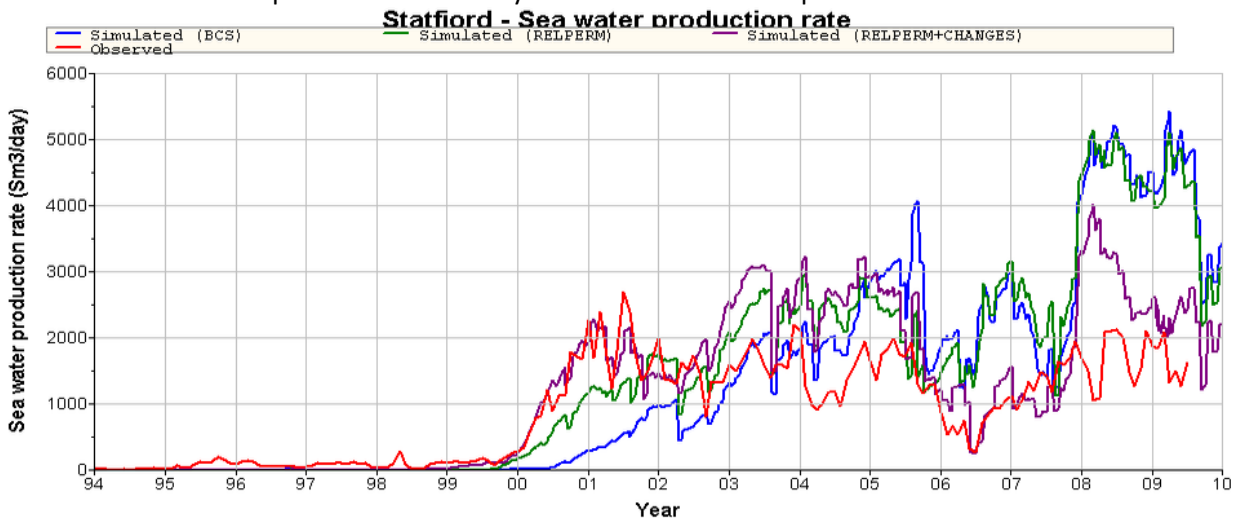

Figure 12.1: Statfjord Fm sea water production rate.

The field WCT is shown in Figure 12.2, where it is seen that the WCT is higher in the first 15 years, mainly due to the new relperm. This was expected since the model had previously been history matched based on WCT and the sea water breakthrough times were generally too late for downflank producers. The work related to reducing production of formation water was outside the scope of this study. After 1995, the WCT is nearly unchanged. For the individual platforms (Figures E.4-E.6), it is also seen that the initial WCT is higher, which is expected when using an oil-water relperm with higher water mobility. For SFA, this has improved the match, as the BCS WCT was too low up to 1990. But for SFB and SFC it has worsened the match, as the WCT here was already overestimated in BCS.

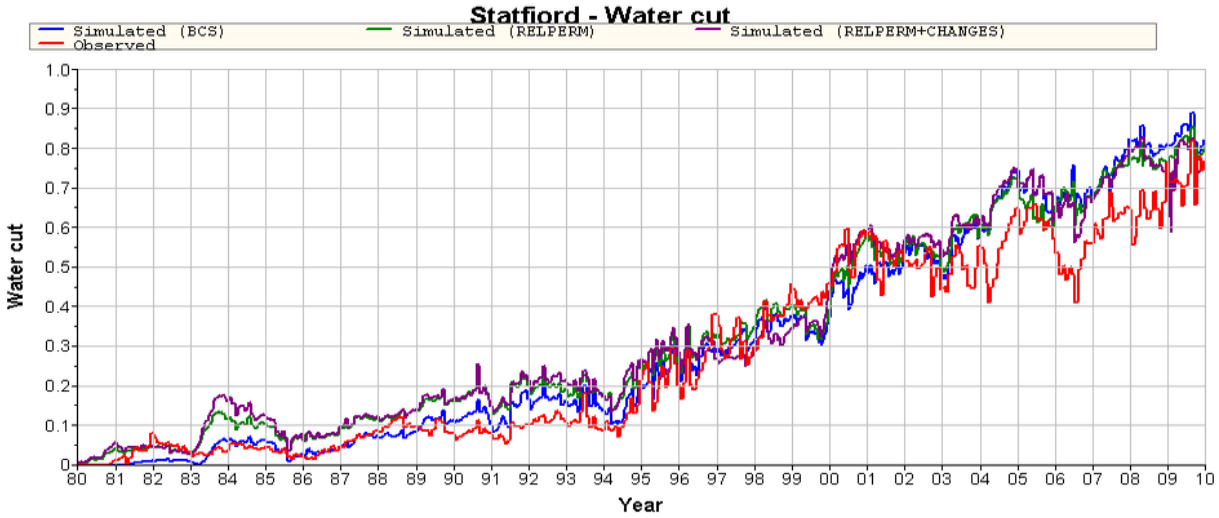

Figure 12.2: Statfjord Fm water cut.

The gas-oil ratio has changed very little, as seen in Figure 12.3. For SFA (Figure E.7), the new relperm resulted in a too low GOR from 2005 onwards, but the additional changes put the match nearer to BCS. For SFB (Figure E.8), the GOR is almost identical to BCS up to 2006, after which it has been lowered and better matched, both due to the new relperm and the local changes. The GOR for SFC (Figure E.9) is practically unchanged.

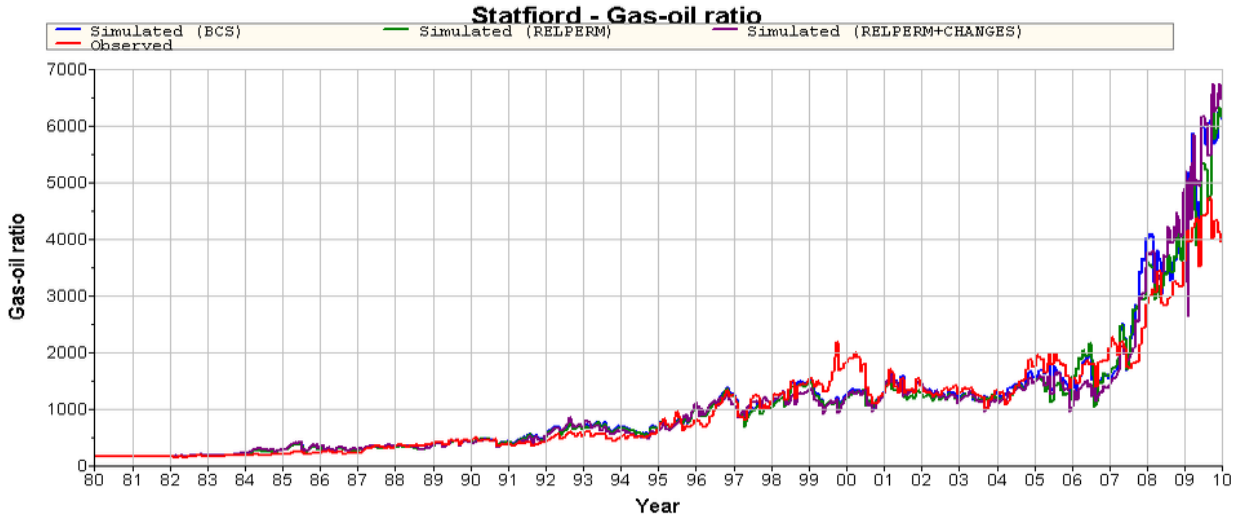

Figure 12.3: Statfjord Fm gas-oil ratio.

Cumulative production volumes of water, oil and gas is shown in Figures 12.4-12.6, respectively.

With a much higher water mobility, the new relperm has increased the total water production massively. It is clear that the relperm itself is mostly to blame for this, as the history matched case is only slightly different from the case with only the relperm. This additional water production has actually improved the match for SFA (Figure E.10) from startup until 1997. After 1997, the new relperm causes excessive water production, though the additional changes have eliminated a significant portion of this.

Water production for SFB (Figure E.11) has been raised both by the new relperm and the local changes. It turned out that the fault introduced between B-1C and the injector B-1B has actually resulted in increased water production for some SFB producers south of the F-11 fault.

No water was injected south of F-11, but gas injection continued in this region when GCWI started elsewhere. However, gas injection south of F-11 was not sufficient to maintain the same pressure support as that achieved north of F-11. Some injected water has therefore moved through F-11 as a result of the pressure being lower, and thereby providing additional pressure support. Simulation results show that water has a tendency to move through F-11 downflank more easily than upflank.

The increased water production of SFB producers south of F-11 can therefore be explained by the new fault directing more of the injected water downflank towards the “opening” in F-11, where it has resulted in a more rapid rise of the oil-water contact and higher water production. The validity of this new fault could therefore be questioned, and for a match of the entire field, an exclusion of the fault could be considered.

As expected, only the new relperm has affected SFC (Figure E.12), in the form of increased water production.

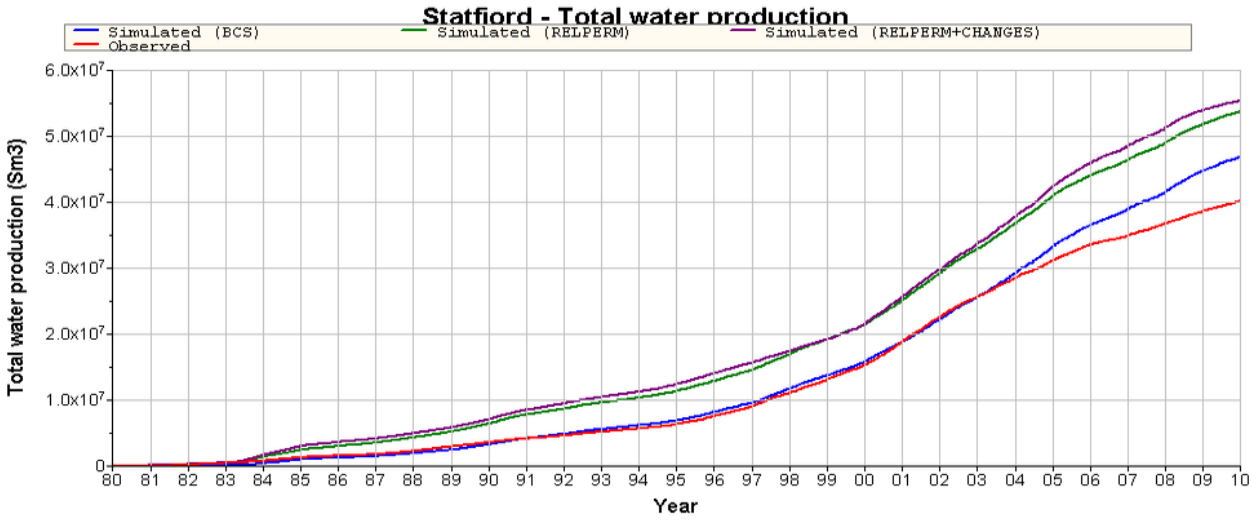

Figure 12.4: Statfjord Fm cumulative water production.

Cumulative oil and gas production for Statfjord is shown in Figures 12.5 and 12.6. The final total for both oil and gas has decreased, corresponding to the increased water production.

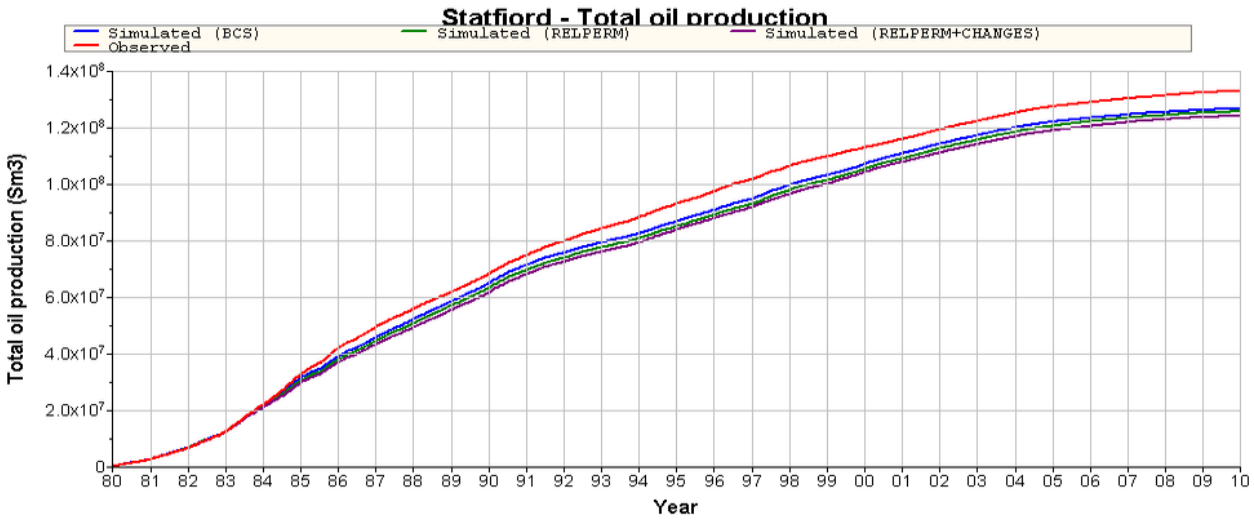

Figure 12.5: Statfjord Fm cumulative oil production.

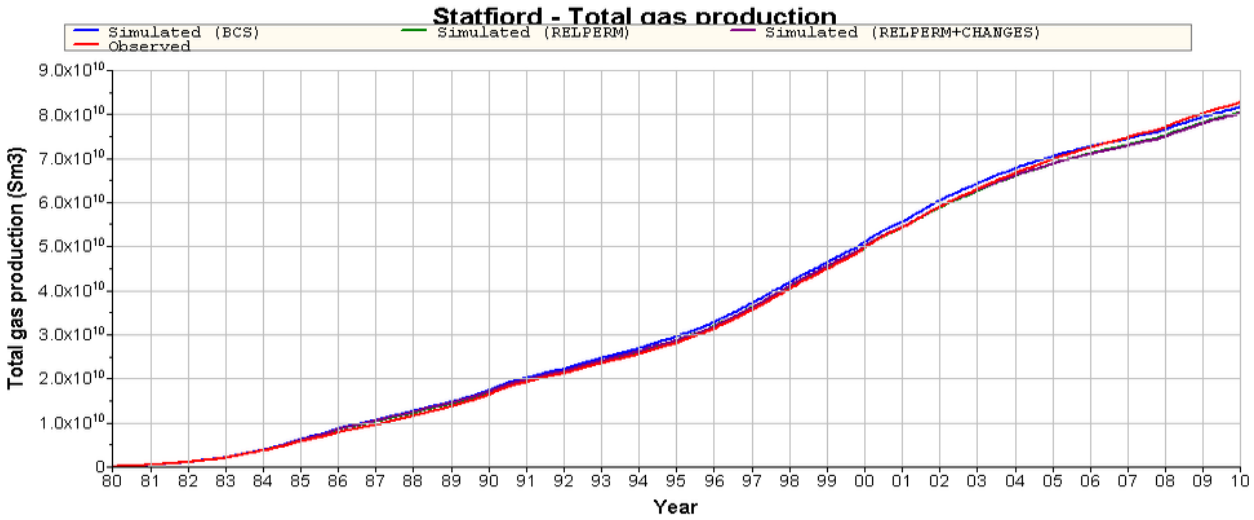

Figure 12.6: Statfjord Fm cumulative gas production.

14 Conclusions

A sea water tracer has been used to perform a history match of the Statfjord Fm model. By comparing model results with the sea water cut in well water samples, several changes have been suggested for implementation in the model. The wells considered were located in the SFA and SFB area north of the F-11 fault, where most of the upflank water injection took place.

- Comparisons of upflank and downflank wells indicated that the model had a tendency to spread more of the injected water in a north-south direction at the crest of the field. Observations, on the other hand, showed that the model gave late sea water breakthrough in downflank producers and a too high sea water cut in upflank producers.
- The first step towards accelerating sea water production in downflank wells was to introduce a new water relative permeability that had higher water mobility. This did improve sea water breakthrough times for several wells, but also resulted in excessive water production.
- Further, it was attempted to improve the match by modifying existing faults, adding new faults and changing permeability in selected layers. These efforts were largely successful in improving breakthrough times for sea water and the general sea water cut match.
    - Downflank wells, particularly in the southern half of the SFA area, obtained a better match, both the SWC match and the volume match for water, oil and gas.
    - Sea water breakthrough times and SWC also improved for northen downflank SFA wells, but the volume match was not as good.
    - In general, upflank wells had a too high SWC, which turned out to be difficult to reduce, even with extensive faults acting as barriers for the water. While the match for most wells improved, the discrepancy between the model and observations is still notable.
    - Two East Flank blocks are also located upflank, and were not isolated with faults in the base case. After implementing the faults, the sea water cut was reduced in wells within these blocks, thereby improving the match.
- The combined sea water production rate for all Statfjord Fm wells show that the sea water breakthrough occurs almost a year earlier than the base case, now matched accurately with the observed breakthrough.

The main objective of this study was to improve the sea water cut match in the southern SFA and northern SFB area. Changes implemented have resulted in a better match. This has been the first step towards matching the model based on the sea water cut. Further work is needed to match the remaining wells and to reduce formation water production.

15 Nomenclature

3D	: Three Dimensional
CPU	: Central Processing Unit
EF	: East Flank
EOR	: Enhanced Oil Recovery
FFM	: Full Field Model
Fm	: formation
GCWI	: Gas Cap Water Injection
GIIP	: Gas Initial In Place
GOR	: Gas Oil Ratio
GRR	: Gravity Reference Rate
IOR	: Improved Oil Recovery
LS	: Lower Statjord
MF	: Main Field
MMP	: Minimum Miscibility Pressure
NNC	: Non-Neighbor Connection
OWC	: Oil Water Contact
SFA	: Statfjord A
SFB	: Statfjord B
SFC	: Statfjord C
SFLL	: Statfjord Late Life
STOIIP	: Stock Tank Oil Initial In Place
STOOIP	: Standard Tank Oil OriginalllyIn Place
US	: Upper Statfjord
SW	: Sea water
SWC	: Sea water cut
SWBT	: Seawater-Breakthrough
WAG	: Water-Alternating-Gas
WCT	: Water Cut
WI	: Water Injection

16 References

[1] A.K. Danona and R.A. Morse, "Down-Dip Waterflooding of an Oil Reservoir Having a Gas Cap," SPE paper, 5086 (1975).

[2] J. A. Adamson and D. L. Flock, "Prediction of Miscibility," SPE paper (1962).

[3] T. Ahmed, "Reservoir Engineering Handbook 2nd ed, Pinciples of Waterflooding " Gulf Professional Publishing (2001).

[4] D. S. Asgarpour, "An Overview of Miscible Flooding," JCPT paper, Volume 33, No. 2 (1994).

[5] L. E. Baker, "Three-Phase Relative Permeability Correlations," SPE paper 17369 (1988).

[6] R. Boge, A. Brendsdal, T. Flatebø, D. Frafjord, A. Gjesdal, A.-G. Hansen, L. Kirkevollen, S. Kvernes, S. O. Netland, E. F. Nilsson, P. T. Sandbakken, M. Skeide, K. Skår, E. Stangeland, and P. Theriault, "Status of Surveillance of the Statfjord Formation at the Statfjord Field January 2003," Statoil (2003).

[7] R. Boge, S. K. Lien, A. Gjesdal, and A. G. Hansen, "Turning a North Sea Oil Giant Into a Gas Field - Depressurization of the Statfjord Field," SPE paper, SPE 96403 (2005).

[8] W. J. Carrigan, H. A. Nasr-El-Din, S. H. Al-Sharidi, and I. D. Clark, "Geochemical characterization of injected and produced water from Paleozoic oil reservoirs in Central Saudi Arabia," SPE paper, 37270 (1997).

[9] T. Ertekin, J. H. A. Kassem, and G. R. King, "Intoduction" In "Basic Applied Reservoir Simulation" Vol. 7 (SPE Textbook Series), Society of Petroelum Engineers Inc., Richardson, Texas, 2001.

[10] J. R. Fanchi, PRINCIPLES OF APPLIED RESERVOIR SIMULATION, 2nd ed, 2001.

[11] E. Hegre, V. Dalen, and H. O. Strandenaes, "IOR Potential With Updip Water Injection in the Statfjord Fm at the Statfjord Field," SPE paper, SPE 28841 (1994).

[12] O. Huseby, C. Chatzichristos, J. Sagen, J. Muller, R. Kleven, B. Bennett, S. Larter, A. K. Stubos, and P. M. Adler, "Use of natural geochemical tracers to improve reservoir simulation models," SPE paper (2005).

[13] Jan Inge Logstein, Eirik Fekjær Nilsson, Egil Boye Petersen Jr., Frode Sedberg, Bjarte Gil, Sigurd Haugen, and A. Zerzar, "The Statfjord Field FFM2005 Study. Part 2 – Reservoir Engineering Dynamic Model and Forecasts," Statoil ASA, Internal document (2005).

[14] B. Jhaveri, G. Youngren, J. Dozzo, L. Schnell, and M. Maguire, "Pressure Support Through Large Scale Gas Cap Water Injection At Prudhoe Bay," SPE paper, SPE 76728 (2002).

[15] S. E. Kindem, "Statfjord Formation Dynamic Model," Statoil (Internal Document) (2009).

[16] O. Kjørholt, "RESVIEW: A Practical 3-D Tool for Reservoir Engineers," SPE paper, SPE 24270 (1992).

[17] H. Kleppe, "Reservoir Simulation," University of Stavanger (2007).

[18] L. F. Koederitz, LECTURE NOTES ON APPLIED RESERVOIR SIMULATION, World Scientific Publishing Co. Pte. Ltd., 2005.

[19] K. Lejon and O. Vikane, "The use of Scale Dissolver and Scale Inhibitor Squeeze Treatments to Repair and Prevent Formation Damage in Two Statfjord Field Wells," SPE paper (1996).

[20] S.M. Skjæveland and J. Kleppe, "Recent Advances in Improved Oil Recovery Methods for North Sea Sandstone Reservoirs; Gasflooding," Norwegian Petroleum Directorate (1992).

[21] Schlumberger, "ECLIPSE Reference Manual," (2009).

[22] Schlumberger, "FloViz User Guide 2009.1," (2009).

[23] Schlumberger, "Reservoir Engineering Software," 29.03, 2010, <http://www.slb.com/services/software/reseng.aspx>.

[24] E. Stangeland, "Upflank Water Injection Statfjord Fm," Statoil (Internal Document) (2010).

[25] E. Stangeland, P. Labes, S. V. Lundbo, T. N. Monsen, K. Helland, A. Jonassen, E. Evensen, H. Breivik, G. Løklingholm, S. L. Rygh, H. C. Magelsen, and E. Ø. Bjørnestad, "Statfjord Reservoir Development Plan 2007," Statoil (2007).

Appendix

A Figures for chapter 2

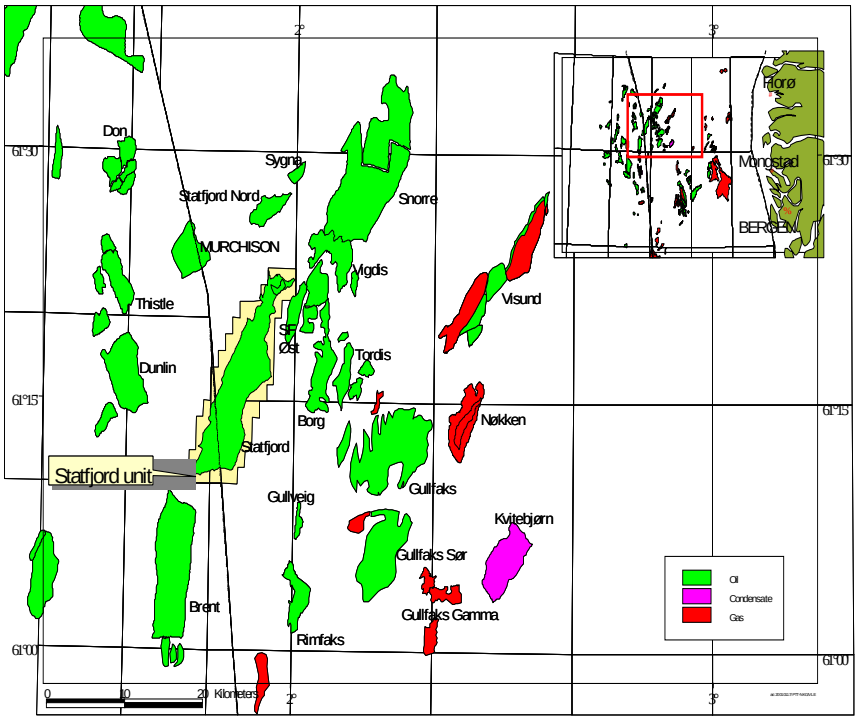

Figure A.1: Statfjord Unit and Tampen area [24].

Figure A.2: Size of Statfjord Field imposed on a map of the Stavanger region [24].

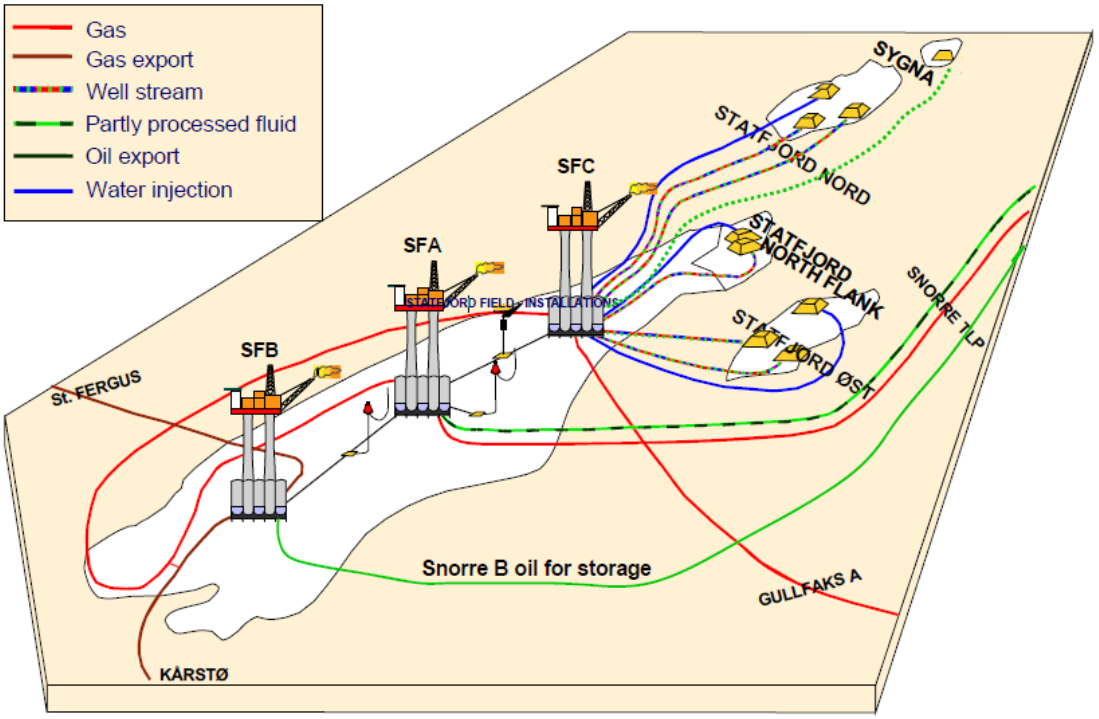

Figure A.3: The Statfjord Field installations and tie-ins [25].

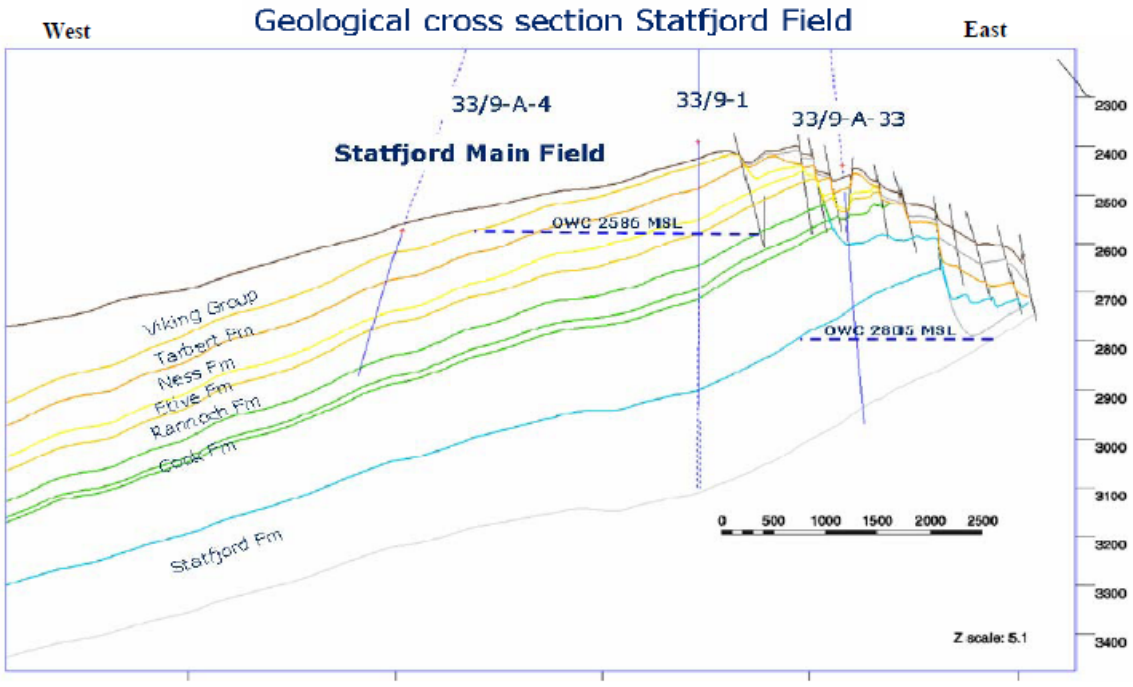

Figure A.4: Geological cross section Statfjord Field [25].

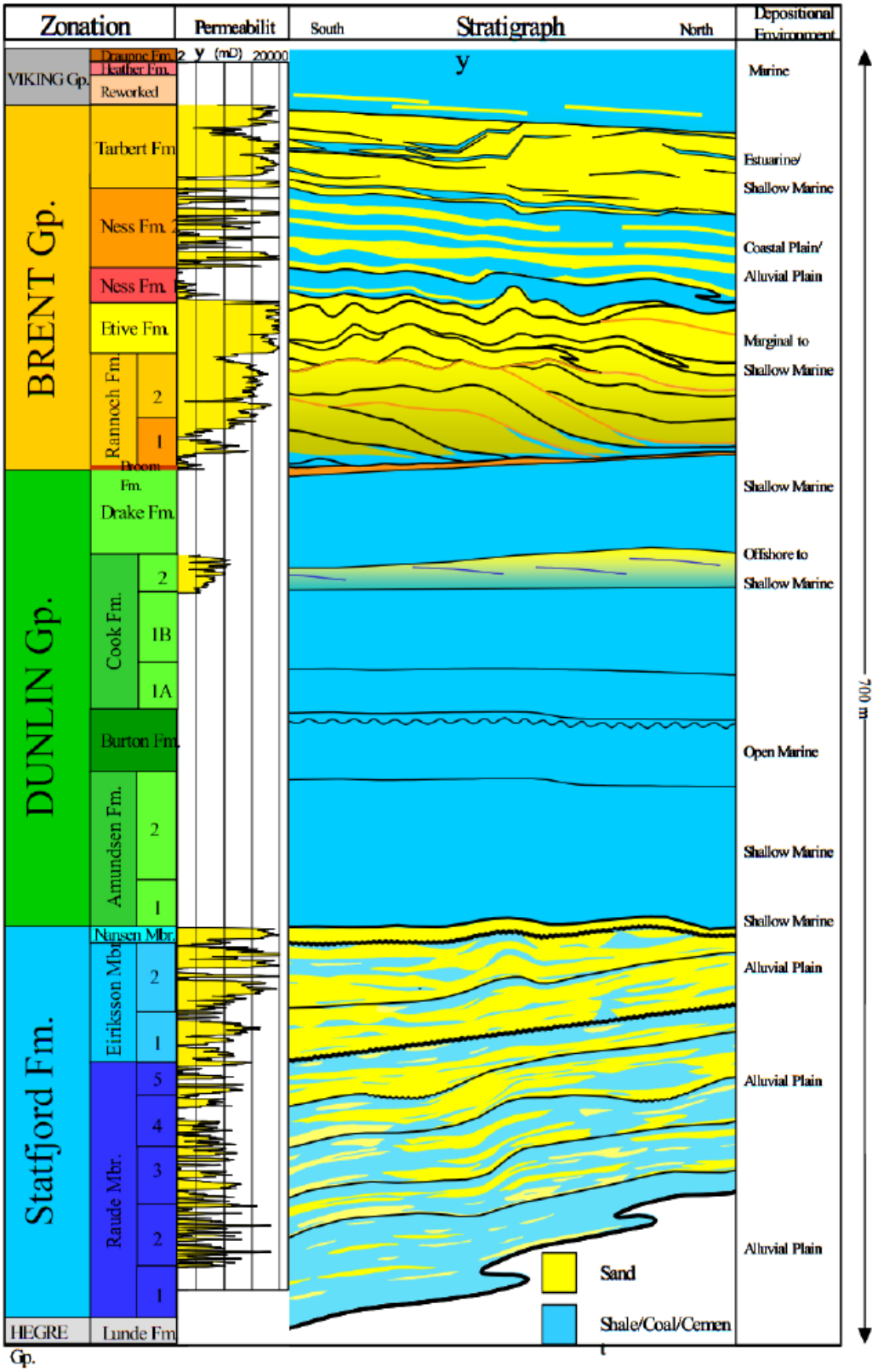

Figure A.5: Lithostratigraphic overview of Statfjord Field [25].

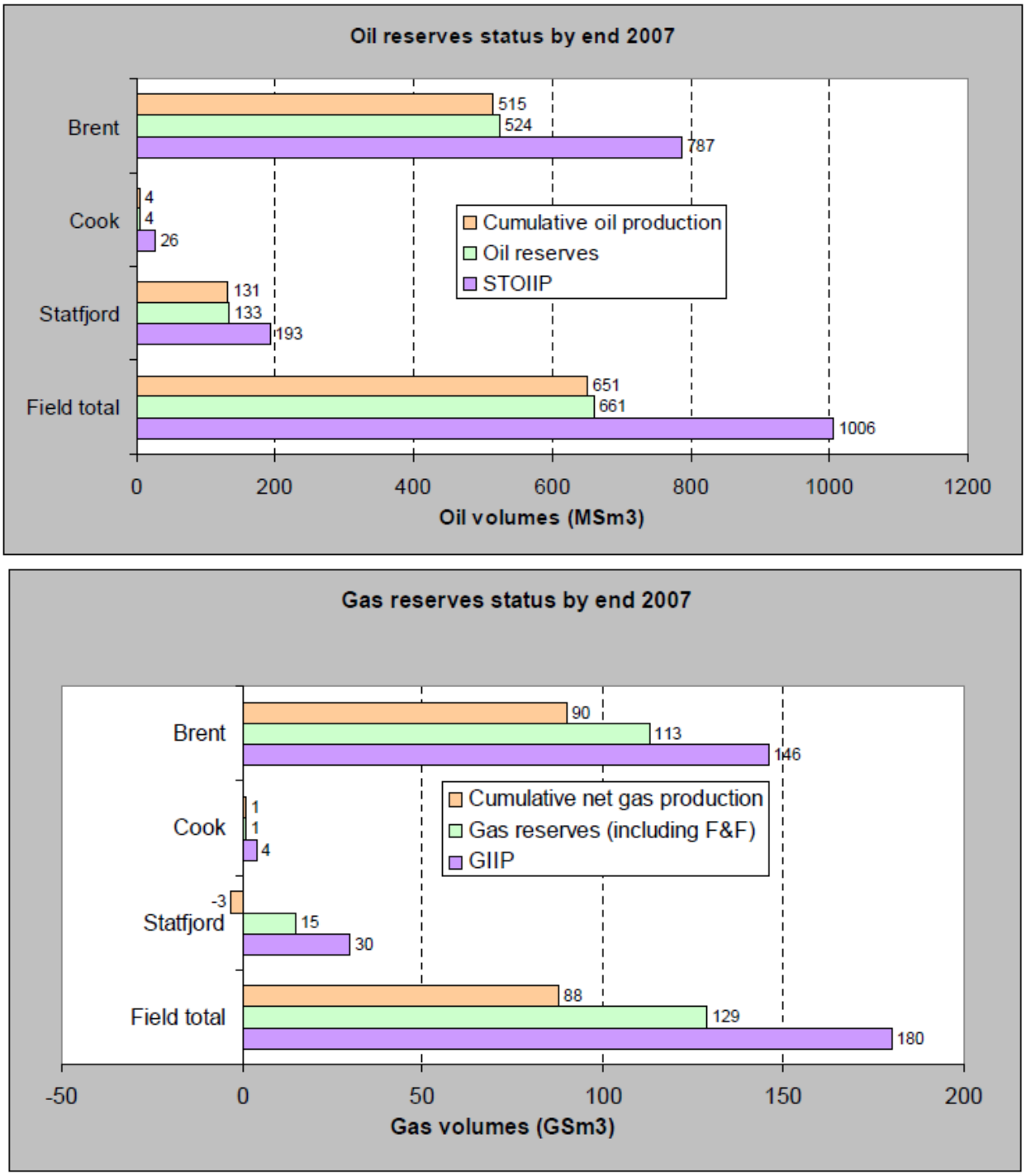

Figure A.6: Oil and gas volumes from the Statfjord field [25].

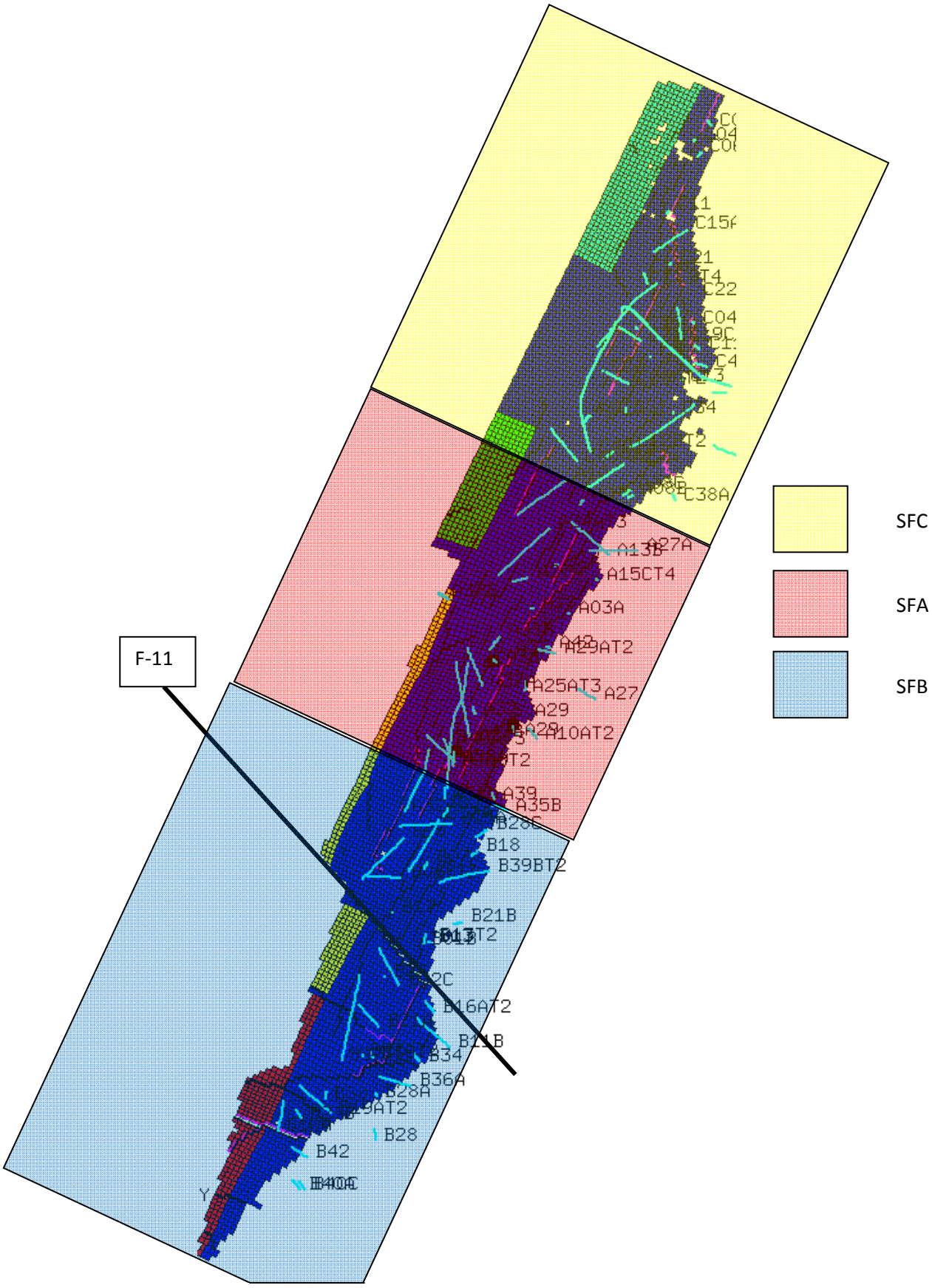

Figure A.7: SFA, SFB and SFC areas, including the major fault F11.

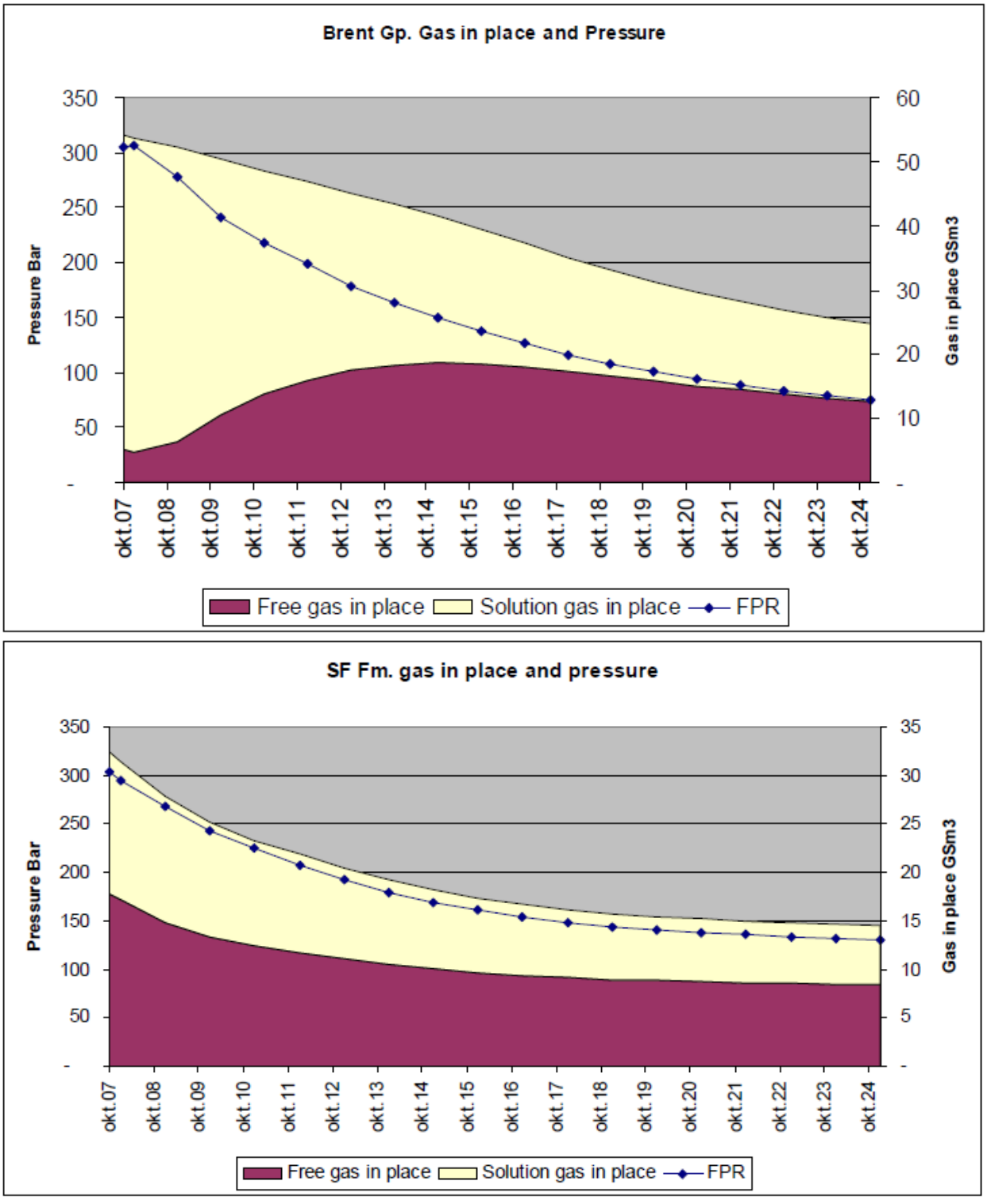

Figure A.8: Development in free and associated gas for both Brent Gp and Statfjord Fm [25].

B Figures and tables for chapters 9 - 10

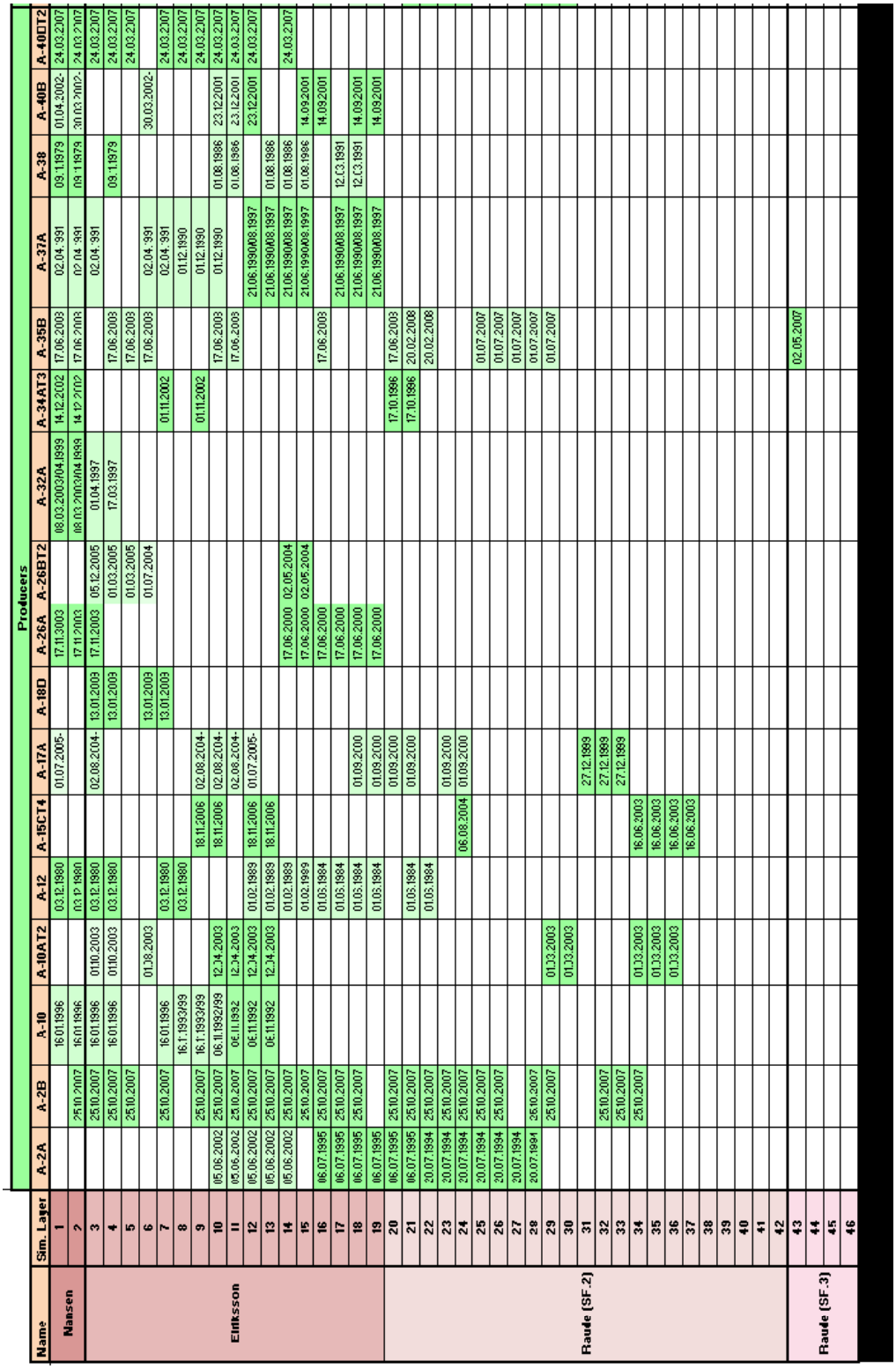

Name	Sim. Layer	Producers																				
		A-2A	A-2B	A-10	A-10AT2	A-12	A-15CT4	A-17A	A-18D	A-26A	A-26BT2	A-32A	A-34AT3	A-35B	A-37A	A-38	A-40B	A-40DT2
Nansen	1			16.01.1996		03.12.1980		01.07.2005-		17.11.2003		18.03.2003/04.1999	14.12.2002	17.06.2003	02.04.1991	09.11979	01.04.2002-	24.03.2007
	2		25.10.2007	16.01.1996		03.12.1980				17.11.2003		18.03.2003/04.1999	14.12.2002	17.06.2003	02.04.1991	09.11979	30.03.2002-	24.03.2007
Eriksson	3		25.10.2007	16.01.1996	01.10.2003	03.12.1980		02.08.2004-	13.01.2009	17.11.2003	05.12.2005	01.04.1997			02.04.1991			24.03.2007
	4		25.10.2007	16.01.1996	01.10.2003	03.12.1980			13.01.2003		01.03.2005	17.03.1997		17.06.2003		09.11979		24.03.2007
	5		25.10.2007								01.03.2005			17.06.2003				24.03.2007
	6				01.08.2003				13.01.2003		01.07.2004			17.06.2003	02.04.1991		30.03.2002-	
	7		25.10.2007	16.01.1996		03.12.1980			13.01.2003				01.11.2002		02.04.1991			24.03.2007
	8			16.1.1993/99		03.12.1980									01.12.1990			24.03.2007
	9		25.10.2007	16.1.1993/99			18.11.2006	02.08.2004-					01.11.2002		01.12.1990			24.03.2007
	10	05.06.2002	25.10.2007	06.11.1992/99	12.04.2003		18.11.2006	02.08.2004-						17.06.2003	01.12.1990	01.08.1986	23.12.2001	24.03.2007
	11	05.06.2002	25.10.2007	06.11.1992	12.04.2003	01.02.1989	18.11.2006	02.06.2004-						17.06.2003		01.08.1986	23.12.2001	24.03.2007
	12	05.06.2002	25.10.2007	06.11.1992	12.04.2003	01.02.1989	18.11.2006	01.07.2005-							21.06.1990/08.1997		23.12.2001	24.03.2007
	13	05.06.2002	25.10.2007	06.11.1992	12.04.2003	01.02.1989	18.11.2006								21.06.1990/08.1997	01.08.1986		
	14	05.06.2002	25.10.2007			01.02.1989				17.06.2000	02.05.2004				21.06.1990/08.1997	01.08.1986		24.03.2007
	15		25.10.2007			01.02.1989				17.06.2000	02.05.2004				21.06.1990/08.1997	01.08.1986	14.09.2001	
	16	06.07.1995	25.10.2007			01.05.1984				17.06.2000				17.06.2003			14.09.2001	
	17	06.07.1995	25.10.2007			01.05.1984				17.06.2000					21.06.1990/08.1997	12.03.1991		
	18	06.07.1995	25.10.2007			01.05.1984		01.09.2000		17.06.2000					21.06.1990/08.1997	12.03.1991	14.09.2001	
	19	06.07.1995				01.05.1984		01.09.2000		17.06.2000					21.06.1990/08.1997		14.09.2001	
Raude (SF.2)	20	06.07.1995	25.10.2007					01.09.2000					17.10.1996	17.06.2003				
	21	06.07.1995	25.10.2007			01.05.1984		01.09.2000					17.10.1996	20.02.2008				
	22	20.07.1994	25.10.2007			01.05.1984								20.02.2008				
	23	20.07.1994	25.10.2007				06.08.2004	01.09.2000										
	24	20.07.1994	25.10.2007					01.09.2000						01.07.2007				
	25	20.07.1994	25.10.2007											01.07.2007				
	26	20.07.1994	25.10.2007											01.07.2007				
	27	20.07.1994												01.07.2007				
	28	20.07.1994	26.10.2007		01.03.2003									01.07.2007				
	29		25.10.2007		01.03.2003									01.07.2007				
	30				01.03.2003													
	31							27.12.1999										
	32		25.10.2007					27.12.1999										
	33		25.10.2007					27.12.1999										
	34		25.10.2007		01.03.2003		16.06.2003											
	35				01.03.2003		16.06.2003											
	36				01.03.2003		16.06.2003											
	37						16.06.2003											
	38																	
	39																	
	40																	
	41																	
	42																	
Raude (SF.3)	43													02.05.2007				
	44																	
	45																	
	46																	

Table B.1: Perforation history for SFA wells. See description in sec. 9.1.

Name	Sim. Layer	B-1C	B-2C	B-6BT2	B-10A	B-11C	B-15	B-15A	B-17	B-17AT3	B-19AT2	B-21B	B-23B	B-24	B-27T2	B-31A	B-37AT2	B-38A	B-40A	B-40C	B-42
Nansen	1	01.11.2008		31.07.2000	20.10.1995	24.04.2007			09.12.1982	15.08.2007				30.10.1982	01.11.1995	01.02.2009	02.06.2009				03.01.1996
	2	01.11.2008	16.06.2008	31.07.2000	20.10.1995	24.04.2007			09.12.1982	15.08.2007	10.04.2003			30.10.1982	01.11.1995		02.06.2009				03.01.1996
Eiriksson	3	01.11.2008				24.04.2007			09.12.1982	15.08.2007	10.04.2003			30.10.1982	01.11.1995			01.07.2000#03.2001	14.03.2004	01.04.1995
	4	01.11.2008	16.06.2008			24.04.2007	21.08.1995#08.1997-		09.12.1982	15.08.2007				30.10.1982	01.11.1995			01.07.2000#03.2001	14.03.2004	01.04.1995
	5	01.11.2008	16.06.2008			24.04.2007	01.08.1995-			15.08.2007				30.10.1982	01.11.1995	01.02.2009			01.05.2003	01.04.1995
	6	01.11.2008	16.06.2008			24.04.2007	28.05.1999-			15.08.2007					14.10.1997				01.05.2003	01.04.1995
	7		16.06.2008			24.04.2007	28.05.1999-	21.11.2003		15.08.2007			15.05.2008		01.09.1993-				08.09.2002	
	8	01.11.2008				24.04.2007	28.05.1999-			15.08.2007			15.05.2008	01.10.1989	01.09.1993-			13.10.2006	03.04.2001#03.2001		10.10.1994
	9	01.11.2008	05.07.2007			24.04.2007	12.03.1994-	21.11.2003		15.08.2007			15.05.2008	01.10.1989				13.10.2006	03.04.2001#03.2001		10.10.1994
	10	01.11.2008				24.04.2007	12.03.1994-	16.03.2002		15.08.2007	10.04.2003			01.10.1989		07.11.2008			03.04.2001#03.2001	01.02.2002	10.10.1994
	11	01.11.2008		12.06.2000			12.03.1994-	16.03.2002		15.08.2007	10.04.2003		15.05.2008	01.10.1989		07.11.2008				01.02.2002	10.10.1994
	12	01.11.2008	05.07.2007			24.04.2007	12.03.1994-	16.03.2002		15.08.2007		01.12.2005	08.10.2006	01.10.1989		07.11.2008		01.03.2006		01.02.2002	10.10.1994
	13	01.11.2008				24.04.2007				15.08.2007	15.10.2000	01.12.2005	08.10.2006	08.01.1994			17.10.2006	01.03.2006		01.02.2002	10.10.1994
	14	01.11.2008				24.04.2007			01.10.1988	15.08.2007		01.12.2005	11.06.2003	08.01.1994		07.11.2008	17.10.2006				10.10.1994
	15					24.04.2007			01.10.1988	15.08.2007	15.10.2000	01.12.2005		08.01.1994		21.02.2006	17.10.2006				10.10.1994
	16	01.11.2008		15.02.2000		24.04.2007			01.10.1988	15.08.2007	15.10.2000	01.12.2005				21.02.2006	30.11.2002				
	17		27.07.2005	15.02.2000					01.10.1988	15.08.2007	15.10.2000	01.12.2005				07.12.2003	30.11.2002				
	18	01.11.2008	07.05.2001	15.02.2000		24.04.2007			01.10.1988	15.08.2007	15.10.2000	01.12.2005				07.12.2003	30.11.2002				
	19	01.11.2008	07.05.2001			24.04.2007			01.10.1988	15.08.2007	15.10.2000	01.12.2005				07.12.2003	30.11.2002				
Raude (SF.2)	20										15.10.2000									15.12.2001	
	21	16.02.2008							01.10.1988	15.08.2007		25.07.2005#2.2005									
	22	16.02.2008				24.04.2007				15.08.2007		25.07.2005									
	23	16.02.2008				24.04.2007				15.08.2007		25.07.2005									
	24	16.02.2008								15.08.2007		06.04.2001									
	25											06.04.2001									
	26									15.08.2007		06.04.2001								15.12.2001	
	27					24.04.2007				15.08.2007											
	28	16.02.2008				24.04.2007				15.08.2007											
	29	16.02.2008								15.08.2007		06.04.2001									
	30	16.02.2008										06.04.2001									
	31																				
	32																				
	33																				
	34										10.12.2000										
	35									15.08.2007											
	36										10.12.2000										
	37										10.12.2000										
	38																				
	39																				
	40																				
	41																				
	42																				
Raude (SF.3)	43																				
	44																				
	45																				
	46																				

Table B.2: Perforation history for SFB wells. See description in sec. 9.1.

Table B.3: Perforation history for WAG/Water injectors. See description in sec. 9.2.

		Water/WAG Injectors															
Name	Sim. Layer	A-2A	A-3A	A-8C	A-25AT3	A-38A	A-38B	B-1B	B-8	B-18	B-38	B-38A	C-1A	C-4A	C-4B	C-14A	C-34
Nansen	1		01.01.1996											18.05.2001	10.07.2003		01.12.1999
	2		01.01.1996					16.04.2000						18.05.2001	10.07.2003		01.12.1999
Eiriksson	3		01.01.1996							01.02.1998				18.05.2001	10.07.2003		
	4		01.01.1996							01.02.1998					10.07.2003		
	5							16.04.2000						18.05.2001	10.07.2003		
	6		01.01.1996		01.06.1999			16.04.2000		01.02.1998				18.05.2001	10.07.2003		01.12.1999
	7		01.01.1996		01.06.1999									18.05.2001	10.07.2003		01.12.1999
	8		01.01.1996		01.06.1999					01.02.1998				18.05.2001	10.07.2003		01.12.1999
	9		01.01.1996											18.05.2001	10.07.2003		01.12.1999
	10		01.01.1996											18.05.2001	10.07.2003		01.12.1999
	11			01.12.2000	01.06.1999									18.05.2001	10.07.2003		01.12.1999
	12		01.01.1996	01.12.2000										18.05.2001	10.07.2003		01.12.1999
	13		01.01.1996	01.12.2000	01.06.1999					01.02.1998				18.05.2001	10.07.2003		01.12.1999
	14		01.01.1996		01.06.1999					01.02.1998					10.07.2003		
	15		01.01.1996		01.06.1999									18.05.2001	10.07.2003		
	16	19.12.1997	01.01.1996											18.05.2001	10.07.2003		
	17	19.12.1997	01.01.1996	01.12.2000										18.05.2001	10.07.2003		
	18	19.12.1997	01.01.1996	01.12.2000						01.02.1998							
	19	19.12.1997		01.12.2000													
Raude (SF.2)	20	19.12.1997	01.01.1996														
	21	19.12.1997				01.09.1998					03.09.1994		29.05.1996				
	22	19.12.1997				01.05.1998					03.09.1994		29.05.1996			29.12.2002	
	23	19.12.1997				01.05.1998					03.09.1994		29.05.1996			29.12.2002	
	24	19.12.1997									03.09.1994		29.05.1996				
	25	19.12.1997				01.05.1998											
	26	19.12.1997				01.03.1998						01.11.1997	29.05.1996				
	27	19.12.1997				01.03.1998			01.06.1991			01.11.1997	29.05.1996				
	28	19.12.1997				01.05.1998			01.06.1991			01.11.1997	29.05.1996			29.12.2002	
	29					01.05.1998										29.12.2002	
	30					01.03.1998						28.01.1998					
	31					01.03.1998			01.06.1991								
	32								01.06.1991			01.11.1997	29.05.1996			29.12.2002	
	33					01.03.1998						01.11.1997	29.05.1996			29.12.2002	
	34					01.03.1998						01.11.1997					
	35					01.03.1998							29.05.1996				
	36					01.03.1998			01.06.1991				29.05.1996				
	37					01.05.1998			01.06.1991			01.11.1997	29.05.1996			29.12.2002	
	38					01.05.1998	01.07.2003					01.11.1997	29.05.1996				
	39					01.05.1998	01.07.2003					01.11.1997	29.05.1996			29.12.2002	
	40					01.03.1998						28.01.1998				29.12.2002	
	41					01.03.1998						28.01.1998					
	42					01.05.1998	01.07.2003									29.12.2002	
Raude (SF.3)	43					01.05.1998						28.01.1998					
	44						01.07.2003									29.12.2002	
	45															29.12.2002	
	46																

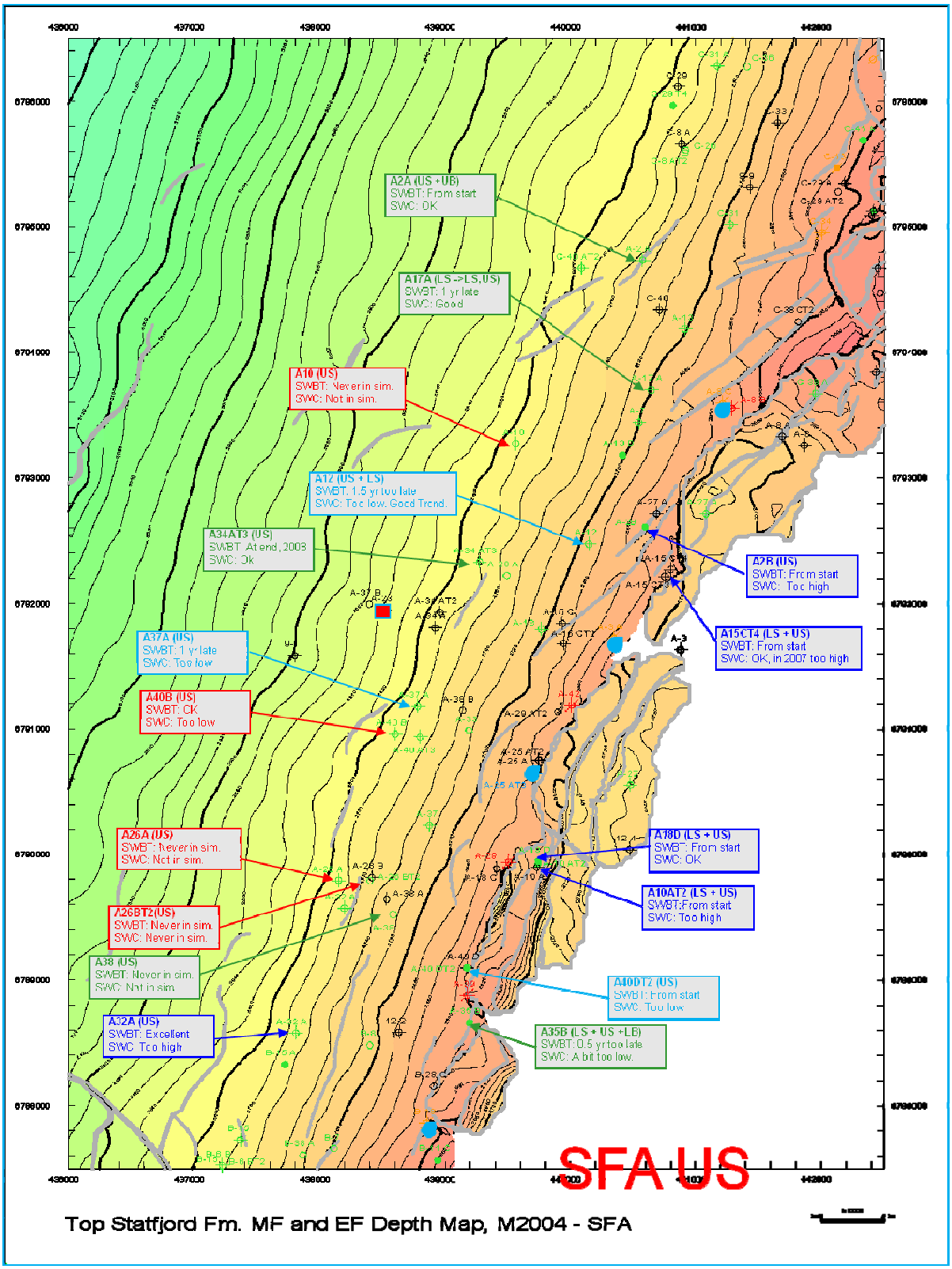

Figure B.1: Upper Statfjord, SFA - Quality of match between simulated and observed SWCT. See description in sec. 10.1.

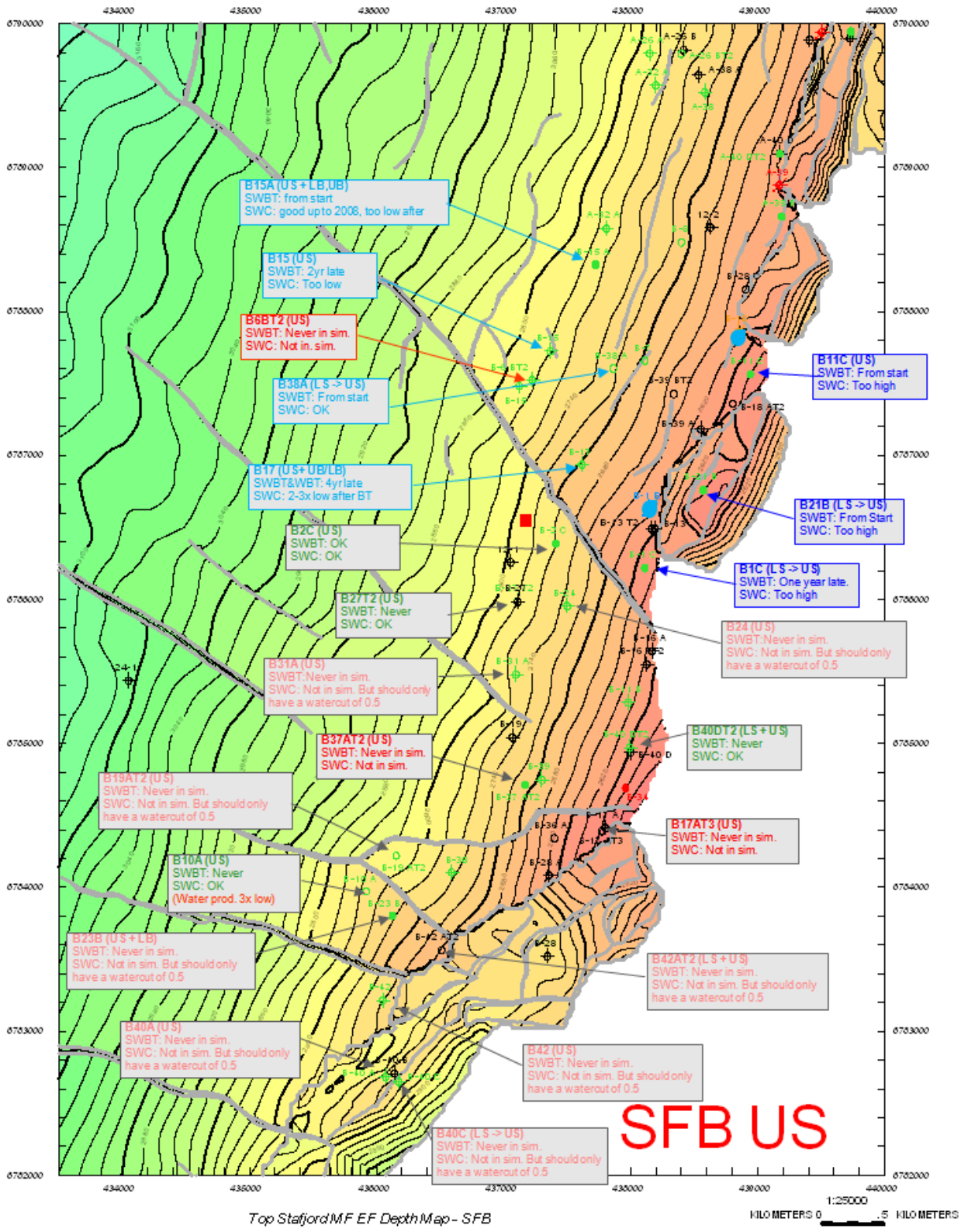

Figure B.2: Upper Statfjord, SFB - Quality of match between simulated and observed SWCT. See description in sec. 10.1.

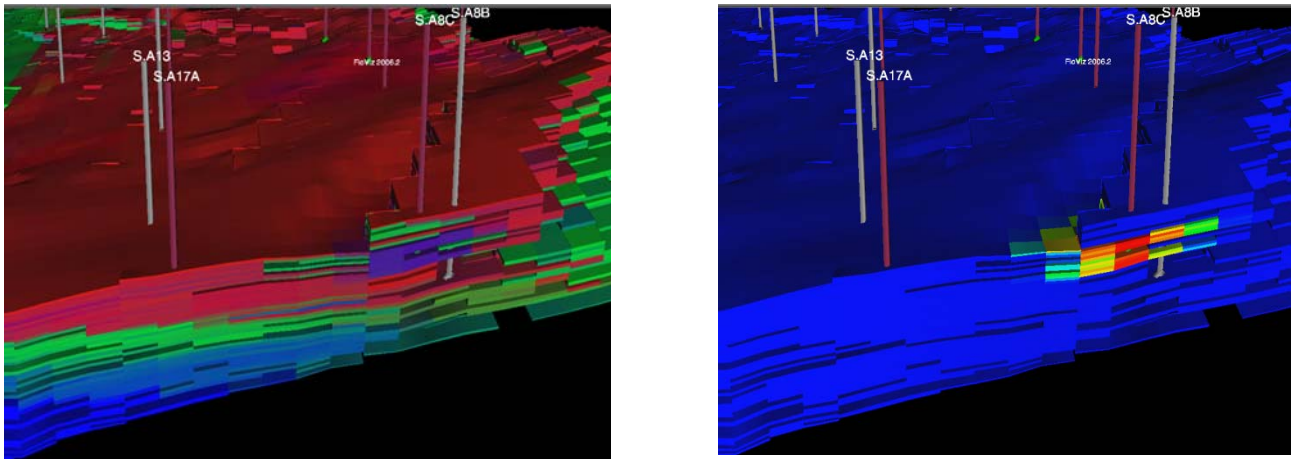

(a) 2001

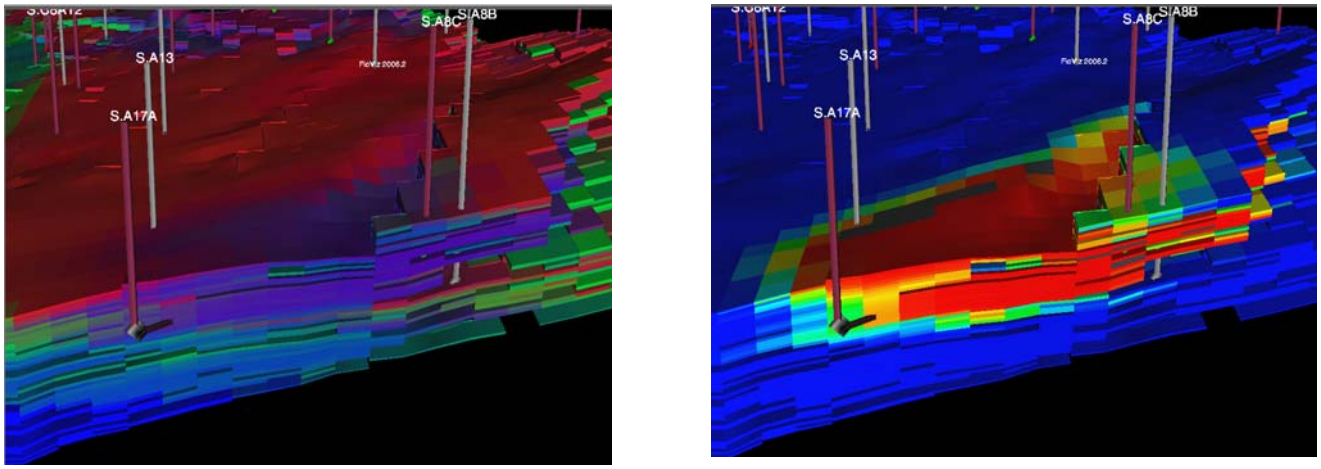

(b) 2005

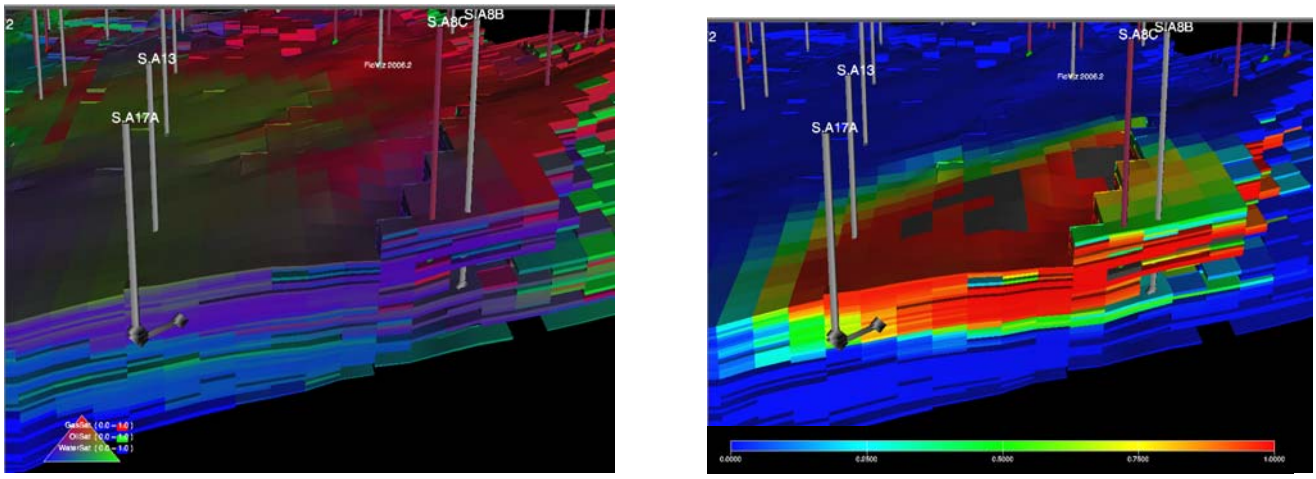

(c) 2009

Figure B.3: SWC in the reservoir and ternary figures from FLOVIZ is shown to illustrate the movement of the upflank water over time for injector A-8C.

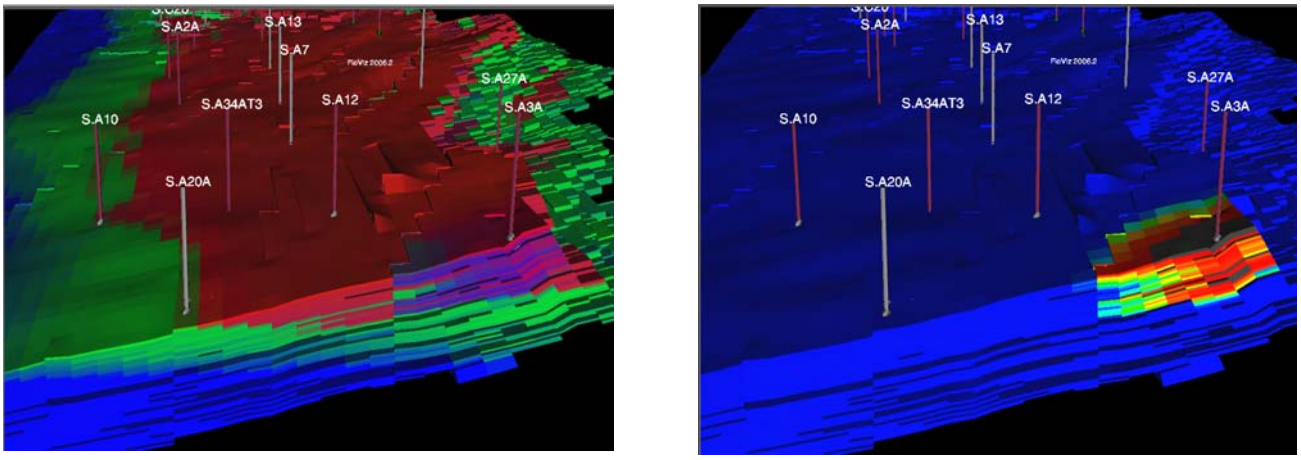

(a) 1997

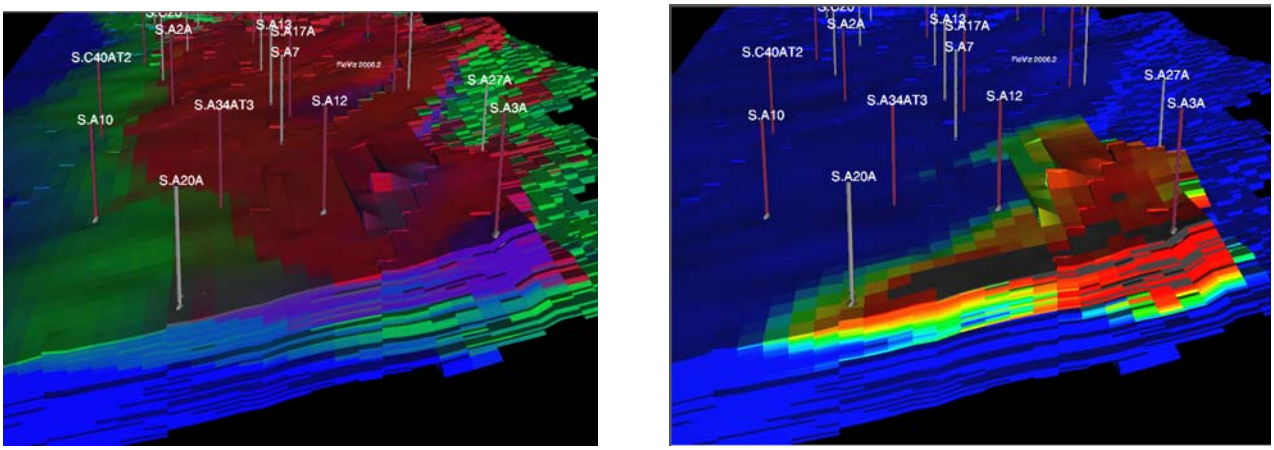

(b) 2002

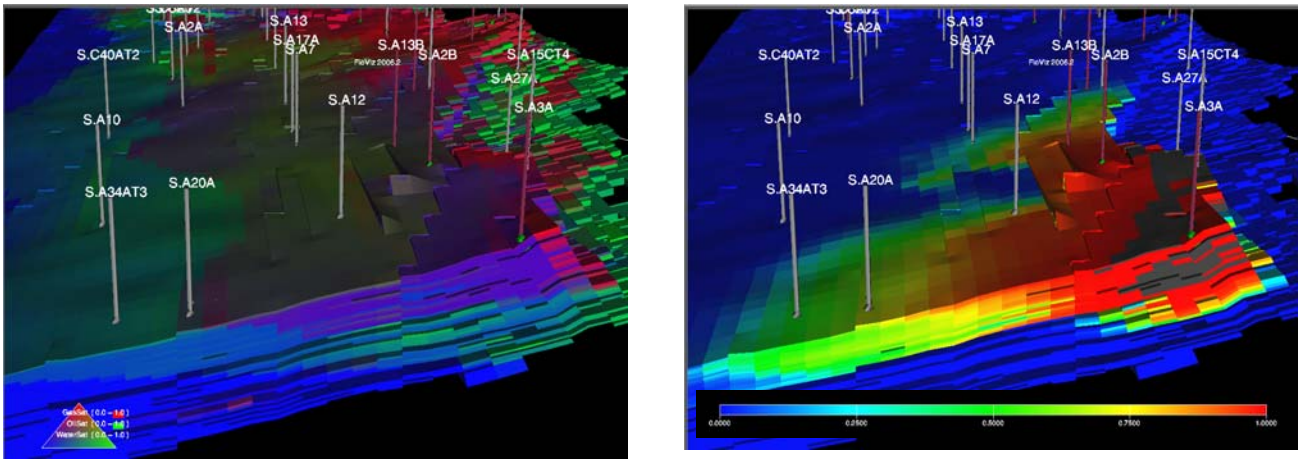

(c) 2009

Figure B.4: SWC in the reservoir and ternary figures from FLOVIZ is shown to illustrate the movement of the upflank water over time for injector A-3A.

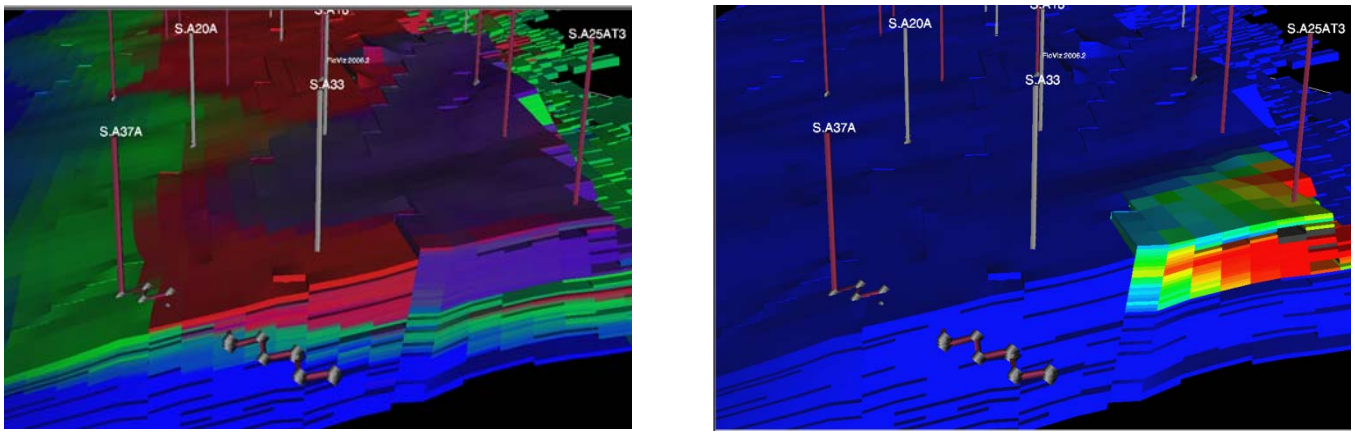

(a) 2000

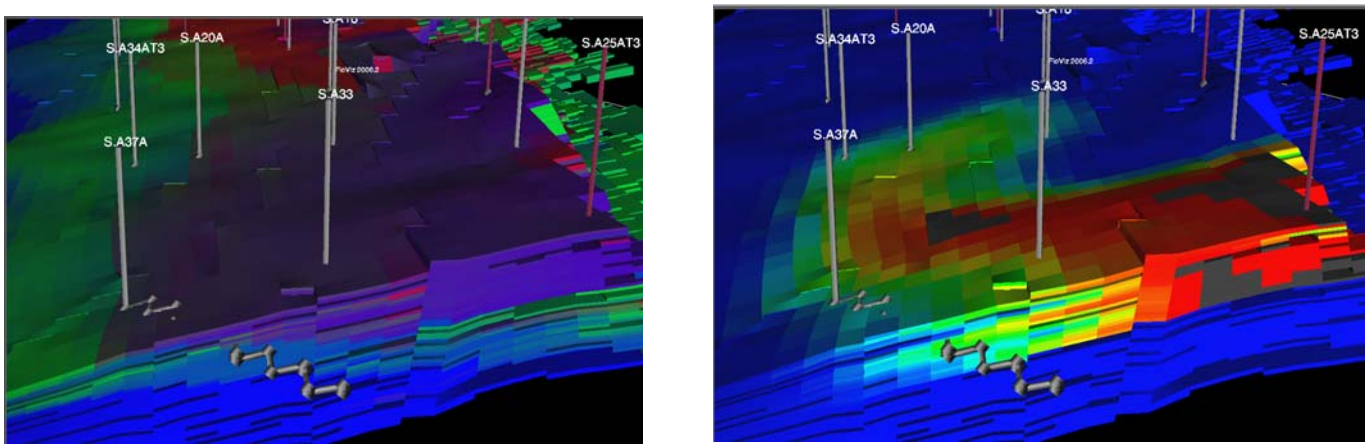

(b) 2005

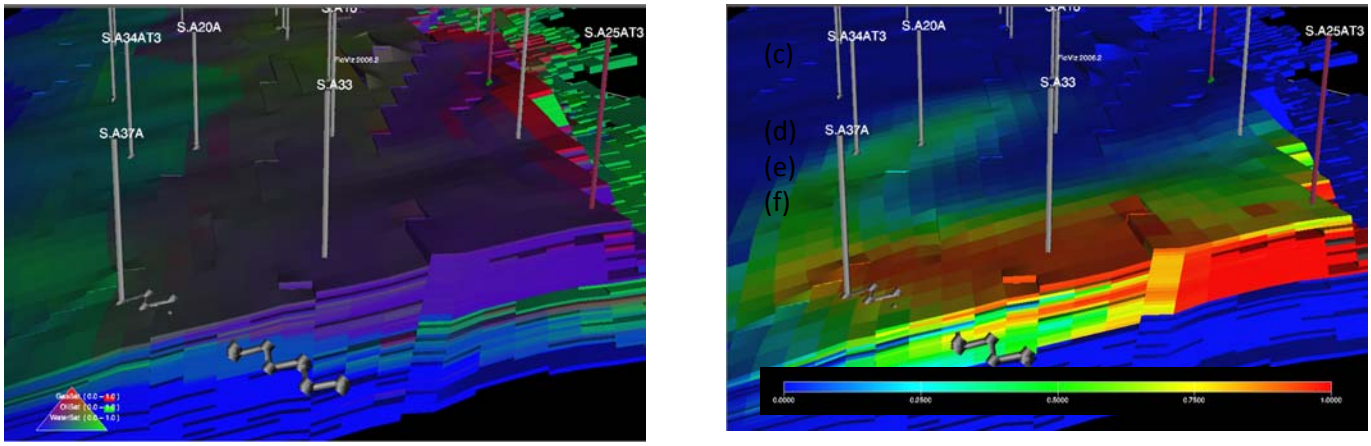

(c) 2009

Figure B.5: SWC in the reservoir and ternary figures from FLOVIZ is shown to illustrate the movement of the upflank water over time for injector A-25AT3.

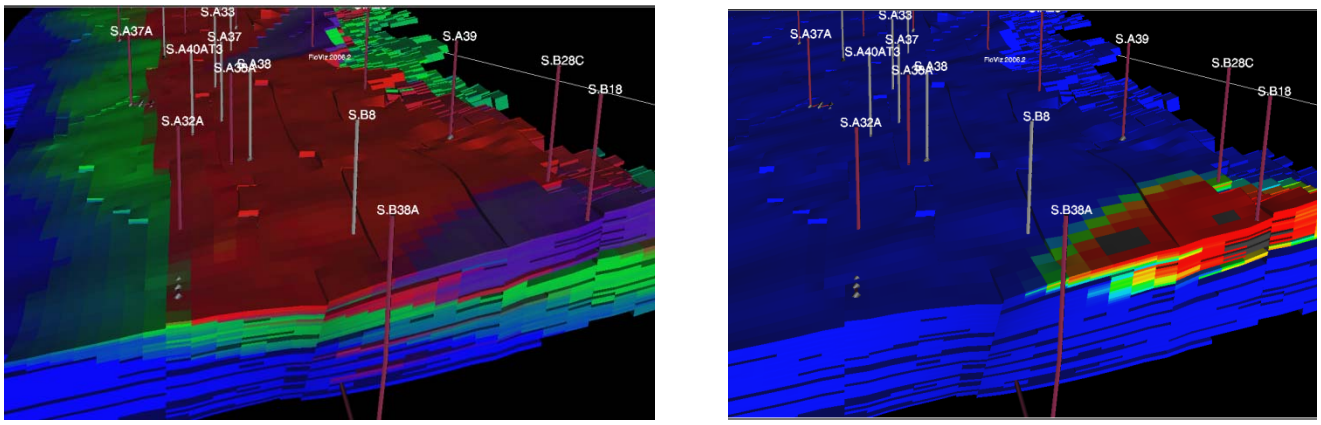

(a) 1999

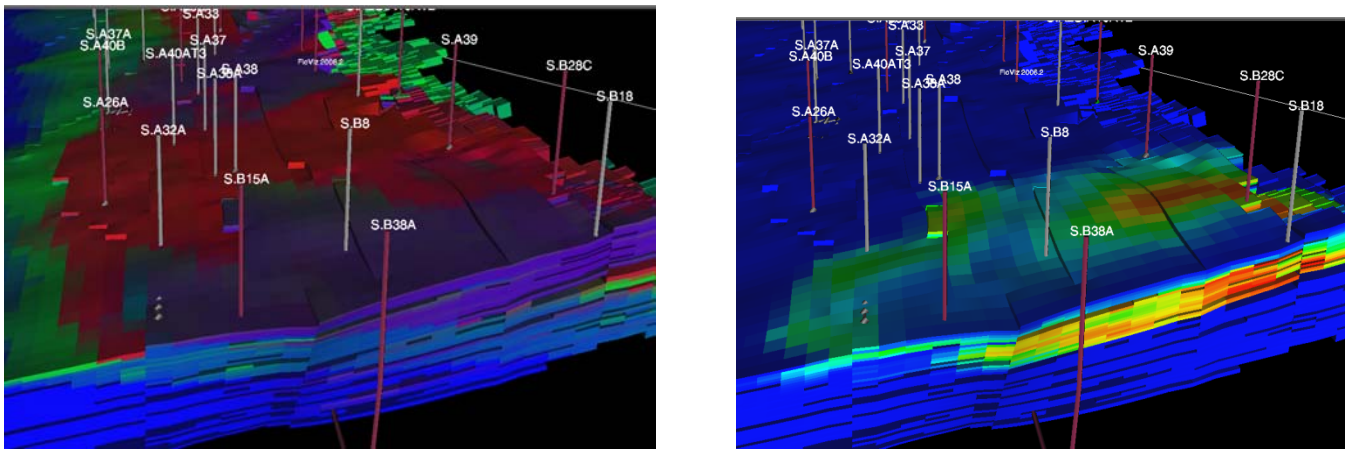

(b) 2004

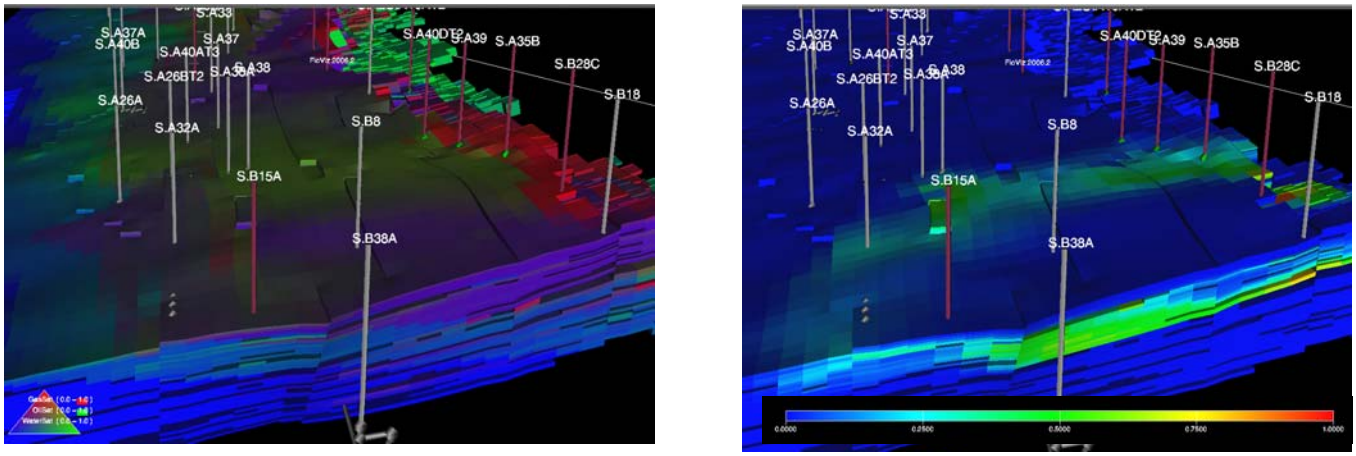

(c) 2009

Figure B.6: SWC in the reservoir and ternary figures from FLOVIZ is shown to illustrate the movement of the upflank water over time for injector B-18.

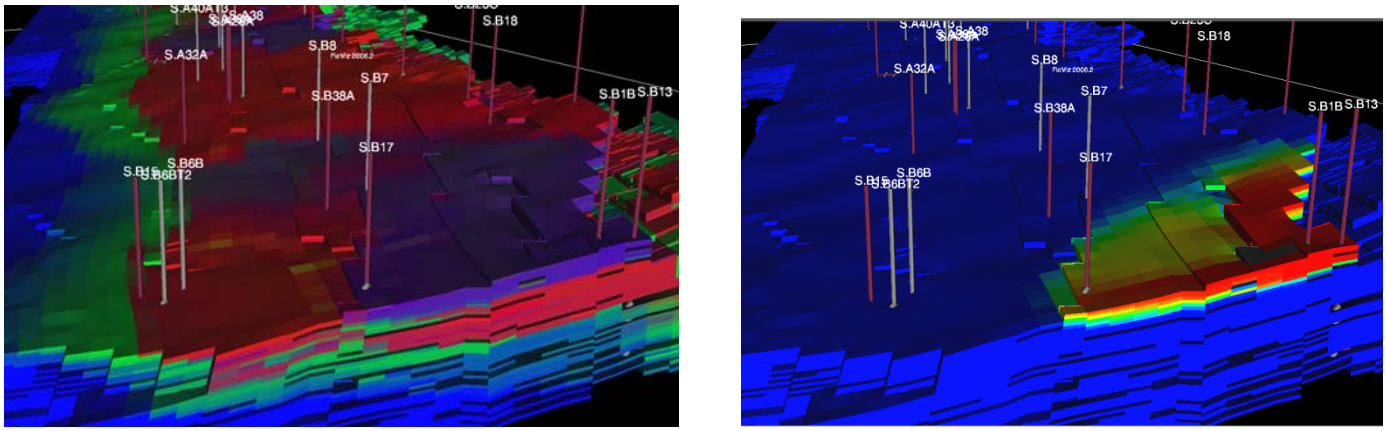

(a) 2001

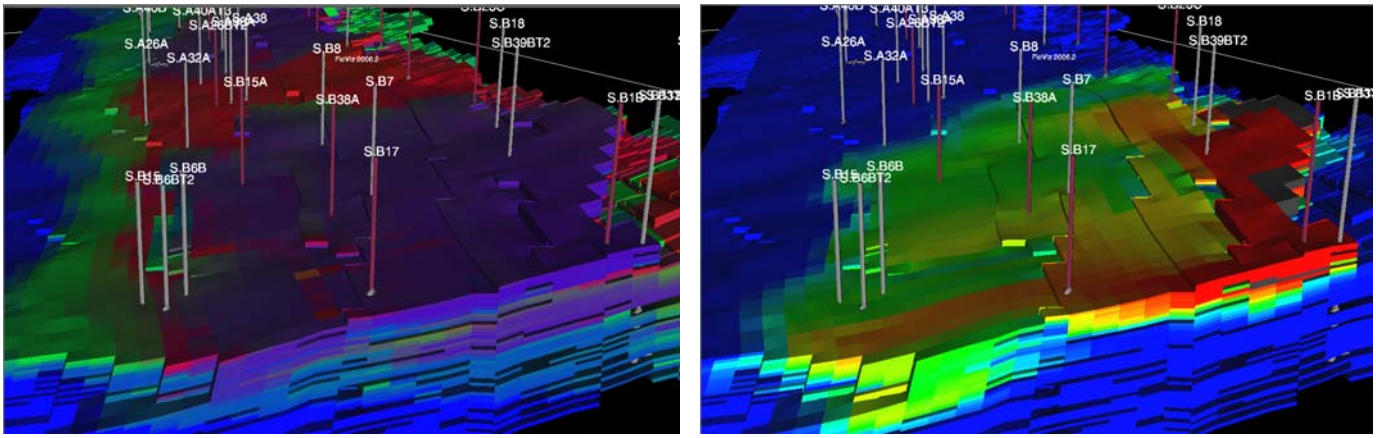

(b) 2005

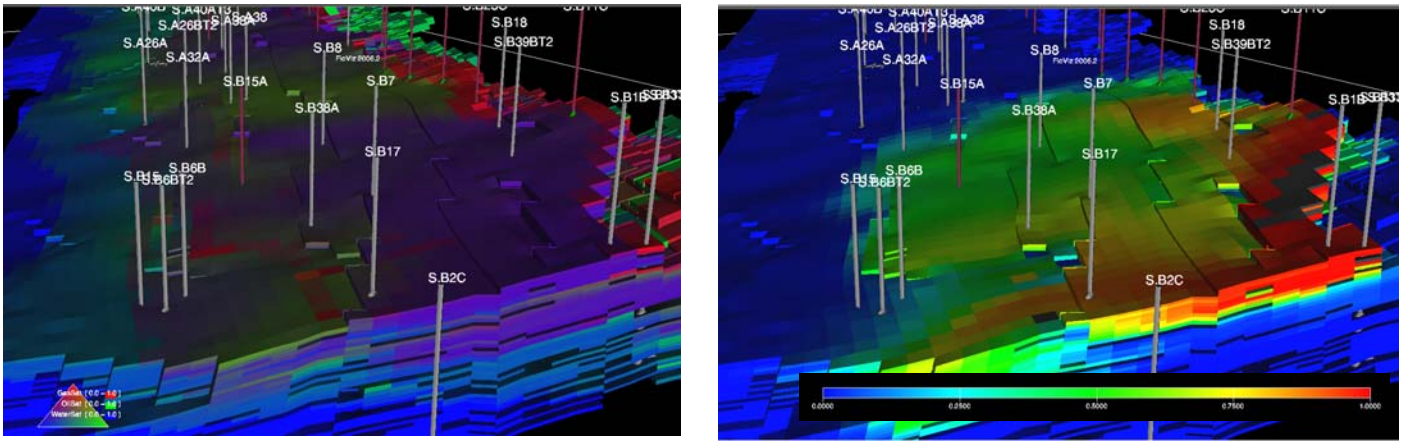

(c) 2009

Figure B.7: SWC in the reservoir and ternary figures from FLOVIZ is shown to illustrate the movement of the upflank water over time for injector B-1B.

C ECLIPSE input and figures for chapter 11

C.1 ECLIPSE input for new relative permeability curves

```
SWOF
0 0 1 2
0.05 0.05 0.914254034 0.715732
0.1 0.1 0.818462281 0.636497
0.15 0.15 0.715715587 0.562249
0.2 0.2 0.610089698 0.492941
0.25 0.25 0.506118771 0.428522
0.3 0.3 0.408124713 0.368937
0.35 0.35 0.319600457 0.314132
0.4 0.4 0.242821516 0.264045
0.45 0.45 0.178757157 0.218614
0.5 0.5 0.127236983 0.177769
0.55 0.55 0.087261466 0.141436
0.6 0.6 0.05734151 0.109537
0.65 0.65 0.035789009 0.081982
0.7 0.7 0.020925394 0.058674
0.75 0.75 0.011208245 0.039502
0.8 0.8 0.005292713 0.02434
0.85 0.85 0.002048582 0.013038
0.9 0.9 0.000551313 0.005409
0.95 0.95 6.09448E-05 0.001202
1 1 0 0
/ reservoir 1 drainage and imbibition
0 0 1 2
0.05 0.001187802 0.914254034 0.715732
0.1 0.005658126 0.818462281 0.636497
0.15 0.014285858 0.715715587 0.562249
0.2 0.027767538 0.610089698 0.492941
0.25 0.046690113 0.506118771 0.428522
0.3 0.071521075 0.408124713 0.368937
0.35 0.102583494 0.319600457 0.314132
0.4 0.140029864 0.242821516 0.264045
0.45 0.183822575 0.178757157 0.218614
0.5 0.233726958 0.127236983 0.177769
0.55 0.289321384 0.087261466 0.141436
0.6 0.350027148 0.05734151 0.109537
0.65 0.415159257 0.035789009 0.081982
0.7 0.483998758 0.020925394 0.058674
0.75 0.555890124 0.011208245 0.039502
0.8 0.630378533 0.005292713 0.02434
0.85 0.707438704 0.002048582 0.013038
0.9 0.787985351 0.000551313 0.005409
0.95 0.875624529 6.09448E-05 0.001202
1 1 0 0
/ reservoir 2 drainage and imbibition
```

C.2 Modifications for individual wells

Producers located in Statfjord A area

C.2.1 A-10

```
EQUALS
      MULTX 3     29    36    94    109   7     7     /
      MULTY 3     29    36    94    109   7     7     /
      MULTX 3     16    35    90    97    7     7     /
      MULTY 3     16    35    90    97    7     7     /
      MULTX 4     29    36    94    109   4     4     /
      MULTY 4     29    36    94    109   4     4     /
      MULTX 4     16    35    90    97    4     4     /
      MULTY 4     16    35    90    97    4     4     /

      MULTZ 0.1   17    34    84    99    7     7     /
/
```

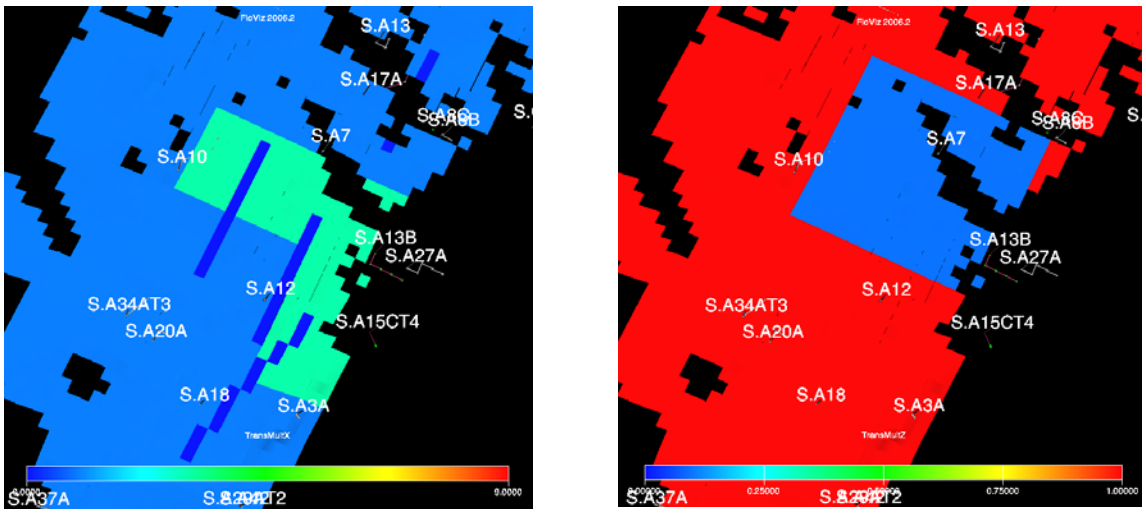

Figure C.1: MULTX-region (left) and MULTZ-region (right)

C.2.2 A-10AT2

```
-- KEYWORD "FAULTS" HAS BEEN WRITTEN FROM RESVIEW.

FAULTS
--     NAME          IX1   IX2     IY1   IY2     IZ1   IZ2    FACE
   'EF_3    '         38    38      132   132       1    46     'Y'    /
   'EF_3    '         37    37      132   132       1    46     'Y'    /
   'EF_3    '         36    36      133   133       1    46     'X'    /
   'EF_3    '         36    36      134   134       1    46     'X'    /
   'EF_3    '         36    36      135   135       1    46     'X'    /
   'EF_3    '         36    36      136   136       1    46     'X'    /
   'EF_3    '         36    36      137   137       1    46     'X'    /
   'EF_3    '         36    36      138   138       1    46     'X'    /
   'EF_3    '         36    36      139   139       1    46     'X'    /
   'EF_3    '         36    36      140   140       1    46     'X'    /
```

```
   'EF_3    '        36   36     141  141       1   46     'X'    /
   'EF_3    '        36   36     142  142       1   46     'X'    /
/


-- KEYWORD "FAULTS" HAS BEEN WRITTEN FROM RESVIEW.

FAULTS
--    NAME          IX1  IX2     IY1  IY2     IZ1  IZ2    FACE
   'EF_3B   '        37   37     142  142       1   46     'Y'    /
   'EF_3B   '        38   38     142  142       1   46     'Y'    /
   'EF_3B   '        39   39     142  142       1   46     'Y'    /
/

MULTFLT
EF_3 0.001 /
EF_3B 0.7 /
/
```

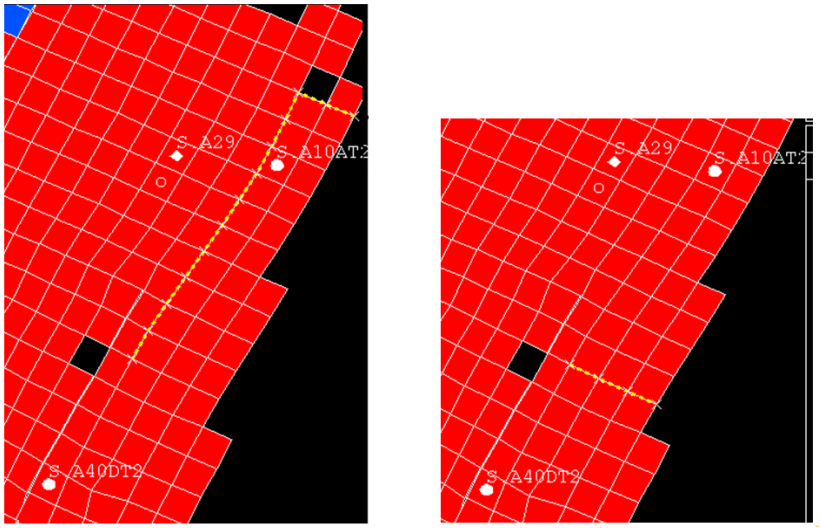

Figure C.2: Fault EF_3 (left) and EF_3B (right)

C.2.3 A-12

```
EQUALS
      PERMX 6000  27    35    103   111   14    14    /
      PERMY 6000  27    35    103   111   14    14    /
/
```

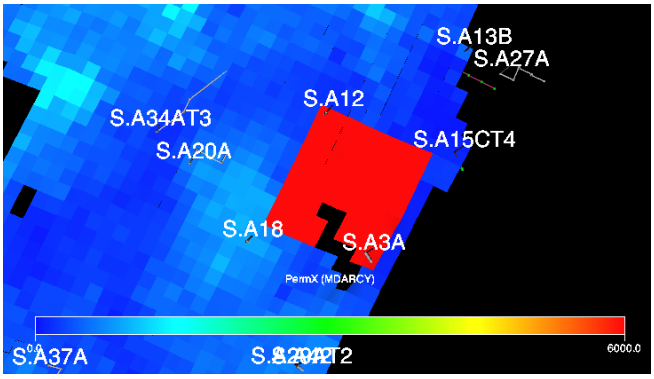

Figure C.3: Permeability region

C.2.4 A-15CT4

```
-- KEYWORD "FAULTS" HAS BEEN WRITTEN FROM RESVIEW.

FAULTS
--    NAME          IX1  IX2     IY1  IY2     IZ1  IZ2    FACE
   'A15CT4  '        36   36     104  104       1   46     'X'    /
   'A15CT4  '        36   36     103  103       1   46     'Y'    /
   'A15CT4  '        35   35     103  103       1   46     'X'    /
   'A15CT4  '        35   35     102  102       1   46     'Y'    /
   'A15CT4  '        34   34     102  102       1   46     'X'    /
/

MULTFLT
A15CT4 0.01 /
/
```

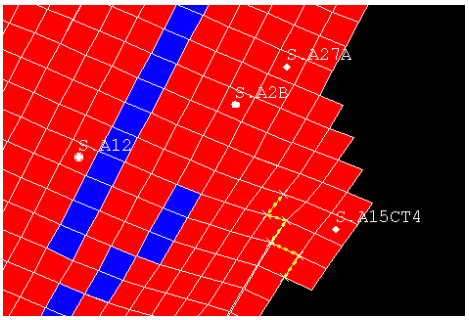

Figure C.4: Fault A15CT4

C.2.5 A-17A

```
EQUALS
      MULTX 0.1   31    31    77    83    1     46    /
/
```

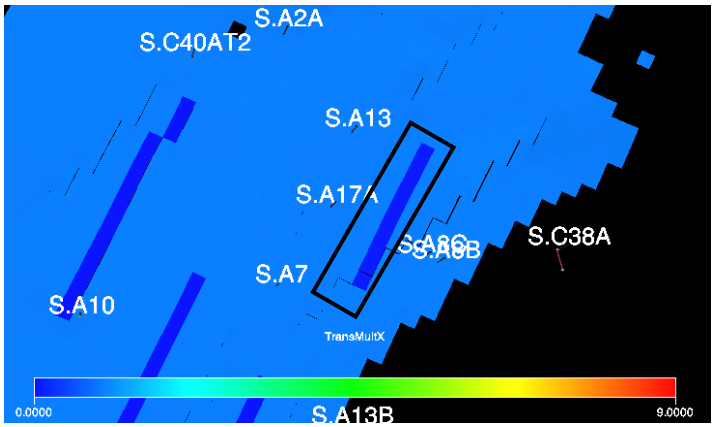

Figure C.5: MULTX-fault

C.2.6 A-18D

See fault A-10AT2 (C.2.2)

C.2.7 A-26A

```
EQUALS
      MULTX 1.5   17    38    143   164   14    17    /
      MULTY 1.5   17    38    143   164   14    17    /
/
```

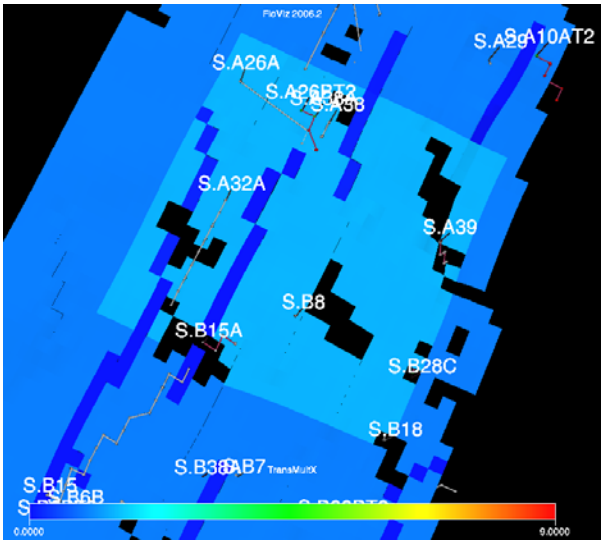

Figure C.6: MULTX/Y region

C.2.8 A-26BT2

```
EQUALS
      MULTX 9     17    26    143   148   4     6     /
      MULTY 9     17    26    143   148   4     6     /
      MULTX 9     27    38    143   164   4     6     /
      MULTY 9     27    38    143   164   4     6     /
/
```

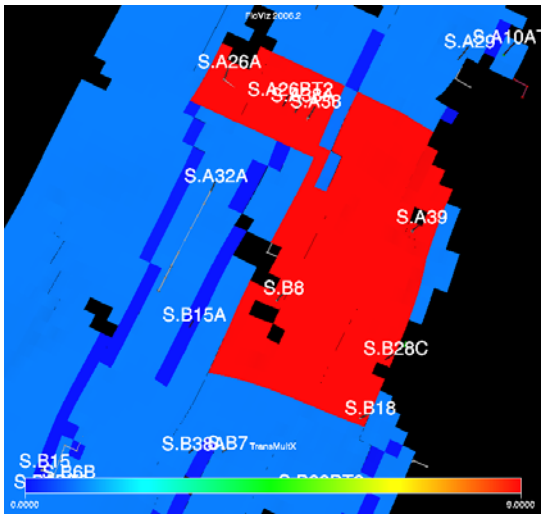

Figure C.7: MULTX/Y region

C.2.9 A-32A

```
EQUALS
      MULTX 0.01  24    24    162   167   1     46    /
/
```

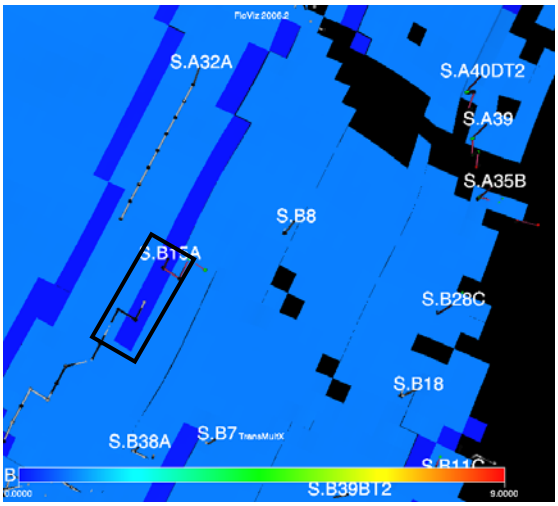

Figure C.8: MULTX-fault extension

C.2.10 A-34AT3

```
EQUALS
      MULTX 0.01  21    21    91    103   1     46    /
/
```

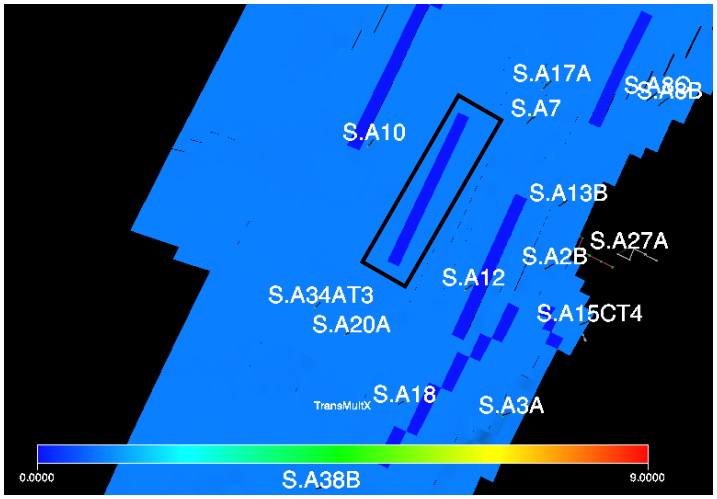

Figure C.9: MULTX-fault

C.2.11 A-35B

```
EQUALS
      PERMX 5000  32    40    150   164   27    29    /
      PERMY 5000  32    40    150   164   27    29    /
/
```

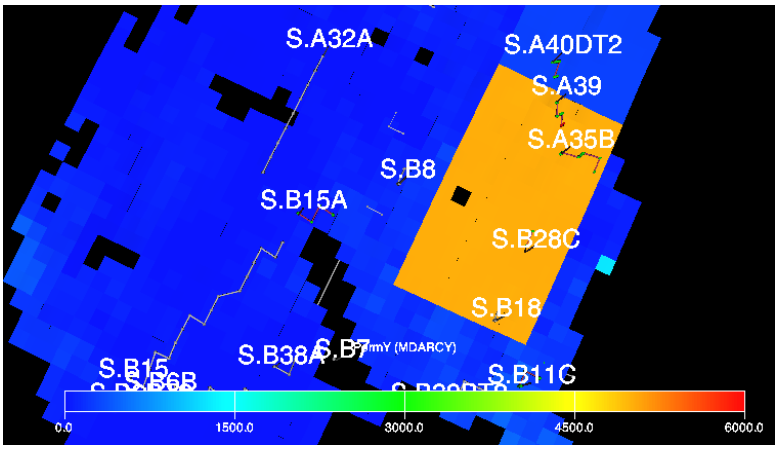

Figure C.10: Permeability region

C.2.12 A-37A

```
EQUALS
      MULTX 100   27    27    124   125   1     19    /
      MULTX 100   26    26    126   128   1     19    /
      MULTX 5     27    27    129   134   1     19    /
/

EQUALS
      PERMX 2000  16    21    121   128   2     2     /
      PERMY 2000  16    21    121   128   2     2     /
/

EQUALS
      PERMX 5000  15    23    121   128   19    19    /
      PERMY 5000  15    23    121   128   19    19    /
/
```

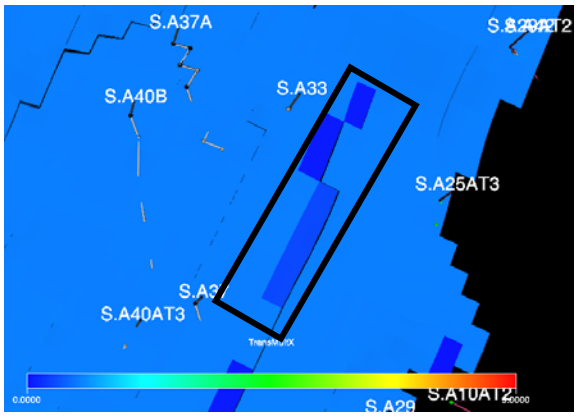

Figure C.11: Modified fault transmissibilities

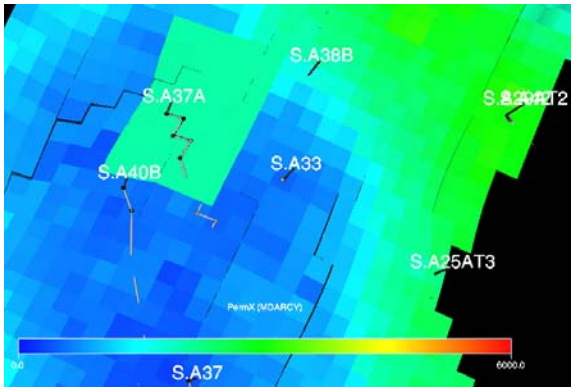

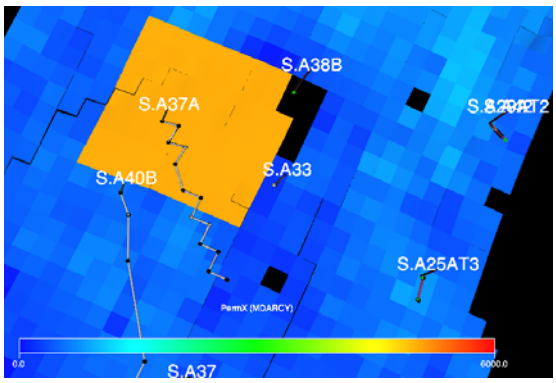

Figure C.12: Permeability region in {2} (left) and in {19} (right)

C.2.13 A-40B

```
EQUALS
      PERMX 4000  17    34    128   137   15    16    /
      PERMY 4000  17    34    128   137   15    16    /
/
```

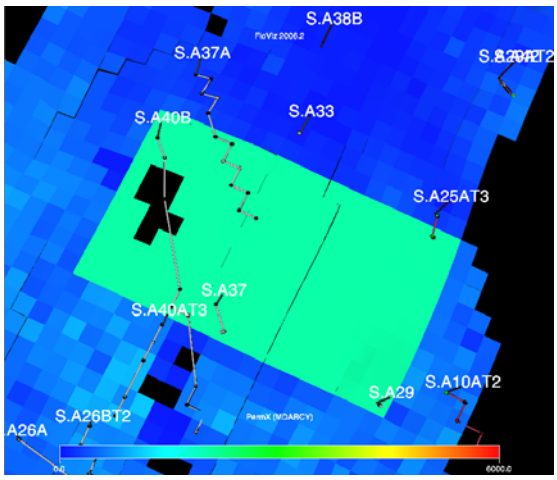

Figure C.13: Permeability region

Producers located in Statfjord B area

C.2.14 B-1C

```
COMPDAT
-- WELL  I    J K1  K2     Sat.   CF    DIAM    KH SKIN ND   DIR   Ro
'S.B1C' 40  188 29 29'OPEN'  1*   15.0  0.178  99.488  2*    'Z'     13.993 /
'S.B1C' 40  188 30 30'OPEN'  1*   15.0  0.178  297.653 2*    'Z'     14.055 /
```

(CF before in layer 29 1.054; CF before in layer 30 3.150)

```
EQUALS
      PERMX 4000  32    42    183   191   30    30    /
      PERMY 4000  32    42    183   191   30    30    /
/

-- KEYWORD "FAULTS" HAS BEEN WRITTEN FROM RESVIEW.

FAULTS
--    NAME          IX1  IX2     IY1  IY2     IZ1  IZ2    FACE
   'FLT_B1C '        40   40     185  185       1   19     'Y'    /
   'FLT_B1C '        39   39     185  185       1   19     'Y'    /
   'FLT_B1C '        38   38     185  185       1   19     'Y'    /
   'FLT_B1C '        37   37     185  185       1   19     'Y'    /
   'FLT_B1C '        36   36     185  185       1   19     'Y'    /
   'FLT_B1C '        35   35     185  185       1   19     'Y'    /
   'FLT_B1C '        34   34     185  185       1   19     'Y'    /
   'FLT_B1C '        33   33     185  185       1   19     'Y'    /
   'FLT_B1C '        32   32     185  185       1   19     'Y'    /
   'FLT_B1C '        31   31     185  185       1   19     'Y'    /
   'FLT_B1C '        30   30     185  185       1   19     'Y'    /
   'FLT_B1C '        29   29     185  185       1   19     'Y'    /
   'FLT_B1C '        28   28     185  185       1   19     'Y'    /
   'FLT_B1C '        27   27     185  185       1   19     'X'    /
   'FLT_B1C '        27   27     184  184       1   19     'Y'    /
   'FLT_B1C '        26   26     184  184       1   19     'X'    /
   'FLT_B1C '        26   26     183  183       1   19     'Y'    /
/

MULTFLT
FLT_B1C 0.001 /
/
```

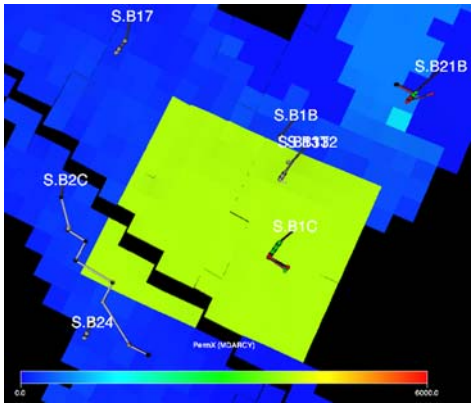

Figure C.14: Permeability region

C.2.15 B-6BT2

```
EQUALS
      MULTX 4     32    37    160   178   1     2     /
      MULTY 4     32    37    160   178   1     2     /
      MULTX 4     18    31    171   178   1     2     /
      MULTY 4     18    31    171   178   1     2     /
/
```

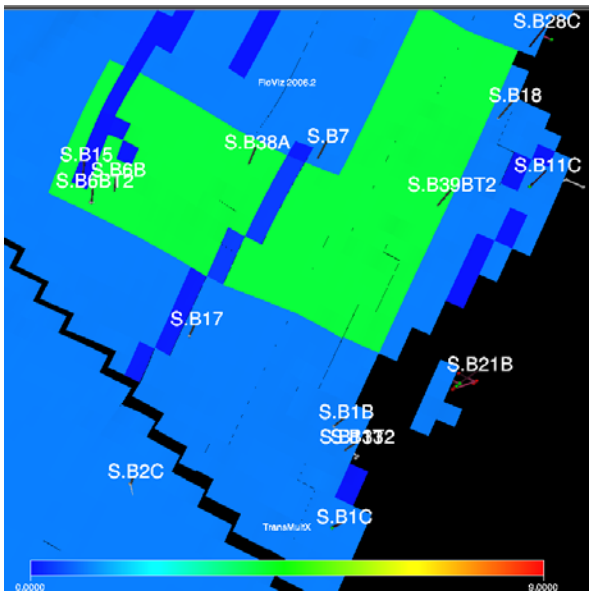

Figure C.15: MULTX/Y-region

C.2.16 B-11C

```
EQUALS
      PERMX 500   38    42    165   178   1     2     /
      PERMY 500   38    42    165   178   1     2     /
/

-- KEYWORD "FAULTS" HAS BEEN WRITTEN FROM RESVIEW.

FAULTS
--    NAME          IX1  IX2     IY1  IY2     IZ1  IZ2    FACE
   'B11C_2  '        42   42     164  164       1   46     'X'    /
   'B11C_2  '        42   42     164  164       1   46     'Y'    /
   'B11C_2  '        41   41     165  165       1   46     'X'    /
   'B11C_2  '        41   41     165  165       1   46     'Y'    /
   'B11C_2  '        40   40     166  166       1   46     'X'    /
   'B11C_2  '        40   40     167  167       1   46     'X'    /
   'B11C_2  '        40   40     167  167       1   46     'Y'    /
   'B11C_2  '        39   39     167  167       1   46     'Y'    /
/

MULTFLT
B11C_2 0.001 /
/
```

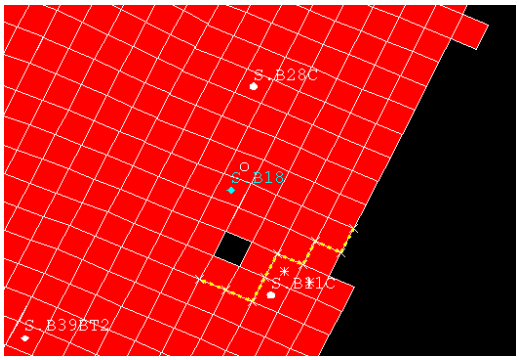

Figure C.16: Fault B11C_2

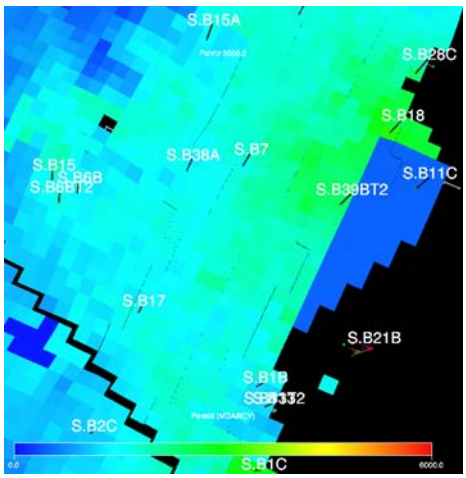

Figure C.17: Permeability region

C.2.17 B-15

```
EQUALS
      MULTX 3.0    20    38    164   177   11    11    /
      MULTY 3.0    20    38    164   177   11    11    /
      MULTX 0.001 19    19    174   177   1     46    /
/
```

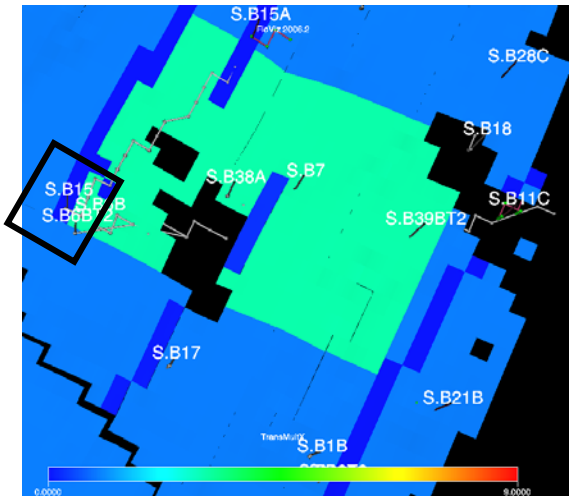

Figure C.18: MULTX/Y region and fault extension

C.2.18 B-21B

```
-- KEYWORD "FAULTS" HAS BEEN WRITTEN FROM RESVIEW.

FAULTS
--    NAME          IX1  IX2     IY1  IY2     IZ1  IZ2    FACE
   'B21B_L'        44   44     168  168       20   46     'Y'    /
   'B21B_L'        43   43     168  168       20   46     'Y'    /
   'B21B_L'        42   42     168  168       20   46     'Y'    /
   'B21B_L'        41   41     169  169       20   46     'X'    /
   'B21B_L'        41   41     170  170       20   46     'X'    /
   'B21B_L'        41   41     170  170       20   46     'Y'    /
   'B21B_L'        40   40     171  171       20   46     'X'    /
   'B21B_L'        40   40     172  172       20   46     'X'    /
   'B21B_L'        40   40     173  173       20   46     'X'    /
   'B21B_L'        40   40     174  174       20   46     'X'    /
   'B21B_L'        40   40     175  175       20   46     'X'    /
   'B21B_L'        40   40     176  176       20   46     'X'    /
   'B21B_L'        40   40     176  176       20   46     'Y'    /
   'B21B_L'        39   39     177  177       20   46     'X'    /
   'B21B_L'        39   39     178  178       20   46     'X'    /
   'B21B_L'        39   39     179  179       20   46     'X'    /
   'B21B_L'        39   39     180  180       20   46     'X'    /
   'B21B_L'        39   39     181  181       20   46     'X'    /
   'B21B_L'        39   39     182  182       20   46     'X'    /
   'B21B_L'        39   39     183  183       20   46     'X'    /
   'B21B_L'        39   39     184  184       20   46     'X'    /
   'B21B_L'        39   39     185  185       20   46     'X'    /
   'B21B_L'        39   39     186  186       20   46     'X'    /
/


-- KEYWORD "FAULTS" HAS BEEN WRITTEN FROM RESVIEW.

FAULTS
--    NAME          IX1  IX2     IY1  IY2     IZ1  IZ2    FACE
   'B21B_U'        44   44     168  168       1   19     'Y'    /
   'B21B_U'        43   43     168  168       1   19     'Y'    /
   'B21B_U'        42   42     168  168       1   19     'Y'    /
   'B21B_U'        41   41     169  169       1   19     'X'    /
   'B21B_U'        41   41     170  170       1   19     'X'    /
   'B21B_U'        41   41     170  170       1   19     'Y'    /
   'B21B_U'        40   40     171  171       1   19     'X'    /
   'B21B_U'        40   40     172  172       1   19     'X'    /
   'B21B_U'        40   40     173  173       1   19     'X'    /
   'B21B_U'        40   40     174  174       1   19     'X'    /
   'B21B_U'        40   40     175  175       1   19     'X'    /
   'B21B_U'        40   40     176  176       1   19     'X'    /
   'B21B_U'        40   40     176  176       1   19     'Y'    /
   'B21B_U'        39   39     177  177       1   19     'X'    /
   'B21B_U'        39   39     178  178       1   19     'X'    /
   'B21B_U'        39   39     179  179       1   19     'X'    /
   'B21B_U'        39   39     180  180       1   19     'X'    /
   'B21B_U'        39   39     181  181       1   19     'X'    /
   'B21B_U'        39   39     182  182       1   19     'X'    /
   'B21B_U'        39   39     183  183       1   19     'X'    /
```

```
   'B21B_U'        39   39     184  184       1   19     'X'    /
   'B21B_U'        39   39     185  185       1   19     'X'    /
   'B21B_U'        39   39     186  186       1   19     'X'    /
/

MULTFLT
B21B_L 0.5 /
B21B_U 0.0001 /
/
```

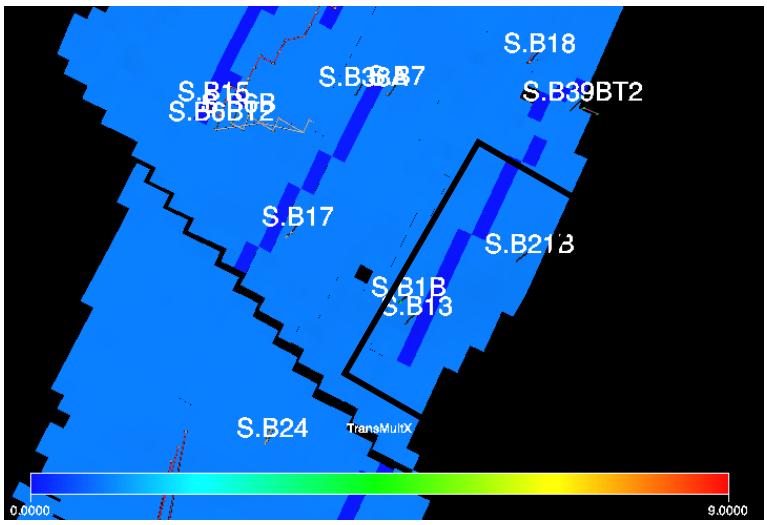

Figure C.19: Fault B21B_U/L

D SWC and WCT for history matched wells

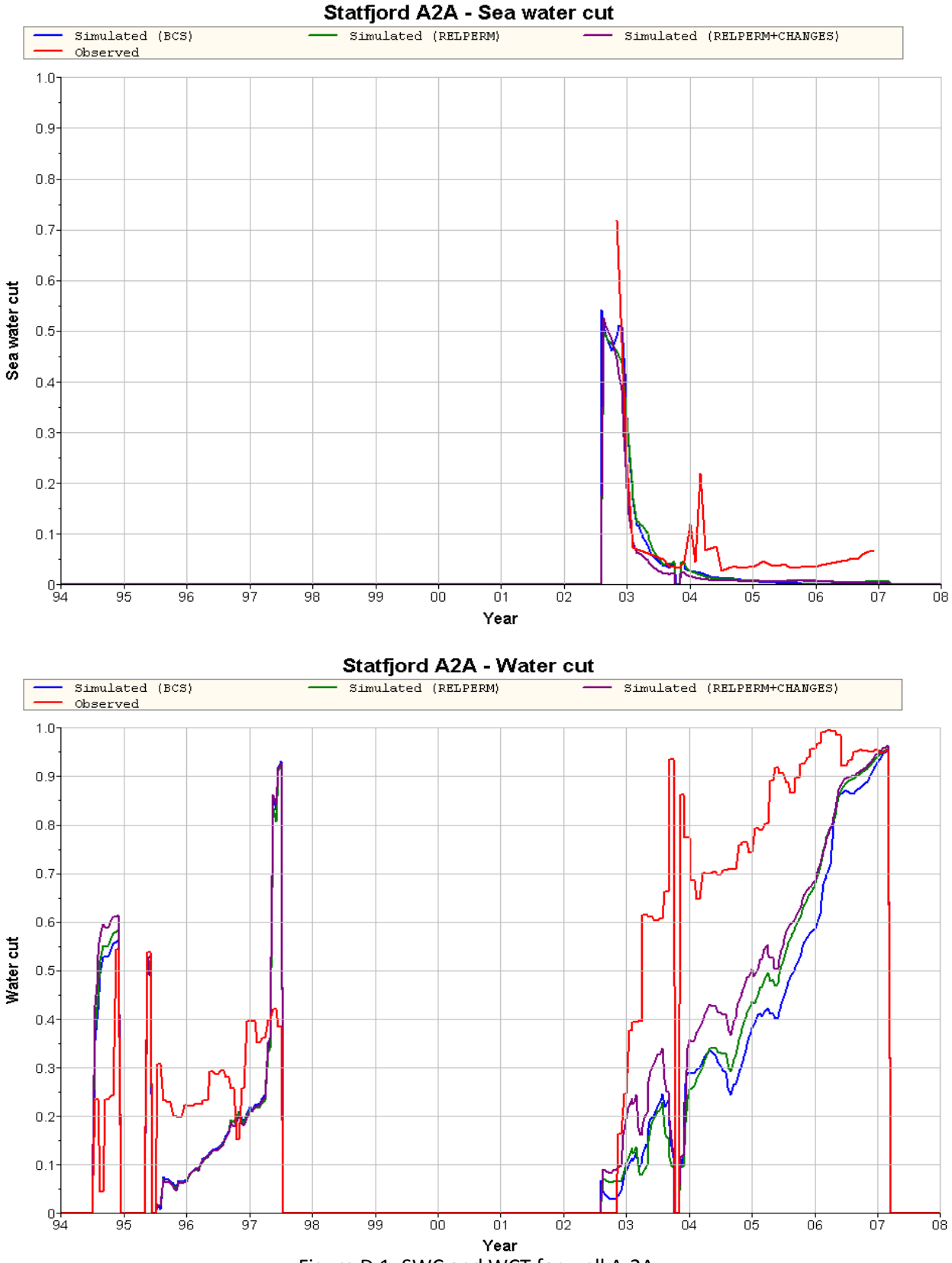

Figure D.1: SWC and WCT for well A-2A

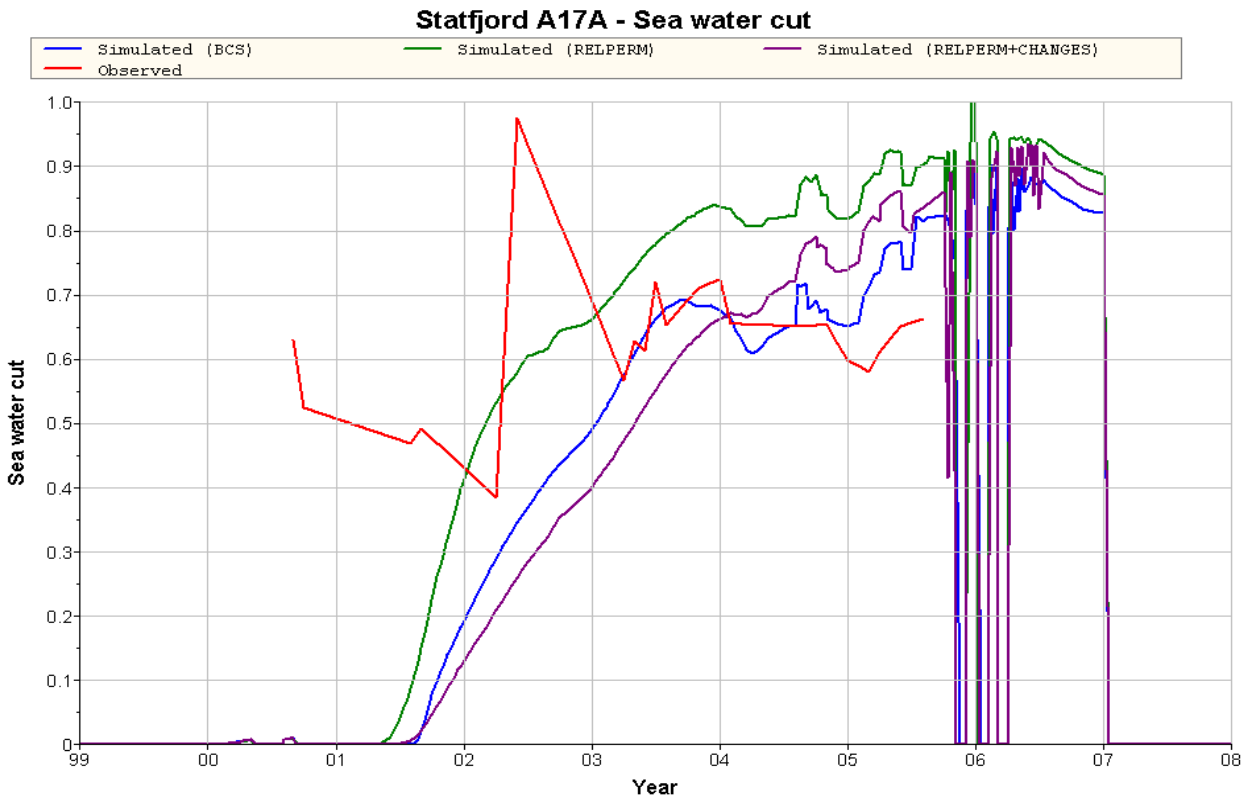

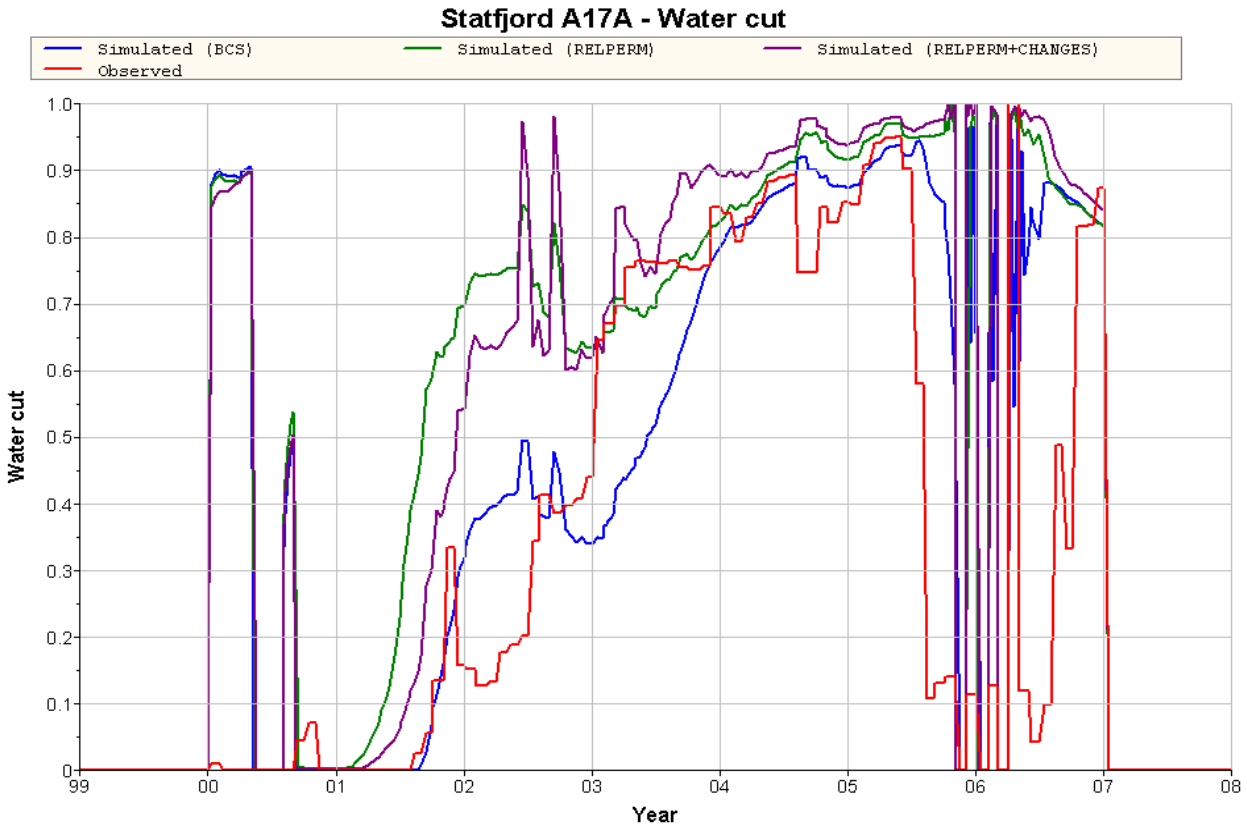

Figure D.2: SWC and WCT for well A-17A

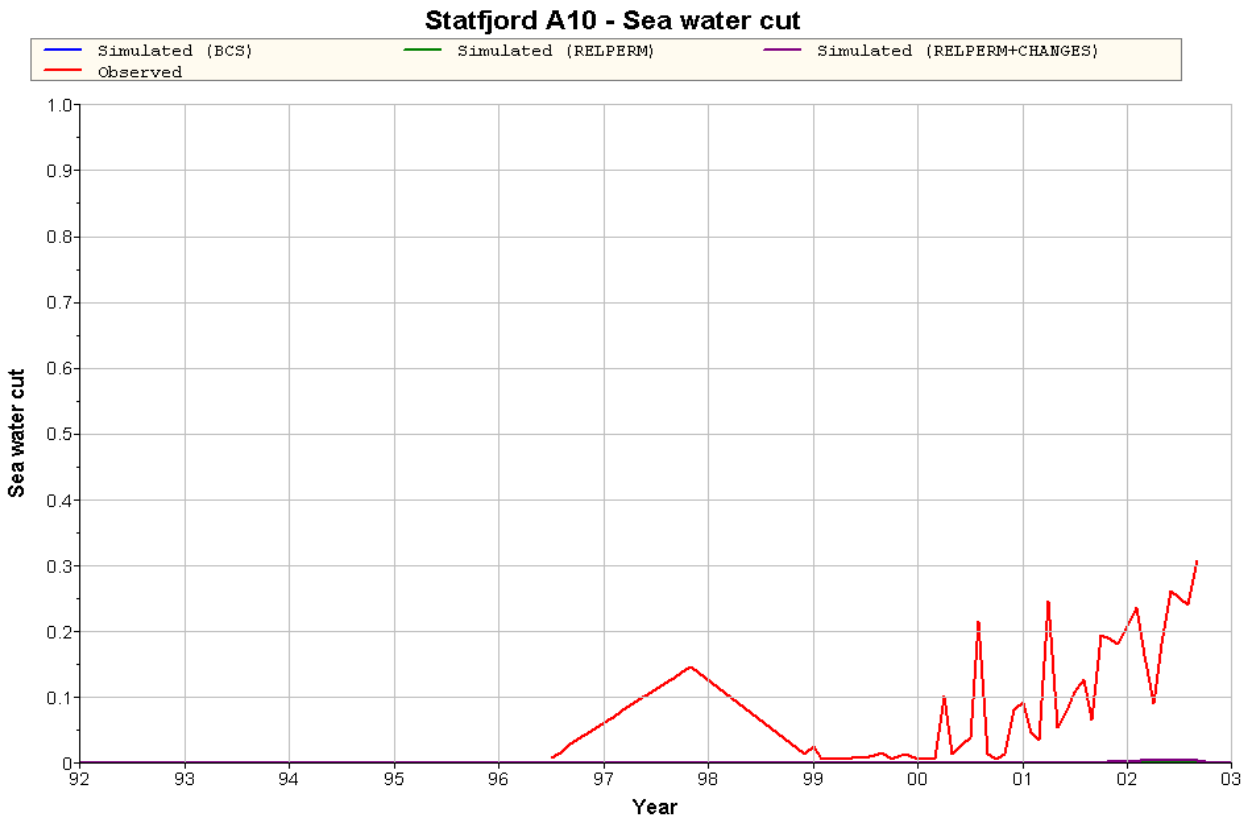

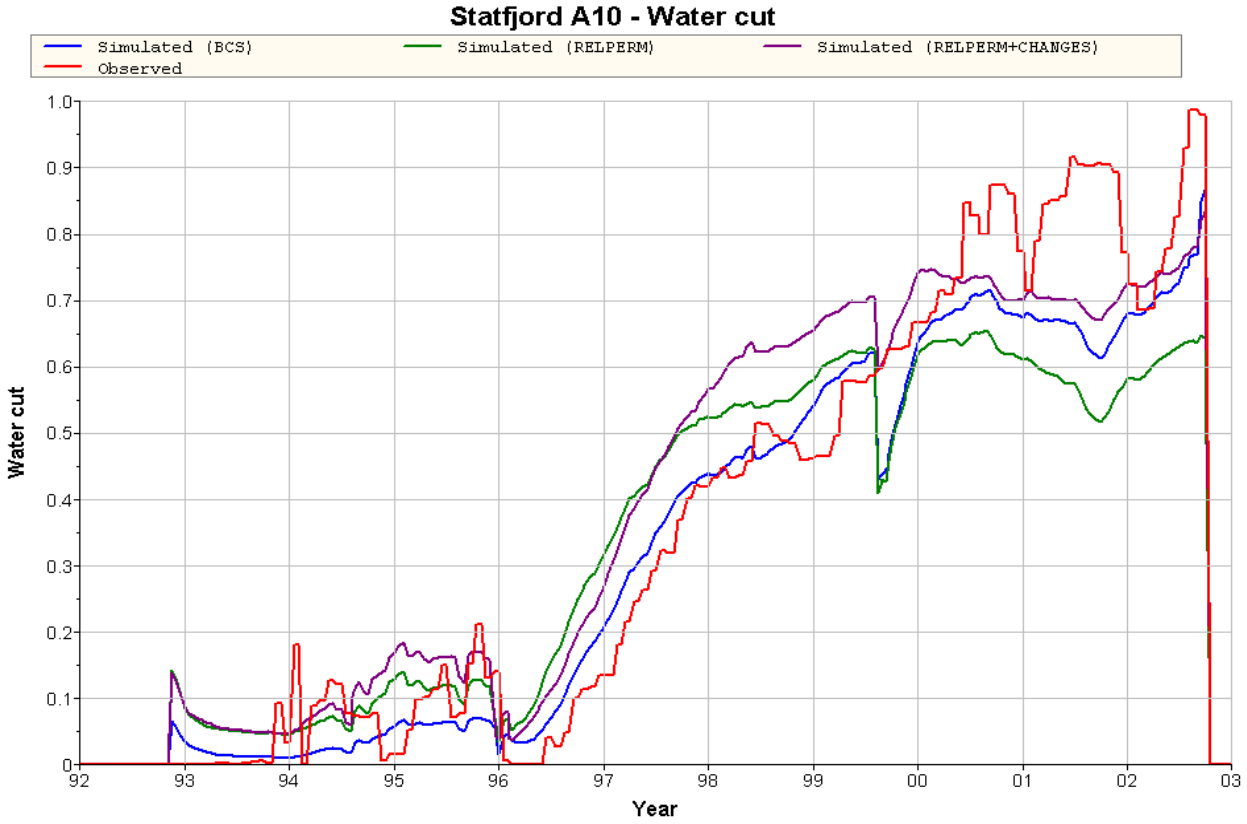

Figure D.3: SWC and WCT for well A-10

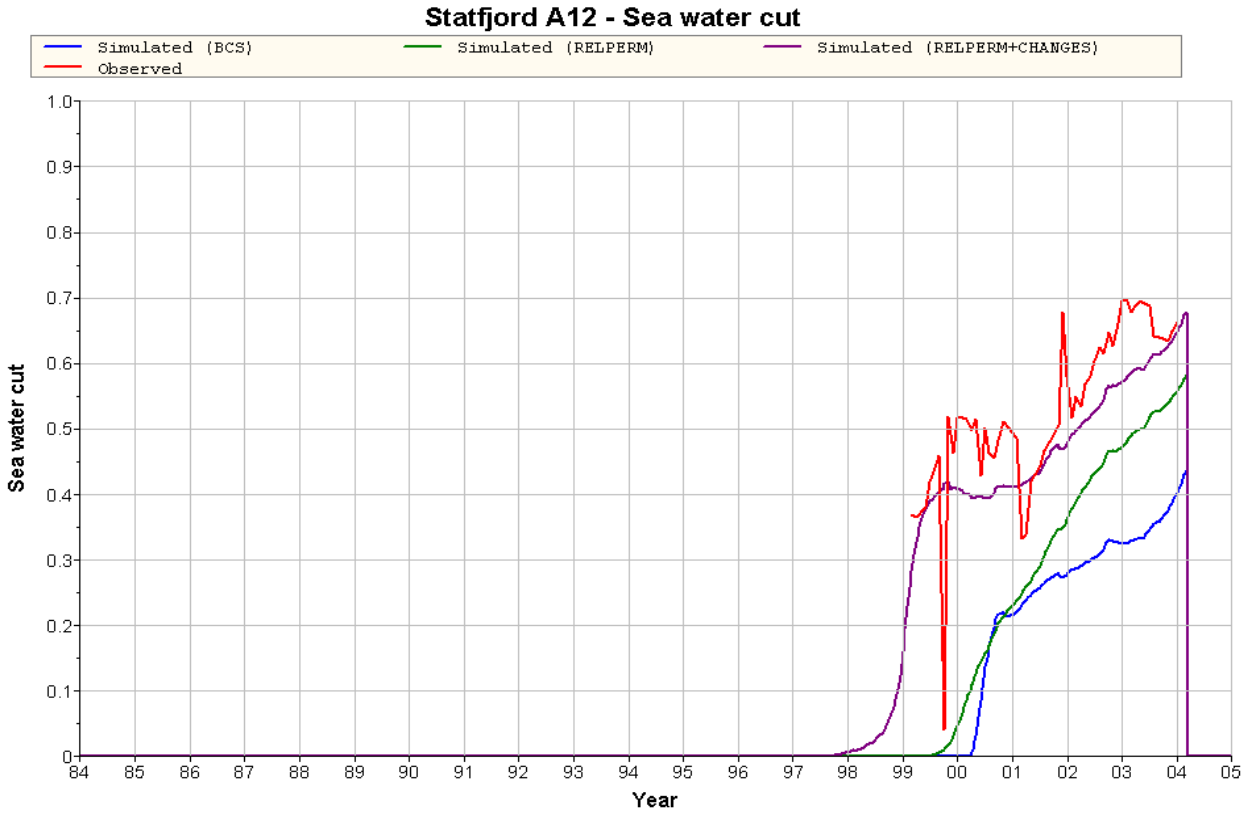

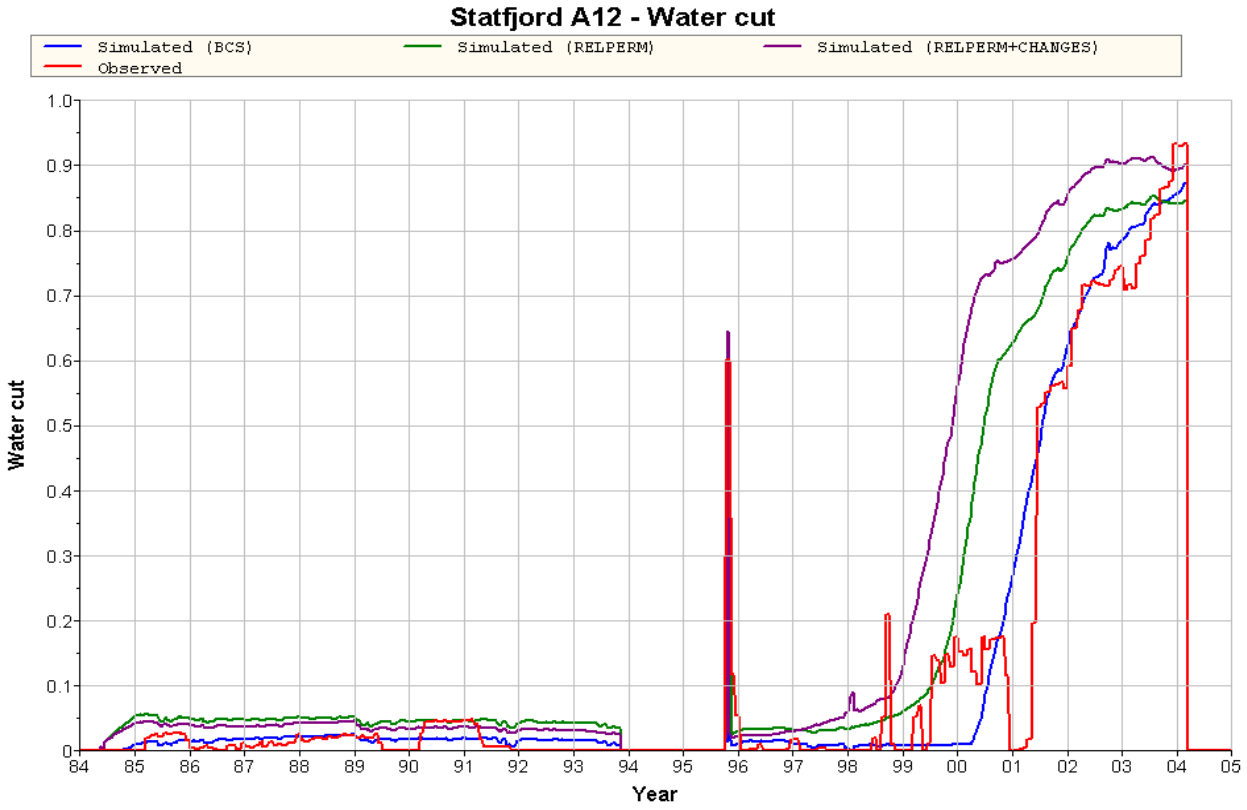

Figure D.4: SWC and WCT for well A-12

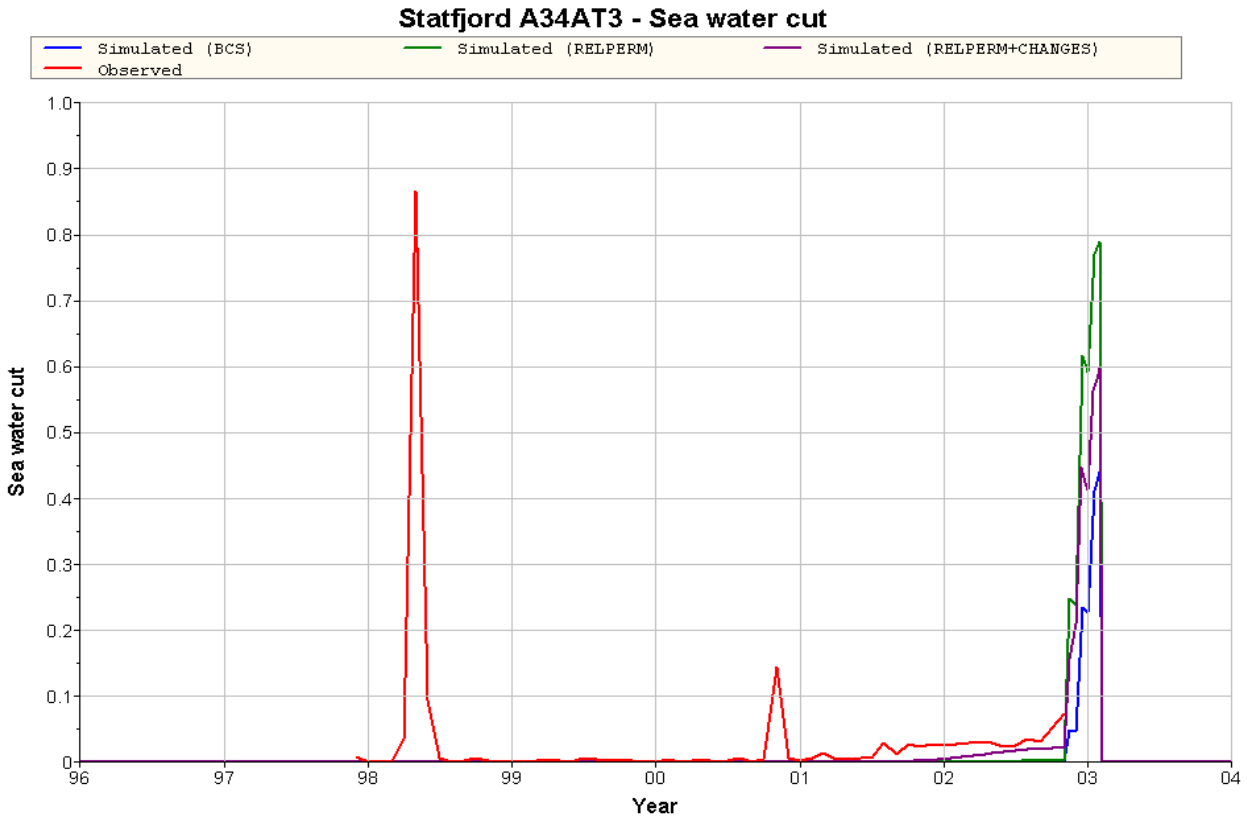

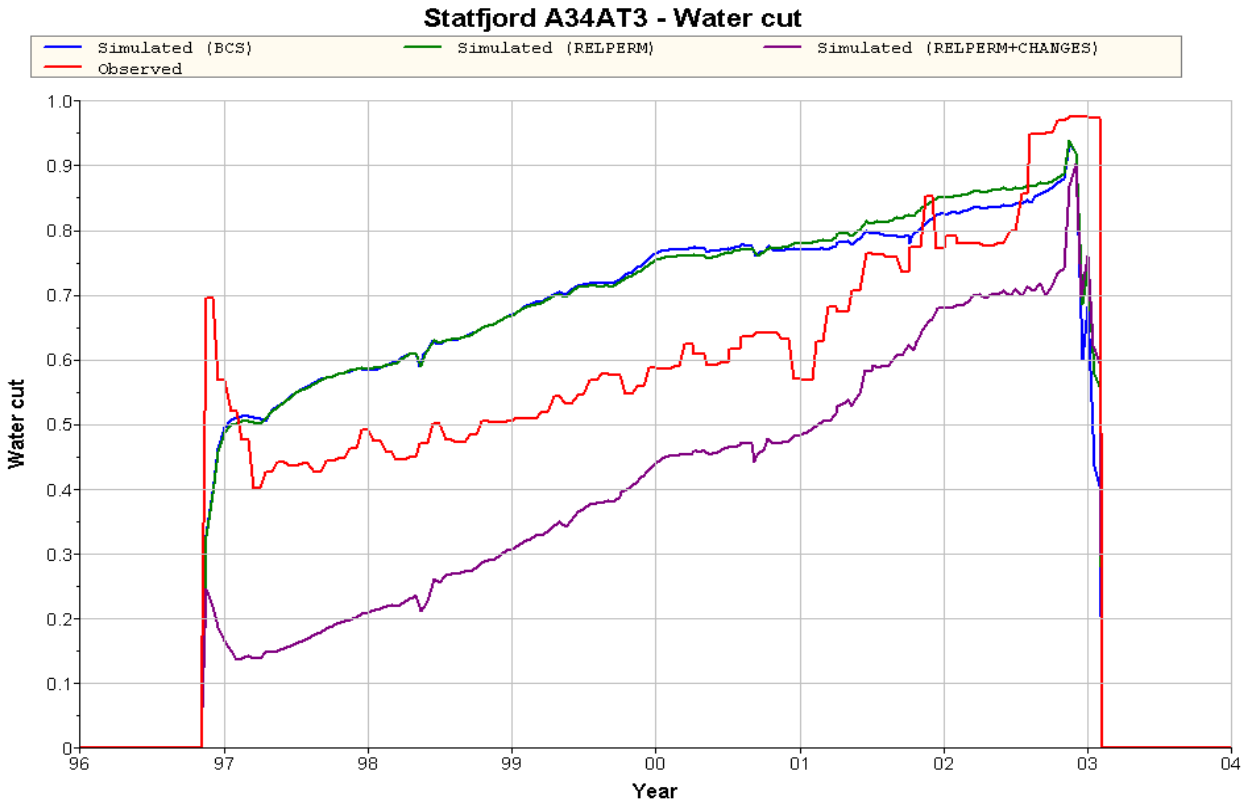

Figure D.5: SWC and WCT for well A-34AT3

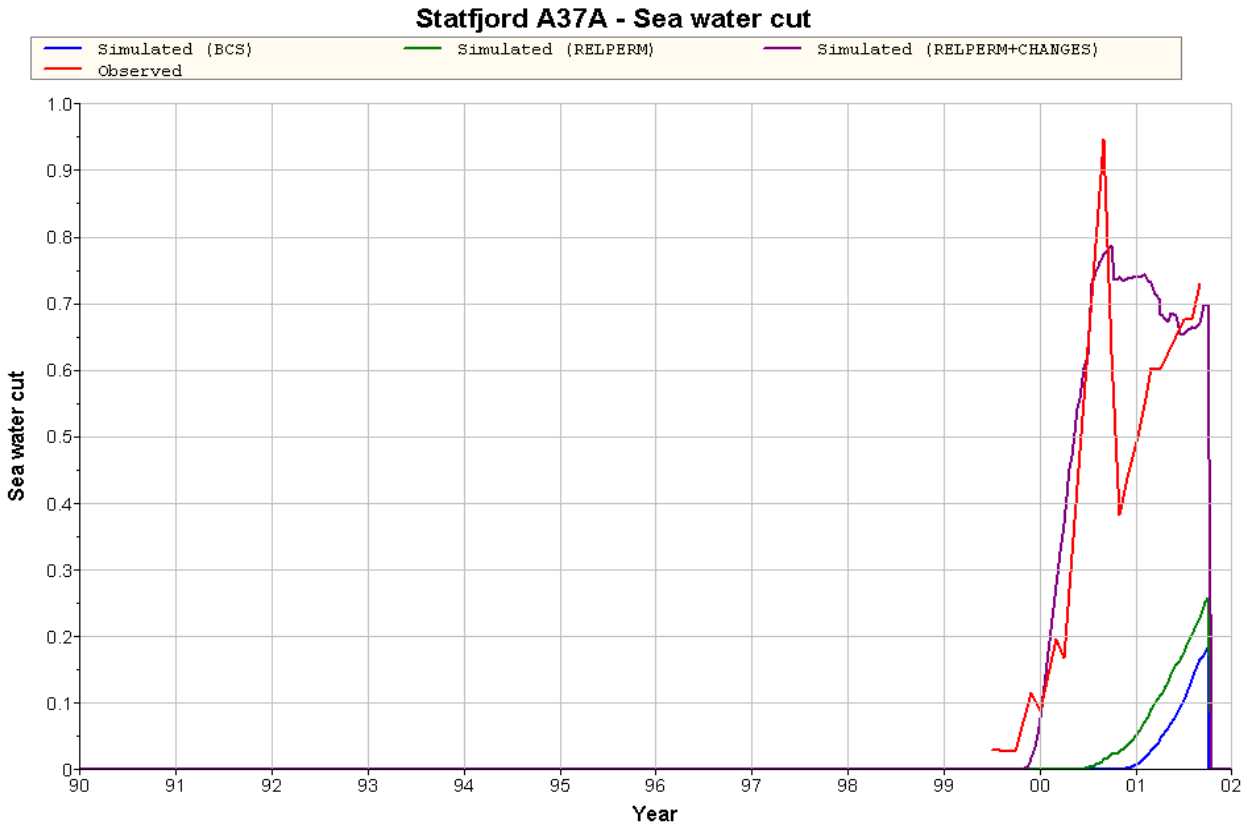

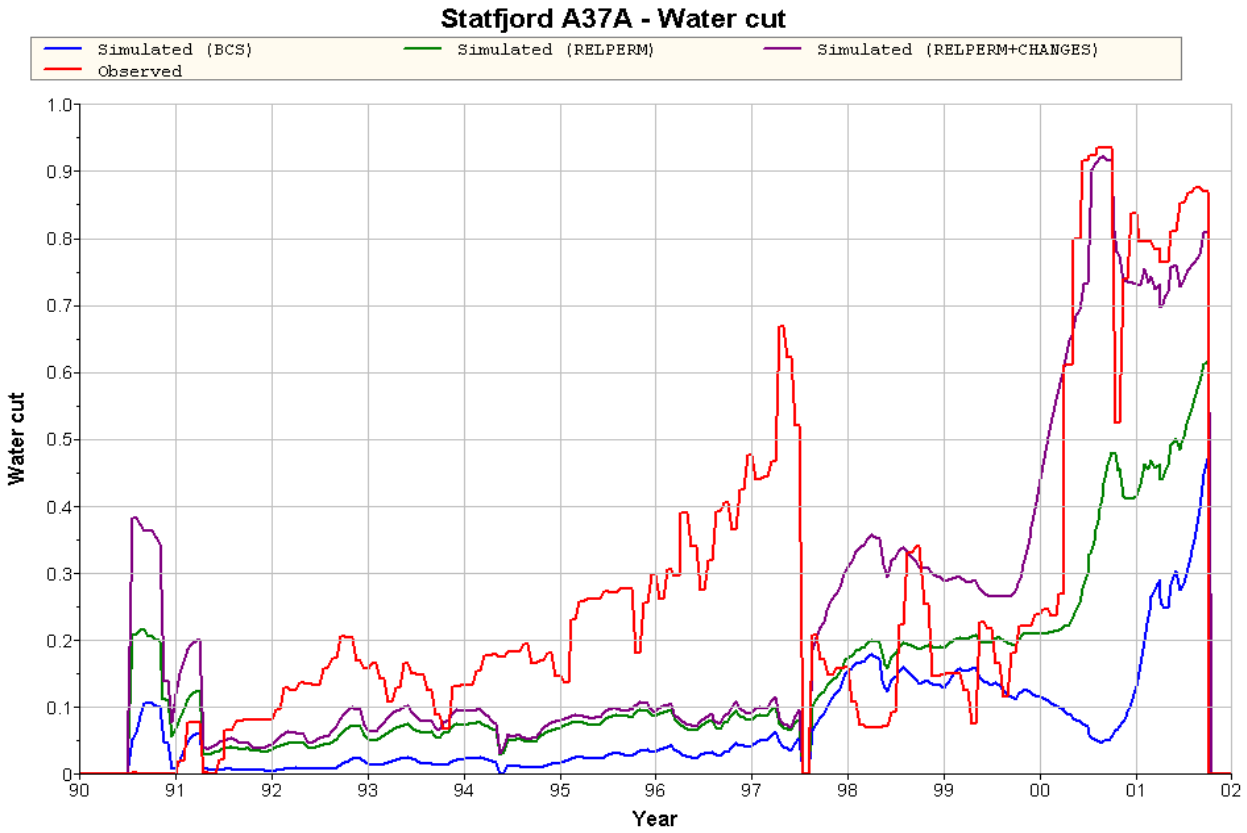

Figure D.6: SWC and WCT for well A-37A

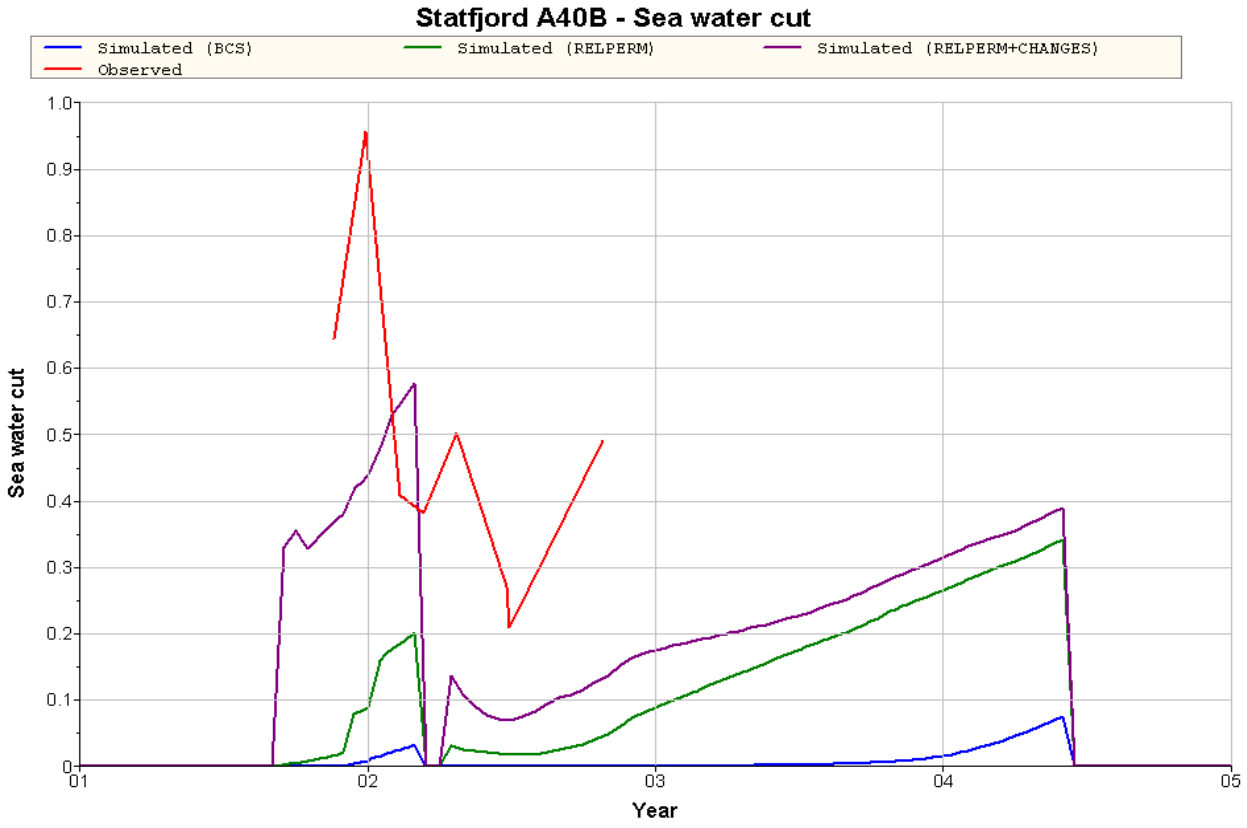

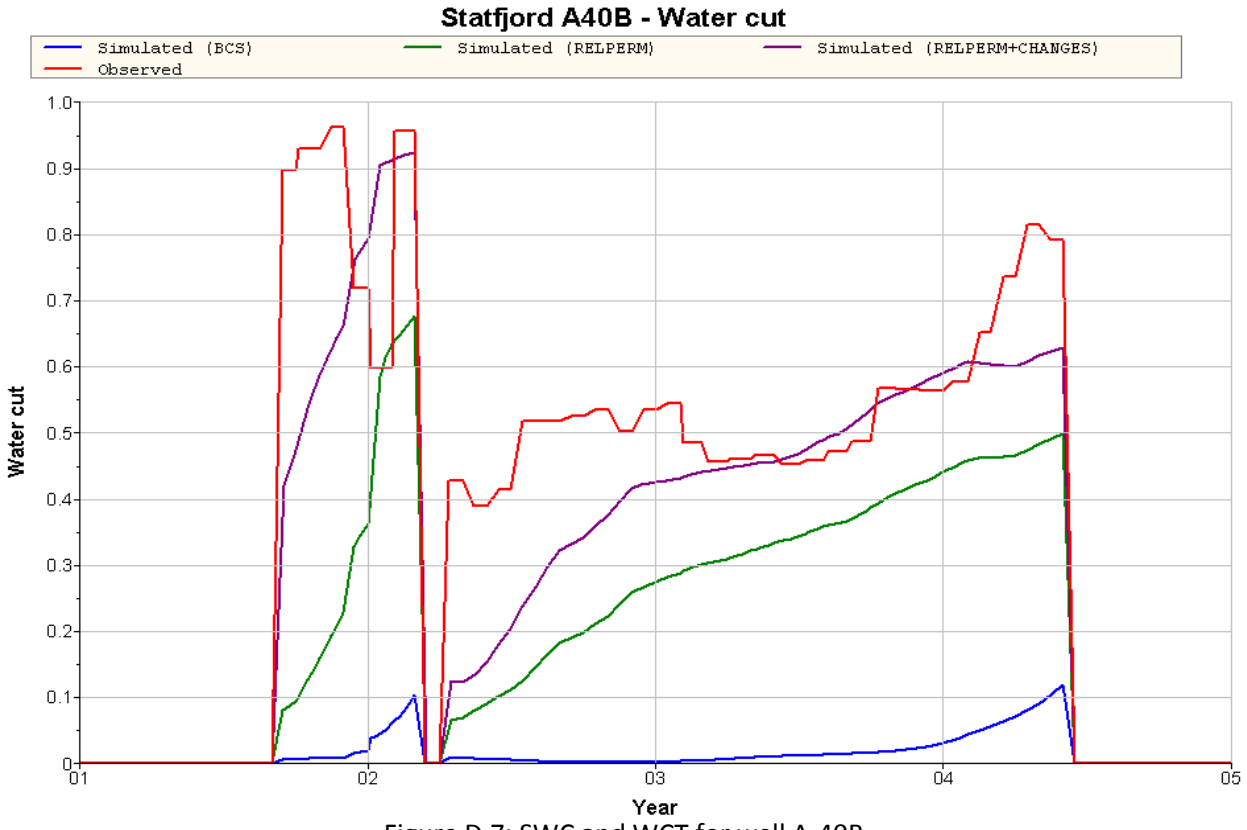

Figure D.7: SWC and WCT for well A-40B

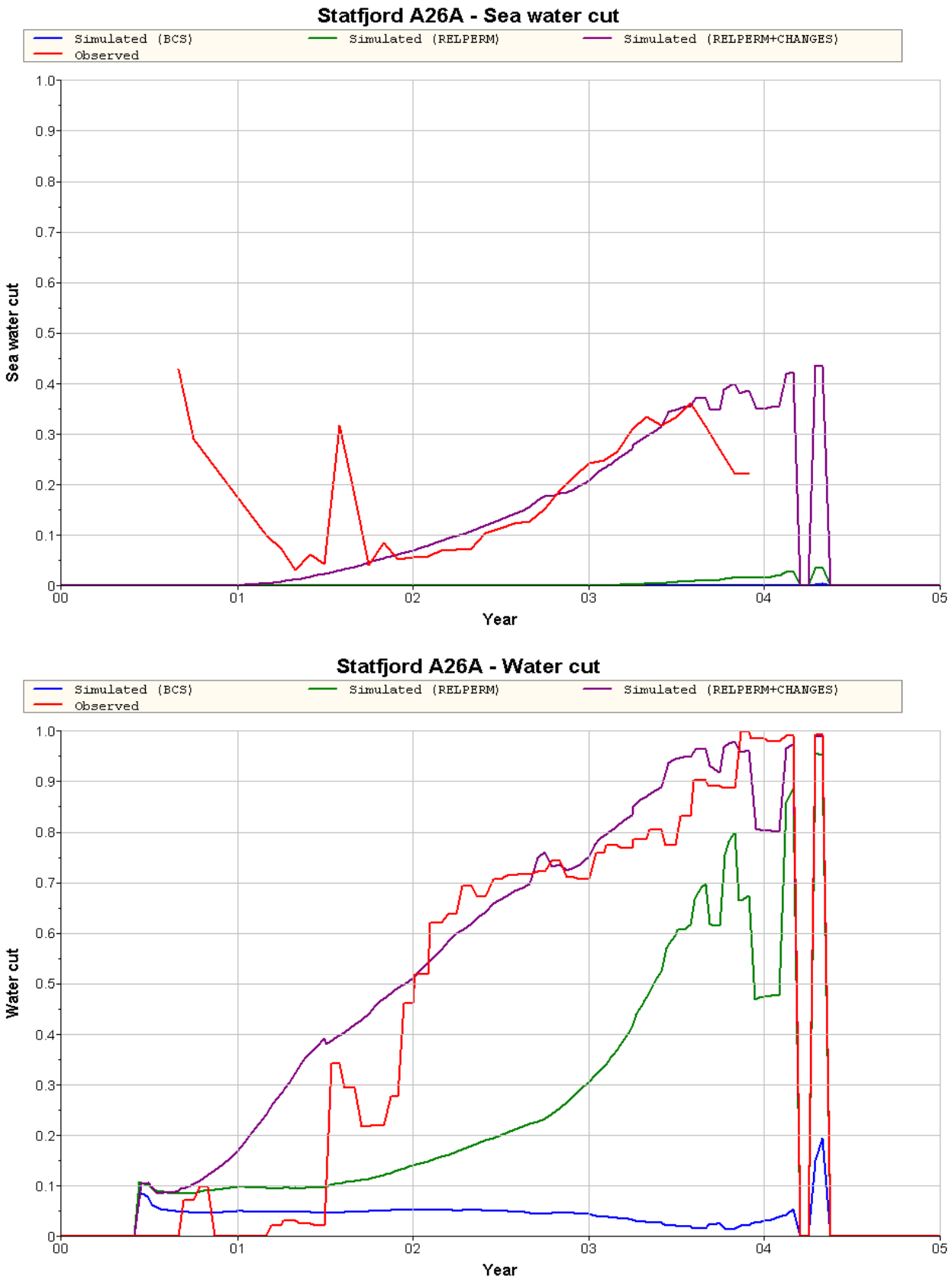

Figure D.8: SWC and WCT for well A-26A

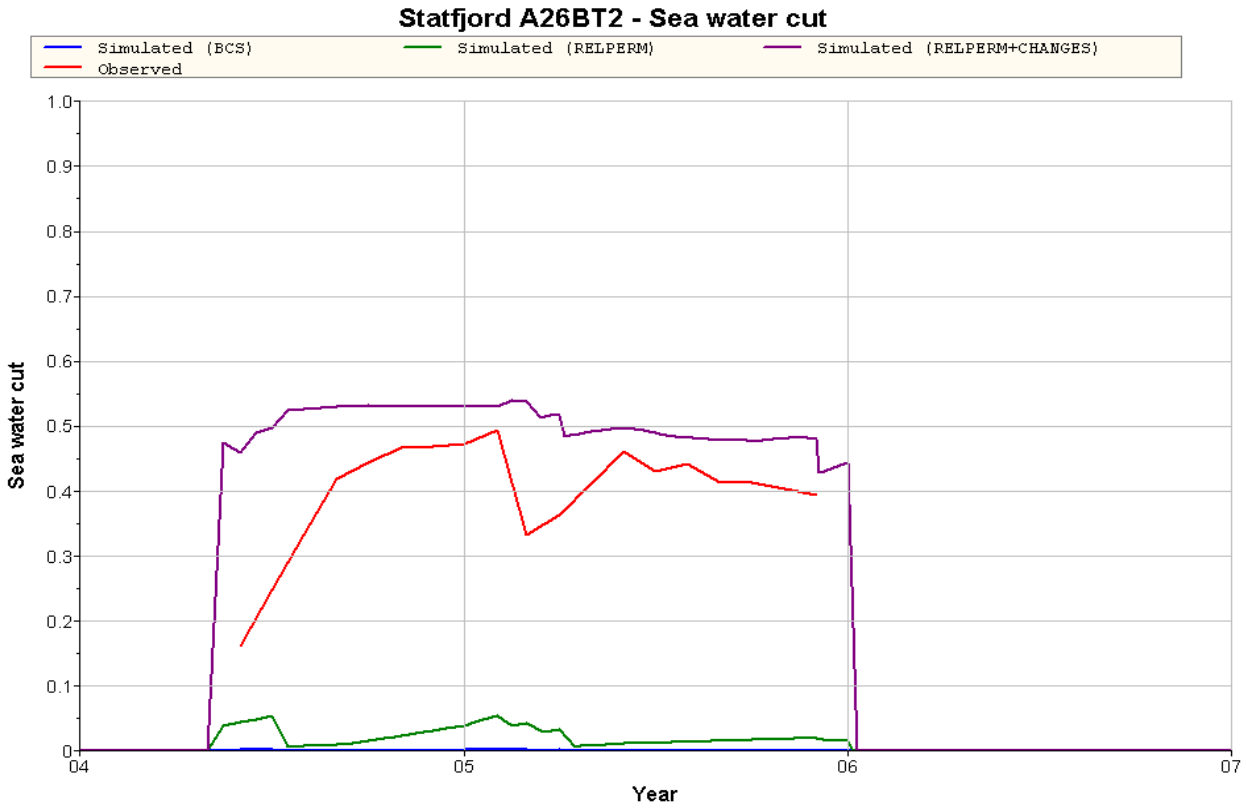

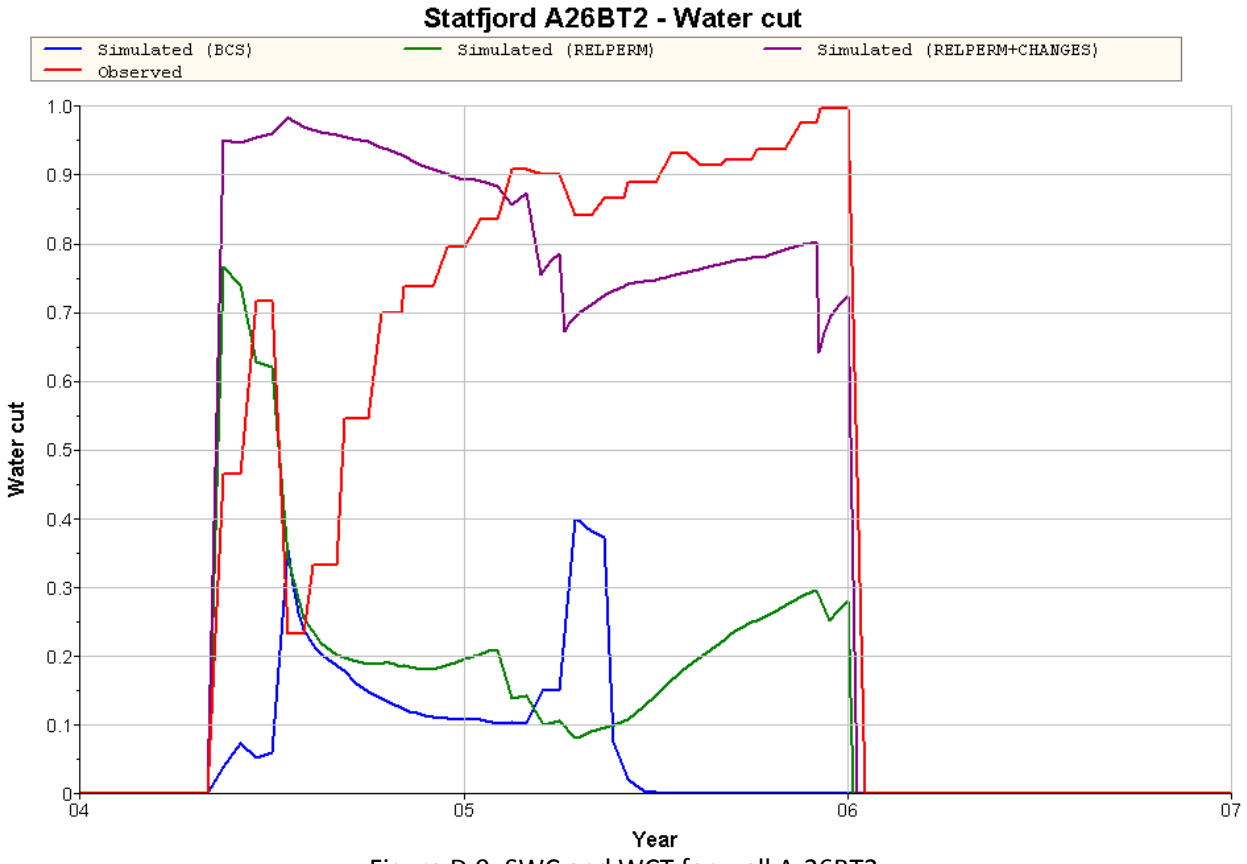

Figure D.9: SWC and WCT for well A-26BT2

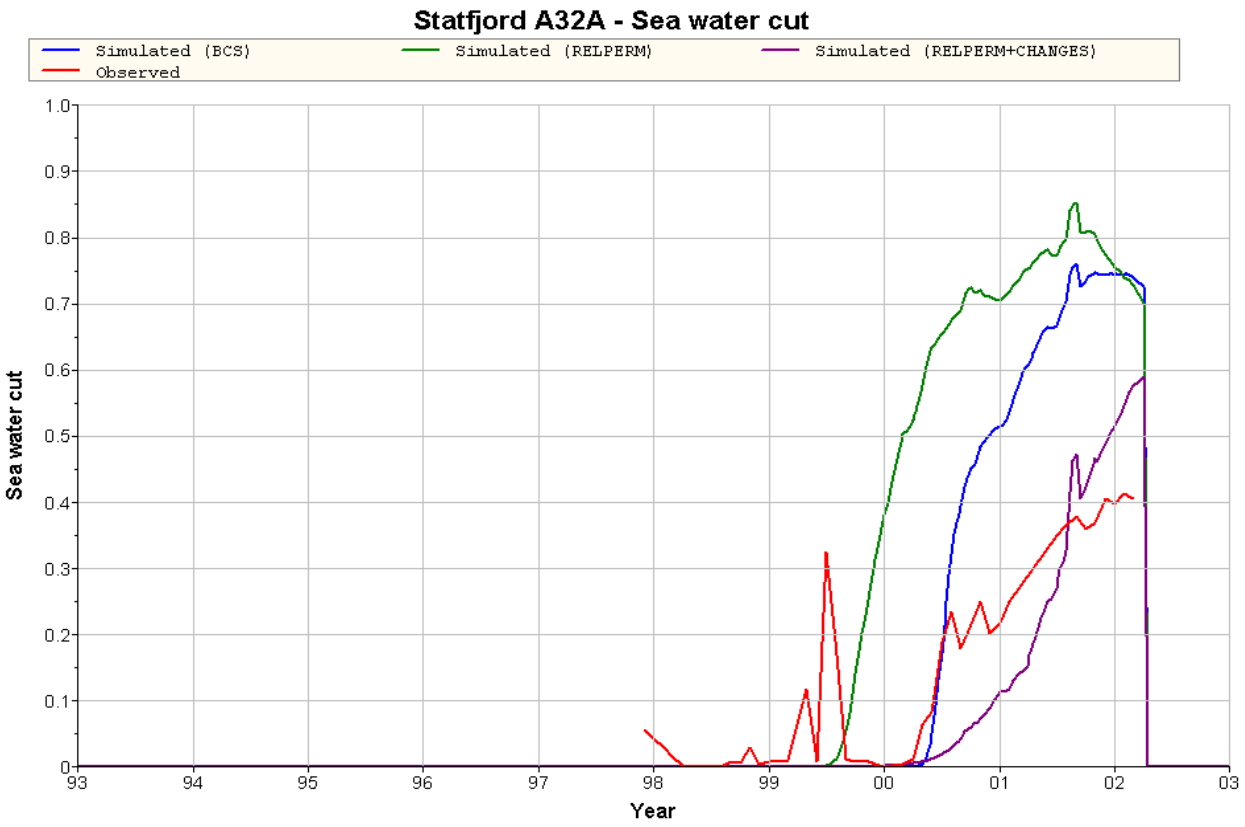

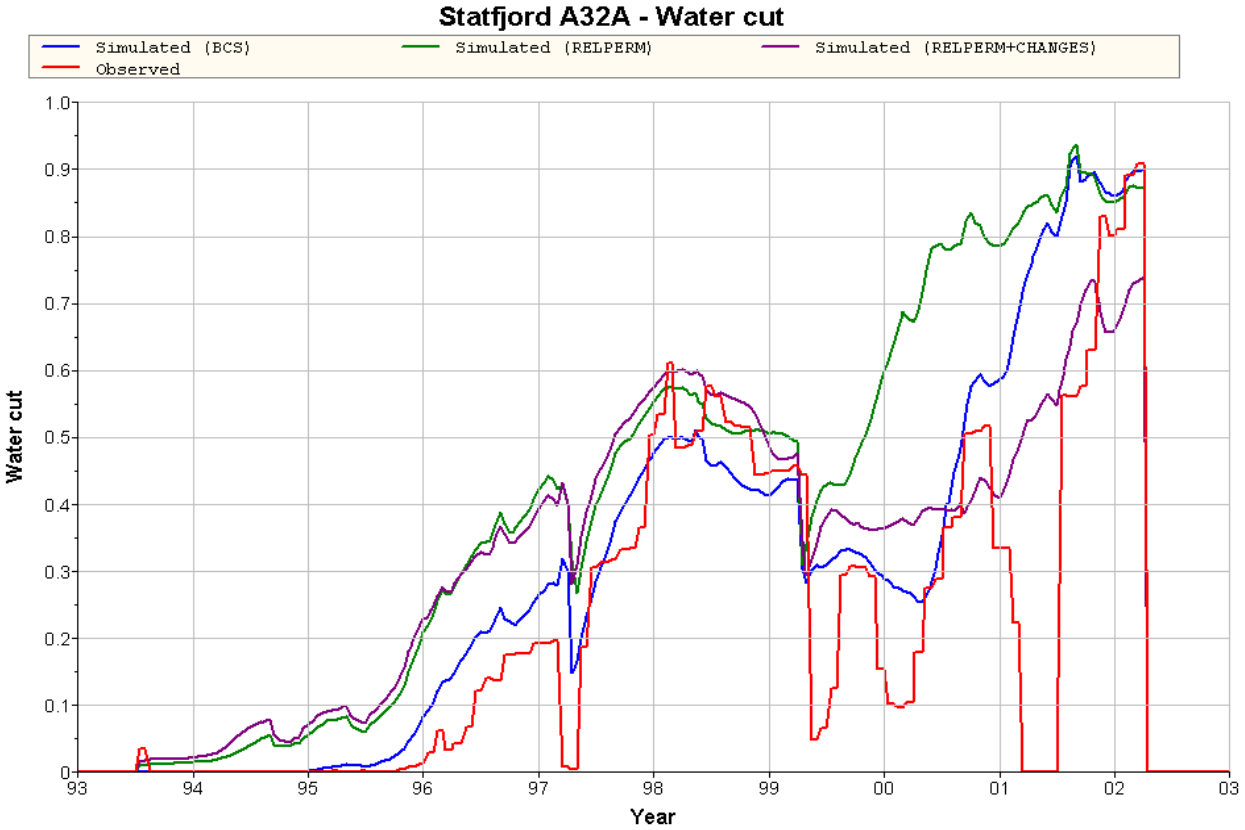

Figure D.10: SWC and WCT for well A-32A

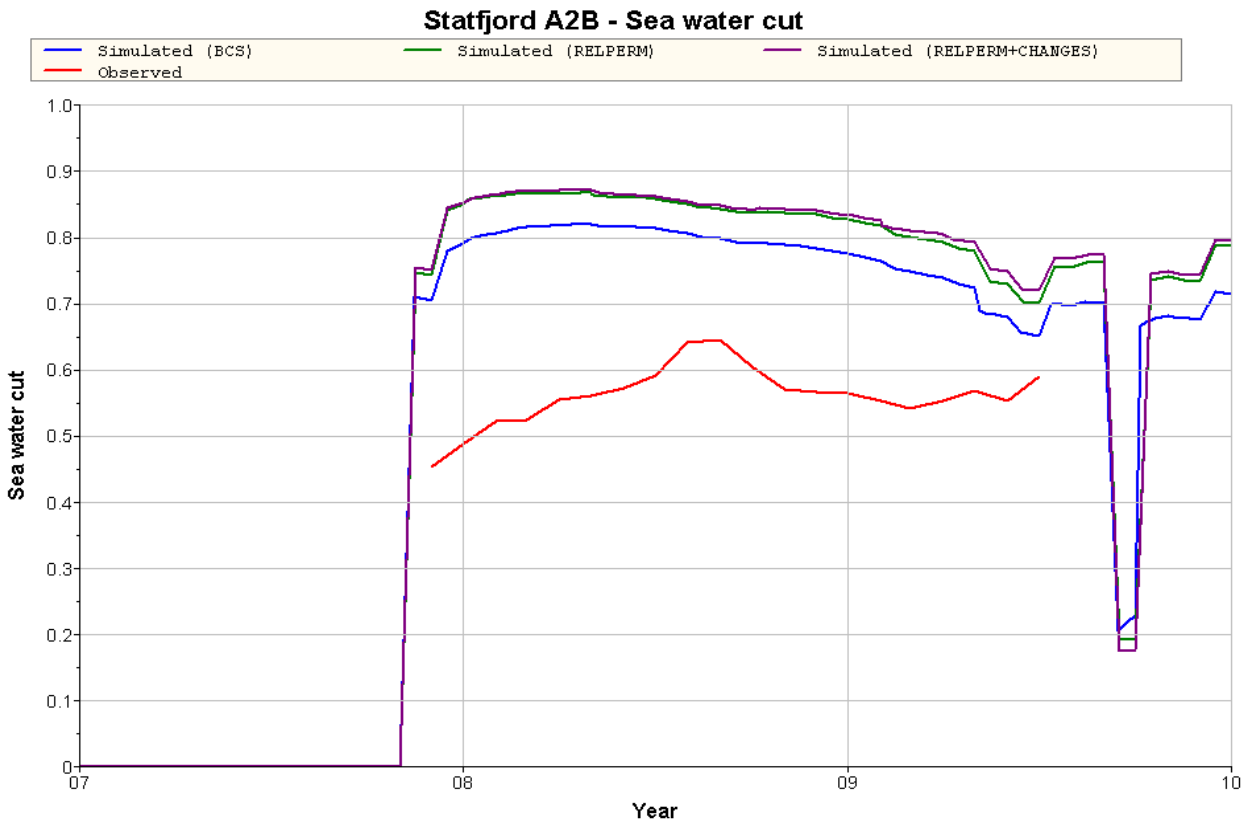

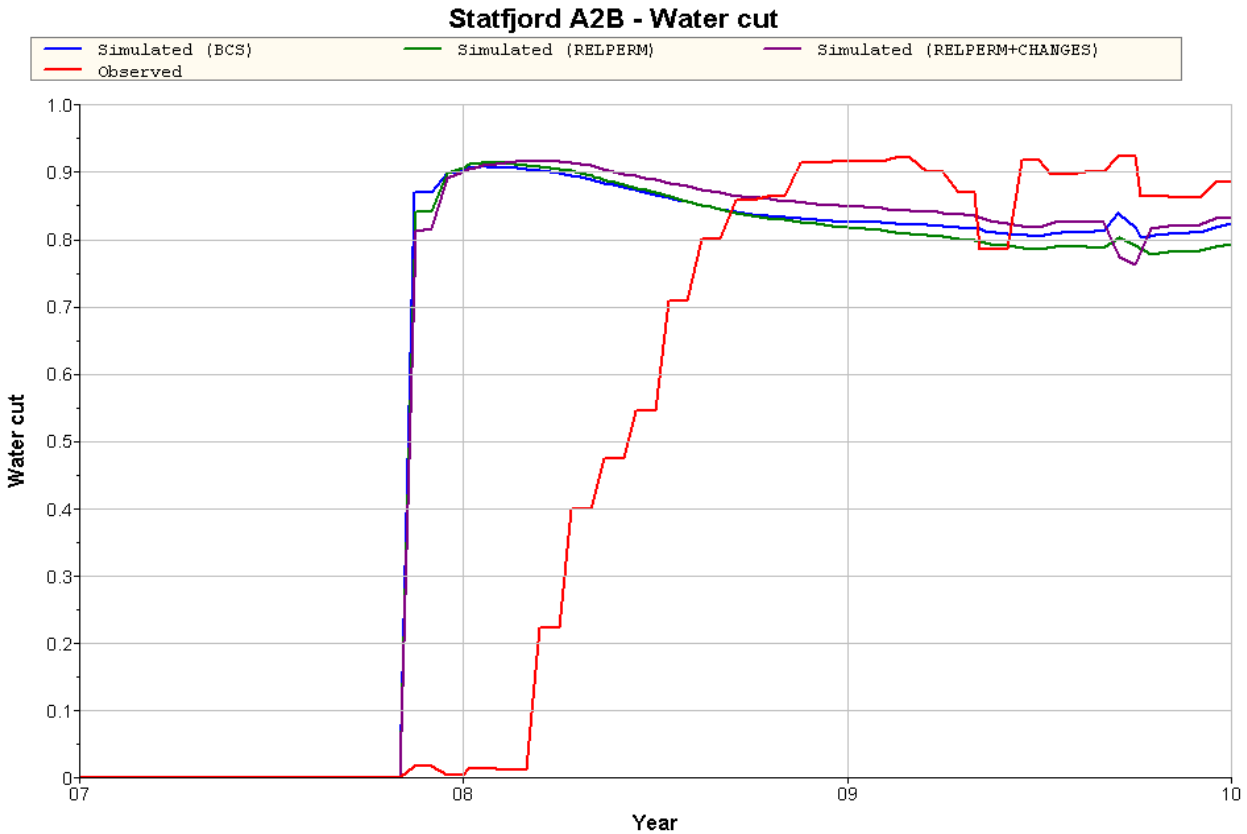

Figure D.11: SWC and WCT for well A-2B

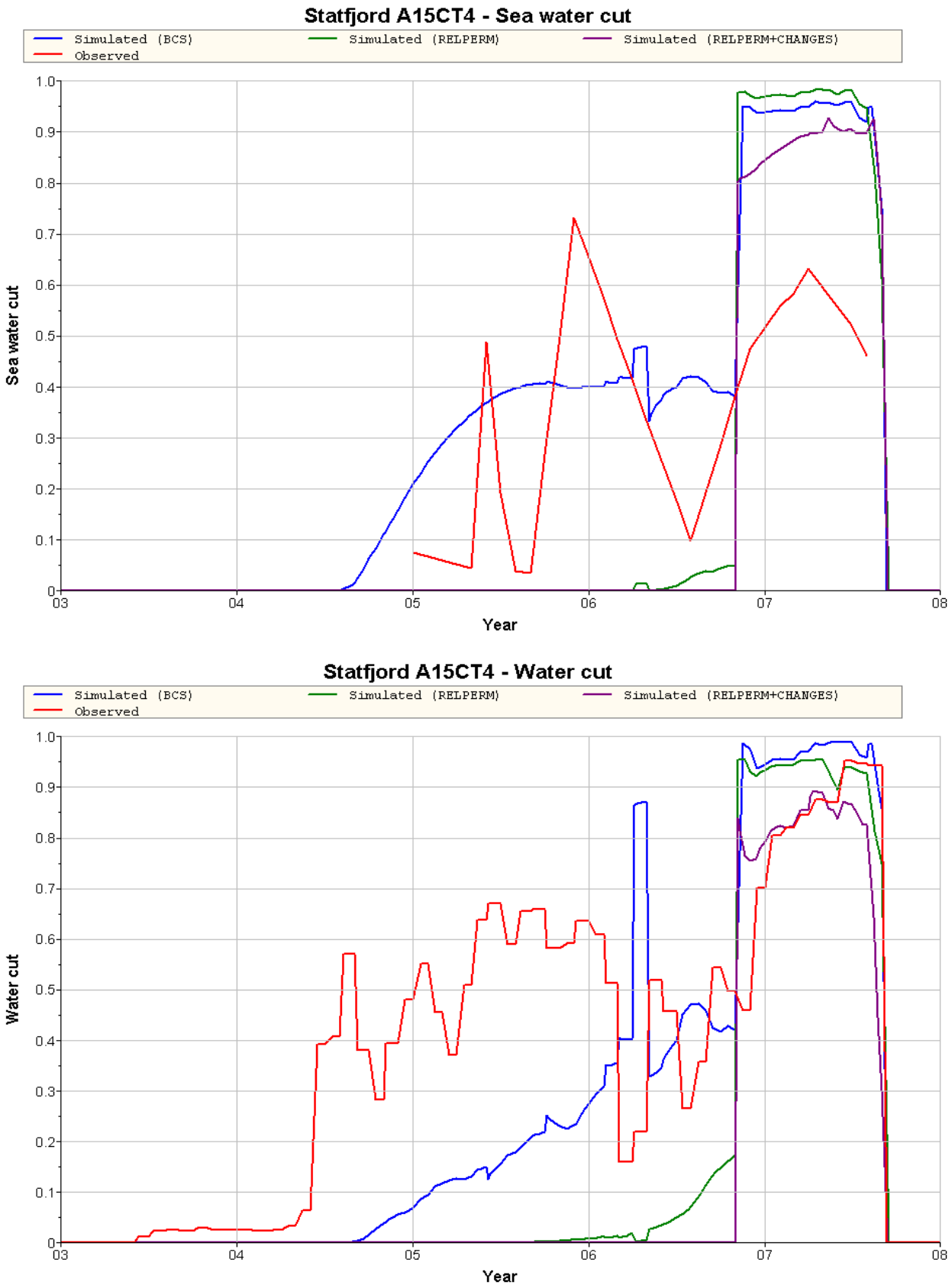

Figure D.12: SWC and WCT for well A-15CT4

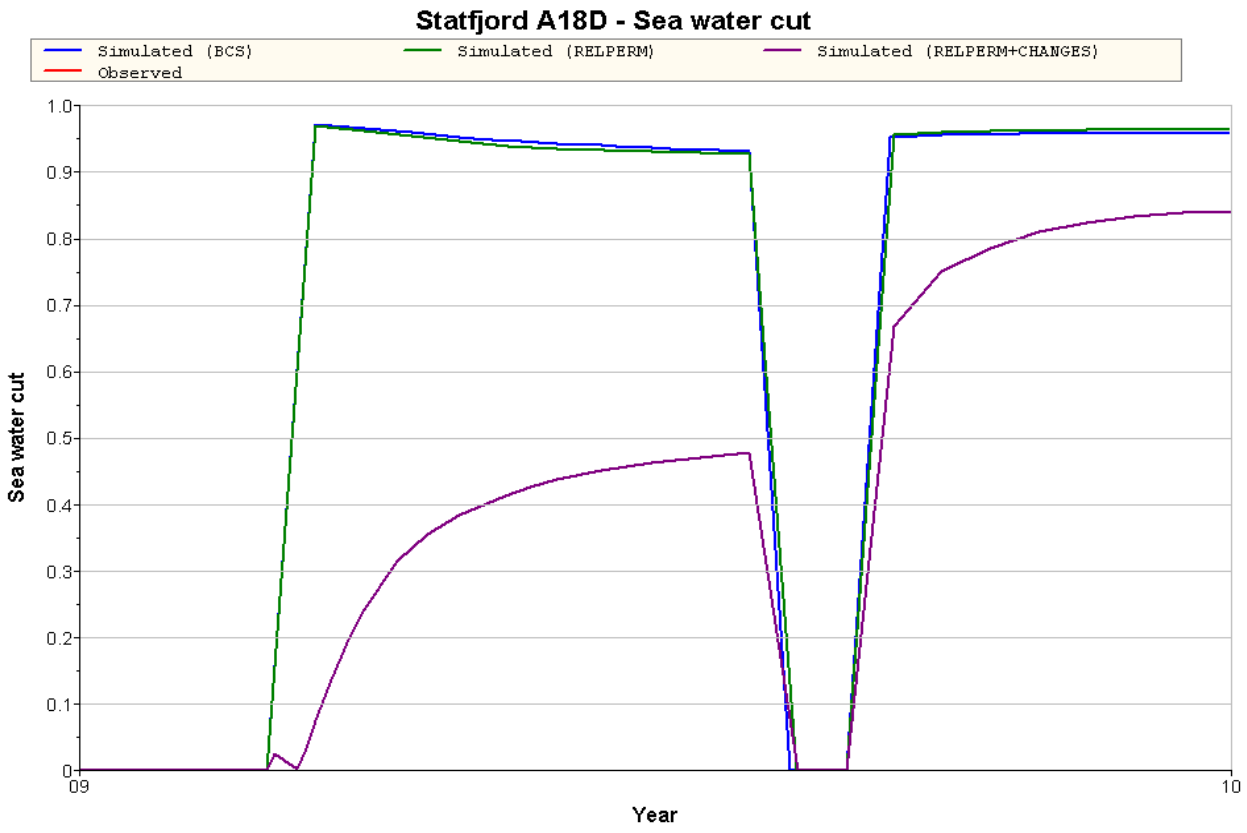

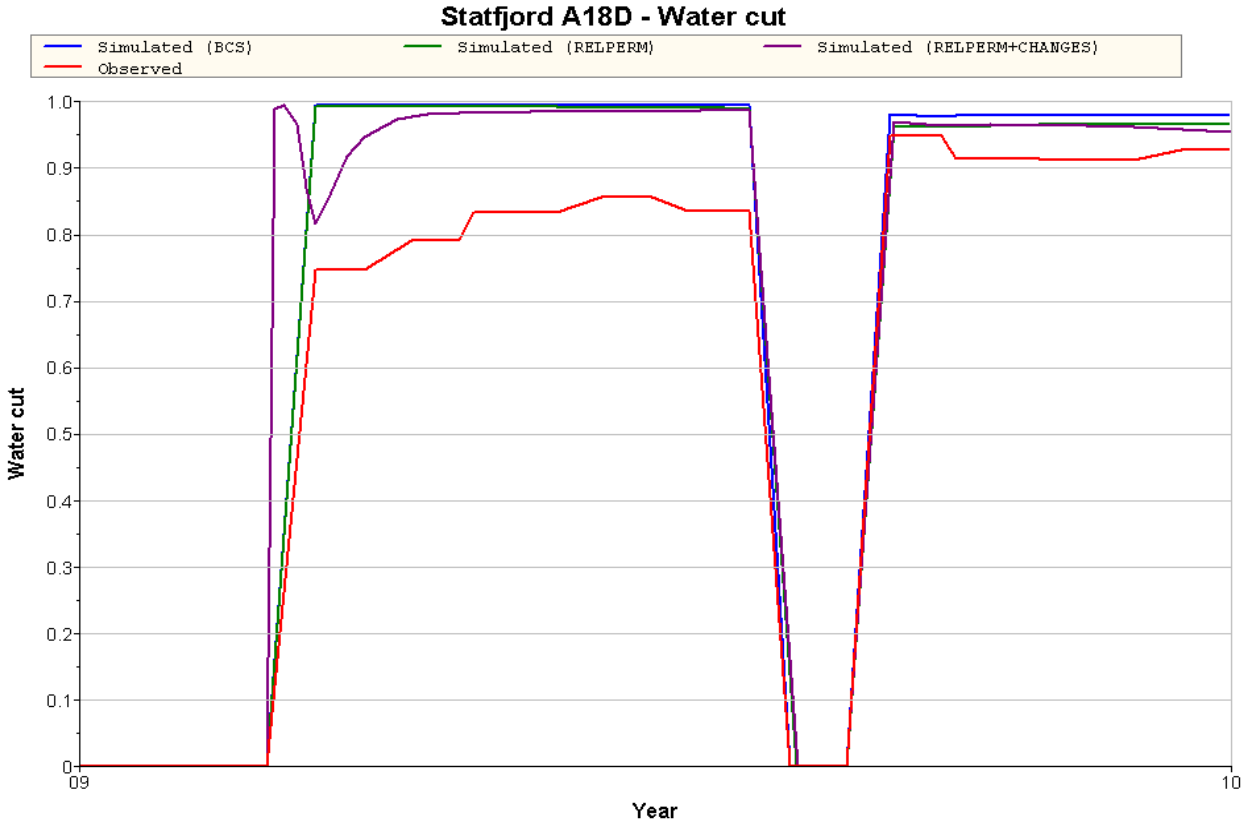

Figure D.13: SWC and WCT for well A-18D

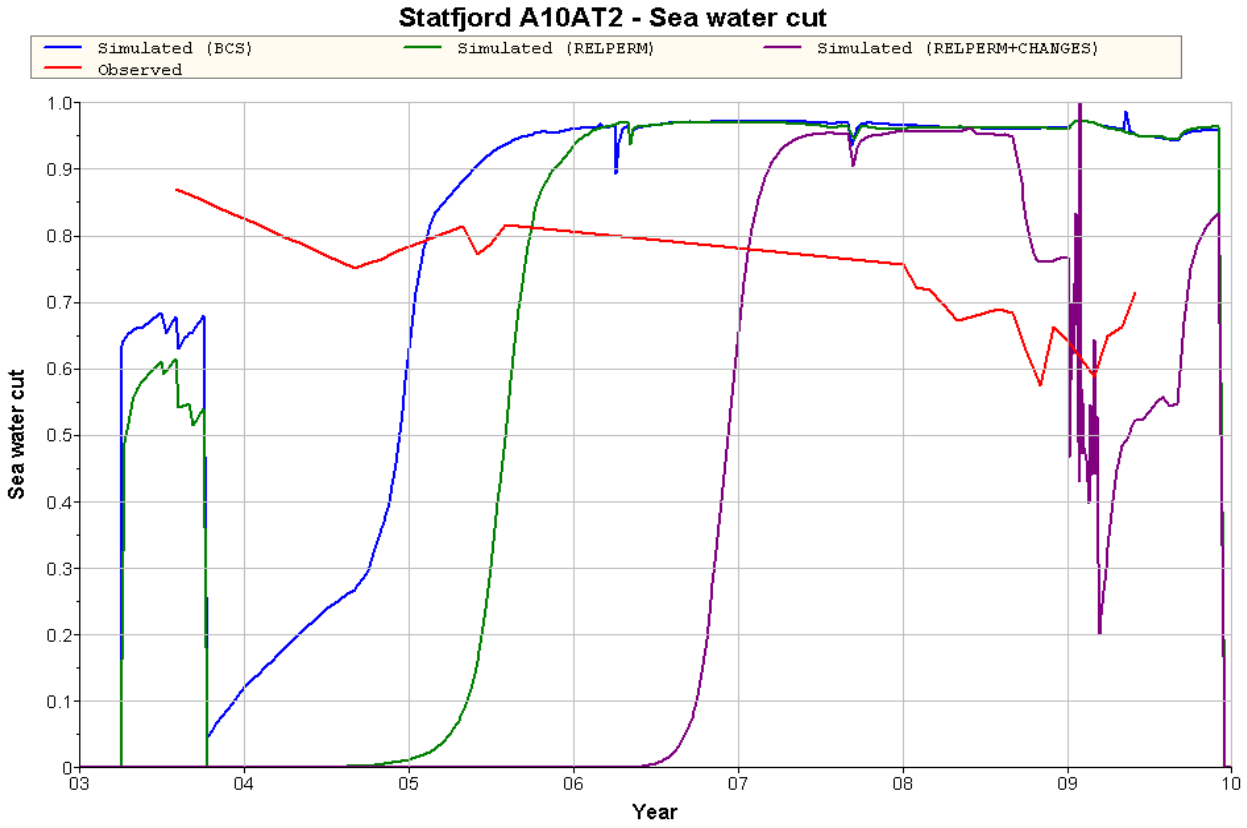

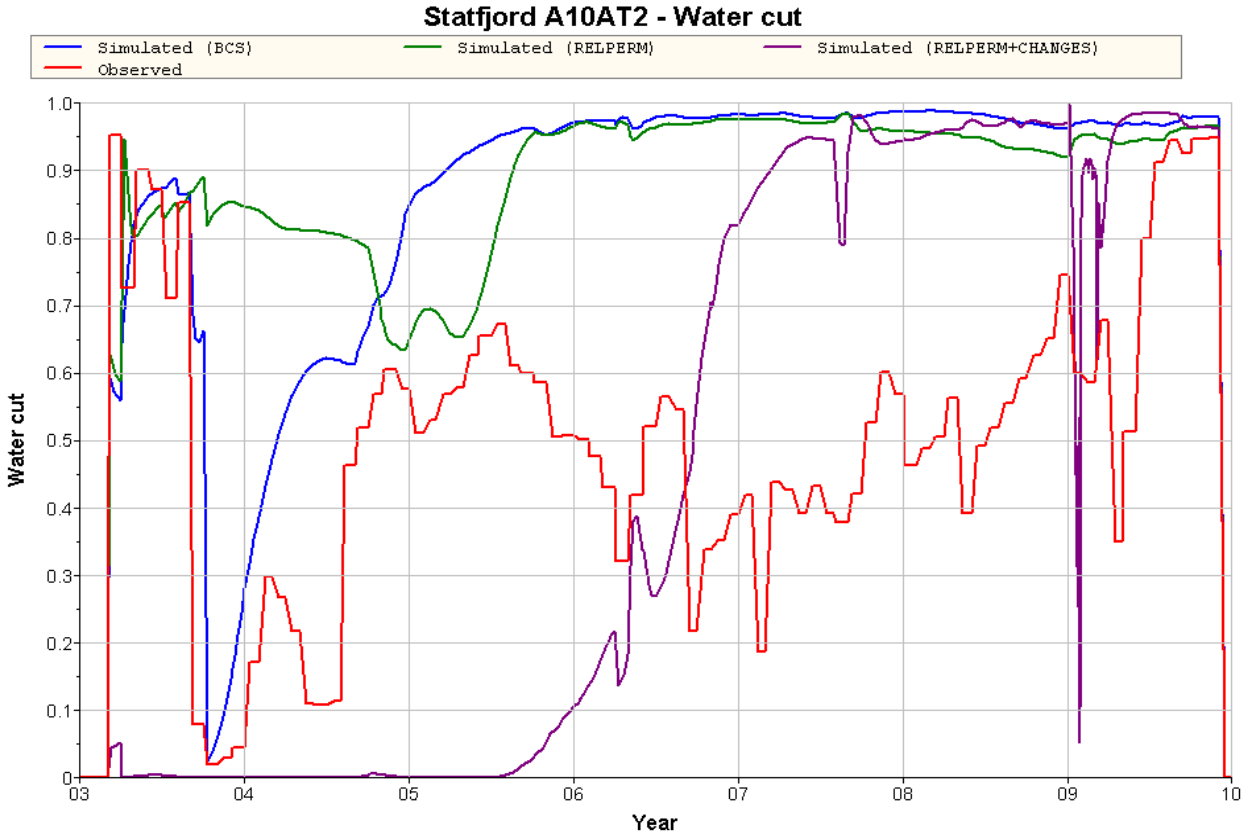

Figure D.14: SWC and WCT for well A-10AT2

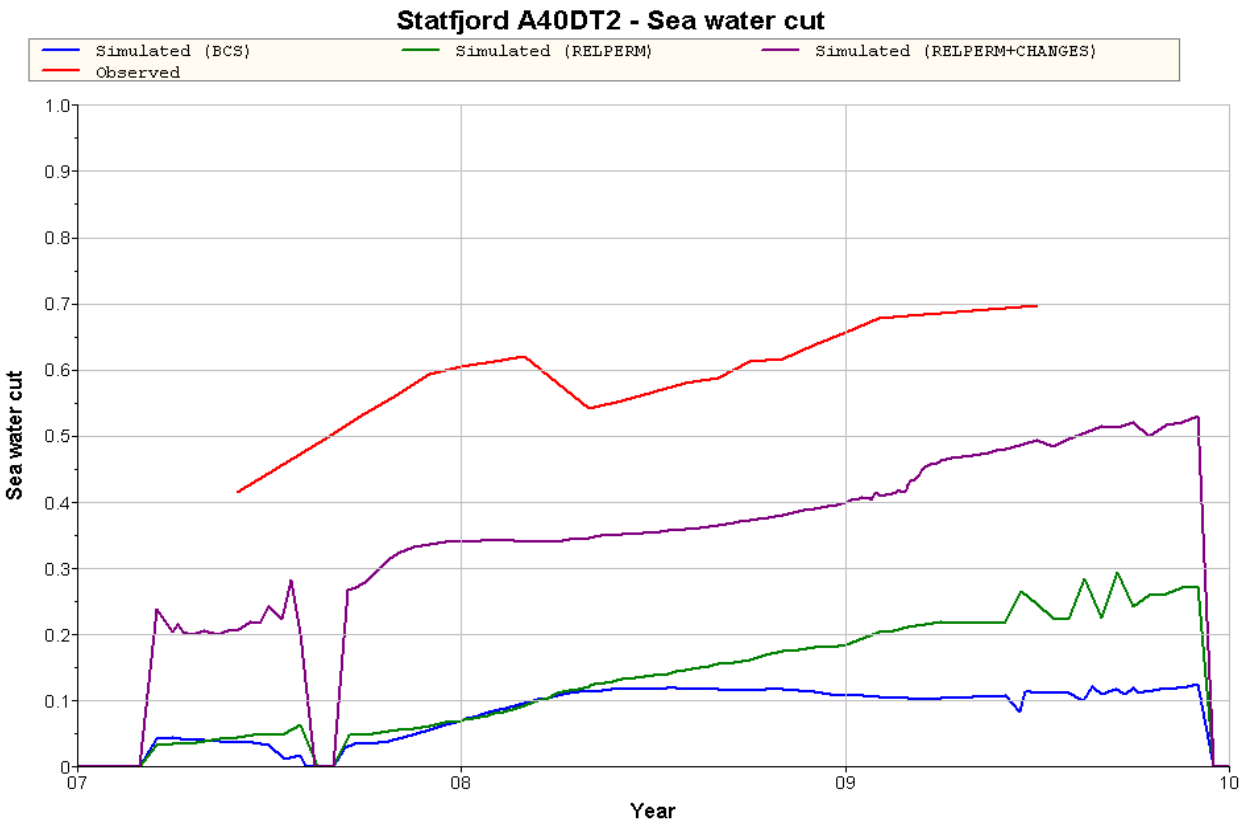

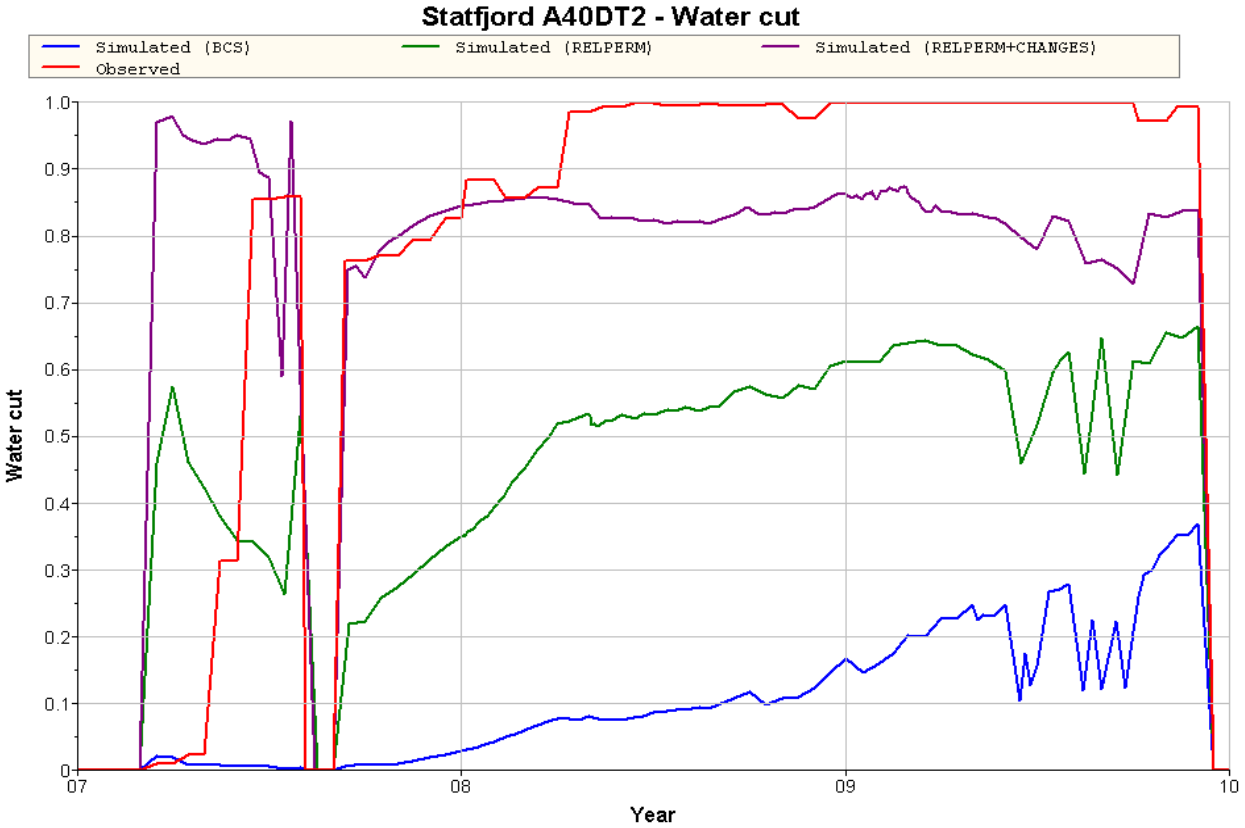

Figure D.15: SWC and WCT for well A-40DT2

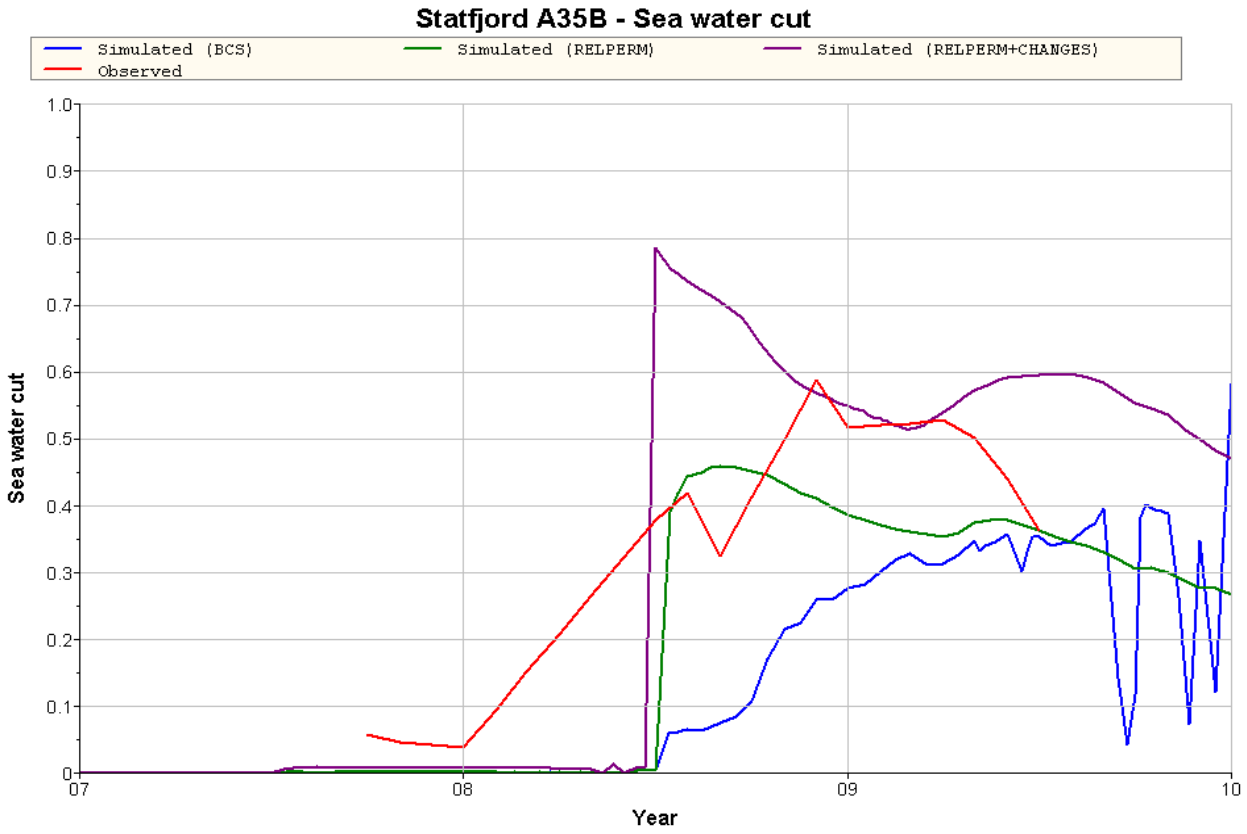

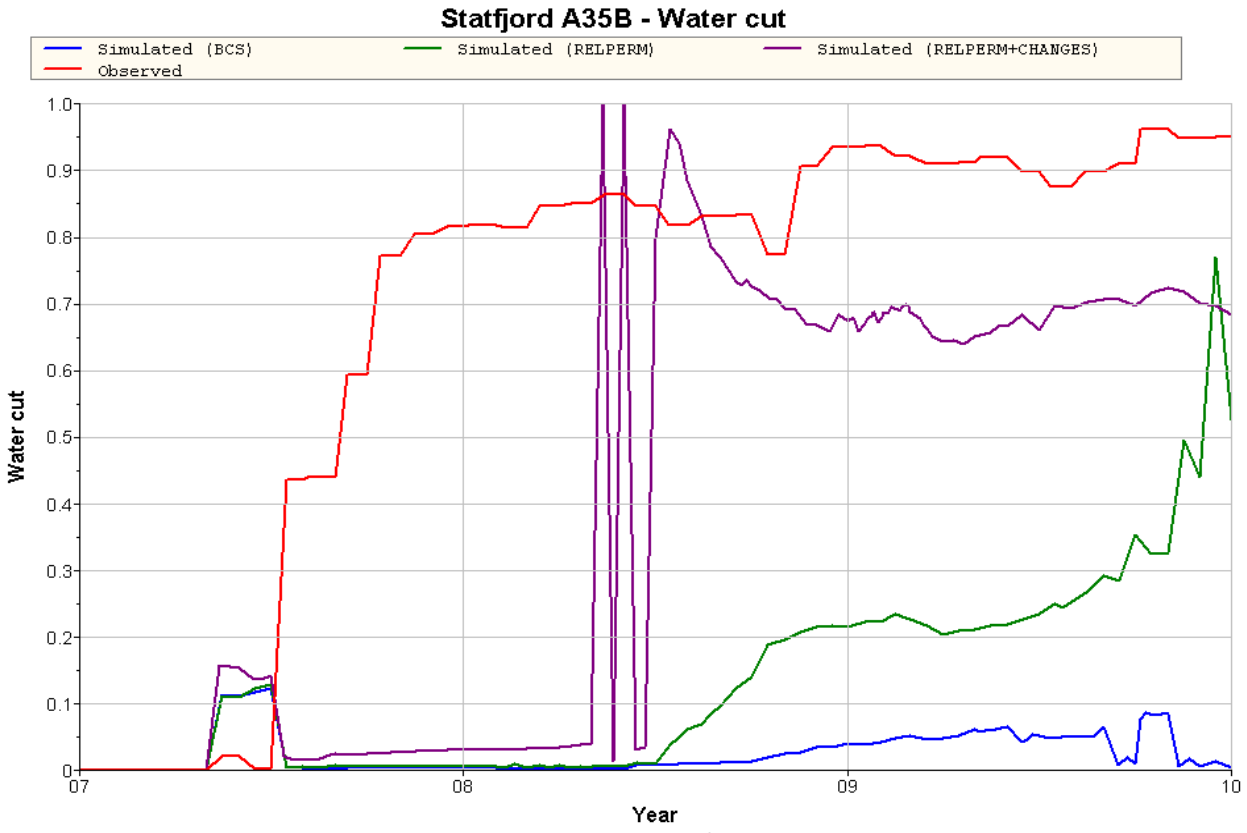

Figure D.16: SWC and WCT for well A-35B

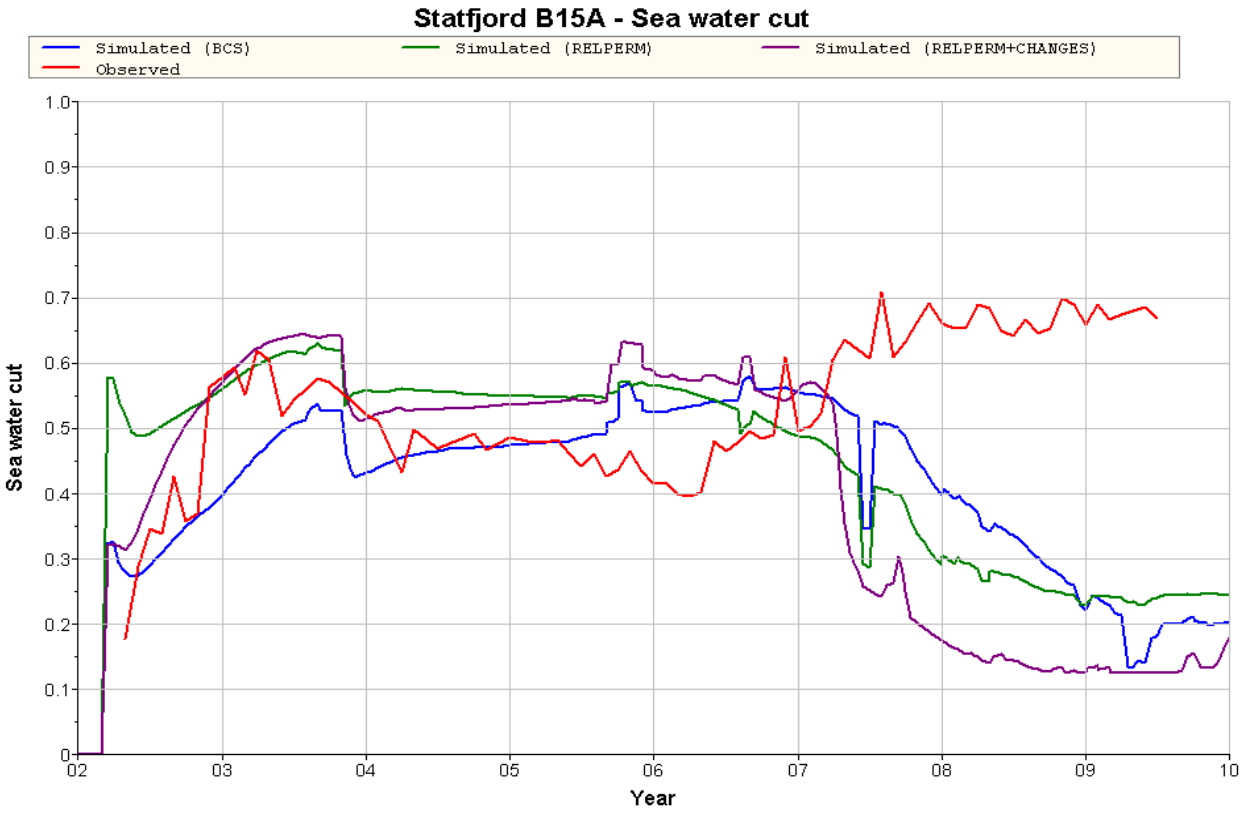

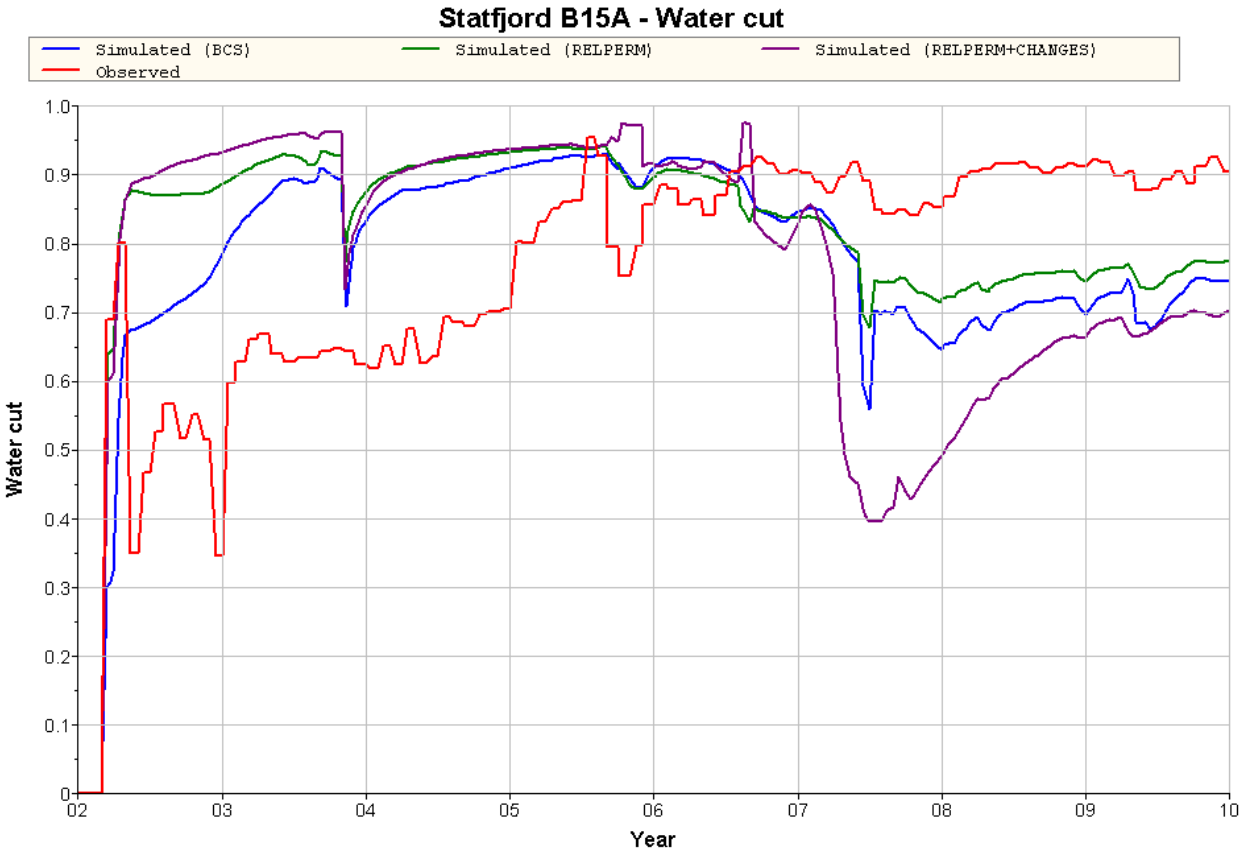

Figure D.17: SWC and WCT for well B-15A

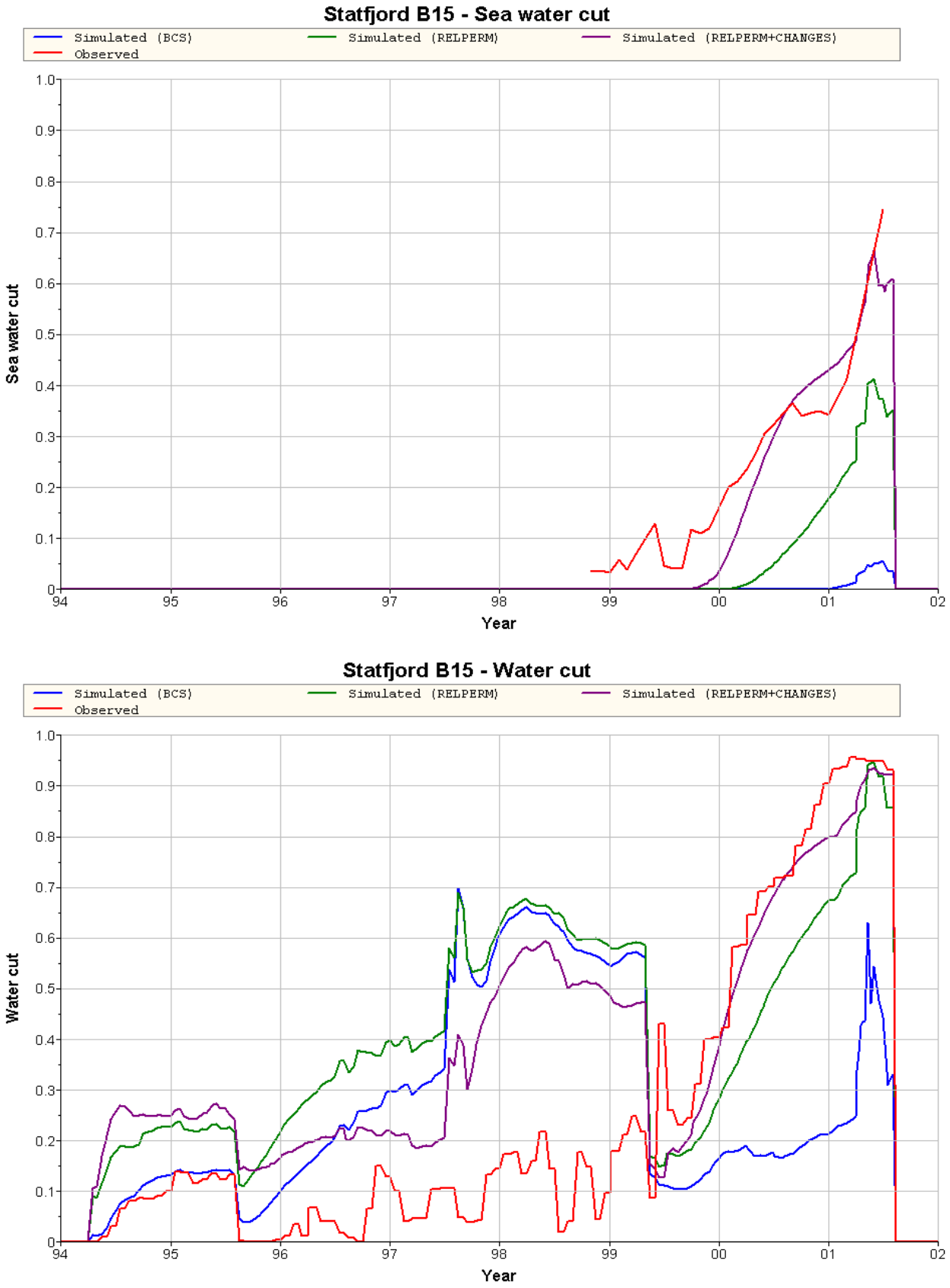

Figure D.18: SWC and WCT for well B-15

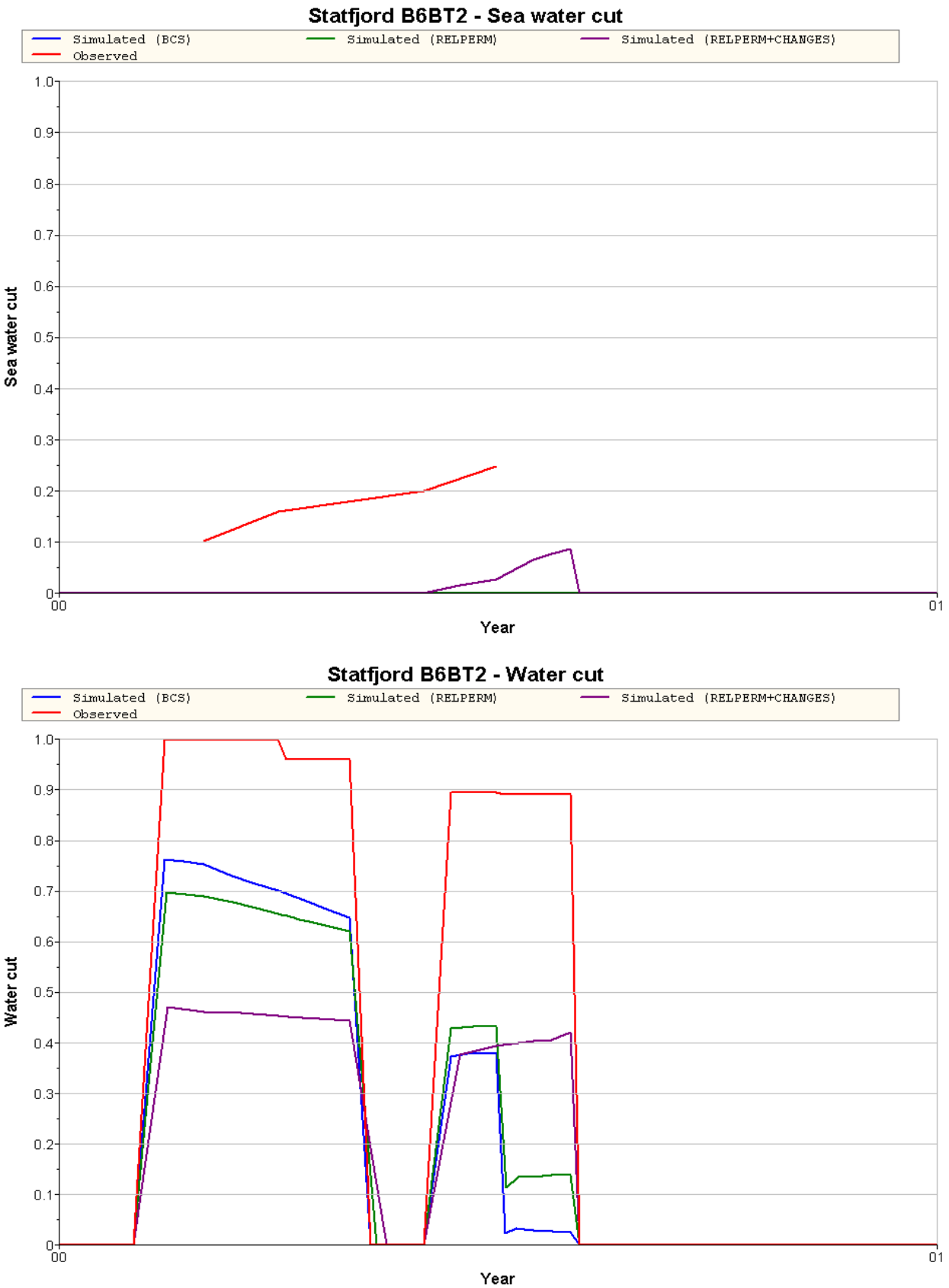

Figure D.19: SWC and WCT for well B-6BT2

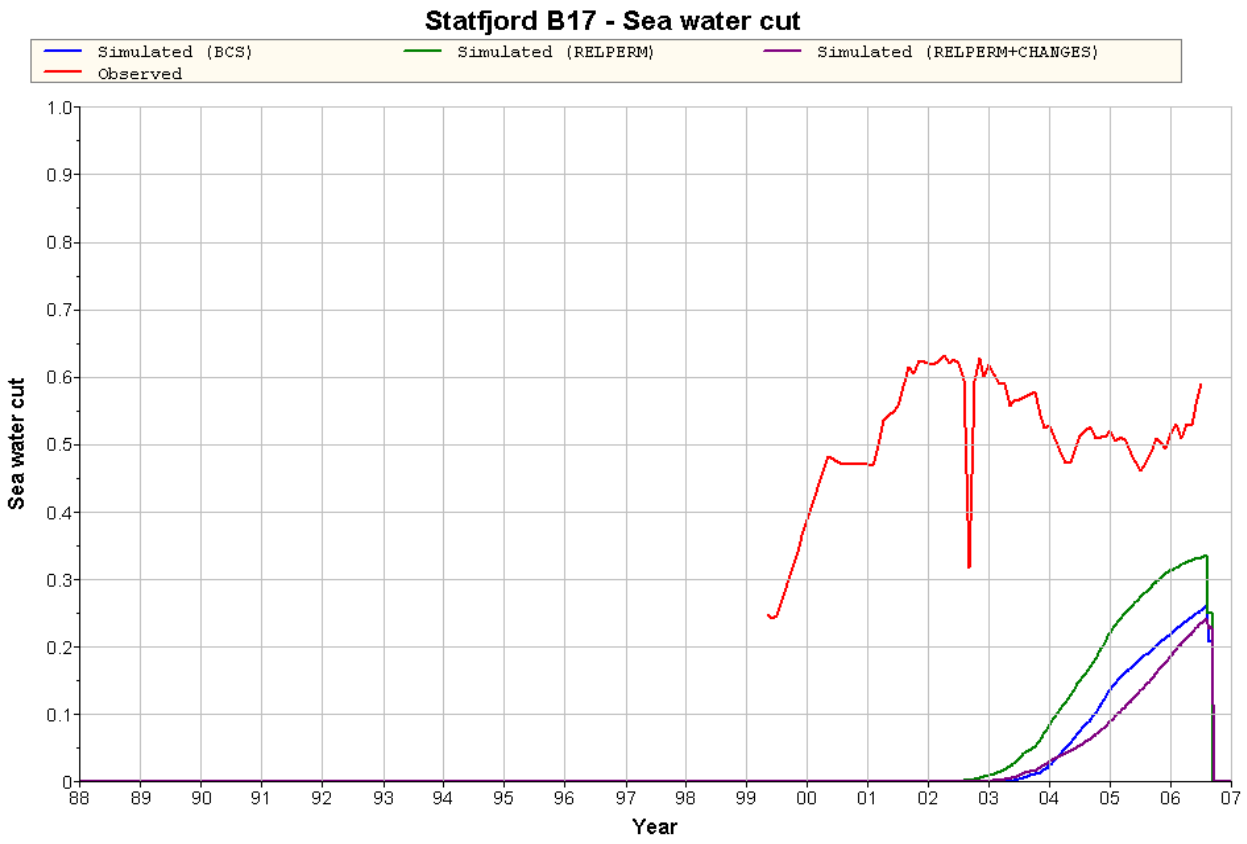

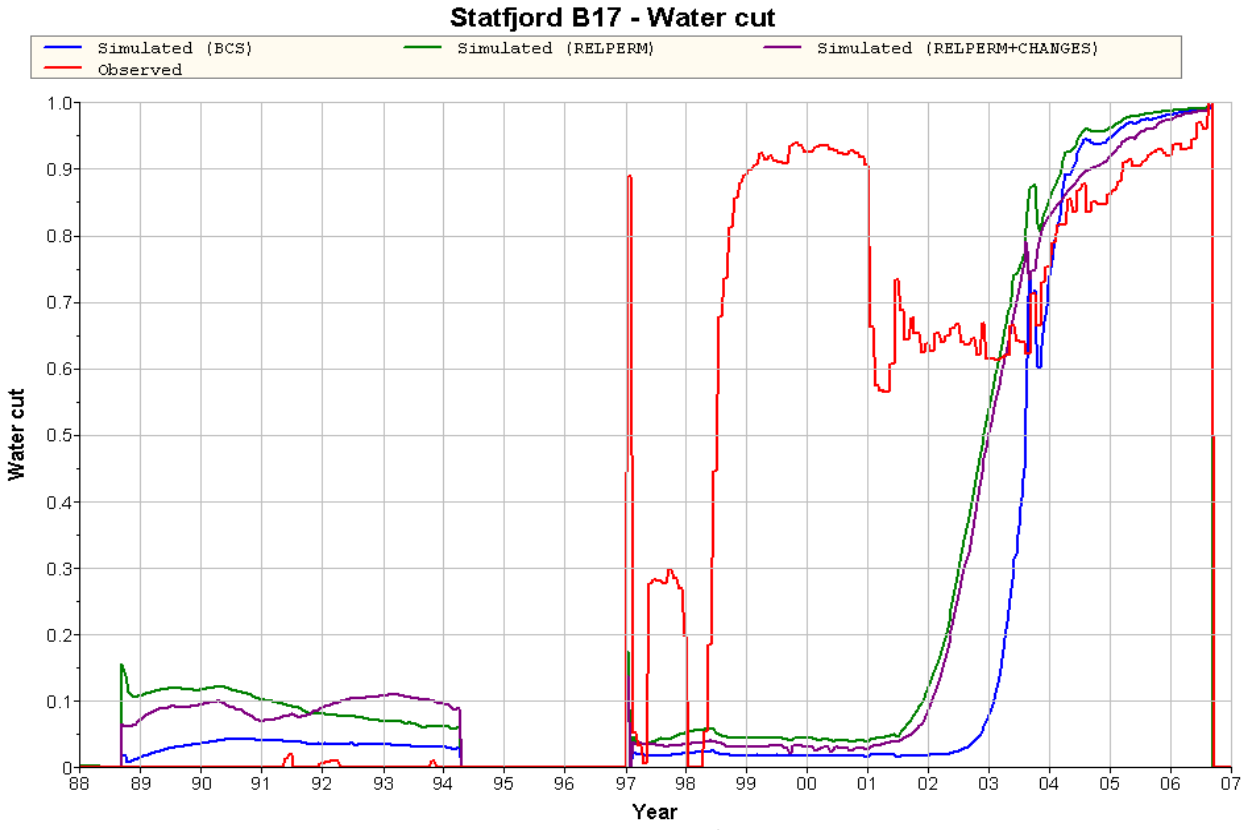

Figure D.20: SWC and WCT for well B-17

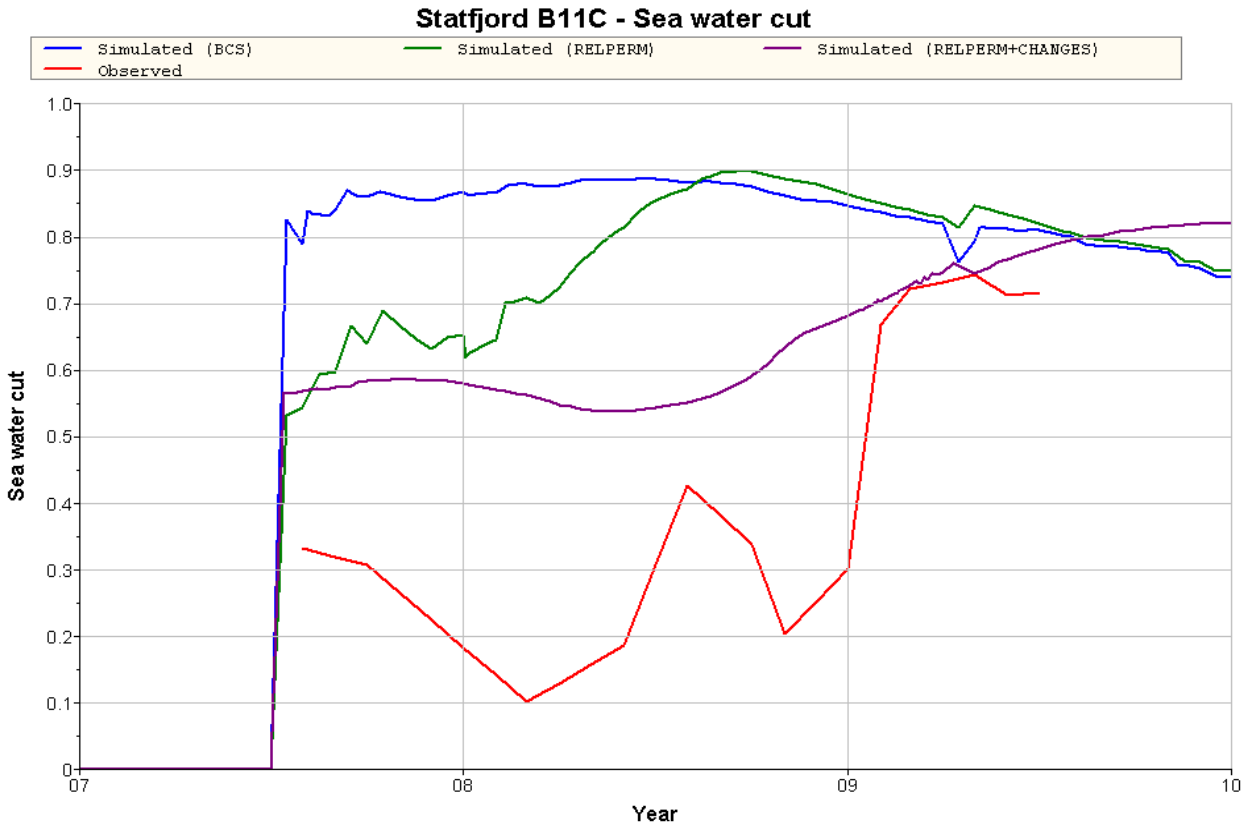

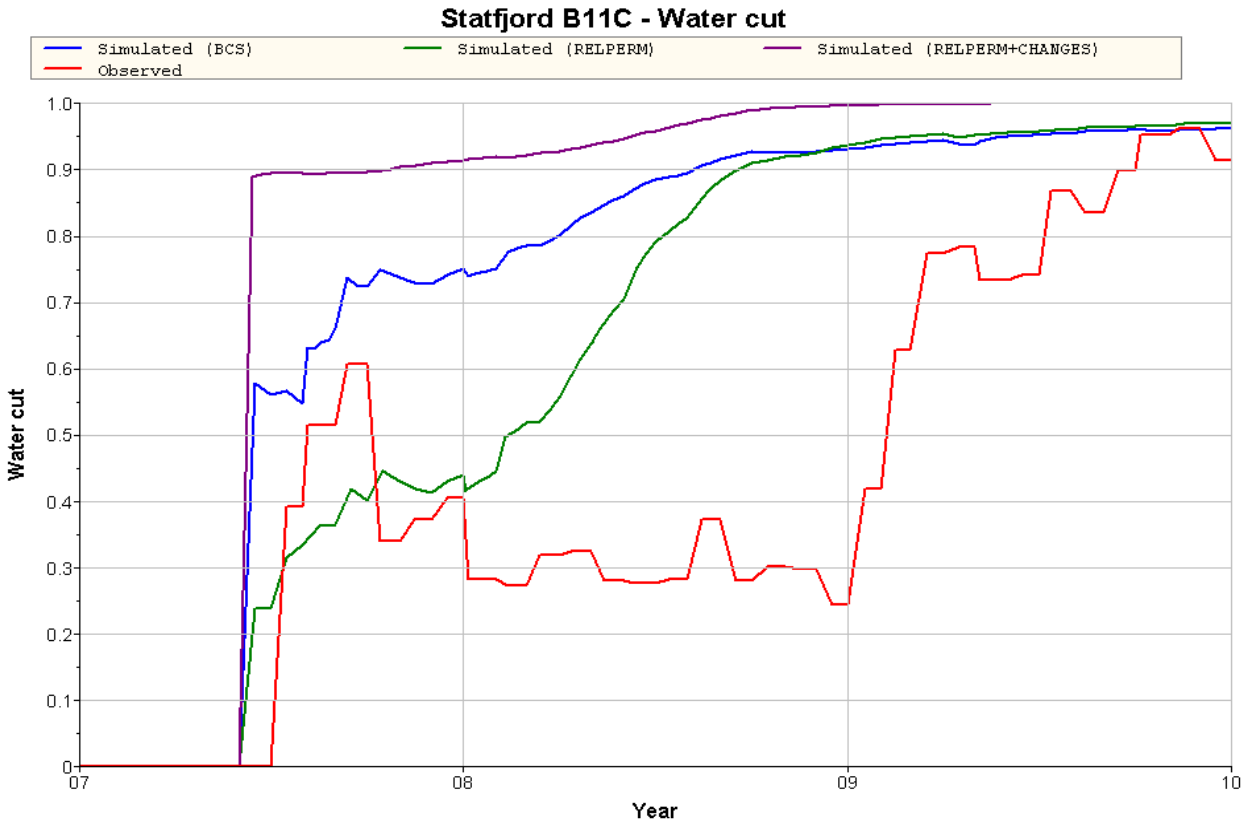

Figure D.21: SWC and WCT for well B-11C

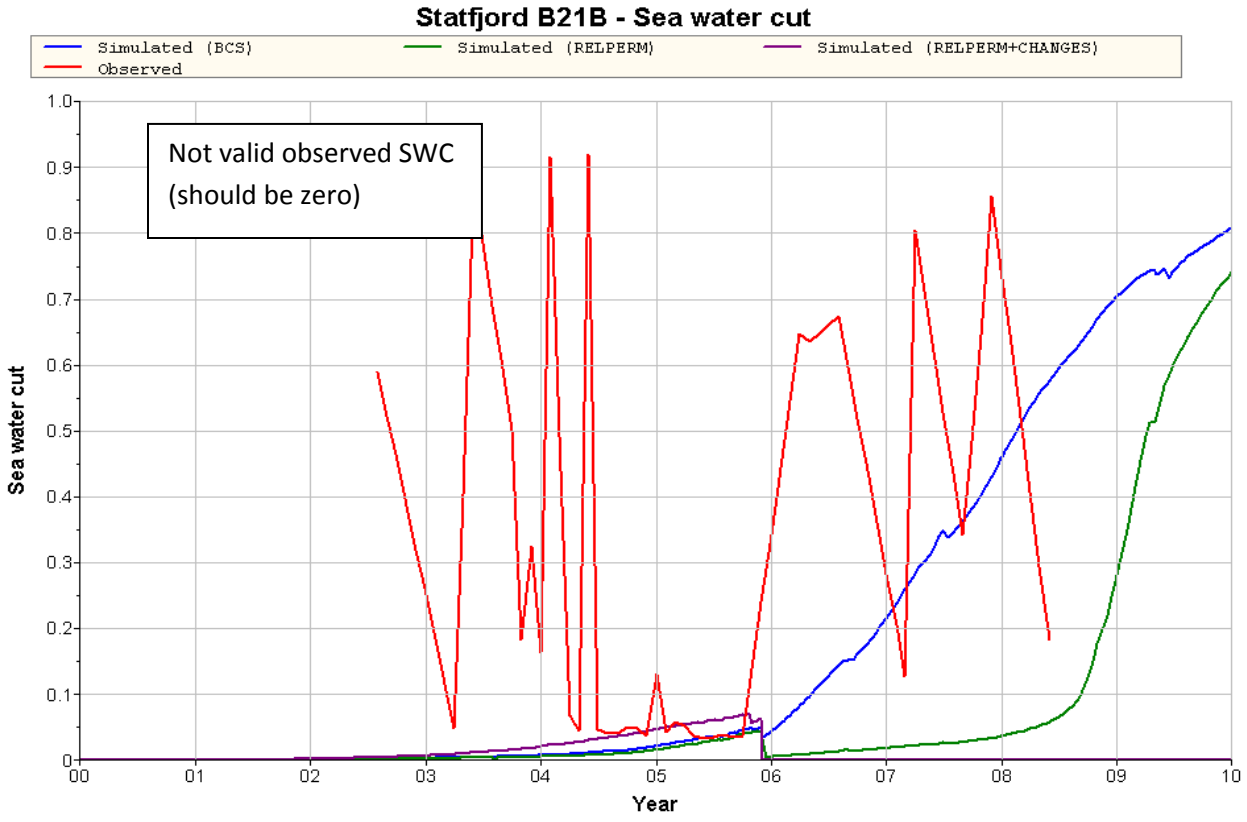

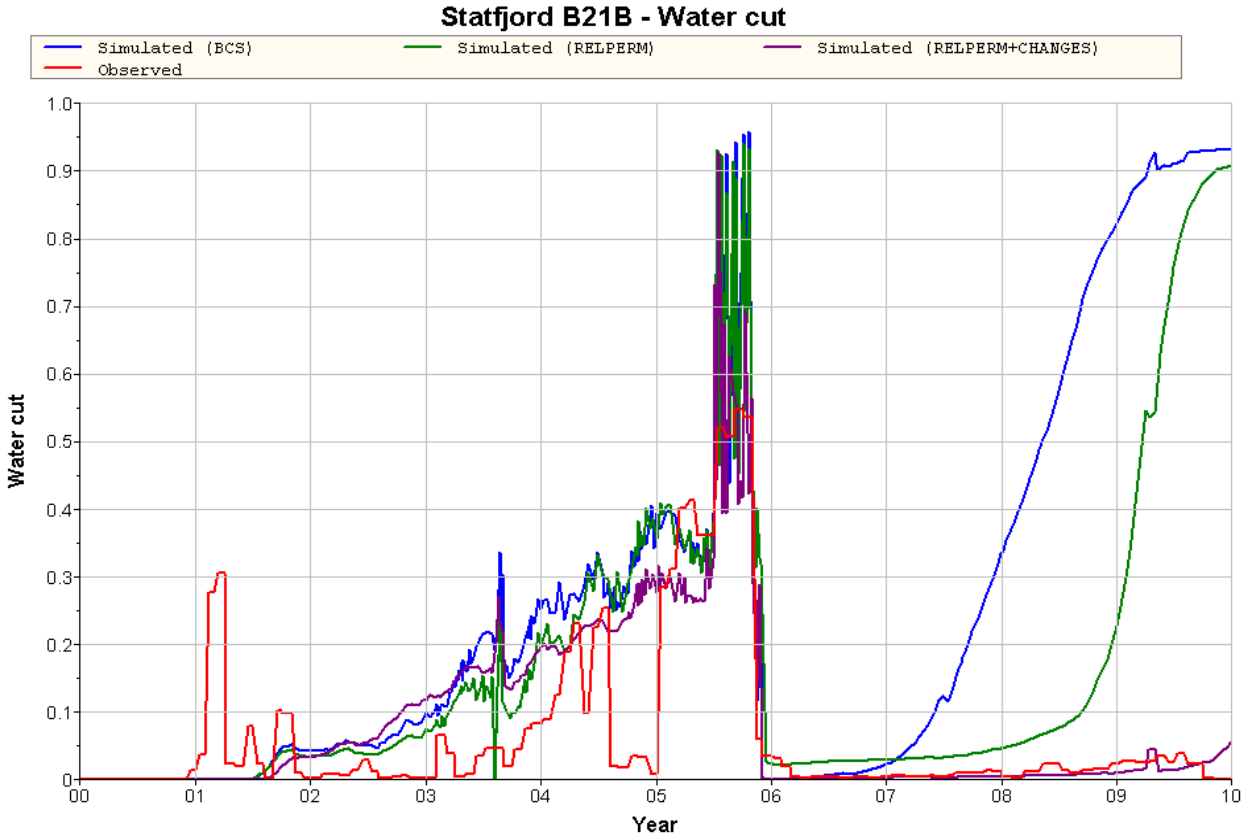

Figure D.22: SWC and WCT for well B-21B

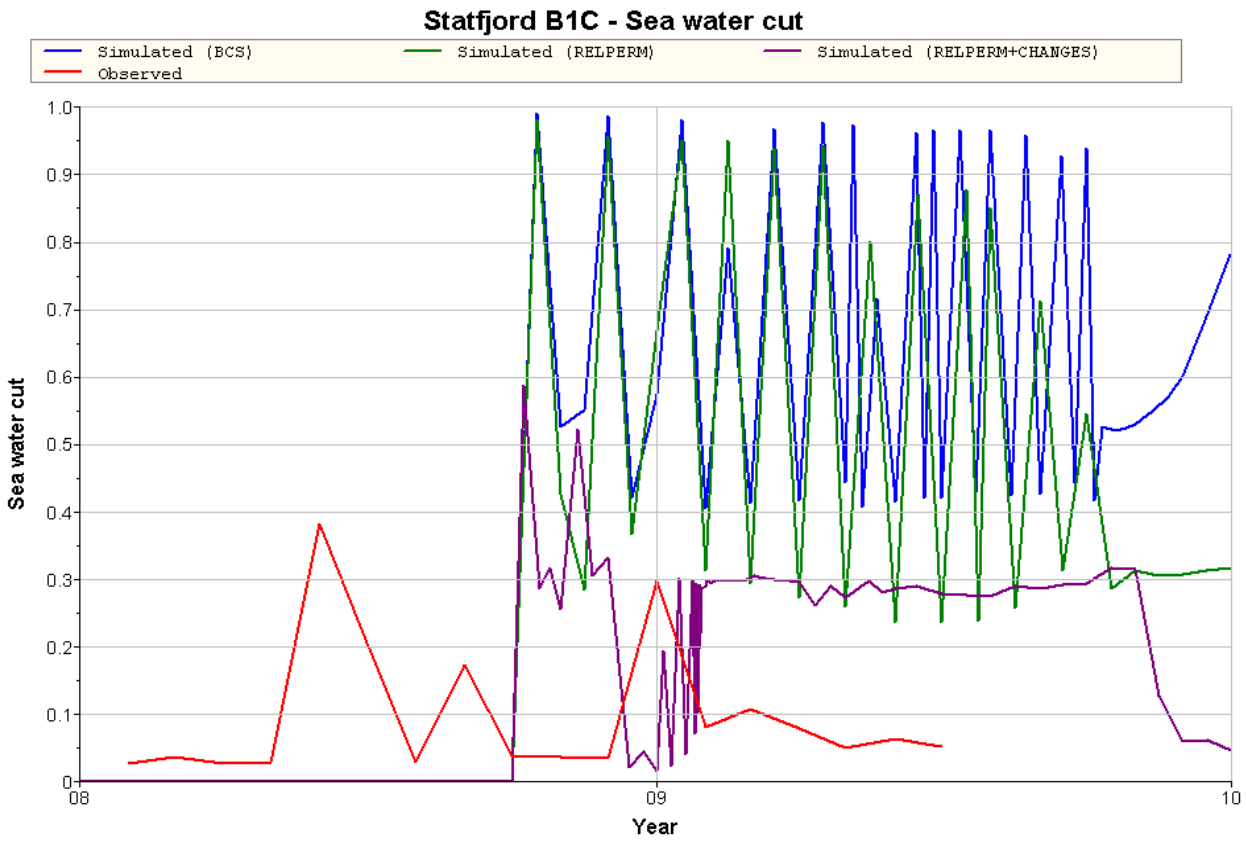

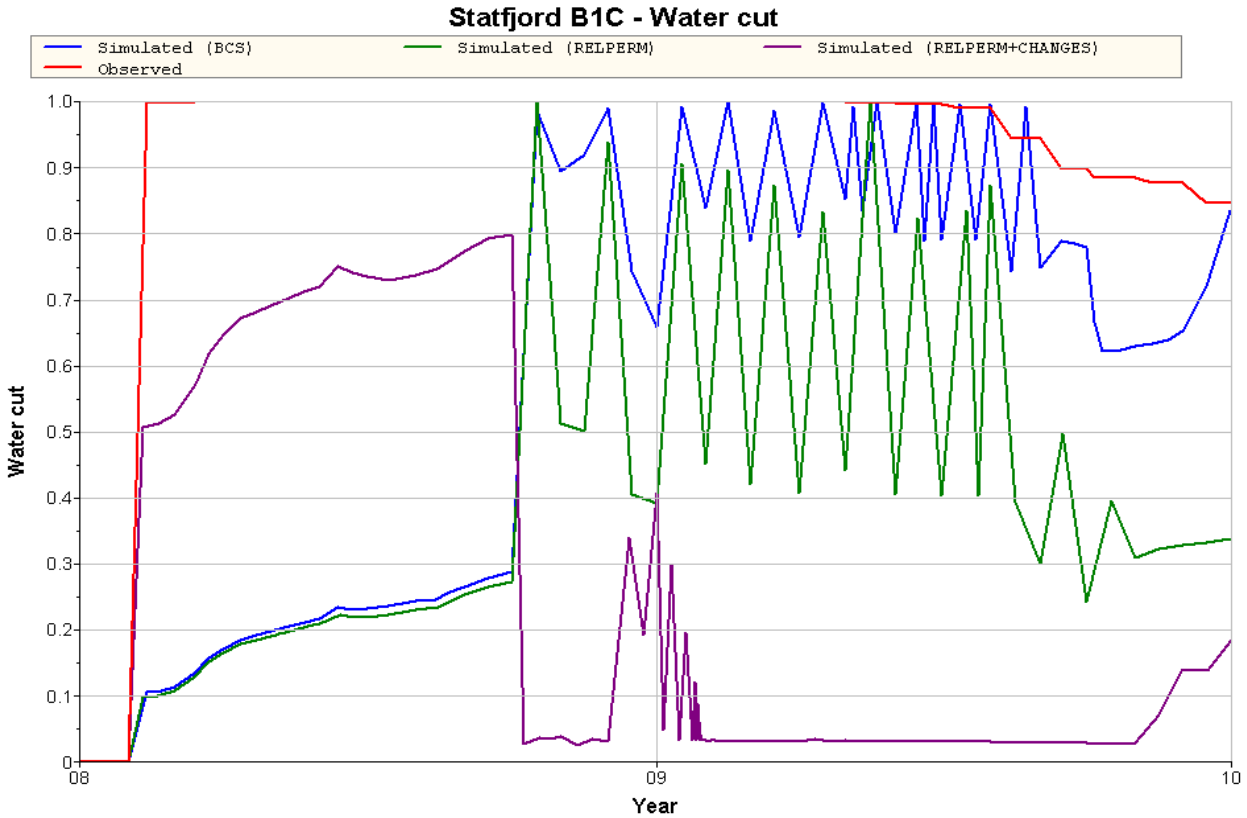

Figure D.23: SWC and WCT for well B-1C

E Field and platform results

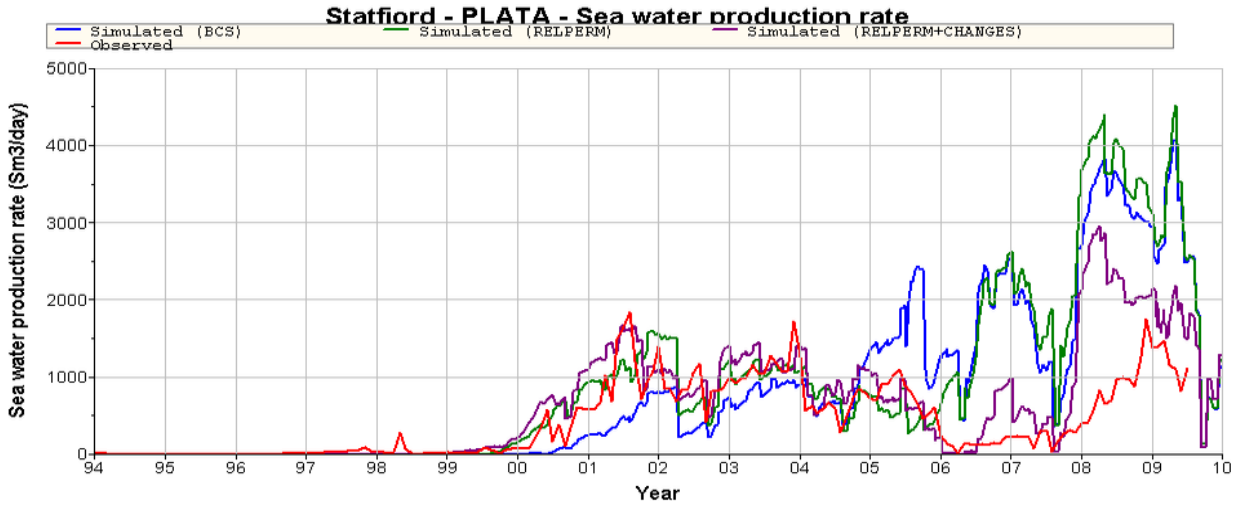

Figure E.1: Sea water production rate – SFA

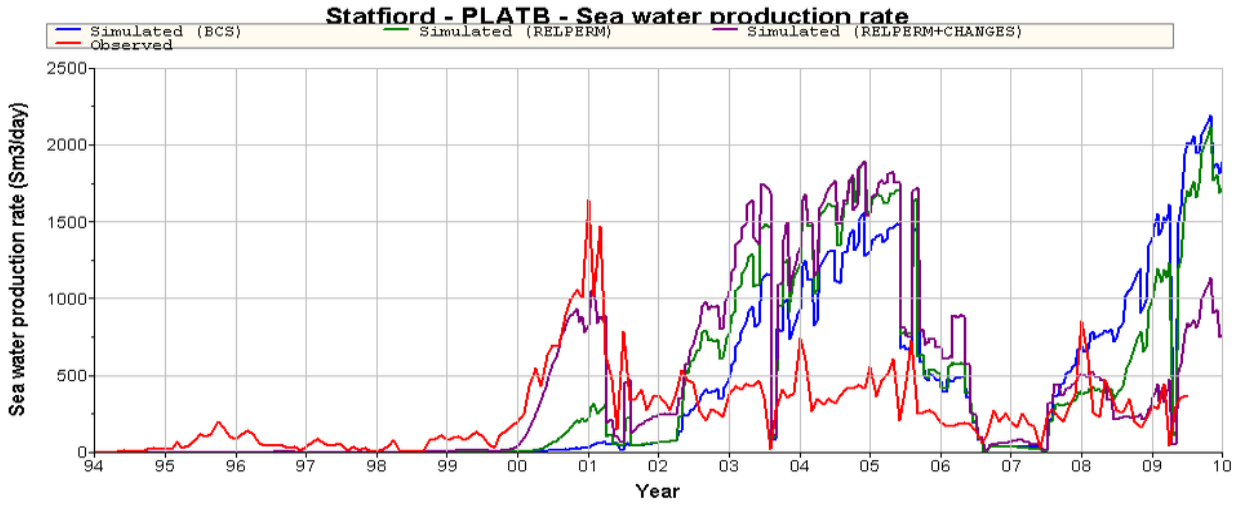

Figure E.2: Sea water production rate – SFB

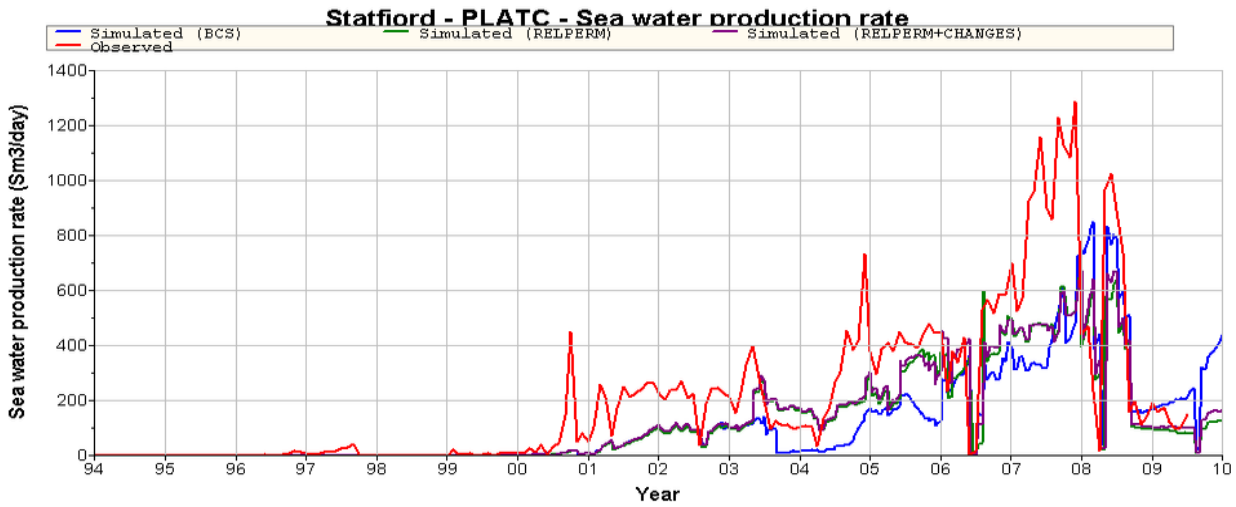

Figure E.3: Sea water production rate – SFC

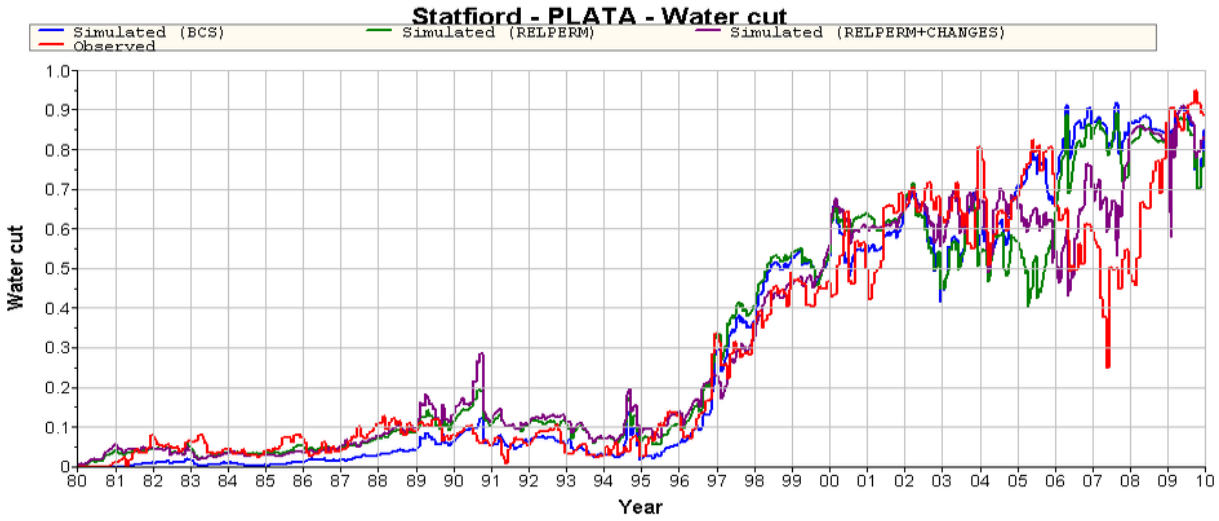

Figure E.4: Water cut – SFA

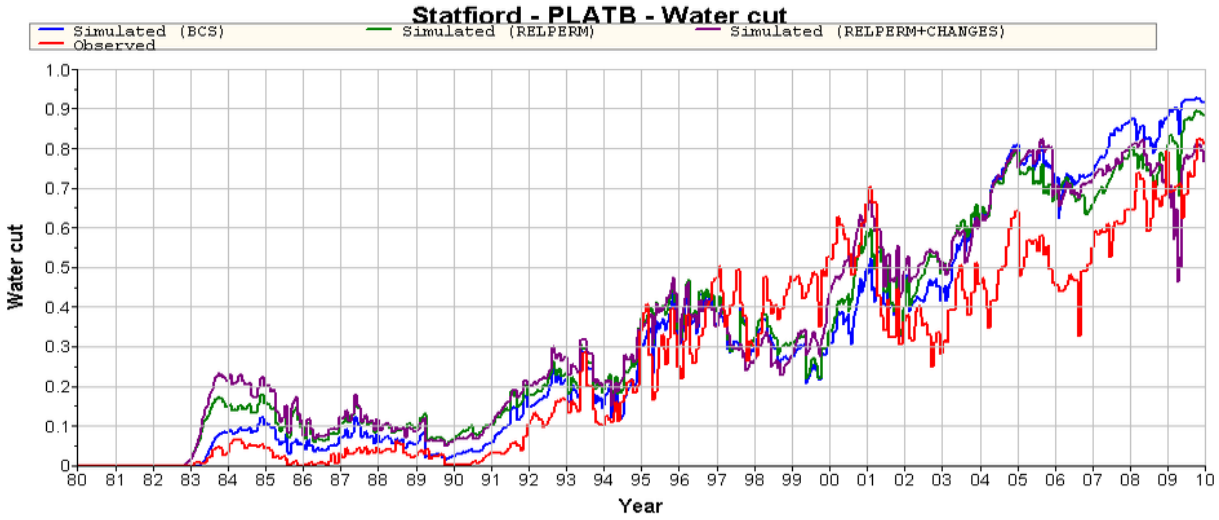

Figure E.5: Water cut – SFB

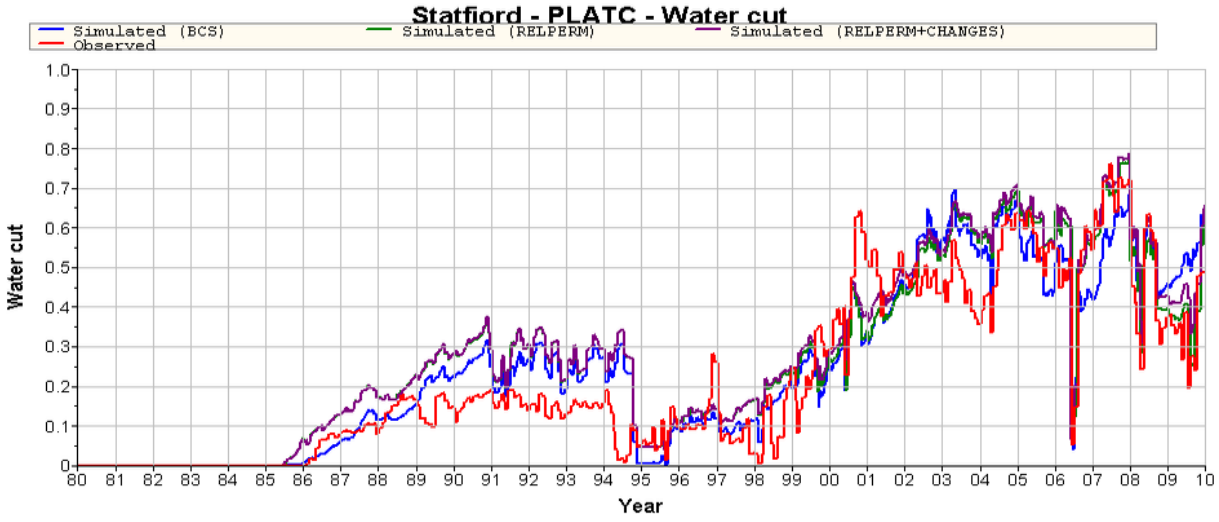

Figure E.6: Water cut – SFC

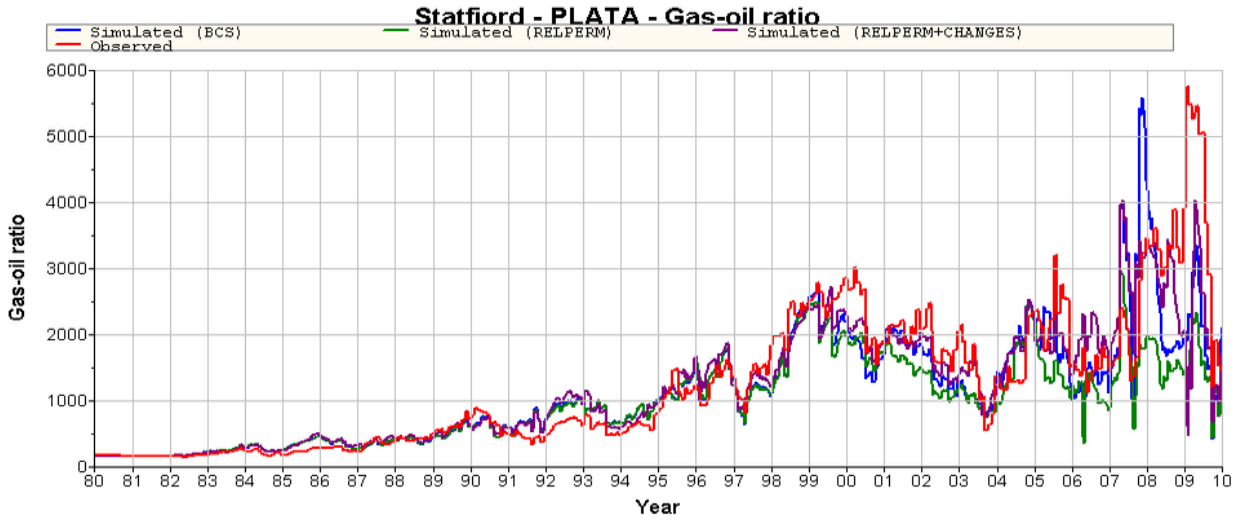

Figure E.7: Gas-oil ratio – SFA

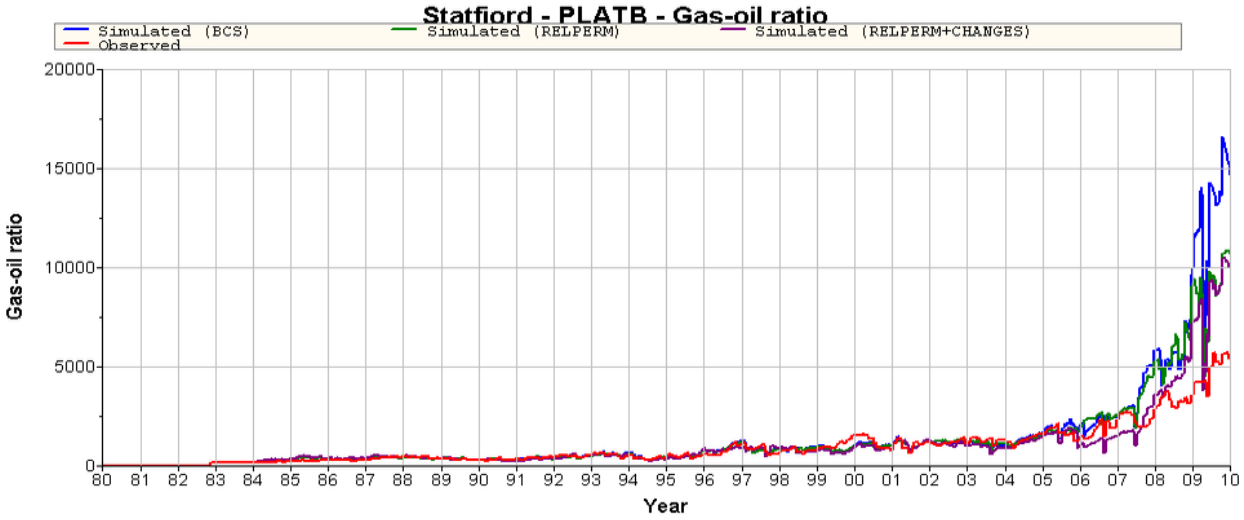

Figure E.8: Gas-oil ratio – SFB

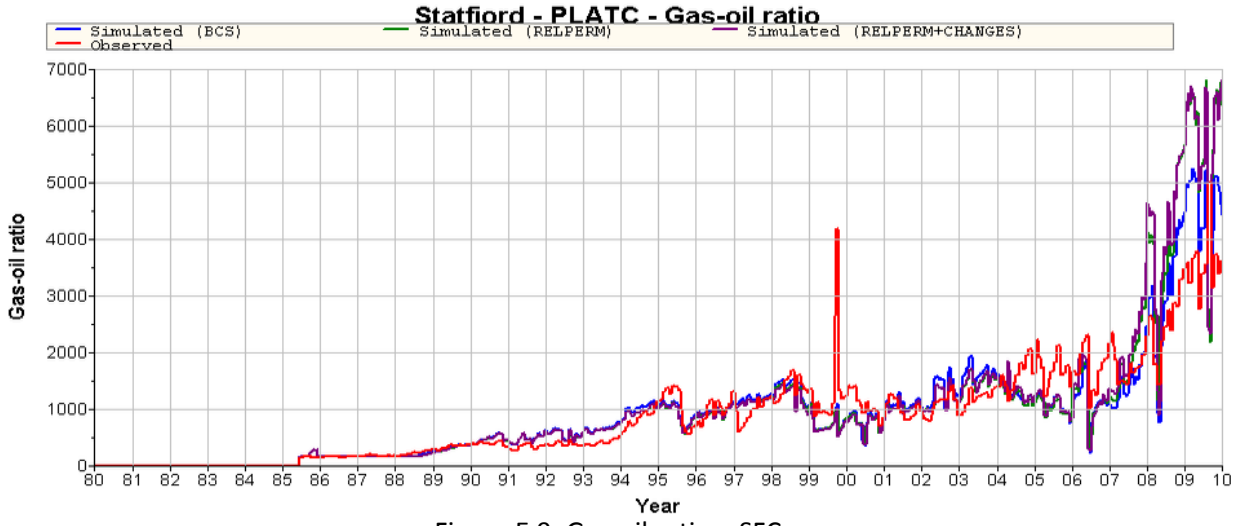

Figure E.9: Gas-oil ratio – SFC

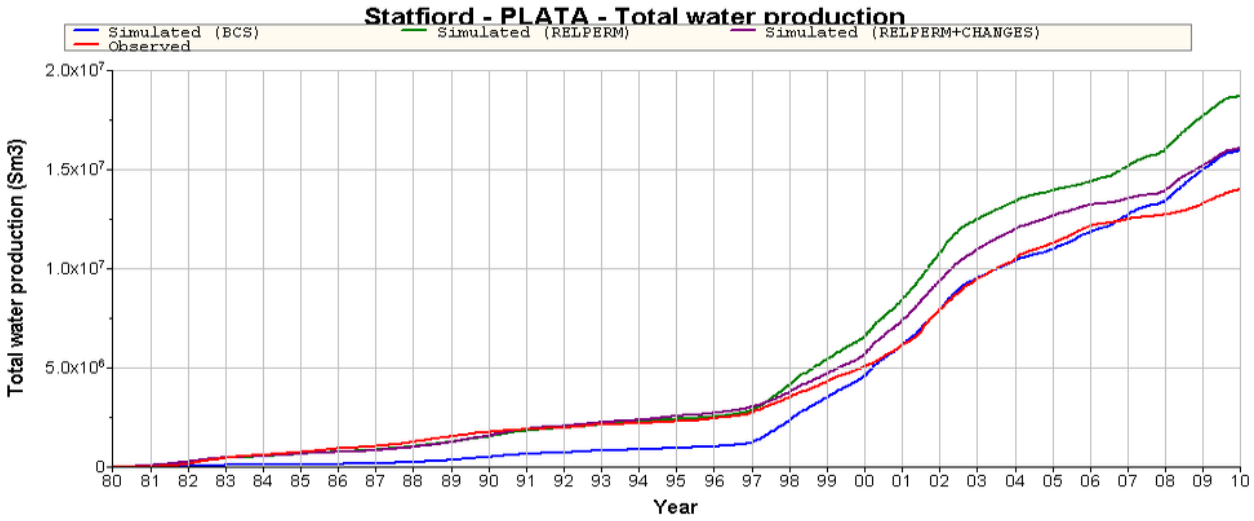

Figure E.10: Total water production – SFA

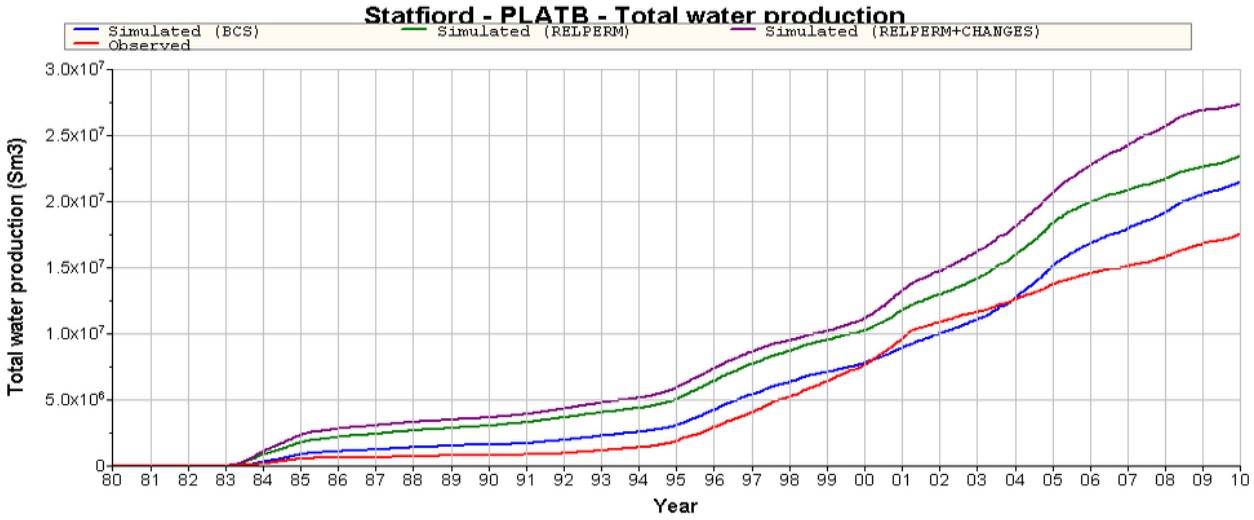

Figure E.11: Total water production – SFB

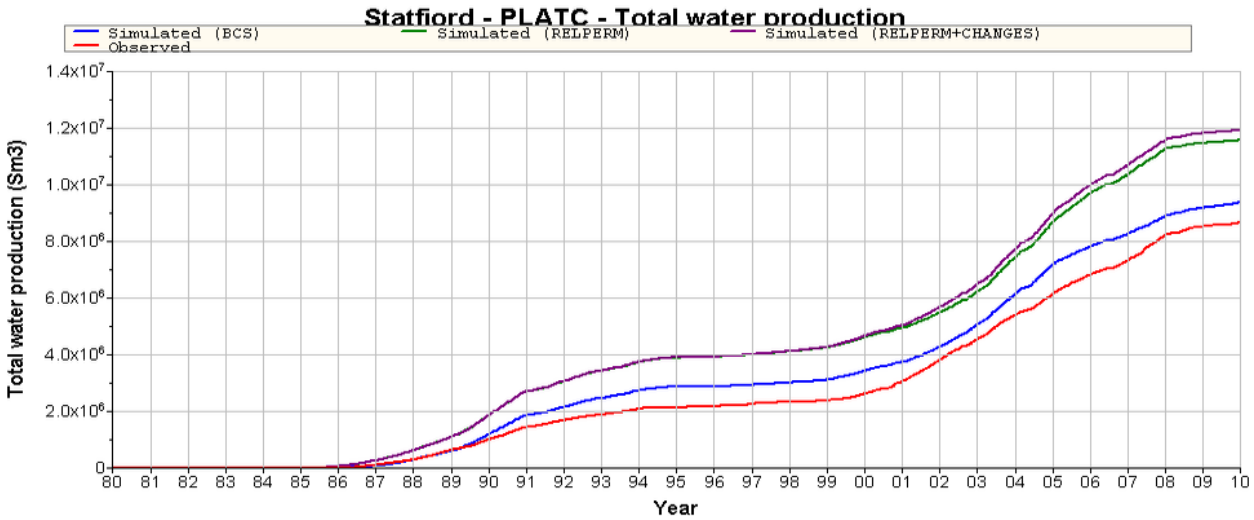

Figure E.12: Total water production – SFC